University of Alberta

Chemical Synthesis and Biological Evaluation of Unusual Sulfur-Containing Peptides and Efforts Toward Chemical Synthesis of Crocin

by

Zedu Huang

A thesis submitted to the Faculty of Graduate Studies and Research
in partial fulfillment of the requirements for the degree of

Doctor of Philosophy

Department of Chemistry

Fall, 2012
Edmonton, Alberta

Abstract

In order to minimize side reactions when preparing peptides containing a C-terminal cysteine residue, a method of protection of the carboxyl of the C-terminal cysteine as a cyclic ortho ester was developed. *N*-Fmoc-*S*-S*t*Bu cysteine cyclic ortho esters **31** (L) and **32** (D) were synthesized with excellent enantiomeric purity. This moiety was incorporated onto a solid support via a disulfide linkage, and model tripeptides (Gly-Phe-Cys) and the analgesic peptide, crotalphine, were synthesized with excellent diastereomeric purity.

In the second chapter of this thesis, a structure-activity relationship (SAR) study of the crotalphine was developed. Eleven analogs were prepared to elucidate the essential structural features for the analgesic activity and identify an active analog with increased metabolic stability. The biological evaluation of these analogs is ongoing in the laboratory of our collaborators.

The Vederas group discovered a new family of Class II bacteriocins, such as thuricin-β, featuring sulfur to α-carbon bridges. In the third chapter, efforts toward asymmetric synthesis of a bis-amino acid containing a thioether bridge were attempted. This bis-amino acid could be used as a standard to confirm the stereochemistry at the α-carbon of the modified residues using chiral GC-MS. Bis-amino acid derivative (**126**) was synthesized as a single diastereomer using chiral tricycloiminolactone **129** and efforts toward the removal of the auxiliary are ongoing.

In the second part of the third chapter, a SAR study of thuricin-β was performed. The cysteine residues of thuricin-β were replaced by glycine, serine or alanine. All of the

synthetic analogs were inactive against *Bacillus firmus*. In the future, cyclic analog **163**, will be synthesized and evaluated for antimicrobial activity.

Crocin is a major component of saffron and shows activity against various diseases. The last project of this thesis was towards chemical synthesis and biological evaluation of crocin and its analogs. The polyene acid **198** was synthesized in 10 steps from geranyl acetate. Attempts to attach this acid to β-D-glucose were unsuccessful. In the future, polyene ester **214** will be coupled to β-D-glucose or β-gentibiose. When the glycosylated products are obtained, they will be subjected to cross metathesis conditions to form crocin and its analogs.

Acknowledgements

I would like to thank my research supervisor, Professor John C. Vederas for his constant support, encouragement and understanding. As an excellent teacher and mentor, he has provided a stimulating learning environment. I have been inspired by his enthusiastic attitude towards science and his commitment to promoting independent thought. The time spent in his group has undoubtedly prepared me for the journey ahead.

I would like to thank Drs. Jennifer Chaytor and David Dietrich for their careful proofreading of this manuscript. I am thankful to all the past and present members of the Vederas group who have contributed to a positive and enjoyable work environment.

I would especially like to thank Dr. Darren Derksen for his collaboration in the cyclic ortho ester and crotalphine projects, Dr. David Dietrich for his collaboration in the crocin project, and Christopher Lohans for his collaboration in the tridecaptin A project. I would also like to thank Stephen Cochrane for his work on a collaborative research project not described in this thesis.

I would like to thank my collaborators outside the Vederas group, Dr. M. Joanne Lemieux, Dr. Yara Cury, and Dr. Cory Brooks. Their excellent collaboration and support had enormous impacts on my research projects.

I also want to thank all of the staff members from the service labs of the Department of Chemistry at the University of Alberta. Dr. Randy Whittal, Dr. Angie Morales-Izquierdo, Jing Zheng, Bela Reiz and Wayne Moffat all provided tremendous help.

Lastly, but most importantly, thank you to my parents and sisters for their unconditional love and support. Whenever I felt frustrated or depressed, they were always

ready to listen to me and cheer me up. Without these overseas conversations, I could not finish my PhD studies. Thanks to all of you for always believing in me and helping me realize my goals.

Table of Contents

List of Figures

List of Schemes

List of Abbreviations

$[\alpha]_D$	specific rotation
Ac	acetyl
Acm	acetamidomethyl
Ac_2O	acetic anhydride
ACS	American Chemical Society
Ala or A	alanine
Ar	aryl
Arg	arginine
Asn or N	asparagine
Asp or D	aspartic acid
atm	atmosphere
BHA	butylated hydroxyanisole
Bn	benzyl
Boc	*tert*-butyloxycarbonyl
Bu	butyl
c	concentration
cat.	catalytic
Cbz	carbobenzyloxy
CD	circular dichroism
CHCA	α-cyano-4-hydroxy cinnamic acid
CM	cross metathesis
C-terminal	carboxy terminal

Cys or C	cysteine
δ	chemical shift
d	doublet
Da	dalton
5’-dA	5’-deoxyadenosine
DBU	1,8-diazabicyclo[5.4.0]undec-7-ene
DCC	dicyclohexylcarbodiimide
DCE	dichloroethane
DCU	dicyclohexylurea
DIC	diisopropylcarbodiimide
DIPEA	diisopropylethyl amine
DMAP	4-dimethylaminopyridine
Dmb	dimethoxybenzyl
DMF	dimethylformamide
DMSO	dimethylsulfoxide
DNs	2,4-dinitrosulfonyl
<E	pyroglutamic acid
e.e.	enantiomeric excess
ESI	electrospray ionization
Et	ethyl
Et_2O	diethylether
Et_3N	triethylamine
EtOAc	ethyl acetate

equiv.	equivalents
Fmoc	9-fluorenylmethyloxycarbonyl
FT	Fourier transform
GC	gas chromatography
Glc	glucose
Gln or Q	glutamine
Glu or E	glutamic acid
Gly or G	glycine
h	hour
HBTU	2-(1*H*-benzotriazole-1-yl)-1,1,3,3-tetramethyl-uronium-hexafluoro-phosphate
HMPA	hexamethylphosphoramide
HOBt	1-hydroxybenzotriazole
HPLC	high performance liquid chromatography
HRMS	high resolution mass spectrometry
Hz	hertz
IBX	2-iodoxybenzoic acid
Ile	isoleucine
IR	infrared
J	coupling constant
JCSG	Joint Center for Structure Genomics
LC	liquid chromatography
LDA	lithium diisopropylamide

Leu or L	leucine
LRMS	low resolution mass spectrometry
Lys or K	lysine
m	multiplet
MALDI	matrix assisted laser desorption ionization
MBom	4-methoxybenzyloxymethyl
Me	methyl
MeOH	methanol
Met or M	methionine
MHz	megahertz
min	minute
mol	mole
Ms	methanesulfonyl
MS	mass spectrometry
MS/MS	tandem mass spectrometry
NMP	*N*-methyl-2-pyrrolidone
NMR	nuclear magnetic resonance
NOESY	nuclear Overhauser effect spectroscopy
N-terminal	amino terminal
PDB	protein data bank
PEG	polyethylene glycol
PG	protecting group
Ph	phenyl

Phe or F	phenylalanine
Pro or P	proline
pNZ	para-nitrobenzyl
ppm	part per million
Pr	propyl
PyBOP	benzotriazole-1-yl-oxy-tris-pyrrolidino-phosphonium hexafluorophosphate
q	quartet
rt	room temperature
RP	reversed phase
rpm	revolutions per minute
s	singlet
SAM	*S*-adenosylmethionine
SAR	structure activity relationship
sat.	saturated
Ser or S	serine
sp.	species
SPPS	solid phase peptide synthesis
t	triplet
*t*Bu or *t*-Bu	*tertiary*-butyl
TCEP	tris(2-carboxyethyl)phosphine
TFA	trifluoroacetic acid
THF	tetrahydrofuran

Thr or T	threonine
TIPS	triisopropylsilane
TLC	thin layer chromatography
TOF	time of flight
t_R	retention time
Trn-α	thuricin α
Trn-β	thuricin β
Trp or W	tryptophan
Trt	trityl
Tyr or Y	tyrosine
Val or V	valine
UDP	uridine diphosphate
UV	ultra violet
ZCD	zeaxanthin cleavage dioxygenase

Chapter 1 : Preparation and Use of Cysteine Cyclic Ortho Esters for Solid-Phase Peptide Synthesis

1.1 Introduction

1.1.1 Fmoc-based solid phase peptide synthesis

Proteins are primary metabolites in nature and fundamental components of organisms. Proteins are involved in many important processes within cells, such as immune response, cell signaling, and cell adhesion. As well, many proteins are enzymes that catalyze essential biochemical reactions. Proteins are made of one or more peptide chains and usually adopt well-folded structures.

Peptides (Figure 1.1) are polymers of amino acids connected by amide bonds (peptide bonds) between the carboxy and amino groups of the adjacent amino acid residues.[1] Except cyclic peptides, all peptides contain a N-terminus and a C-terminus. The side chains R of amino acids play an important role in biochemical processes.[1] For example, the thiol group in the side chain of a cysteine residue can act as a nucleophile to participate in a Michael addition reaction. Two thiol groups can form a disulfide bond to facilitate peptide or protein folding.

For simplicity, a bead structure is also used to represent a peptide in this thesis (Figure 1.1). In a typical bead structure, a three-letter code is assigned to each amino acid residue. For instance, Cys represents a cysteine residue.

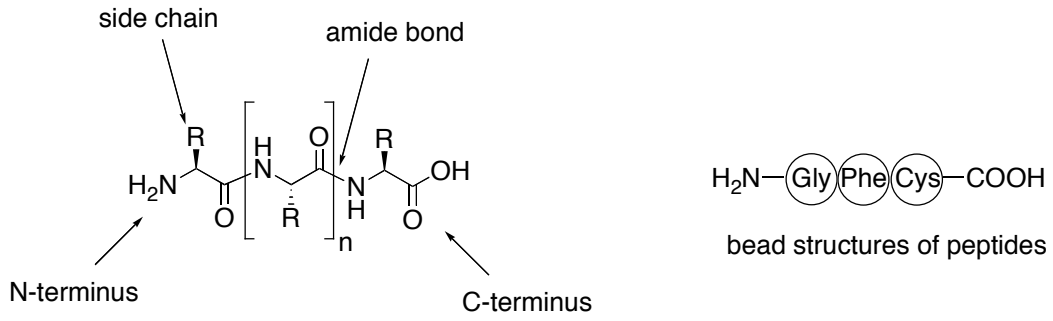

Figure 1.1 The general structure of peptides

In nature, many peptides are ribosomally synthesized and sometimes undergo post-translational modification. Alternatively, peptides can also be non-ribosomally synthesized, usually catalyzed by enzymes. Both of these two processes are quite efficient.

In addition to these biological processes, chemical synthesis of peptides is an attractive alternative because it can be used to prepare peptides that are difficult or impossible to make by biological methods. For example, unnatural amino acids, including D-amino acids, can be incorporated into peptide targets. Chemical synthesis of peptides can be performed in solution phase as well as on a solid support. In the classical solution phase synthesis, the peptide product needs to be purified and characterized at each step. This purification and characterization requires a considerable amount of labor and time, although the product can be obtained in high purity.[1] In contrast, less work is required in the purification of intermediates in the peptide synthesis using a solid support. In fact, since its introduction by Merrifield[2] in the early 1960s, solid phase peptide synthesis (SPPS) has become a frequently used tool to chemically assemble peptides and proteins. Using SPPS, peptides that are up to 50 amino acids in length can be readily

synthesized. In combination with native chemical ligation (Scheme 1.1),[3] a method developed to ligate two unprotected peptide segments, modern peptide chemists have synthesized peptides consisting of 200 amino acids.

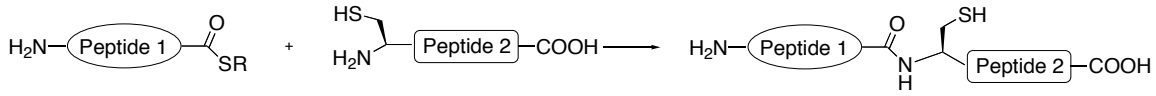

Scheme 1.1 A general representation of native chemical ligation

There are two commonly used forms of SPPS based on the N-terminal protecting group, specifically, 9-fluorenylmethyloxycarbonyl (Fmoc)- and *tert*-butoxycarbonyl (Boc)- based synthesis (Figure 1.2). In this thesis, all the peptide syntheses were performed using Fmoc-based SPPS.

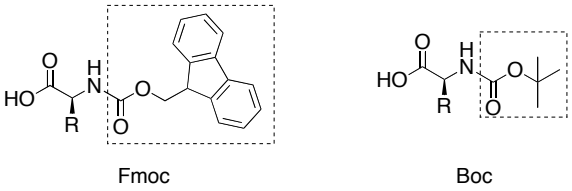

Figure 1.2 Generalized Fmoc-protected amino acid and Boc-protected amino acid

A typical Fmoc-based SPPS consists of five steps: 1) loading the C-terminal *N*-Fmoc-amino acid onto a resin, 2) deprotection of the Fmoc group, 3) coupling the following amino acid, 4) capping the unreacted amino groups and 5) cleavage of the final peptide from the resin. In the beginning of the synthesis, an Fmoc-protected amino acid is activated at the free carboxylate by forming an activated ester, such as a benzotriazole ester (Scheme 1.2). This activation step is necessary as the free amino acid is not readily coupled to an amino group of the next residue. The activated ester reacts with a resin

bearing a nucleophilic moiety to finish the loading of the C-terminal amino acid. The resin usually consists of a polymer that contains a linker with a functional group. For example, the commercially available Wang resin is made of polystyrene and bears a hydroxybenzyl linker (Scheme 1.2).

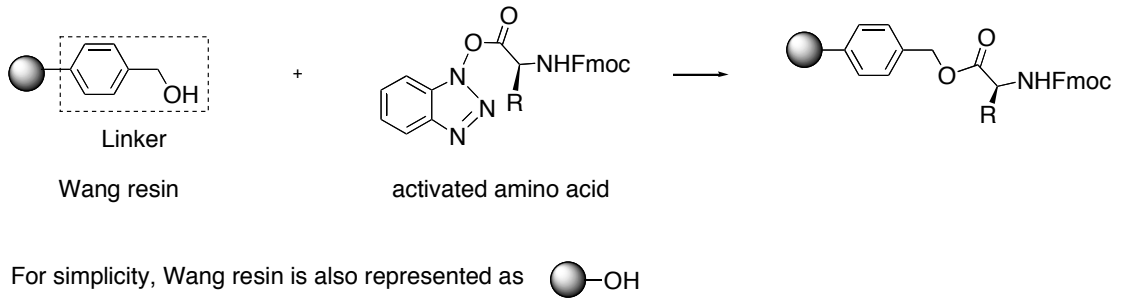

Scheme 1.2 Loading the C-terminal amino acid onto a resin

Once the amino acid is loaded onto the solid support, the Fmoc group is removed using 20% piperidine in DMF (Scheme 1.3). This cleavage results in a dibenzofulvene-piperidine adduct, which can be monitored by UV absorbance at 301 nm, to ensure deprotection is complete.

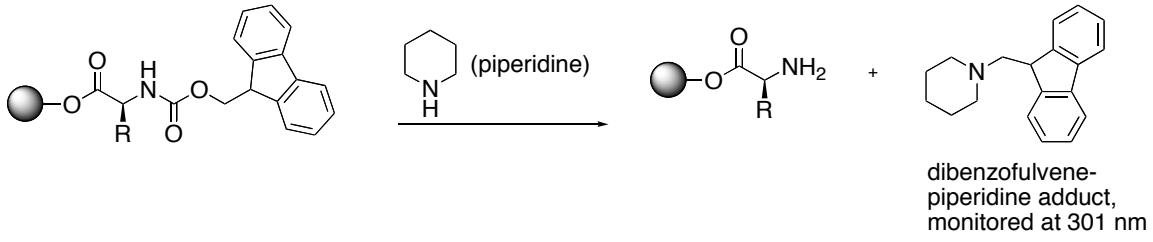

Scheme 1.3 Deprotection of the Fmoc group

The liberated amine is then ready to be coupled to another activated *N*-protected amino acid to achieve peptide chain elongation (Scheme 1.4).

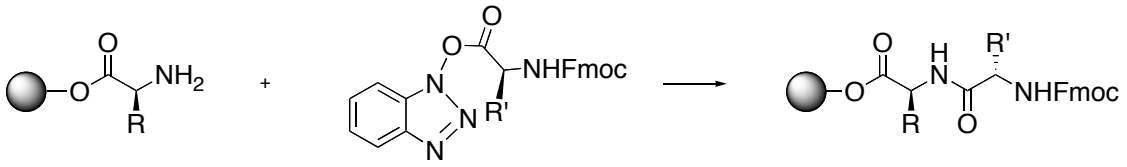

Scheme 1.4 Coupling the following amino acid to recently deprotected N-terminus

In order to minimize the formation of truncated peptides, any unreacted free amino group following the coupling step is acylated by treatment with acetic anhydride (Scheme 1.5).

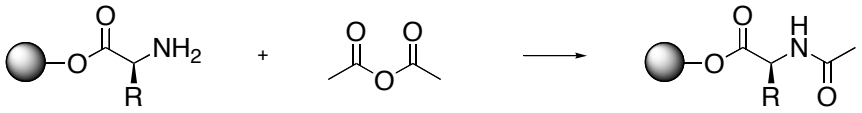

Scheme 1.5 Capping unreacted amino groups

By repeating this deprotection-elongation cycle, the peptide with the desired sequence as well as length will be obtained. At this stage, a final Fmoc deprotection followed by acidic treatment will cleave the peptide from the resin with concomitant removal of side chain protecting groups (Scheme 1.6). Protecting groups, such as trityl (Trt) or *t*-butyl (*t*-Bu) are incorporated onto certain amino acid side chains to minimize undesired side reactions during SPPS.

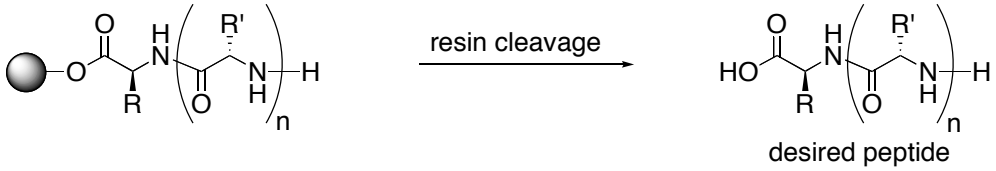

Scheme 1.6 Cleavage of the final peptide from the resin

1.1.2 Naturally occurring peptides containing C-terminal cysteine

A C-terminal cysteine residue occurs in many biologically active peptides found in natural sources. Three examples are shown in Figure 1.3. Somatostatin (**1**) is a well-known peptide hormone that contains a C-terminal cysteine and is produced by neurons.[4] It regulates the endocrine system and affects neurotransmission through interaction with G-protein coupled somatostatin receptors. Somatostatin inhibits the release of many other secondary hormones as well. Crotalphine (**2**) is a potent orally available analgesic peptide.[5, 6] Crotalphine will be discussed in detail in the second chapter of this thesis. Neopetrosiamides (**3**) are a pair of diastereomeric peptides recently discovered by the Andersen group from the marine sponge *Neopetrosia* sp..[7, 8] These peptides effectively inhibit human tumor cell invasion in cancer metastasis. All these peptides, as well as many other naturally occurring peptides, share the common feature of a cysteine residue located at the C-terminus.

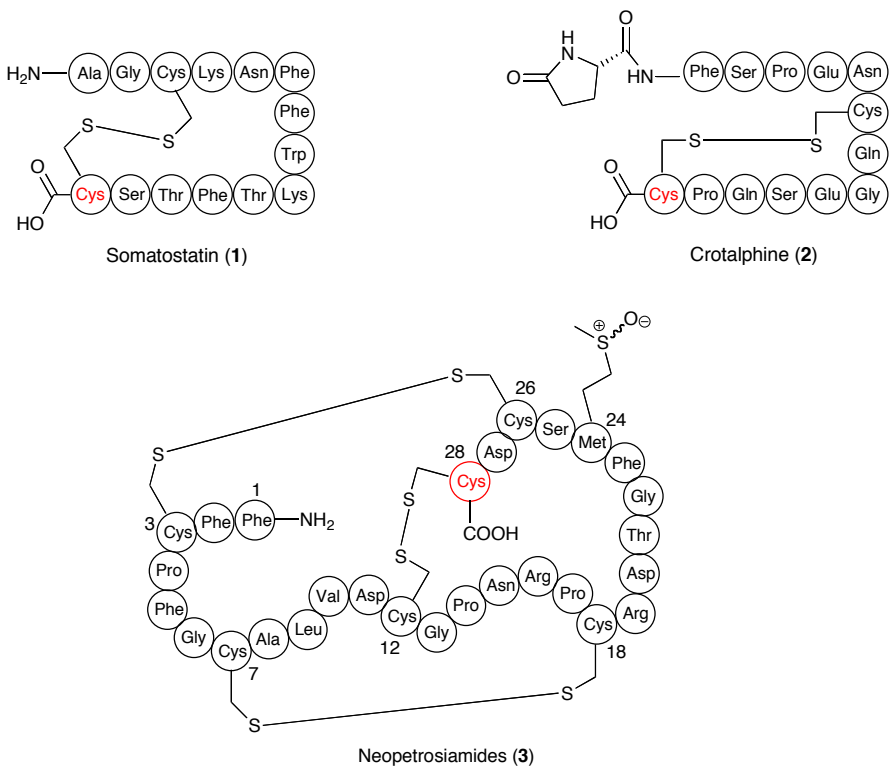

Figure 1.3 Some representative naturally occurring peptides containing a C-terminal cysteine residue

1.1.3 Fmoc-based SPPS of peptides containing C-terminal cysteine

1.1.3.1 Epimerization and piperidine adduct formation during Fmoc-based SPPS

Significant advances have been made in SPPS over the years. For example, human lysozyme, an enzyme with a length of 130 amino acids was successfully prepared by the combination of SPPS and native chemical ligation.[9] In spite of these achievements, some common problems still occur. For instance, diketopiperazine formation (Scheme 1.7) is a common side reaction found in SPPS, especially in the presence of certain residues such as proline, glycine or *N*-methylamino acids.[10, 11] Formation of this

undesired side product reduces the yield of the desired peptide. As well, the synthesis of long, hydrophobic peptides can be quite difficult.[12]

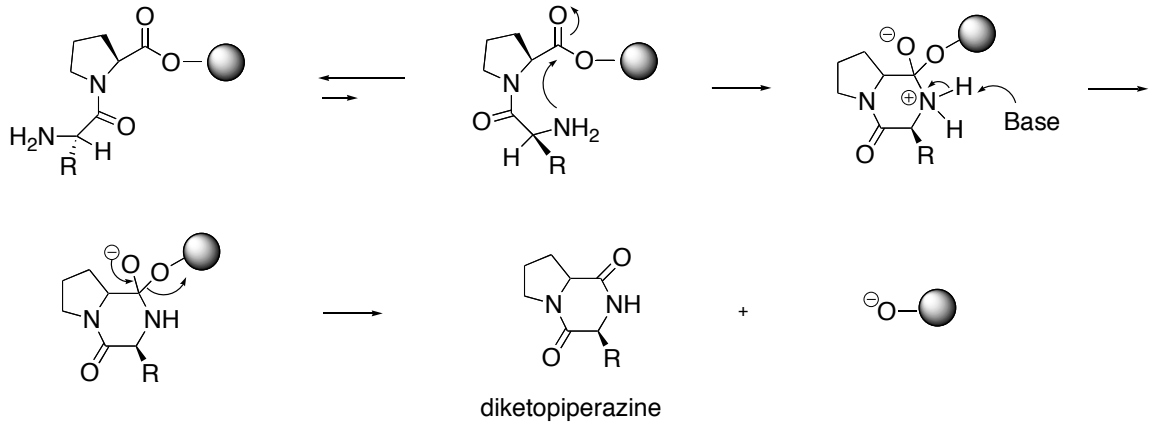

Scheme 1.7 Diketopiperazine formation during SPPS

The efficiency of SPPS is highly sequence-dependent. For example, it is known that two possible side reactions can happen in the SPPS of peptides containing a C-terminal cysteine. As the C-terminal amino acid is attached to the solid support via an ester bond, the acidity of the α-proton of the C-terminal amino acid is greater than the α-proton of internal residues with amide bonds (ΔpKa ~ 5). During Fmoc deprotection, the α-proton of the C-terminal amino acid is more likely to be removed by piperidine (Scheme 1.8). The resulting carbanion is stabilized by the sulfur atom through the interaction between the p-orbital of the α-carbon and the d-orbital of the sulfur atom of the cysteine side chain.[13] Removal of this relatively acidic α-proton leads to the formation of an epimerized product upon re-protonation. A recent report supports this sulfur stabilization hypothesis.[14] Nishiuchi and co-workers found that when 4-methoxybenzyloxymethyl (MBom) was used as the protecting group for C-terminal

cysteine, a decreased amount of epimerized peptide was formed compared to the use of trityl or acetamidomethyl (Acm) protecting groups (Figure 1.4). To rationalize this result, they proposed that the carbanion was less stabilized due to the electron-donating ability of MBom group.

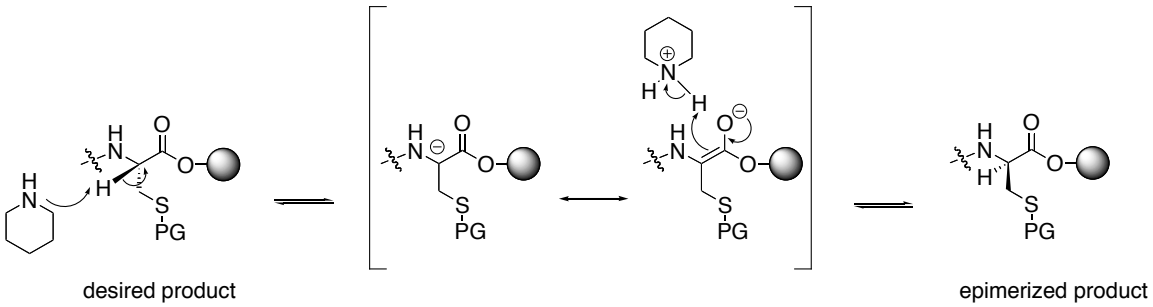

Scheme 1.8 Epimerization during the Fmoc-based SPPS of peptides containing a C-terminal cysteine residue

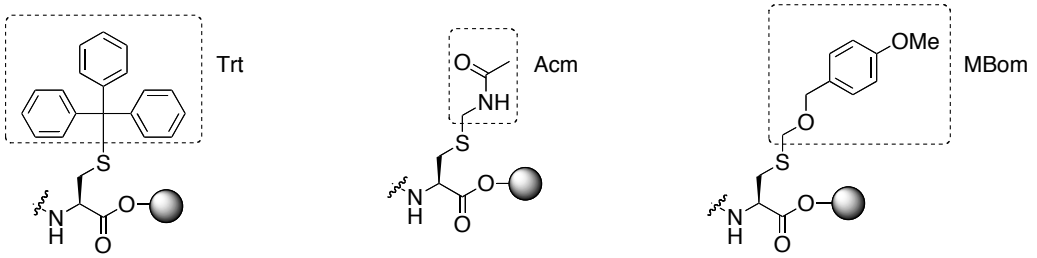

Figure 1.4 Protecting group on sulfur affects the efficiency of peptide synthesis

In addition to epimerization, peptides containing a C-terminal cysteine are also prone to the formation of piperidine adducts (Scheme 1.9).[15] After abstraction of the α-proton, thiolate eliminates to generate the dehydroalanine residue, which is attacked by piperidine to give a stable adduct. This side reaction happens due to the good leaving

ability of thiolate. A significant amount of epimerized peptides and piperidine adducts could form during the synthesis of long peptides.[15] Since these undesired side products are structurally very similar to the desired peptides, separation may become quite tedious and it may even be impossible to obtain the pure desired products.

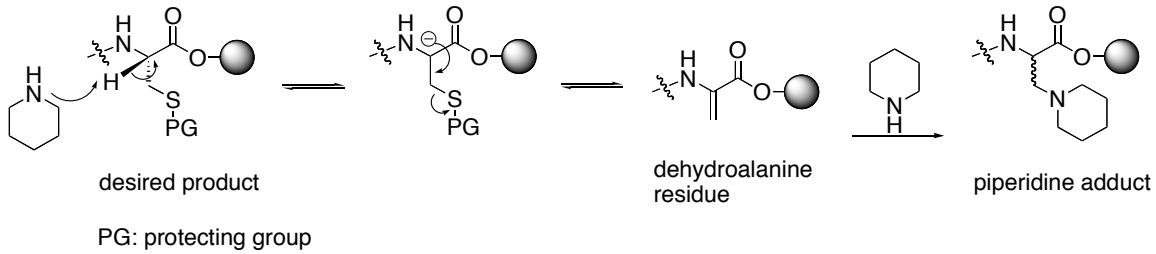

Scheme 1.9 Piperidine adduct formation during the Fmoc-based SPPS of peptides containing a C-terminal cysteine residue

1.1.3.2 Established methods to prevent or reduce undesired side reactions during Fmoc-based SPPS of peptides containing a C-terminal cysteine residue

1.1.3.2.1 Use of trityl resin

One general approach to address the above side reactions is to use a trityl resin rather than a Wang resin (Figure 1.5). The steric hindrance of trityl esters makes the α-proton less likely to be removed by base during Fmoc deprotection.[16] For intermediate length peptides, this strategy is sufficient. In the synthesis of hydrophobic peptides consisting of more than 30 residues, sometimes it is necessary to use bases stronger than piperidine to remove the Fmoc group. In this case, a significant amount of epimerized product may be formed, meaning a decreased yield of the desired product.

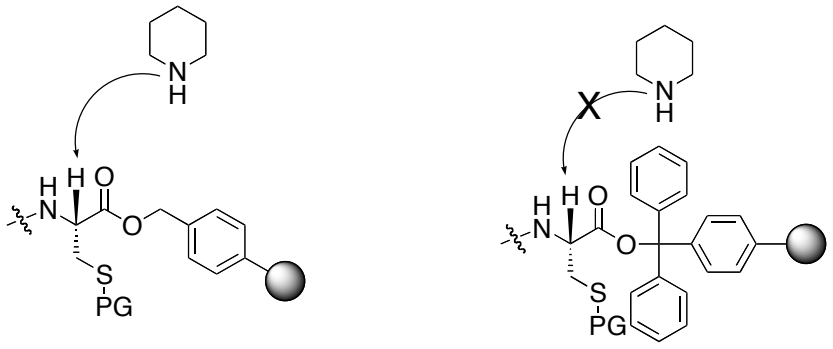

Figure 1.5 Trityl resin is superior to Wang resin for prevention of side reactions during Fmoc deprotection

1.1.3.2.2 Side-chain anchoring strategy

Barany and co-workers used an alternative method to address this problem.[17] Their C-terminal cysteine was anchored onto a solid support via the side chain thiol rather than the C-terminal carboxyl group (Figure 1.6). As the C-terminus was protected as a *tert*-butyl ester, the α-proton remained equally acidic as in the conventional method. This approach has one benefit that any by-product containing dehydroalanine, generated from thiolate elimination reaction, would be washed into waste.

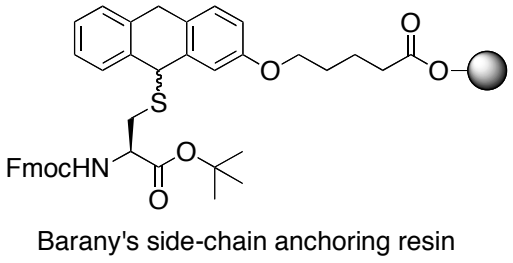

Figure 1.6 Barany's side-chain anchoring strategy

1.1.4 Serine cyclic ortho esters

In the 1990s, Lajoie and co-workers prepared a serine derivative with the carboxyl group protected as a cyclic ortho ester (Scheme 1.10).[18-20] Following a $BF_3 \bullet Et_2O$ catalyzed rearrangement (Scheme 1.11), the oxetane ester **5** was converted to the desired serine cyclic ortho ester **6**. Under Swern oxidation conditions, compound **6** was further transformed to the corresponding aldehyde **7**, which fully retained the enantiomeric purity as determined by NMR spectroscopy using the chiral shift reagent $Eu(hfc)_3$. Since the carboxyl is protected as a cyclic ortho ester, the acidity of the α-proton is decreased dramatically compared to the parent compound. While the serine aldehyde is prone to epimerization, its equivalent, compound **7**, is more resistant to epimerization due to the lower acidity of the α-proton. This unique property enables it to undergo many useful transformations while leaving the stereochemistry of the α-carbon intact. Three commonly used reagents, Grignard (RMgX), Reformatsky ($BrZnCH_2CO_2tBu$) and Wittig reagents ($Ph_3P{=}CHCO_2CH_3$) were all shown to react with compound **7** in a stereoselective fashion. Interestingly, the Fmoc group was stable under these reaction conditions. The cyclic ortho ester functionality can be converted back to a carboxyl group under mild conditions. This generated free amino acid **11** retained an excellent enantiomeric purity using HPLC analysis.[18]

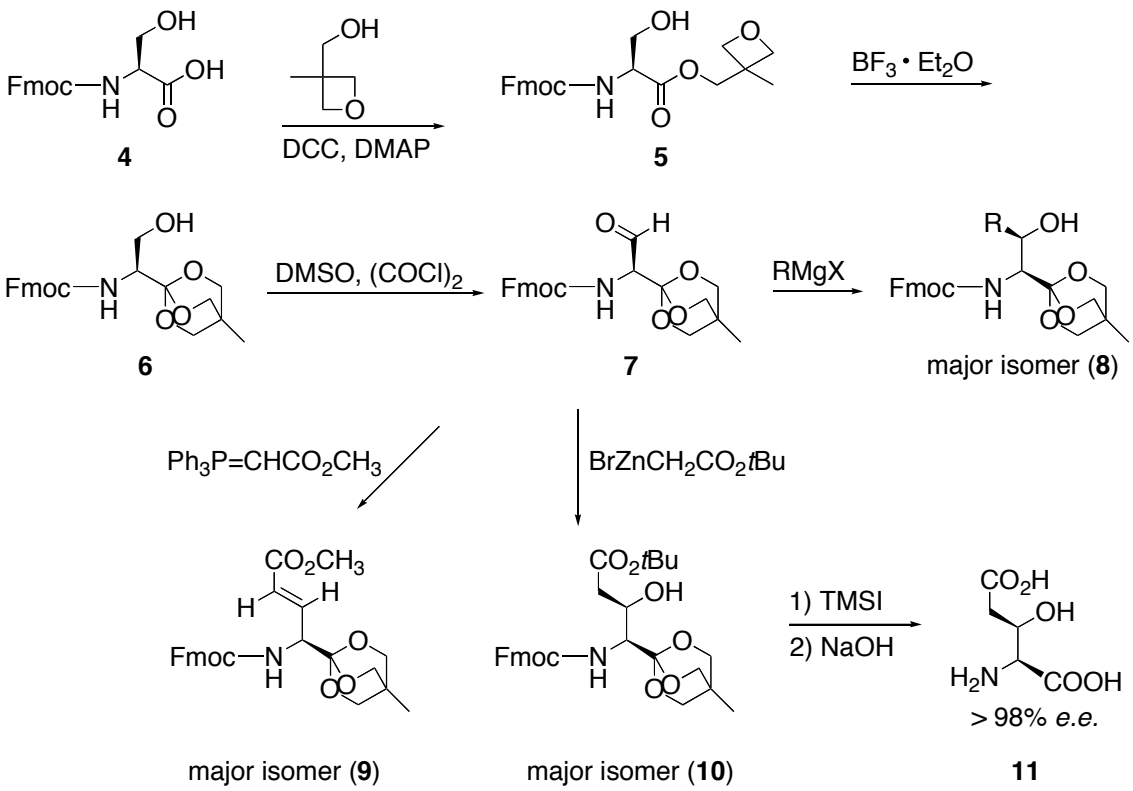

Scheme 1.10 Preparation and application of serine cyclic ortho esters[18]

The use of cyclic ortho esters to protect the carboxyl of amino acids has proven to be very useful in organic synthesis. This strategy has been widely used in the synthesis of unnatural amino acids and peptidomimetics.[21-24] Herdeis and co-workers prepared a pyroglutamic acid derivative (**12**) with the carboxyl protected as a cyclic ortho ester (Scheme 1.12).[21] Compound **12** was successfully converted into 3-substituted pyroglutamic acid **13** and glutamic acid derivative **14**. The cyclic ortho ester functionality has two effects in this synthesis. In addition to decreasing the acidity of the α-proton, it also serves as a bulky group to direct the stereoselective introduction of the substituent at the 3-position.

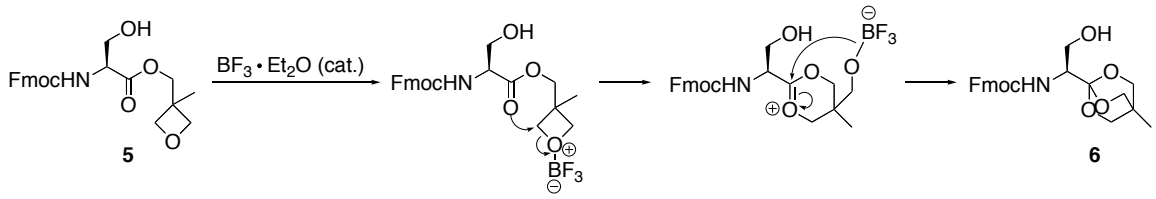

Scheme 1.11 Proposed mechanism for the formation of the cyclic ortho ester **6**[18]

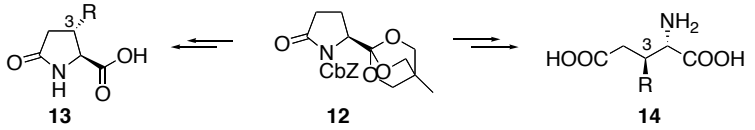

Scheme 1.12 Stereoselective synthesis of 3-substituted (*S*)-pyroglutamic acid **13** and glutamic acid **14** via a cyclic ortho ester derivative (**12**)[21]

Amino acids containing cyclic ortho esters are also useful intermediates in the synthesis of natural products and natural product-like molecules.[25-27] Nenajdenko and co-workers reported an interesting study of Ugi multi-component reactions using the chiral cyclic ortho ester of an α-isocyano containing acid **16** as a substrate (Scheme 1.13).[28, 29] The authors found that the corresponding product (**18**) retained its configuration due to the lower acidity of the α-proton in **16**. In contrast, the related α-isocyano ester **15** was epimerized during the reaction.

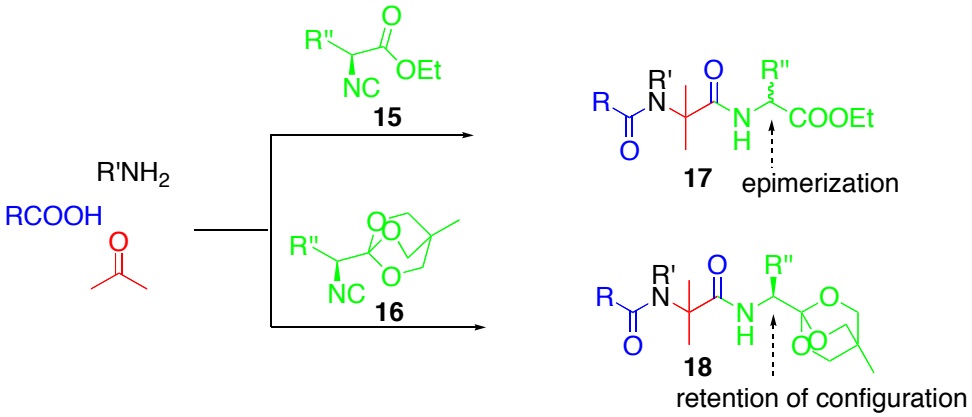

Scheme 1.13 Comparison of Ugi multi-component reaction utilizing α-isocyano ester **15** or its cyclic ortho ester **16**[28, 29]

As shown above, since the cyclic ortho ester functionality can effectively prevent epimerization, the use of this moiety to protect the carboxyl of amino acids has found wide application in the synthesis of unnatural amino acids and peptidomimetics. However, prior to our work no cysteine-derived ortho ester was reported.

1.2 Project objectives: Fmoc-based SPPS of peptides containing C-terminal cysteine residues without epimerization or piperidine adduct formation by the protection of the carboxyl group as a cyclic ortho ester

Many natural biologically active peptides contain a cysteine residue located at the C-terminus. The goal of this project is to develop a general and efficient methodology for Fmoc-based SPPS of peptides containing C-terminal cysteines without undesired epimerization or piperidine adduct formation. As discussed previously, the acidic nature of the terminal α-proton is the fundamental reason causing these side reactions. We

hypothesized that by the protection of the carboxyl group as a cyclic ortho ester, the α-proton of compound **20** would be much less acidic (Scheme 1.14). After incorporation onto a solid support using a side-chain anchoring strategy, the standard Fmoc-based SPPS ideally would only produce the desired peptides without significant amounts of side products. To examine the efficiency of the developed method, two diastereomeric tripeptides H-Gly-Phe-L-Cys-OH (**24**) and H-Gly-Phe-D-Cys-OH (**25**) will be used as model compounds since they are known to be separable using RP-HPLC.[17] This methodology will then be applied to the synthesis of the natural peptide crotalphine (**2**).

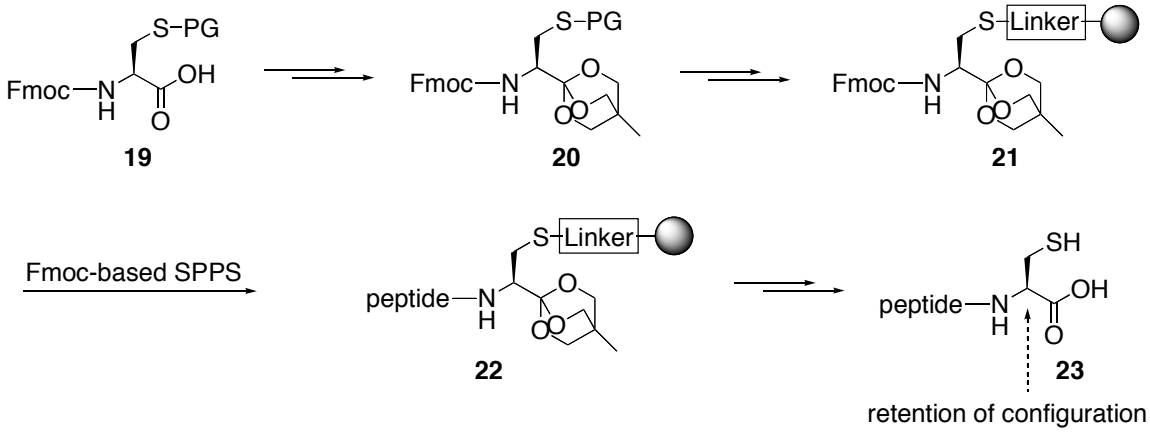

Scheme 1.14 Proposed synthetic route towards formation of peptides with retention of configuration at the α-carbon of the C-terminal cysteine residue

1.3 Results and discussion

1.3.1 Synthesis and chiral HPLC analyses of cysteine cyclic ortho esters

In order to study epimerization of peptides containing C-terminal cysteine residues using RP-HPLC, it was envisioned that both L-cysteine and D-cysteine cyclic ortho esters would be required (Scheme 1.16). The Fmoc group is base labile and the cyclic ortho ester functionality is acid labile. Therefore, the *S*-*t*-butyl group was selected as the cysteine thiol protecting group, as it could be removed under neutral reducing conditions. The synthesis started from reaction between the commercially available Fmoc-Cys(S-*t*Bu)-OH and 3-methyl-3-(hydroxymethyl)-oxetane (**28**) under standard DCC/DMAP coupling conditions. The desired oxetane esters **29** and **30** were obtained in moderate to good yields ranging from 55-73%. With these precursors in hand, the next step was to form the key cysteine cyclic ortho esters. A former graduate student in the Vederas group, Dr. Darren Derksen, initiated this project and had no success in the synthesis of these cysteine cyclic ortho ester compounds. Following the conditions reported by Lajoie and co-workers in their synthesis of serine cyclic ortho ester,[18] initial attempts to prepare compound **31** by using 10 mol % $BF_3 \bullet Et_2O$ as a catalyst were made. A variety of other Lewis acids, including $TiCl_4$, $MgBr_2$, $SnCl_4$, $La(OTf)_3$, $Gd(OTf)_3$ and $Lu(OTf)_3$ were also attempted at 10 mol % catalyst loading.[30] Unfortunately, no product was observed in any of these conditions. The lack of product formation was possibly due to the preferential coordination of the Lewis acids to the sulfur atom instead of the oxetane oxygen, preventing the desired rearrangement (Scheme 1.15). It was proposed that increasing the amount of the Lewis acid could solve this problem. Fortunately, when 2.5 equivalents of $BF_3 \bullet Et_2O$ were used, the desired cysteine cyclic ortho esters **31** and **32**

were indeed obtained in 67% and 70% yields, respectively (Scheme 1.16).[31] The necessity of using stoichiometric amounts of Lewis acid for sulfur-containing substrates is not uncommon. For instance, in a previous synthesis conducted in our group, four equivalents of BF_3•Et_2O were used in the synthesis of lanthionine **35**, compared to 0.1 equivalent used in the synthesis of the corresponding oxygen analog **38** (Scheme 1.17).[32, 33]

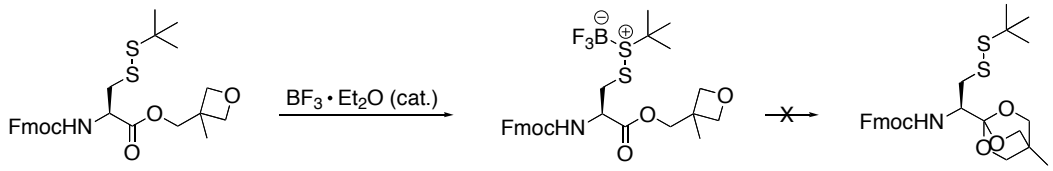

Scheme 1.15 Proposed mechanism for lack of formation of the cysteine cyclic ortho ester using a catalytic amount of Lewis acid

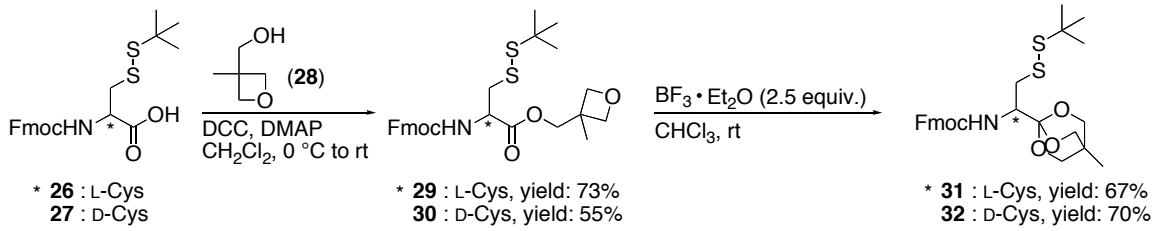

Scheme 1.16 Synthesis of cysteine cyclic ortho esters **31** and **32**

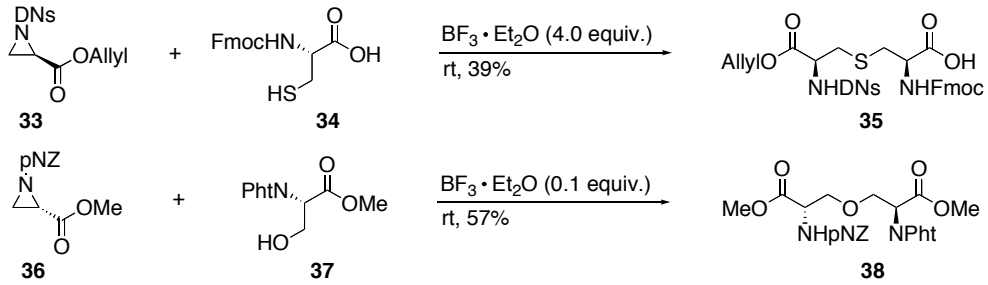

Scheme 1.17 Synthesis of orthogonally protected lanthionine **35** and its oxygen analog **38** using BF_3•Et_2O[32, 33]

Before incorporation onto a solid support, the evaluation of the enantiomeric purity of cysteine cyclic ortho esters **31** and **32** was performed using chiral HPLC analysis (Figure 1.7). Integration of the peaks in HPLC revealed that compound **31** contained 99.4% major enantiomer and 0.6% minor enantiomer. Similarly, compound **32** contained 99.6% major enantiomer and 0.4% minor enantiomer.

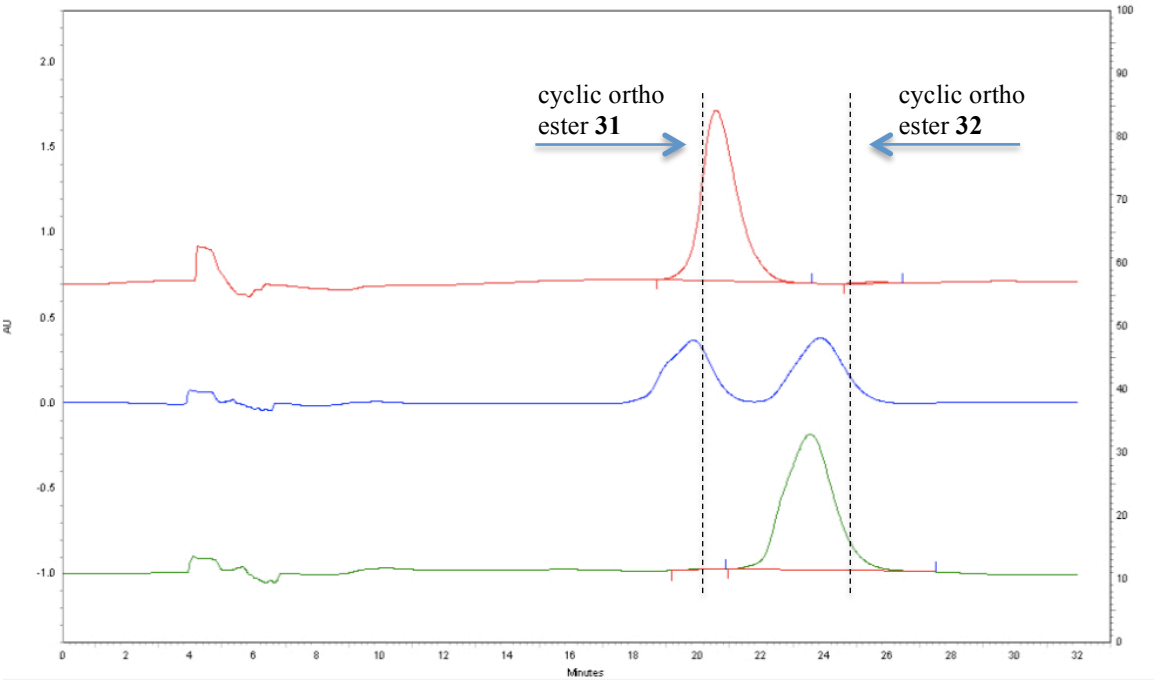

HPLC trace for cyclic ortho ester **31**

HPLC trace for co-injection of cyclic ortho esters **31** and **32**

HPLC trace for cyclic ortho ester **32**

Figure 1.7 Chiral HPLC analyses of cyclic ortho esters **31** and **32**

In the peptide community, there is increasing interest in using disulfide-based linkers in peptide synthesis.[34-37] For example, Woggon and co-workers developed a disulfide linker for single-bead analysis of peptide libraries.[35] Recently, a cysteine-based

disulfide linker was also reported for Fmoc-based SPPS of cyclic peptides and peptide libraries.[34] Encouraged by these achievements, we also aimed to incorporate our cysteine cyclic ortho esters onto a solid support via a disulfide linker. The *S*-*t*-butyl groups of compounds **31** and **32** were removed in the presence of tributylphosphine (Scheme 1.18). The newly formed free thiols were reacted with 2,2'-pyridine disulfide (**39**) to afford the desired asymmetric disulfide compounds **40** and **41** in moderate yields.

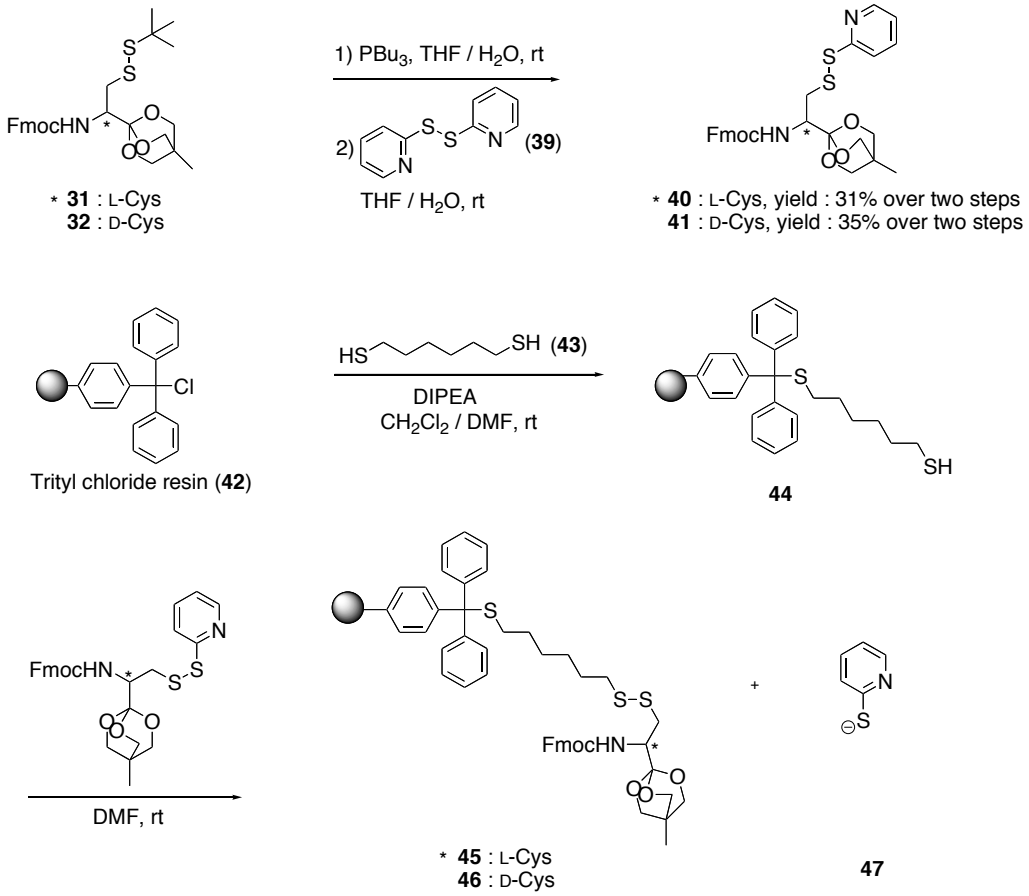

Scheme 1.18 Incorporation of cysteine cyclic ortho esters onto a solid support via a disulfide linkage

Commercial trityl chloride resin (**42**) was then reacted with 1,6-hexanedithiol (**43**) to produce resin **44** bearing a free thiol. A disulfide exchange reaction occurred between

the cyclic ortho esters **40** and **41** and the synthetic thiol resin **44** to furnish the resin bound cyclic ortho esters **45** and **46**. This reaction proceeds with the loss of pyridine thiolate **47**, which is a good leaving group. The formation of pyridine thiolate **47** drives the reaction forward.

1.3.2 Synthesis and evaluation of epimerization of model tripeptides

Two diastereomeric tripeptides H-Gly-Phe-L-Cys-OH (**24**) and H-Gly-Phe-D-Cys-OH (**25**) were used as models to examine the efficiency of the modified resins in minimizing epimerization during SPPS. Starting from pre-loaded resins **45** and **46**, Fmoc-based SPPS generated resin bound tripeptides **48** and **49** (Scheme 1.19). Then tripeptide esters **50** and **51** were produced by Fmoc deprotection, followed by resin cleavage. Finally, hydrolysis followed by disulfide reduction with tris(2-carboxyethyl)phosphine (TCEP) furnished the desired model tripeptides **24** and **25**.

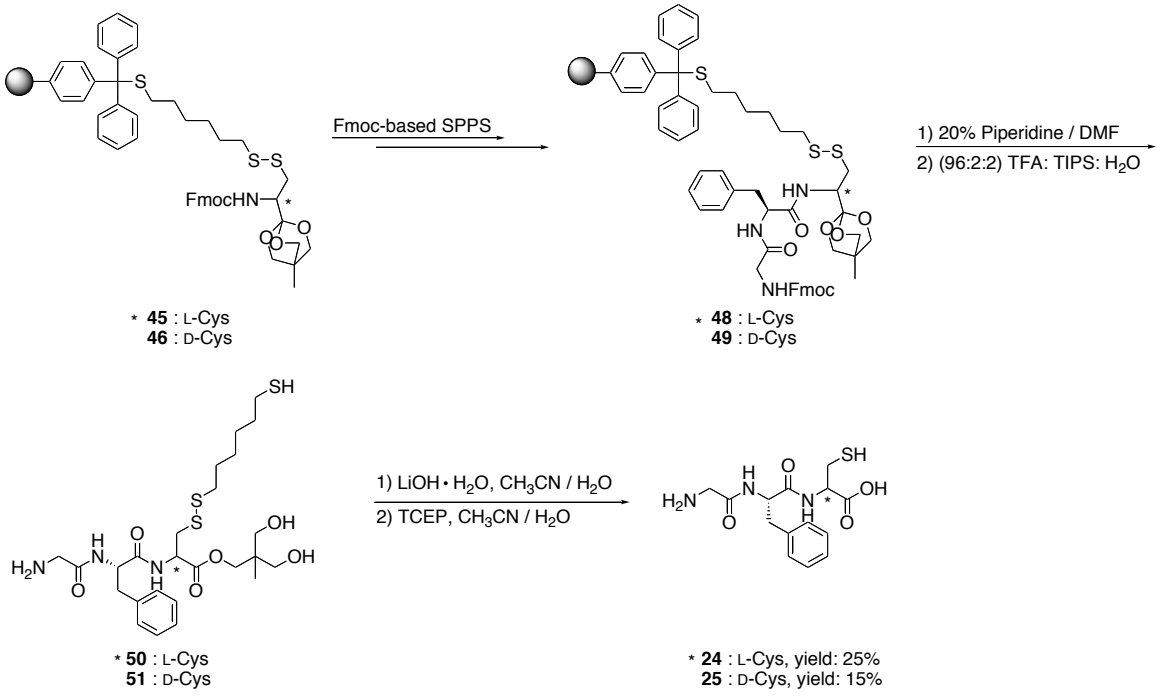

Scheme 1.19 Synthesis of model tripeptides **24** and **25**

The amount of epimerization was first evaluated at the tripeptide ester stage. The crude tripeptide ester, synthesized from L-cysteine cyclic ortho ester resin **45**, contained a 98.3 : 1.7 ratio of tripeptide **50** to **51** according to integration of the peaks in HPLC (Figure 1.8). On the other hand, the crude tripeptide ester synthesized from D-cysteine cyclic ortho ester resin **46**, contained a 3.5 : 96.5 ratio of tripeptide **50** to **51**. Therefore, both SPPS syntheses generated tripeptide esters with excellent diastereomeric purity. The small amount of epimerized peptides may have been formed during the resin cleavage.

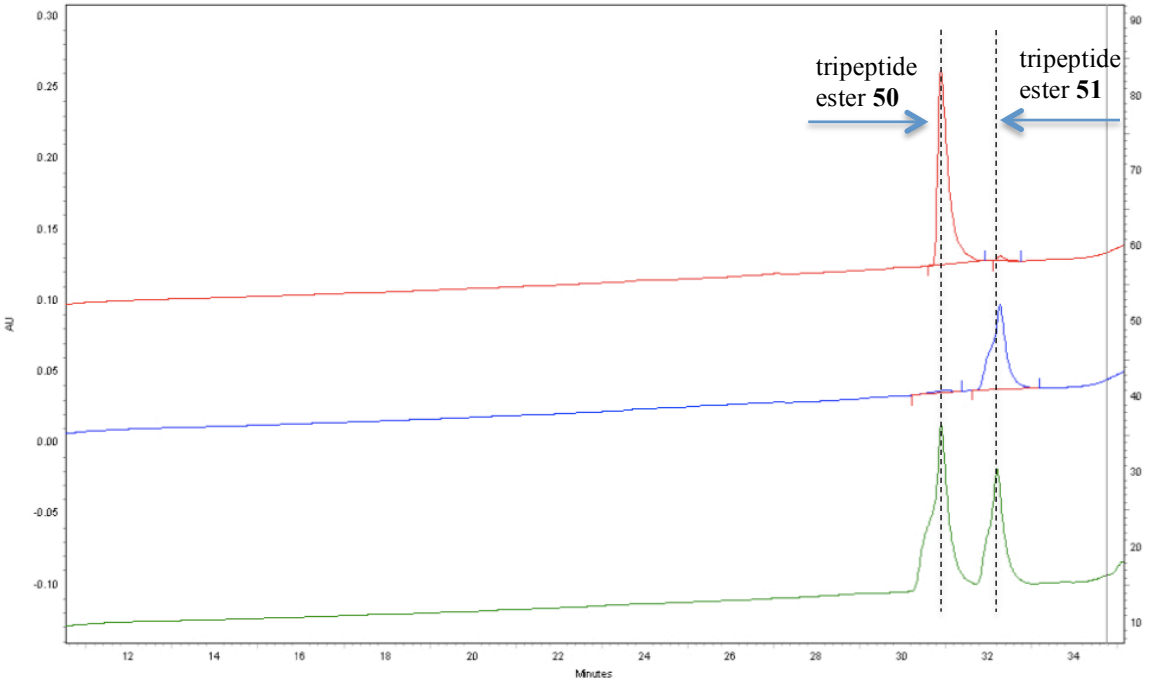

Tripeptide ester crude mixture from cyclic ortho ester resin **45**

Tripeptide ester crude mixture from cyclic ortho ester resin **46**

Co-injection of pure tripeptide ester **50** and pure tripeptide ester **51**

Figure 1.8 Evaluation of epimerization of tripeptide esters

In order to study whether the last two steps, and particularly ester hydrolysis, would cause further epimerization of the C-terminal cysteine residue, crude tripeptide esters were deprotected. Specifically they were hydrolyzed to remove the oxetane ester, and the disulfide was reduced. After these reactions, the diastereomeric purity of the products was again examined using RP-HPLC (Figure 1.9). The crude tripeptide acid, originally synthesized from cyclic ortho ester resin **45**, contained a 96.7 : 3.3 ratio of tripeptide **24** (desired) to **25** (epimerized). Correspondingly, the crude tripeptide acid synthesized from D-cysteine cyclic ortho ester resin **46** contained a 2.9 : 97.1 ratio of tripeptide **24** (epimerized) to **25** (desired). Based on the HPLC analysis of the corresponding tripeptide ester **50**/**51** and tripeptide acid **24**/**25**, no significant epimerization occurred during the hydrolysis or reduction steps. After HPLC purification, tripeptide acid **24** and **25** were obtained in 25% and 15% yields for 10 steps (including all deprotections and couplings) based on the initial loading of trityl chloride resin.

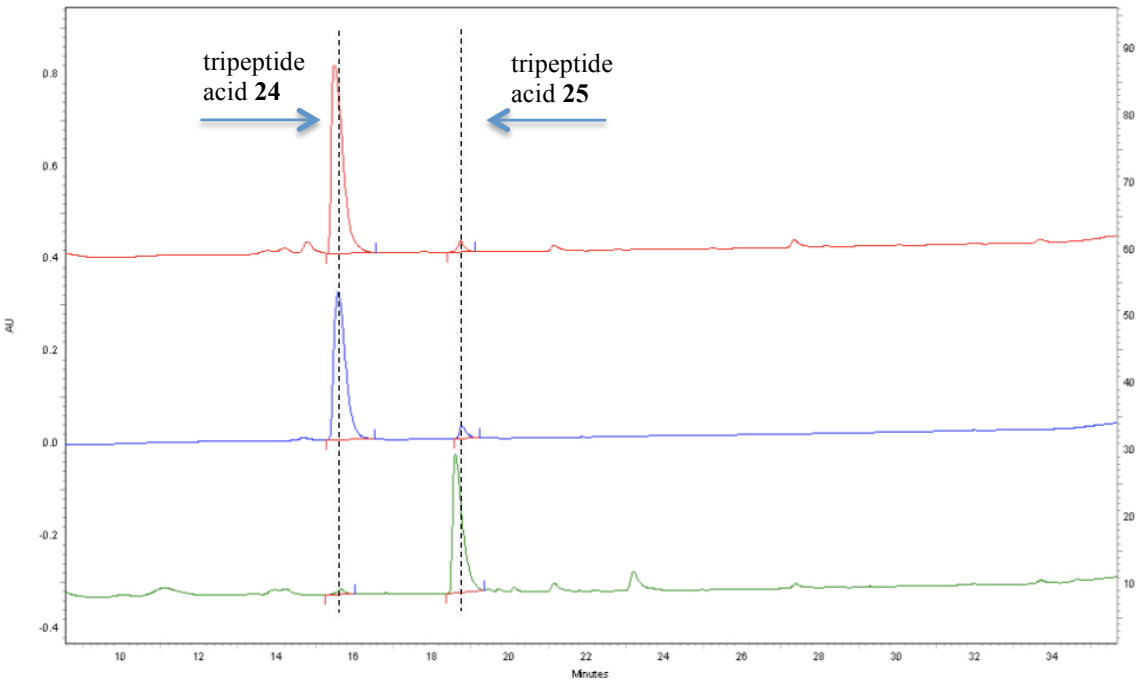

Tripeptide acid crude mixture from cyclic ortho ester resin **45**

Tripeptide acid crude mixture from H-L-Cys(Trt)-2-chloro trityl resin

Tripeptide acid crude mixture from cyclic ortho ester resin **46**

Figure 1.9 Comparison of epimerization of tripeptide acids via commercial 2-chloro trityl resin versus cyclic ortho ester method

In order to compare the efficiency of our synthetic cyclic ortho ester resins to a commercial 2-chloro-trityl resin, the same tripeptide acid **24** was also prepared using commercial H-L-Cys(Trt)-2-chloro-trityl resin (Scheme 1.20). The cysteine residue was pre-loaded onto the resin via an ester bond. Fmoc-based SPPS, followed by the resin cleavage produced the crude tripeptide. HPLC analyses indicated that the crude tripeptide acid, synthesized from this commercial resin, contained a 95.2 : 4.8 ratio of tripeptide **24** to **25** (Figure 1.9). Therefore, based on these results, our cyclic ortho ester

resins showed similar efficiency compared to a commercial 2-chloro-trityl resin. Both of our cyclic ortho ester resins and commercial 2-chloro-trityl resin were superior to commercial Wang resin which generated 8% epimerized tripeptide.[30] As epimerization and piperidine adduct formation could occur at each stage of chain elongation, we envisioned that our modified resins may become superior to commercial 2-chloro-trityl resin in the synthesis of longer peptides.

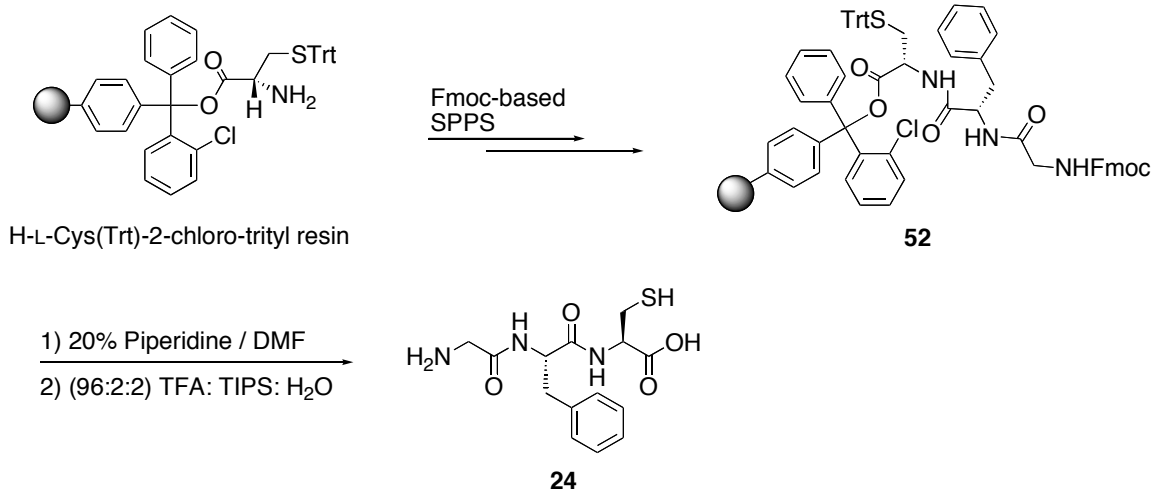

Scheme 1.20 Synthesis of tripeptide **24** using commercial H-L-Cys(Trt)-2-chloro-trityl resin

To test this hypothesis, we decided to make a medium sized peptide, crotalphine (**2**) (Figure 1.3). Crotalphine consists of 14 amino acids, including a C-terminal cysteine residue and N-terminal pyroglutamic acid residue. Crotalphine contains a disulfide bond.

1.3.3 Synthesis and evaluation of epimerization of natural crotalphine (2) and its D-Cys1 diastereomer (53)

Both natural crotalphine (**2**) and its D-Cys1 diastereomer (**53**) were synthesized (Scheme 1.21). In this thesis, the D-Cys1 nomenclature means that a D-cysteine is located at the C-terminus rather than N-terminus. Starting from resin bound cyclic ortho esters **45** and **46**, Fmoc-based SPPS produced resin bound peptides **54** and **55**. Peptide esters **56** and **57** were generated by Fmoc deprotection, followed by acidic cleavage from the resin. Basic hydrolysis, followed by disulfide reduction with TCEP furnished the peptides **58** and **59** containing free thiols. The native disulfide bond was installed under oxidative conditions in ammonium bicarbonate buffer. The desired natural crotalphine (**2**) and its D-Cys1 diastereomer (**53**) were obtained in 5% and 2% yields, respectively, for 33 steps (including all deprotections and couplings), based on the initial loading of trityl chloride resin.

Similar to the tripeptide case, the evaluation of epimerization was first done at the peptide ester stage. The crude peptide ester, synthesized from cyclic ortho ester resin **45**, contained a 98.0 : 2.0 ratio of peptide **56** to **57** based on integration of the peaks in HPLC (Figure 1.10). Correspondingly, the crude peptide ester synthesized from D-cysteine cyclic ortho ester resin **46**, contained a 0.8 : 99.2 ratio of peptide **56** to **57**. Both of these syntheses therefore produced the desired peptide esters in excellent diastereomeric purities. In principle, the small amount of epimerized peptides observed may have been formed during cleavage.

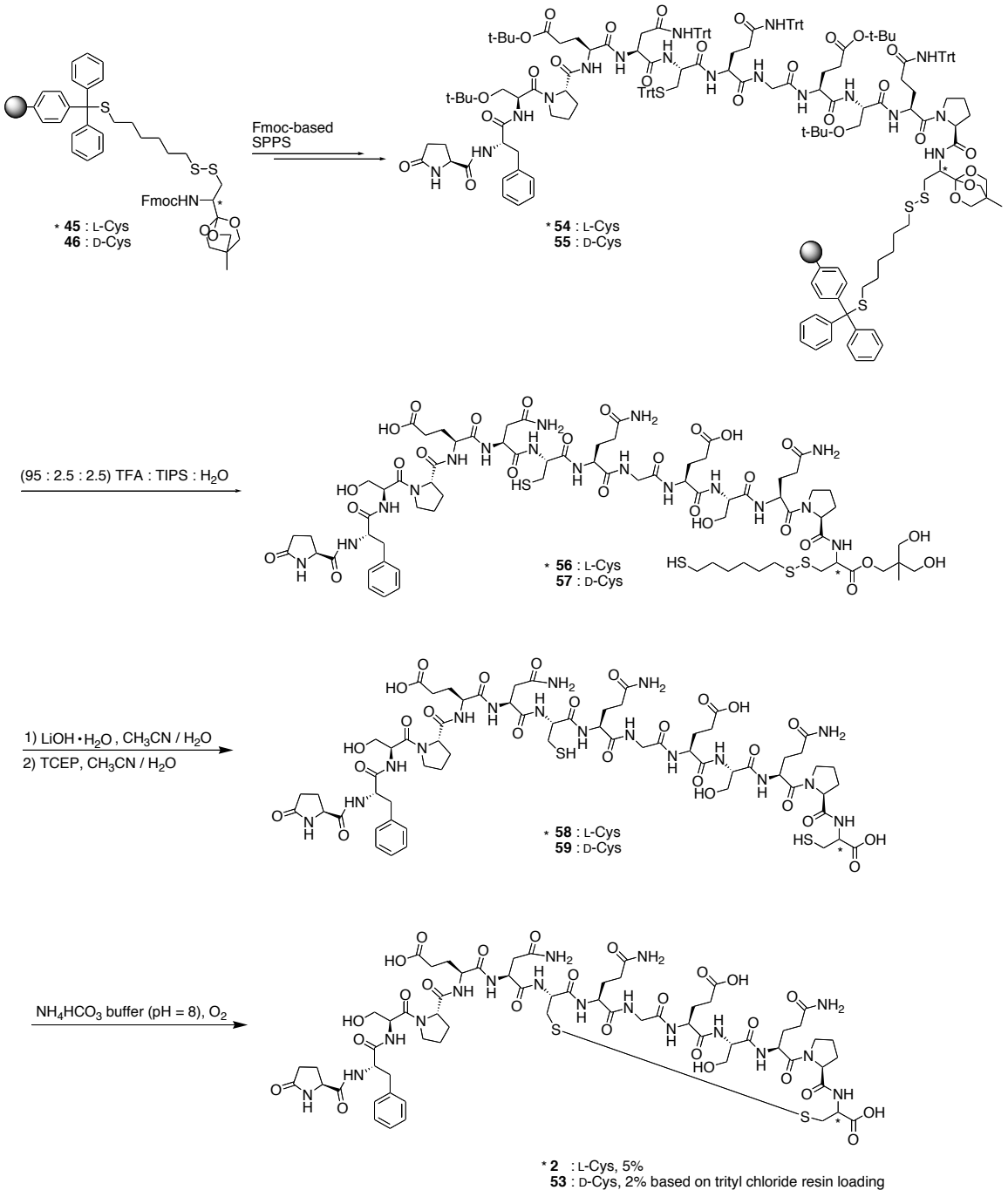

Scheme 1.21 Synthesis of the natural L-Cys crotalphine (**2**) and its D-Cys1 diastereomer (**53**)

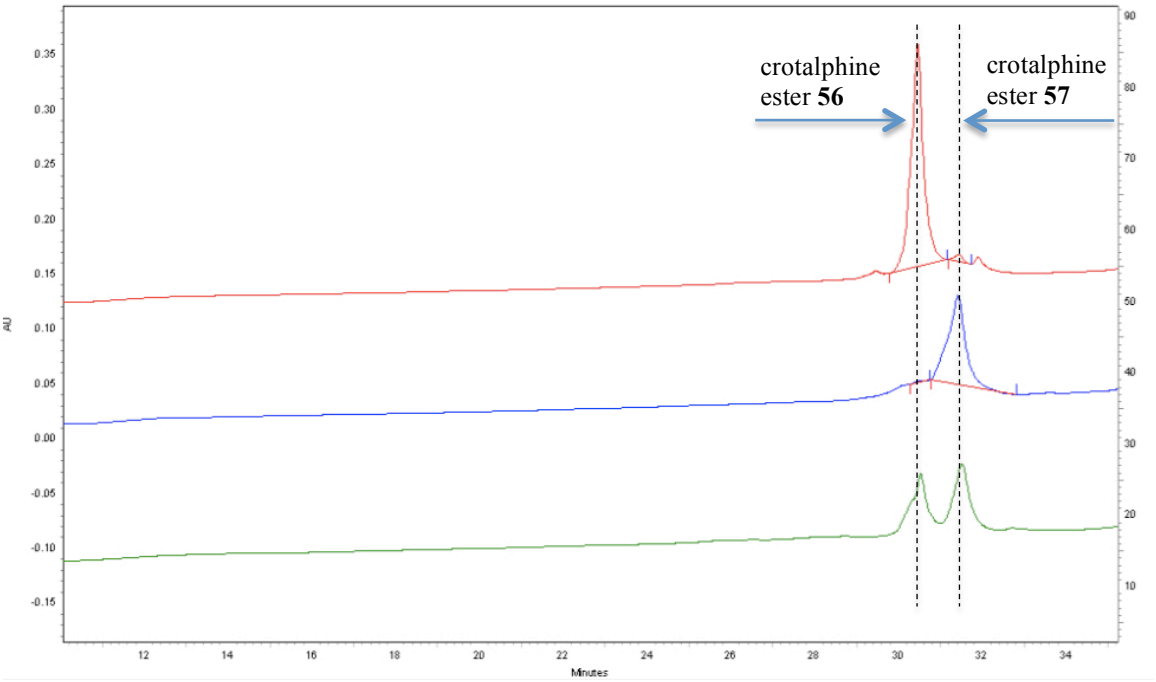

Figure 1.10 Epimerization study of crotalphine esters

The epimerization study was continued for peptide acids **58** and **59**. As mentioned before, in order to study whether the next two steps, and particularly ester hydrolysis, would cause further epimerization of the C-terminal cysteine residue, crude peptide esters were deprotected. Specifically they were hydrolyzed to remove the oxetane ester, and the disulfide was reduced. Following these reactions, the diastereomeric purity of the products was again examined using RP-HPLC (Figure 1.11). The crude peptide acid synthesized from D-cysteine cyclic ortho ester resin **46**, contained a 4.4 : 95.6 ratio of peptide **58** (epimerized) to **59** (desired) based on integration of the peaks in HPLC.

Notably, in the HPLC trace of the crude peptide acid synthesized from L-cysteine cyclic ortho ester resin **45**, a shoulder peak contained both the epimerized peptide **59** and other un-identified impurities, based on matrix assisted laser desorption ionization-mass spectrometry (MALDI-MS) (Figure 1.11). The same impurities were also observed in the peptide synthesized using a commercial H-L-Cys(Trt)-2-chloro trityl resin, when these syntheses were done by former graduate student, Dr. Darren Derksen.[30] These results imply that the impurities are likely sequence-dependent rather than resin-dependent. Due to this co-elution, it was difficult to evaluate the efficiency of L-cysteine cyclic ortho ester resin **45** or the commercial resin. Nonetheless, it was safe to say that no significant epimerization happened in the hydrolysis or reduction steps based on the result obtained from the D-cysteine cyclic ortho ester approach.

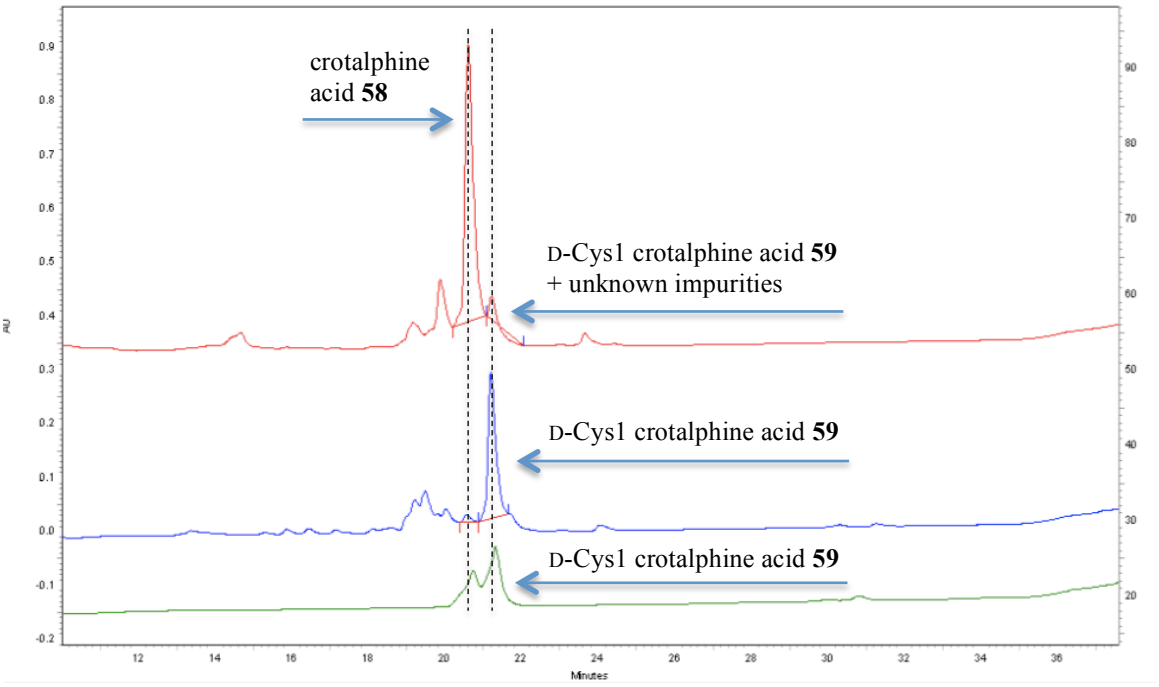

Figure 1.11 Epimerization study of crotalphine acids (free thiols)

Finally, after formation of the native disulfide bond using pure peptides **58** and **59** as substrates, the desired natural crotalphine (**2**) and its D-Cys1 diastereomer (**53**) were purified by RP-HPLC (Figure 1.12). The retention times of these two peptides were so similar that it was impossible to distinguish them. Since diastereomerically pure starting materials **58** and **59** were used, and it was believed that epimerization was unlikely to happen under this reaction condition, the purified crotalphine (**2**) and its D-Cys1 diastereomer (**53**) were considered as diastereomerically pure and epimerization studies were not performed at this stage.

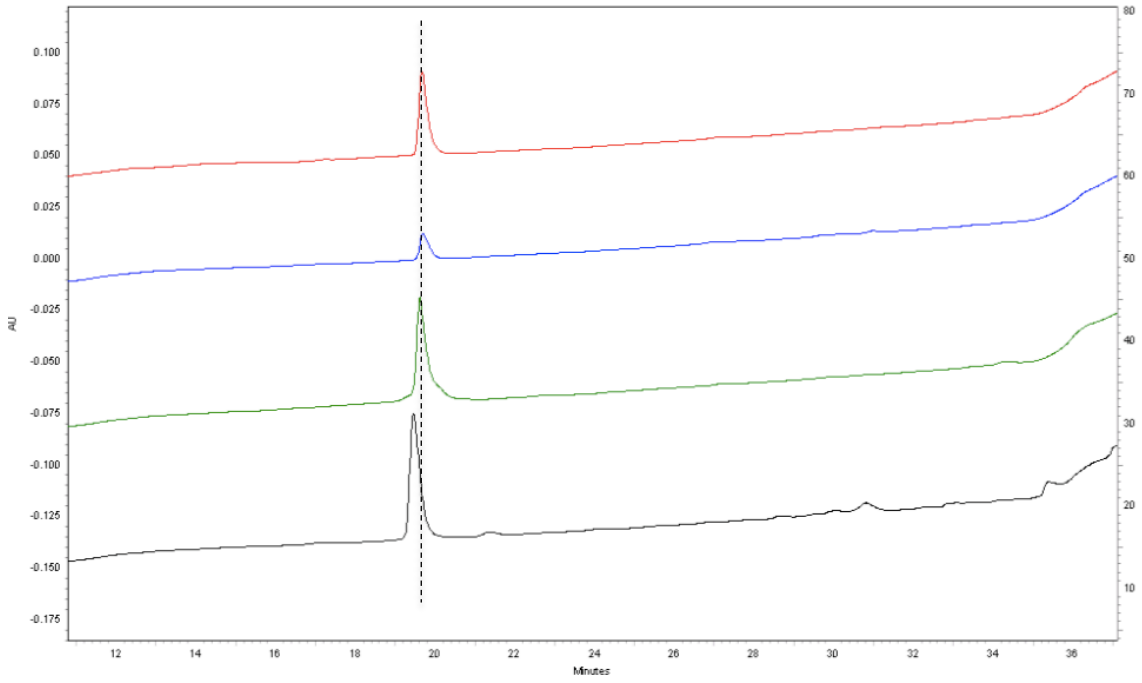

Crotalphine (**2**), generated from disulfide bond formation of pure **58**

Crotalphine diastereomer (**53**), generated from disulfide bond formation of pure **59**

Crotalphine (**2**), synthesized using commercial H-L-Cys(Trt)-2-chloro trityl resin

Co-injection of pure crotalphine (**2**) synthesized from cyclic ortho ester resin **45** and pure crotalphine (**2**) from commercial H-L-Cys(Trt)-2-chloro trityl resin

Figure 1.12 HPLC traces of crotalphine and its D-Cys1 diastereomer

The identity of our synthetic crotalphine (**2**) was examined by comparison to a peptide synthesized from commercial H-L-Cys(Trt)-2-chloro trityl resin. A single peak observed upon co-injection onto a RP-HPLC column indicated they were likely the same peptide (Figure 1.12). As it was already confirmed that the crotalphine synthesized from

H-L-Cys(Trt)-2-chloro trityl resin had the same HPLC trace and mass spectral properties as natural crotalphine,[30] it was logical to conclude that by using the cyclic ortho ester containing resin **45**, the natural product crotalphine was successfully synthesized.

The sequence of synthetic crotalphine (**2**) was further confirmed by LC-MS/MS analysis. Due to the absence of basic residues and the blocked N-terminus (Figure 1.3), it was difficult to obtain direct MS/MS data of crotalphine with the disulfide bridge. Alternatively, alkylation of peptide **58** with free thiols using iodoacetamide generated linear peptide **60** which was subjected to LC-MS/MS sequencing (Scheme 1.22). Fortunately, most of the peptide fragments, with charge retained at N-terminus (b-ions) and at C-terminus (y-ions) in the sequence were observed and the obtained data (Figure 1.13) matched extremely well with the reported MS/MS data,[5] supporting the synthesis of the peptide crotalphine (**2**).

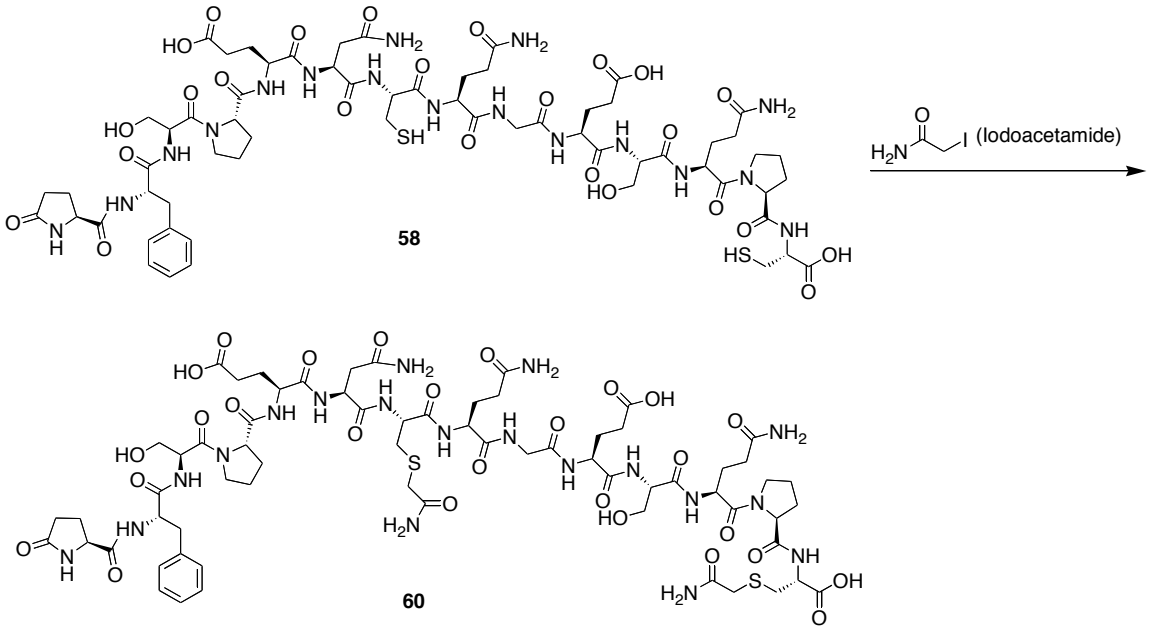

Scheme 1.22 Synthesis of the alkylated crotalphine derivative (**60**)

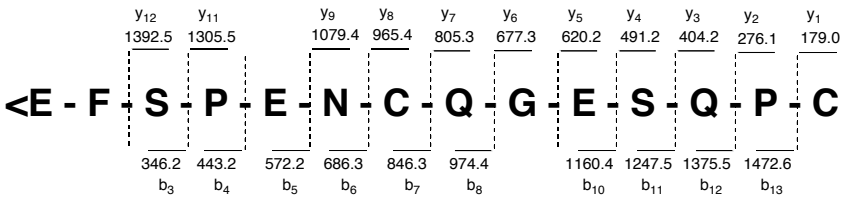

(**<E** stands for pyroglutamic acid)

Figure 1.13 LC-MS/MS analysis of the alkylated crotalphine derivative (**60**)

1.3.4 Synthesis and evaluation of epimerization of all-D crotalphine

As discussed above, the co-elution made it impossible to evaluate the synthetic efficiency of the commercial H-L-Cys(Trt)-2-Cl trityl resin. To approach this problem, a synthesis of all-D crotalphine (**61**) was performed using a commercial H-D-Cys(Trt)-2-chloro trityl resin (Scheme 1.23). The D-cysteine residue was pre-loaded onto the resin via an ester bond. Following Fmoc-based SPPS, all-D crotalphine (**61**) was made using all D-amino acids to give the enantiomer of natural crotalphine (**2**). After synthesis, the amount of epimerization was evaluated again using RP-HPLC. Fortunately, the epimerized peptide formed in this synthesis was indeed separable from the impurity (Figure 1.14).

Integration of the peaks in HPLC showed that the crude peptide acid from this synthesis contained 95% of the desired peptide **63** and 5% of its C-terminal diastereomer (**64**) (Figure 1.14). This result indicated that the commercial 2-chloro trityl resin had similar efficiency as D-cysteine cyclic ortho ester resin (**46**) in the synthesis of a medium sized peptide.

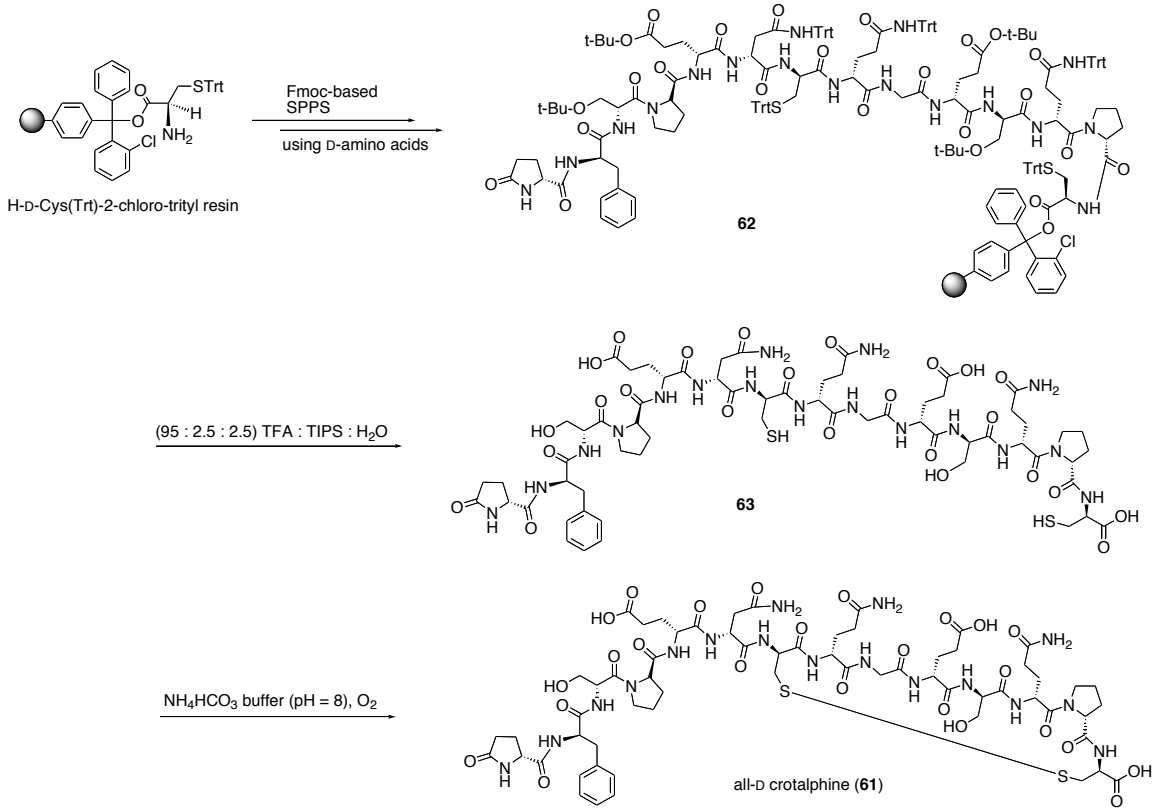

Scheme 1.23 Synthesis of all-D crotalphine (**61**)

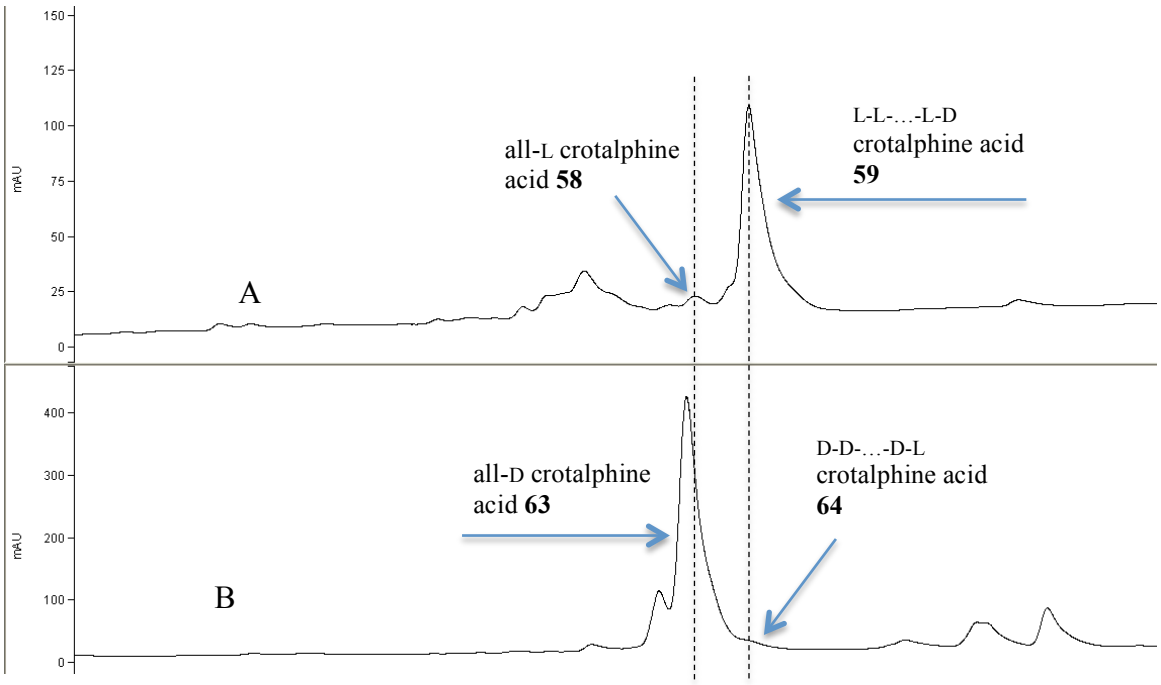

Figure 1.14 HPLC traces of D-crotalphine acids (free thiols). Trace A: Crotalphine acid (free thiols) crude mixture from cyclic ortho esters resin **46**. Trace B: All-D crotalphine acid (free thiols) crude mixture from H-D-Cys(Trt)-2-chloro trityl resin

1.4 Conclusions and future directions

Novel cysteine cyclic ortho esters **31** and **32** were synthesized with excellent enantiomeric purity. These compounds can be versatile synthons for preparing cysteine derivatives that would otherwise be susceptible to epimerization or thiolate elimination. After incorporation of this moiety to a solid support via a disulfide linkage, Fmoc-based SPPS generated model tripeptides and crotalphine with excellent diastereomeric purity. In a comparative synthesis, commercial 2-chloro trityl resin produced the same peptides with a similar purity. At this stage, and based on these model studies, our modified resin is not yet superior to the commercial resin. As epimerization and piperidine adduct formation could occur at each stage of chain elongation using conventional resins, more side products would form in the synthesis of longer peptides, such as hydrophobic peptides with more than 30 amino acids. In contrast, this increasing formation of side products is not expected in our modified cyclic ortho ester resins due to the much lower acidity of the α-proton. Therefore, we believe our cyclic ortho ester resins will be superior in the synthesis of long hydrophobic peptides. This should be explored in the future.

As the cysteine cyclic ortho esters were attached to a trityl resin, one may argue it was the bulky trityl linker, rather than cyclic ortho ester moiety, that led to the observed excellent diastereomeric purity. To test this hypothesis, in the future the cysteine cyclic ortho ester could be incorporated onto Wang resin using a similar disulfide linkage (Figure 1.15). This modified resin **65** could be used for Fmoc-based SPPS of model tripeptides and crotalphine. If an excellent diastereomeric purity is observed, it will be clear that the cyclic ortho ester moiety is the key factor governing this observation as

commercial Wang resin generated the same tripeptides with poor diastereomeric purities.[30]

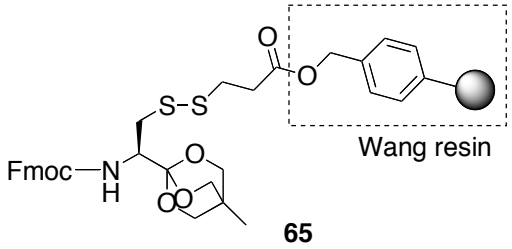

65

Figure 1.15 Cysteine cyclic ortho ester attached to Wang resin

Chapter 2 : Structure-Activity Relationship Study of Crotalphine and Efforts Toward Racemic Crystallization of Crotalphine

2.1 Introduction

2.1.1 Crotalphine and pain relief

According to the International Association for the Study of Pain, pain is classified as *"an unpleasant sensory and emotional experience associated with actual or potential tissue damage, or described in terms of such damage".*[38]

Woolf has classified pain into four groups: nociceptive pain, inflammatory pain, functional pain and neuropathic pain.[39] As pain is a major symptom in many medical conditions, the pharmacology of pain is a multi-billion dollar industry. Human beings have a long history of searching for painkillers, also called analgesics. Small molecules, such as morphine (**66**) and aspirin (**67**) are the most commonly used analgesics (Figure 2.1). Drug tolerance and dependence are often observed after long-term usage of some common analgesics. For instance, patients can develop a severe addiction to morphine. Therefore, it is necessary to develop an analgesic that does not display the above side effects.

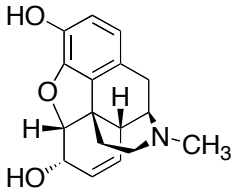

Morphine (66)

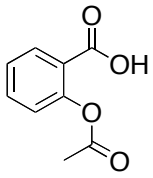

Aspirin (67)

Figure 2.1 Structures of morphine (**66**) and aspirin (**67**), two common analgesics

Recently Cury and co-workers reported that crotalphine (**2**) (Figure 1.3), a peptide isolated from the venom of the South American rattlesnake *Crotalus durissus terrificus*, showed potent oral analgesic activity using rats and mice as animal models.[5] This oral activity is interesting and unique, because most peptides cannot be administered orally due to the rapid inactivation by gastrointestinal enzymes.[40] Crotalphine was reported to be active at low doses, typically less than 10 μg/kg and its activity lasted for up to five days.[6] Interestingly, no tolerance or dependence was observed after prolonged treatment.

Opioid receptors belong to a large group of G protein-coupled receptors that use opioids as ligands.[41] Mu (μ), delta (δ) and kappa (κ) opioid receptors are three important types of proteins that recognize analgesics. For example, morphine binds to the μ–receptor. As well, selective opioid receptor antagonists are known. D-Phe-Cys-Tyr-D-Trp-Orn-Thr-Pen-Thr amide (CTOP) (**68**), *N*,*N*-diallyl-Tyr-Aib-Aib-Phe-Leu (ICI 174864) (**69**) and norbinaltorphimine (nor-BNI) (**70**) (Figure 2.2) are selective antagonists of μ, δ and κ-opioid receptors, respectively. When these three compounds were co-administered with crotalphine in animal models, the analgesic effect was only blocked in the nor-BNI case.[5] This result suggested that this peptide induces the analgesic activity by activation of the κ-opioid receptor. To determine the affinity of crotalphine to

the above three opioid receptors, Dr. Darren Derksen performed an experiment using competitive binding with radiolabeled ligands, and no binding was observed.[30] The above preliminary mechanistic studies suggest that crotalphine activates the κ-opioid receptor but does not directly bind to it at the same site as the κ-ligand U-69593 (**70a**) (Figure 2.2).

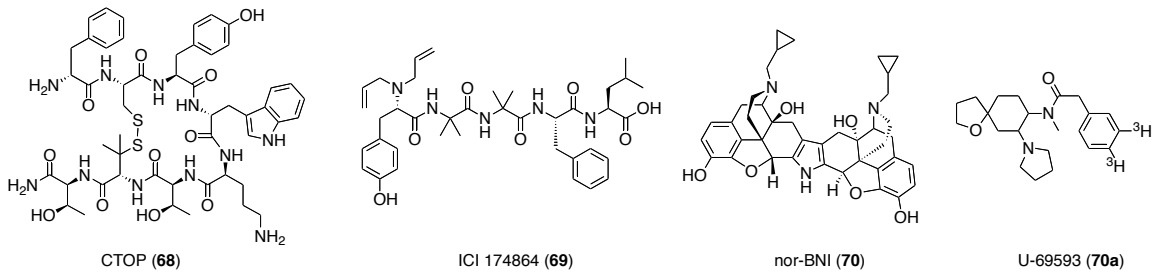

Figure 2.2 Opioid receptor antagonists CTOP **(68)**, ICI 174864 **(69)** and nor-BNI **(70)** and κ-ligand U-69593 (**70a**)

2.1.2 Structure-activity relationship study of crotalphine

The structure-activity relationship (SAR) study of bioactive molecules is a popular research area. Generally speaking, the purpose of an SAR study is to identify the essential structural features for the activity and find an active analog with improved properties, such as stability or solubility. The potent oral analgesic activity and relatively simple structure make crotalphine a suitable candidate for SAR studies. During their structural elucidation study of crotalphine, Cury and co-workers chemically synthesized three crotalphine analogs, with either one or two glutamine residues replaced by lysine (Figure 2.3).[5]

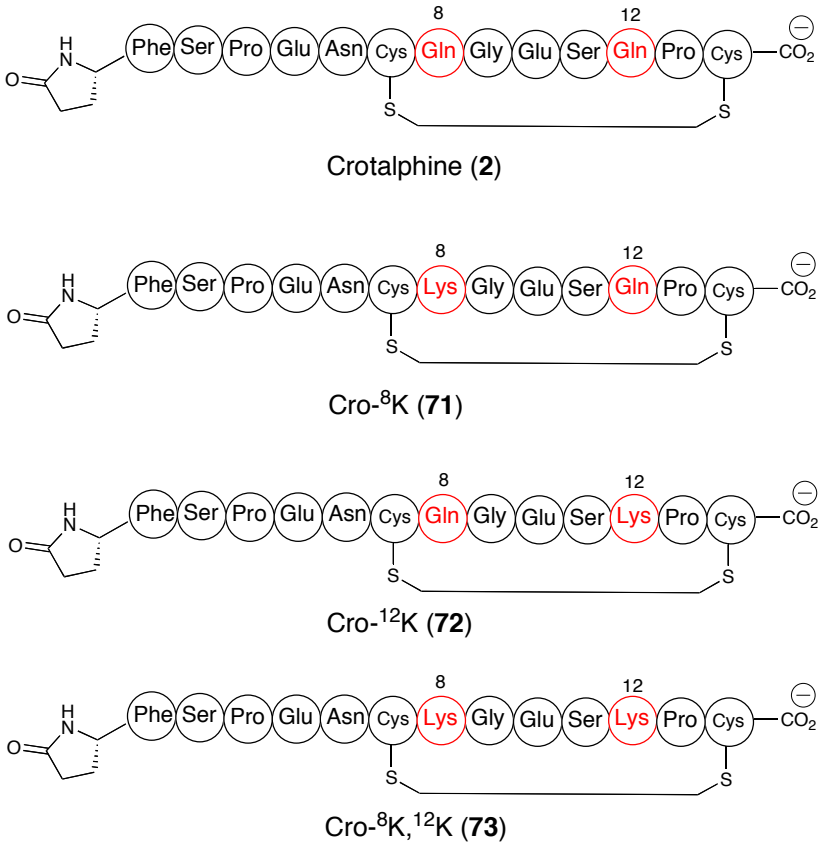

Figure 2.3 Crotalphine and its analogs synthesized by Cury and co-workers[5]

The biological evaluation of these analogs showed analog **72** retained full analgesic activity, while analogs **71** and **73** completely lost activity. This result implied that it is possible to modify position 12. Although no further SAR study was reported, we were encouraged by the full retention of activity for compound **72**.

Inspection of the structure of crotalphine indicates three important features for SAR study. First, if we can replace the N-terminal pyroglutamic acid with a proteinogenic amino acid, such as proline, then the modified peptide would only be made of proteinogenic amino acids. This peptide analog could be produced not only by chemical synthesis but also by biological methods, for instance, using heterologous

expression. Second, related to our cyclic ortho ester project, we were interested to see if peptide analogs, the D-Cys1 diastereomer (**53**) and all-D crotalphine (**61**) would retain any analgesic activity. Peptide **53**, containing a D-cysteine at the C-terminus, is a diastereomer of natural crotalphine. The selective substitution of D-amino acids within a peptide has been shown to be an effective method to identify a bioactive peptide analog with increased stability.[42, 43] Lee and co-workers found that when the C-terminal residue or N-terminal residue of the antimicrobial peptide KSLK (**74**) (Figure 2.4) was replaced by the corresponding D-amino acid, similar antimicrobial activity and greatly improved stability in serum were observed.[42] Occasionally, the all-D enantiomer of a natural peptide can retain bioactivity.[42, 44, 45] All-D enantiomers have also been used to probe the conformational requirements of ligand-receptor interactions.[30, 42, 45, 46] For example, the all-D enantiomer of leucocin A (**75**) (Figure 2.5) completely abolished antimicrobial activity, which indicated that chiral recognition was required.[30, 46] In contrast, Lee and co-workers found that the all-D enantiomer of peptide KSLK retained full activity, suggesting that a chiral recognition may be not involved.[42]

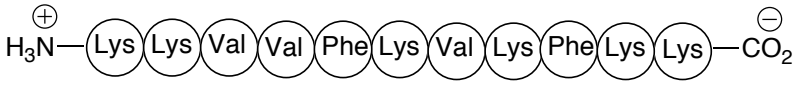

KSLK (**74**)

Figure 2.4 Structure of the antimicrobial peptide KSLK (**74**)[42]

Another interesting modification is the replacement of disulfide bonds. Disulfide bonds are commonly found in naturally occurring peptides. This covalent linkage between two cysteine thiols plays an important role in the folding and stability of some biologically active peptides. Disulfide bonds are susceptible to reduction and thiol

exchange, often resulting in loss of activity. It is interesting to study the replacement of disulfide bonds with other stable moieties. Recently reported results from the Vederas group suggest that the replacement of a disulfide-bond with hydrophobic residues may lead to an active peptide analog with increased stability.[47, 48] For instance, leucocin A (**75**) analogs in which the cysteine residues were replaced with phenylalanine (**76**), allylglycine (**77**) or leucine (**78**), all retained significant antimicrobial activity (Figure 2.5). In contrast, the serine analog (**79**) completely lost activity. Interestingly, the product of a ring-closing metathesis between the allylglycine residues (**80**) was also active.[49-52] We wanted to determine if similar hydrophobic substitutions would lead to the discovery of active crotalphine analogs.

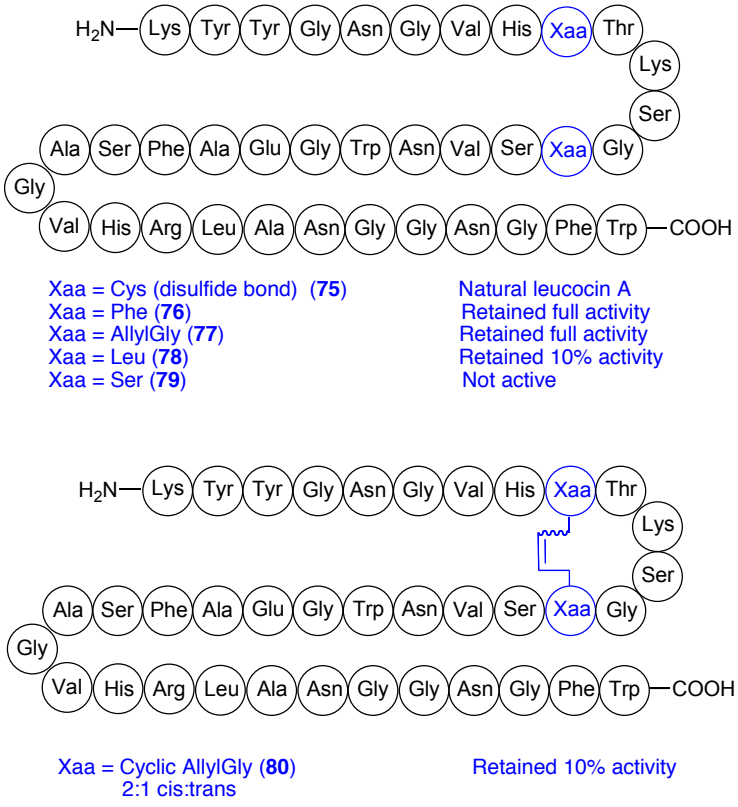

Figure 2.5 Leucocin A (**75**) and its synthetic analogs

2.1.3 Racemic crystallization of peptides

Protein crystallization is an important tool to study protein structure. The tertiary structure of a protein can be obtained by X-ray diffraction of suitable protein crystals. There have been significant advances in recent years in the crystallization of proteins, with over 77000 protein structures available in the Protein Data Bank (PDB) as of 2011, compared to only 7 in 1971 when the PDB was first created.[53] High throughput screening is a widely used method in protein crystallization. It consists of two important features. Firstly, many commercial kits with preassembled ingredients are available. Secondly, robotic screening can test crystallization conditions much faster and more precisely than humans. In spite of these recent advances, however, there are still problems that must be overcome. One difficulty is the crystallization of small peptides, typically those less than 5 kDa in size. Large proteins usually adopt a defined conformation in solution, while small peptides are more likely to exist as random coils. This conformational freedom makes small peptides particularly difficult to crystallize.

One possible solution to small peptide crystallization is racemic crystallization. This method involves growing a peptide crystal using a 1:1 mixture of the L-peptide and its D-peptide enantiomer, which generally can only be made by chemical synthesis. This method can increase the chances of successful peptide crystallization, because out of the possible 230 space groups available for crystallization, 165 are racemic mixtures (centrosymmetric) (72%).[54, 55] In contrast, single enantiomers can crystallize only in the remaining 65 space groups (28%), so the L/D racemate has a higher chance of crystallization. It is also easier to determine the crystal structure of a racemic mixture

than a single enantiomer.[54, 55] These two advantages make racemic crystallization an attractive approach to solve the crystal structure of small peptides.

The Kent group is considered to be the pioneer of the racemic crystallization of peptides and micro-proteins,[56-59] although three small peptide structures were solved using this method prior to their reports.[60-62] In 2009, Kent and co-workers obtained the crystal structure of native scorpion toxin BmBKTx1 (**81**) (Figure 2.6) using the racemic crystallization method (Figure 2.7).[56] Interestingly, no crystal formation was observed for the L-peptide after several weeks at a peptide concentration of 100 mg/mL. In contrast, the racemate, derived from the 1:1 mixture of L-peptide and D-peptide, readily crystallized after several days at concentrations ranging from 25 to 150 mg/mL. This result strongly supports the theory that racemic mixtures crystallize more readily than single enantiomers.

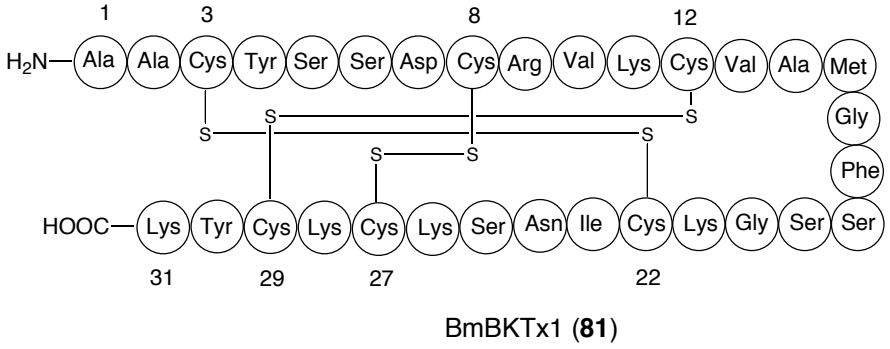

Figure 2.6 Amino acid sequence of BmBKTx1 (**81**)

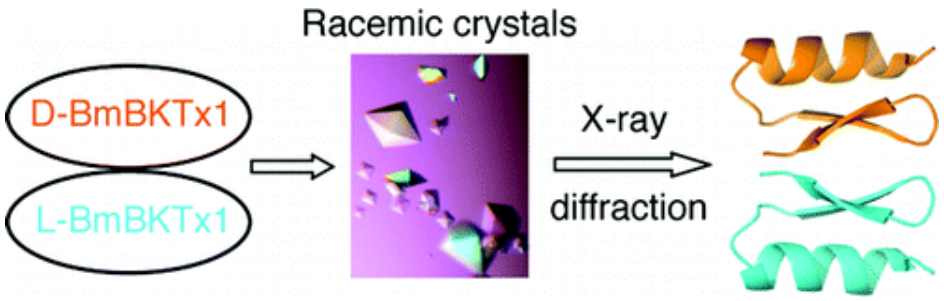

Figure 2.7 Racemic crystallization of native scorpion toxin BmBKTx1 (**81**) (used under permission of ACS Publications)[56]

2.2 Project objectives: Structure-activity relationship study of crotalphine and efforts toward the racemic crystallization of crotalphine

Due to the potent oral analgesic activity of crotalphine, we were interested in performing SAR studies. Our objectives were to identify the essential structural features for the bioactivity and find an active analog with increased metabolic stability. As discussed in the introduction, three groups of analogs would be synthesized and tested for biological activity; these include: (1) replacement of the N-terminal pyroglutamic acid residue; (2) replacement of the L-cysteines with D-cysteines; and (3) replacement of the disulfide bond with hydrophobic residues.

Attempts would also be made to perform the racemic crystallization of crotalphine. First, we were interested in determining the generality of this crystallization method. Second, if a crystal structure is successfully obtained, the analysis of the crystal structure could help to rationally design crotalphine analogs in the future.

2.3 Results and discussion

2.3.1 Synthesis of crotalphine analogs

Eleven crotalphine analogs were prepared for use in an SAR study. These compounds can be divided into three groups. Analogs of the N-terminal pyroglutamic acid, compounds **82** and **83** containing a proline and acetylated proline at the N-terminus respectively were prepared by Dr. Darren Derksen. These syntheses started from commercial 2-chloro trityl resin and Fmoc-based SPPS generated resin bound peptide **84** (Scheme 2.1). At this point, the resin was split into two portions and half of resin was acetylated at the N-terminus using acetic anhydride in DMF to give resin bound peptide **85**. Resin cleavage, followed by disulfide bond formation in $(NH_4)_2CO_3$ buffer furnished the desired crotalphine analogs **82** and **83**. Since analogs **82** and **83** do not contain a pyroglutamic acid at the N-terminus, they are likely less metabolically stable than natural crotalphine. On the other hand, analogs **82** and **83** could be potentially produced using biological methods as they are made of all proteinogenic amino acids.

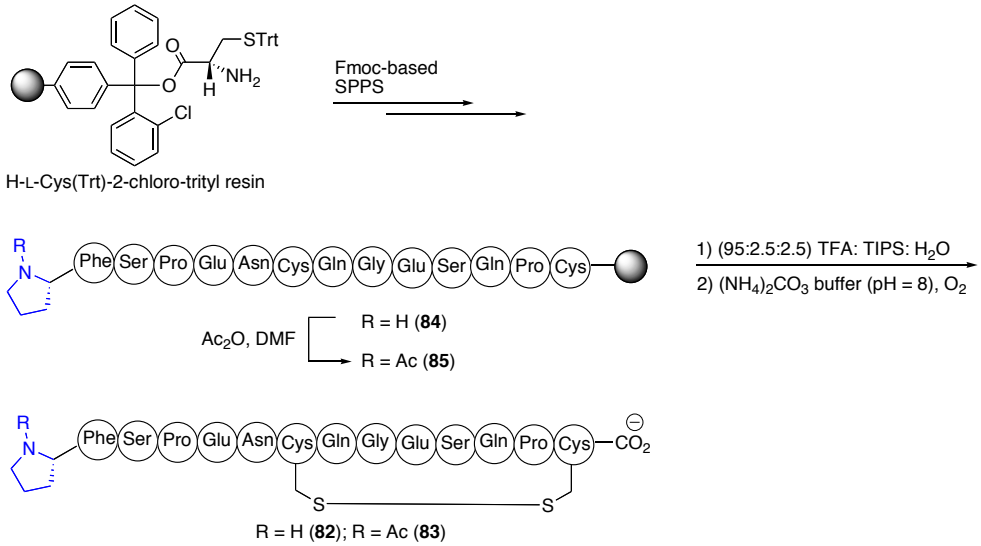

Scheme 2.1 Synthesis of crotalphine analogs **82** and **83**[30]

Crotalphine D-Cys1 diastereomer (**53**) and all-D crotalphine (**61**) previously prepared in Scheme 1.21 and Scheme 1.23, respectively, were used to test the D-amino acid substitution effect. These analogs are believed to have more metabolic stability than natural crotalphine (**2**).[42, 43]

Finally, peptides **86-92** were synthesized to examine the hypothesis that the disulfide bond could be replaced with hydrophobic residues. These peptides could be potentially active analogs with increased metabolic stability. In order to synthesize peptides **88**, **89** and **90**, three Fmoc protected unnatural amino acids, Fmoc-AllylSer-OH (**93**), Fmoc-AllylCys-OH (**94**) and Fmoc-PentenylGly-OH (**95**) were required (Figure 2.8). They were prepared by Stephen Cochrane, another graduate student in the Vederas group, for the use in another project. Peptide analogs **86**, **87** and **92** were synthesized by Dr. Darren Derksen.[30] Analogs **86-91** were prepared using Fmoc-based SPPS with amino acid pre-loaded Wang resin or 2-chloro trityl resin (Scheme 2.2).

Fmoc-AllylSer-OH (**93**) | Fmoc-AllylCys-OH (**94**) | Fmoc-PentenylGly-OH (**95**) | Fmoc-AllylGly-OH (**96**) Commercially available

Figure 2.8 Unnatural amino acids involved in the synthesis of crotalphine analogs **88-91**

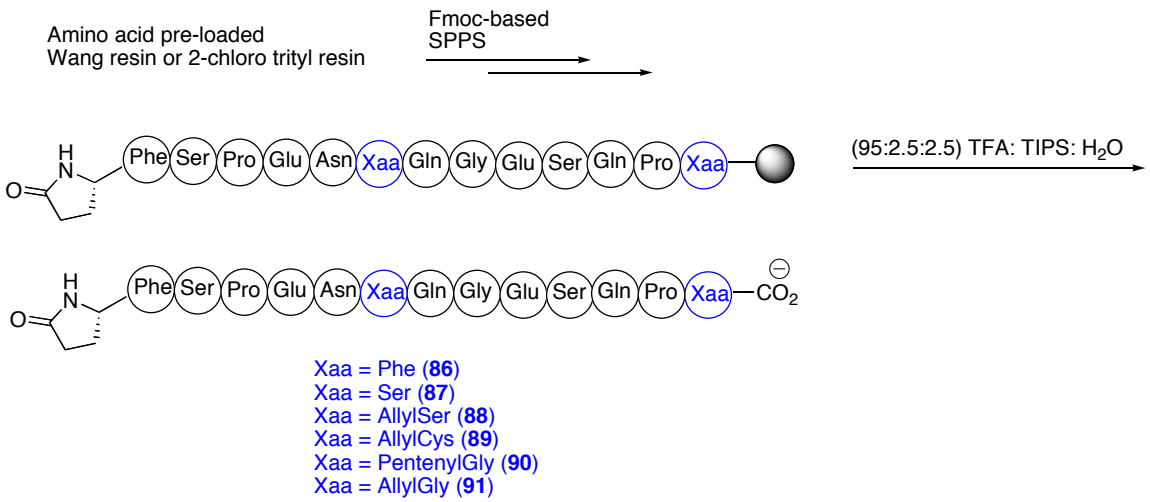

Schme 2.2 Synthesis of crotalphine analogs **86-91**

The synthesis of peptide analog **92** is shown in Scheme 2.3. Using amino acid pre-loaded Wang resin, Fmoc-based SPPS generated resin bound peptide **97**. The key on-resin ring-closing metathesis (RCM) was achieved using a catalytic amount of Grubbs II catalyst to give peptide **98**. Continuing Fmoc-Based SPPS and resin cleavage furnished the desired analog **92**.

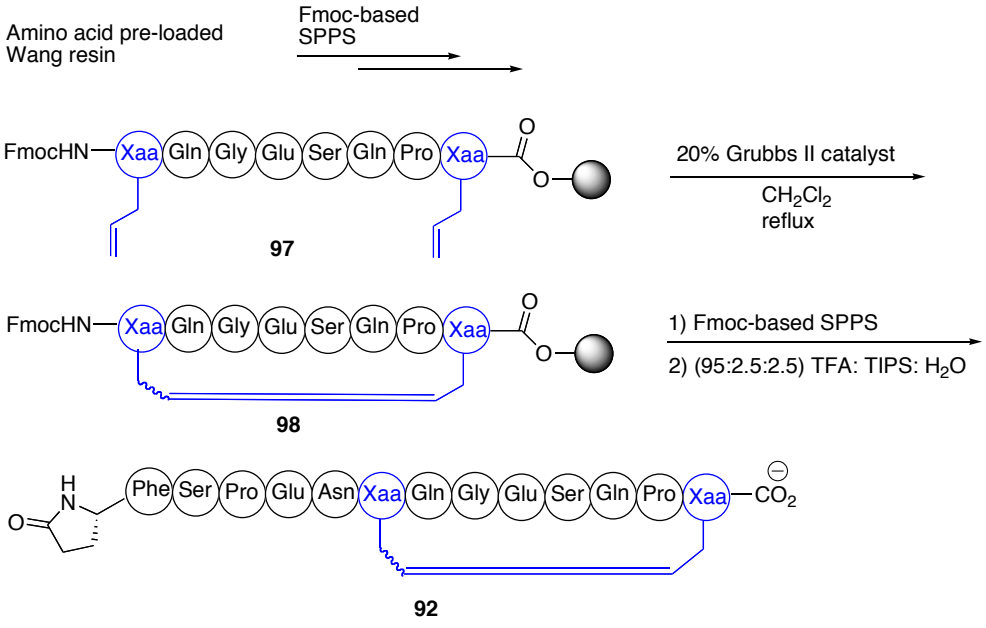

Scheme 2.3 Synthesis of crotalphine analog **92**[30]

2.3.2 Biological evaluation of crotalphine analogs

After chemical synthesis and HPLC purification to homogeneity, all the analogs were sent to our collaborator, Professor Yara Cury in Brazil. The Cury group was the first to isolate and study bioactivity of crotalphine.[5] Evaluation of the analgesic activity of our synthetic analogs using animal models is being performed using a hot-plate test and tail-flick test. This testing is in progress at present.

2.3.3 Racemic crystallization study of crotalphine

As discussed in (Chapter 1), we prepared both natural L-crotalphine (**2**) and its enantiomer all-D-crotalphine (**61**). In collaboration with Professor Joanne Lemieux in the Biochemistry Department at the University of Alberta, the racemic crystallization study of crotalphine was done using a robotic screen with a sitting drop method. About 500 crystallization conditions were screened and four peptide concentrations were attempted: 12, 24, 48 and 100 mg/mL. The peptide solution was prepared by mixing equal amounts of HPLC purified L-peptide and D-peptide. Unfortunately, a peptide crystal has yet to be obtained. To rationalize this, we have considered two possibilities. First, we suspect that the L-peptide and D-peptide were not present exactly in equal amounts. As the exact 1:1 ratio of two enantiomers is the prerequisite to the success of this method, any excess of one isomer may prevent crystal formation. Any contamination from purification may cause the two enantiomeric peptides to be present in different purities, which would make it difficult to prepare an equal amount of two peptides. The error from weighing small amounts of the sample would also possibly lead to unequal amounts of two peptides. The second possibility we considered was the use of an unsaturated peptide solution. For

crystallization to occur, a peptide or protein solution needs to be saturated. As crotalphine contains two glutamic acid residues and several glutamine and asparagine residues, it is very hydrophilic. Its extremely high solubility in water makes it difficult to crystallize, even at the concentration of 100 mg/mL. Generally speaking, when a protein or peptide solution is saturated for crystallization, precipitate would appear in more than 25% of the conditions screened. According to our observations, precipitate appeared in less than 10% of the tested conditions. This result further suggested that our peptide solution was not saturated. Attempts will be made to address these concerns in the future.

2.4 Conclusions and future directions

Eleven rationally designed crotalphine analogs were chemically synthesized using either manual or automated SPPS. The biological evaluation of these compounds is in progress at the laboratory of our collaborator in Brazil. If any of them shows analgesic activity, a second-generation of analogs will be designed, synthesized and tested. Ultimately, by doing this SAR study, we hope we can identify the essential structural features for this analgesic activity and find an active analog with increased metabolic stability.

The racemic crystallization of crotalphine was attempted. So far, no peptide crystal has been obtained. In the future, a precisely measured 1:1 mixture of L-crotalphine and D-crotalphine will be prepared and monitored by circular dichroism (CD) spectrometry. When the L-peptide and D-peptide are at the same concentration, they should have the same magnitude of absorption in the CD spectrum, but with opposite signs. Kent and co-workers showed a nice example in their study of kaliotoxin.[59]

In the future, we will also try to make a saturated peptide solution for crystallization. If we could obtain the peptide crystal, X-ray diffraction will be used to obtain the structure. Analysis of the crystal structure may help to better design crotalphine analogs in the future.

Chapter 3 : Study of New Bacteriocins Featuring Sulfur to α-Carbon Bridges

3.1 Introduction

3.1.1 New members of Class II bacteriocins featuring sulfur to α-carbon bridges

Bacteriocins are antimicrobial peptides produced by bacteria that are usually active against closely related bacteria strains.[63, 64] Bacteriocins are ribosomally synthesized and sometimes undergo extensive post-translational modifications.[65] Several classification systems have been proposed for bacteriocins from Gram-positive bacteria.[66-69] For instance, Ross and co-workers divide bacteriocins into two classes.[69] In Class I are the lantibiotics, which are highly post-translationally modified and contain characteristic structural features: lanthionine (**99**) or β-methyllanthionine (**100**) amino acids (Figure 3.1).[70]

Lanthionine (**99**) β-Methyllanthionine (**100**)

Figure 3.1 Structures of lanthionine **(99)** and β-methyllanthionine **(100)**

In Class II are the non-lantibiotic bacteriocins. Recently, the Vederas group discovered several new class II bacteriocins that share a common structural feature: a bridge between the sulfur of cysteine to the α-carbon of another amino acid (Figure

3.2).[71-74] This type of bridge is very unusual among the ribosomally synthesized peptides from bacteria, and was first observed in subtilosin A (**101**).[71] The N and C termini of subtilosin A are cyclized, whereas two other peptides of this class, thuricin-α (Trn-α) (**102**) and thuricin-β (Trn-β) (**103**), do not display this feature. Interestingly, all these peptides are produced by *Bacillus* species, and they all show antimicrobial activity against a spectrum of *Bacillus* and *Listeria* species. Trn-α and Trn-β form a two-component bacteriocin, which means that they not only show individual activity, but also show strong synergistic activity. Importantly, Trn-α and Trn-β are active against the human pathogen *Clostridium difficile*.[74]

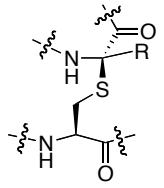

general structure of sulfur to α-carbon bridge

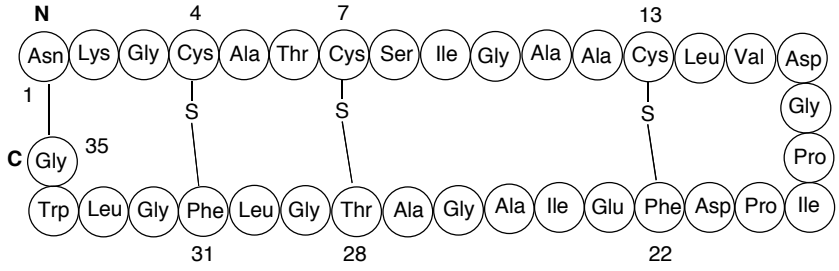

Subtilosin A (**101**)

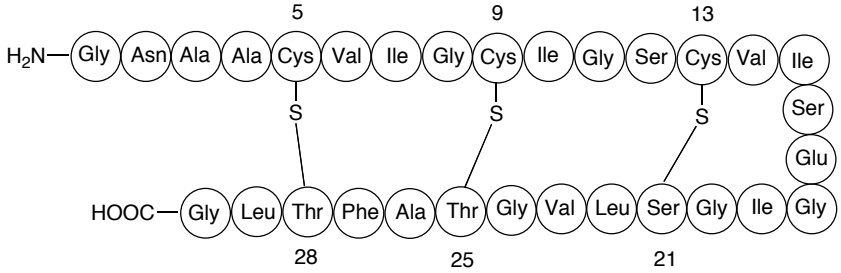

Thuricin-α (**102**)

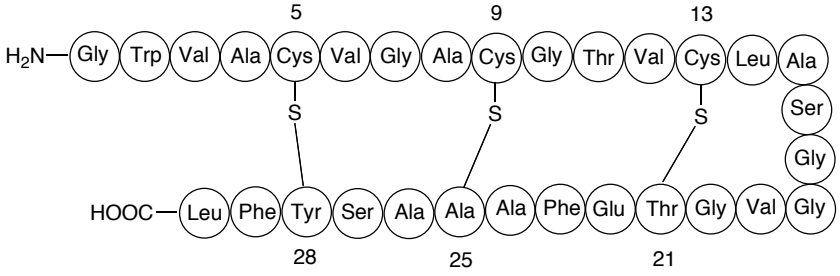

Thuricin-β (**103**)

Figure 3.2 A general structure of sulfur to α-carbon bridge and amino acid sequences of subtilosin A (**101**), thuricin α (**102**) and thuricin β (**103**), members of class II bacteriocins. Positions of sulfur to α-carbon bridges are indicated by solid lines. Backbone cyclization between the N and C termini in subtilosin A is shown by a solid line.

3.1.2 Structural elucidation of peptides containing sulfur to α-carbon bridges

The structural elucidation of these peptides containing sulfur to α-carbon bridges was performed using multiple modern analytical techniques. Taking Trn-β as an example,[75] the sequence generated by infusion MS/MS matched very well with the genetic sequence except at positions 21, 25 and 28 (Figure 3.2).[73] High resolution MALDI and MALDI FT-ICR MS indicated a loss of two hydrogens at each of these residues. In order to elucidate the exact modification, ^{15}N, ^{13}C-labeled Trn-β was prepared using isotopically labeled media. Based on data acquired from extensive multidimensional NMR experiments, including nuclear Overhauser effect spectroscopy (NOESY), a structure containing three sulfur to α-carbon bridges was proposed. The stereochemistry at the modified positions (21, 25, 28) was assigned as *RRS* (Figure 3.3), because this isomer best fit the NMR data when compared using CYANA, a protein structure calculation program.[74] Subtilosin A[71] and Trn-α[74] were analyzed in a similar way.

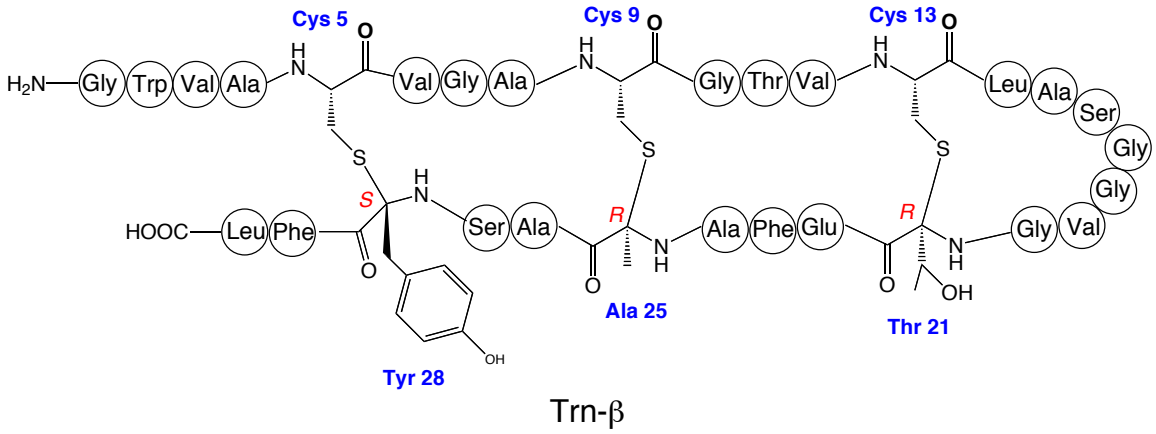

Figure 3.3 The stereochemistry at modified positions 21, 25 and 28 of thuricin-β are proposed to be *RRS* as shown[74]

3.1.3 Mechanism of formation of sulfur to α-carbon bridges

The proposed biosynthesis of subtilosin A is shown in Scheme 3.1.[76] Subtilosin A precursor (SboA) (**104**) is ribosomally synthesized and undergoes sulfur to α-carbon bridge formation catalyzed by the radical *S*-adenosylmethionine (SAM) enzyme AlbA[65] to give peptide **105**, which is converted to subtilosin A under the catalysis of putative proteases AlbE and AlbF.

Scheme 3.1 Proposed biosynthesis of subtilosin A[76]

The mechanism involved in the formation of sulfur to α-carbon bridges was not elucidated until very recently. Marahiel and co-workers successfully reconstituted the enzyme AlbA *in vitro* and demonstrated that indeed this enzyme was responsible for the formation of sulfur to α-carbon bridges during subtilosin A maturation.[76] AlbA is a

radical *S*-adenosylmethionine (SAM) enzyme and harbors two [4Fe-4S] clusters. The authors proposed that four main steps were involved in the formation of the thioether bridge. In the first step, by transferring an electron from the reduced form of the first [4Fe-4S] cluster to SAM, a 5'-deoxyadenosyl radical (5'-dA•) and methionine are generated, with simultaneous oxidation of the first [4Fe-4S] cluster (Scheme 3.2). In the second step, the peptide substrate SboA (**104**) (Figure 3.1), the unmodified subtilosin A precursor with a leader peptide, then coordinates to the second [4Fe-4S] cluster via its cysteine sulfur. In step three, the previously generated 5'-dA• radical then abstracts a hydrogen from the α-carbon of a phenylalanine or threonine residue to release 5'-dA. In the final step, the generated α-carbon radical attacks the coordinated sulfur to form the desired thioether bond (**106**).

The leader peptide in SboA was found to be essential, as the peptide without this leader sequence was unable to form the sulfur to α-carbon bridges. This result supported the proposal that the thioether bond formation is the first post-translational modification in subtilosin A biosynthesis.[76] These authors also demonstrated that the three thioether bridges were installed in a consecutive manner and the formation of the first bridge may be the rate-limiting step.[76] Although no similar biosynthetic study has been reported for thuricin, bioinformatic studies indicate two radical SAM enzymes are present in the biosynthetic gene cluster.[73] Therefore, it is reasonable to believe that radical SAM enzymes are involved in the formation of these unique thioether bridges.

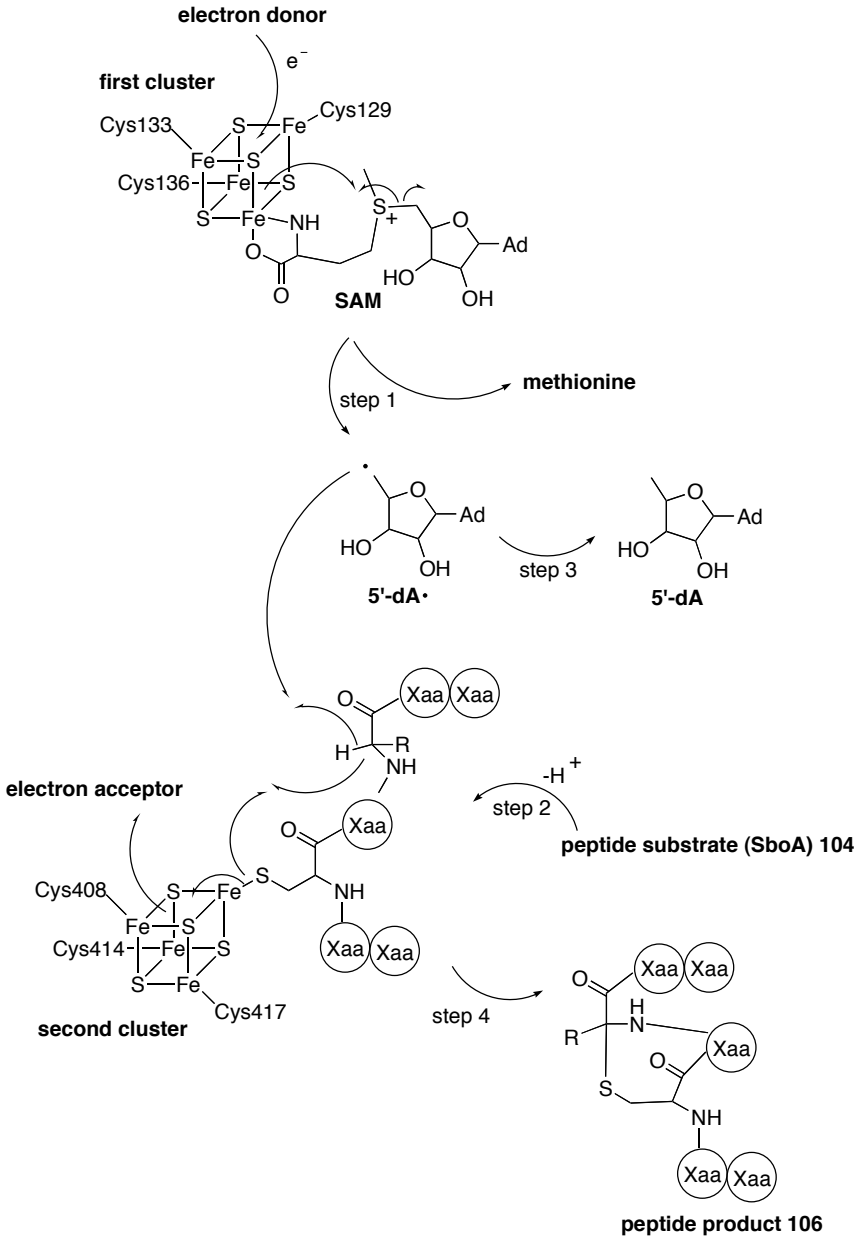

Scheme 3.2 Proposed mechanism for sulfur to α-carbon bridge formation.[76] Step 1: generation of 5'-dA• radical and methionine. Step 2: peptide substrate (SboA) **104** coordinates to the second [4Fe-4S] cluster. Step 3: 5'-dA• radical abstracts a hydrogen from the α-carbon of the modified residue to release 5'-dA. Step 4: formation of the thioether bridge **106**.

3.1.4 Chemical synthesis of sulfur to α-carbon bridges

In addition to biosynthetic study, it is also interesting to study the chemical synthesis of these peptides containing sulfur to α-carbon bridges. Previously the Vederas group has reported a racemic synthesis of some model compounds containing a thioether bridge.[72] When compound **107** was treated with a Lewis acid, $SnCl_4$, a reactive *N*-acyl imine **108** was generated, which was attacked by benzylthiol to give compound **109** in quantitative yield (Scheme 3.3). The chemical shift (68.0 ppm) of the α-carbon of **109** matched well with the corresponding chemical shifts (69.4 and 69.8 ppm) of the modified phenylalanine residues in subtilosin A. This chemical shift similarity is consistent with the cysteine sulfur being attached to the α-carbon of the phenylalanine residues in subtilosin A. To the best of our knowledge, no asymmetric synthesis of compounds containing sulfur to α-carbon bridges has been reported to date.

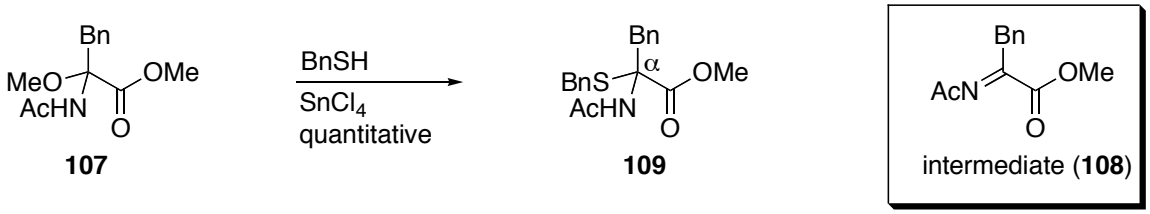

Scheme 3.3 Racemic synthesis of model compound **109**[72]

3.1.5 Structure-activity relationship study of bacteriocins featuring sulfur to α-carbon bridges

The mode of action of subtilosin A was studied using fluorescence spectroscopy, differential scanning calorimetry and solid-state NMR techniques.[77, 78] Subtilosin A was found to insert into phospholipid bilayers and interact with the hydrophobic core of the

membrane. As well, a specific receptor is proposed to be involved in this binding,[79] but further research is required to elucidate the exact mode of action and identity of the receptor.

Due to the synthetic challenge in preparing sulfur to α-carbon bridges, there has only been very limited SAR study of these peptides. Site-directed mutagenesis was used to prepare the T6I mutant of subtilosin A.[80] This mutant exhibited increased activity against *Listeria monocytogenes*, *Enterococcus faecalis* and *Streptococcus pyogenes*. Interestingly, this mutant showed hemolytic activity, unlike native sublitosin A. This improved antimicrobial activity and new hemolytic activity may be caused by the increased hydrophobicity of the mutant. In another study, it was found that desulfurization of subtilosin A using a nickel boride reduction abolished the antimicrobial activity.[72] This result indicates that the thioether bridges are essential for the bioactivity of subtilosin A.

3.2 Project objectives: Stereoselective synthesis of a bis-amino acid containing a sulfur to α-carbon bridge and structure-activity relationship study of thuricin-β

As discussed above, the stereochemistry of the α-carbons at the modified residues were assigned based on NMR data.[71-74, 81] We were interested in developing a complementary approach to confirm the absolute stereochemistry. Taking the modified phenylalanine residue in subtilosin A as an example, if the bis-amino acids **110** and **111** containing thioether bridges can be chemically synthesized in an enantiomerically pure form, these two compounds could possibly be derivatized as pentafluoropropanamide

methyl esters **112** and **113**, respectively (Scheme 3.4). Diastereomers **112** and **113** are expected to be separable via chiral GC-MS or chiral LC-MS. Hydrolysis and derivatization of natural substilosin A would be expected to produce either **112** and **113** depending on the stereochemistry of the modified residues. Therefore, by comparison to the synthetic standards using chiral separation methods, it should be possible to identify the absolute stereochemistry of the α-carbon in the modified residue of the natural product. Previously, such a chiral GC-MS approach was used to successfully elucidate the stereochemistry of lanthionine (**99**) and β-methyllanthionine (**100**) in lantibiotics.[32, 82]

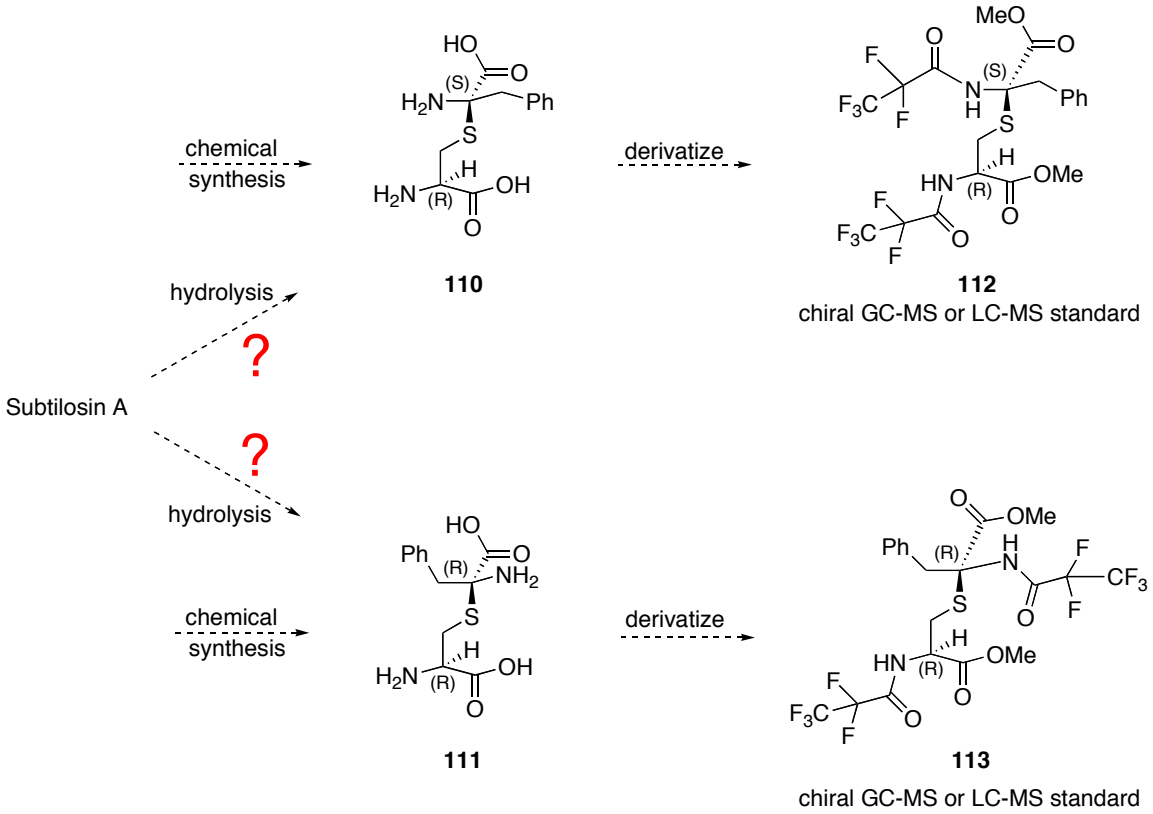

Scheme 3.4 Proposed approach to elucidate the stereochemistry of the α-carbon at the modified residue using chiral GC-MS or LC-MS

In addition to studying the stereochemistry, the developed synthetic method could also potentially allow for the synthesis of this class of peptides. Compound **114** (Figure 3.4) has orthogonal protecting groups on two nitrogens and could be used as a key building block in the solid-phase peptide synthesis of subtilosin A using a on-resin cyclization approach.[32]

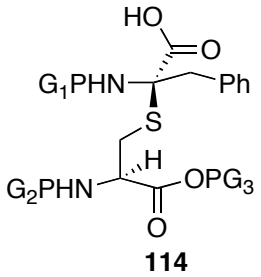

114

PG_1, PG_2, PG_3: protecting groups

Figure 3.4 Orthogonal protected bis-amino acid containing a thioether bridge

Another objective for this project was to conduct an SAR study of Trn-β. We chose Trn-β as the target for two main reasons. First, little has been reported regarding the mode of action of thuricin. It was our hope that an SAR study would shed some light on this. Second, Trn-β is not N to C cyclized and it is more amenable to a chemical synthesis approach.

As discussed above, thioether bridges were found to be essential for the antimicrobial activity of subtilosin A.[72] We were interested to investigate whether this is also true for Trn-β. Therefore, the SAR study would begin with the chemical synthesis and biological evaluation of three linear peptides with the cysteine residues replaced by glycine, serine or alanine residues (Figure 3.5). Notably, L-Thr, L-Ala and D-Tyr would

be used at positions 21, 25 and 28, as these configurations were assigned based on the NMR data.[74]

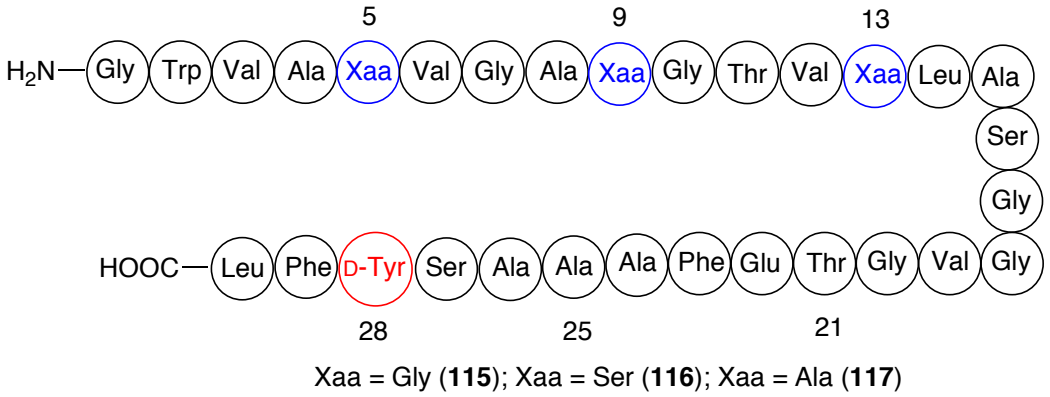

Figure 3.5 Designed thuricin-β analogs for SAR study

3.3 Results and discussion

3.3.1 Efforts toward asymmetric synthesis of a bis-amino acid containing a thioether bridge

Asymmetric synthesis of amino acids has been a subject studied by organic chemists for decades. The common approaches include enzymatic resolution of racemic amino acids,[83] asymmetric Strecker reaction,[84] asymmetric hydrogenation of dehydroamino acids,[85] and chiral auxiliary mediated synthesis of amino acids. Due to its high availability and efficiency, the chiral auxiliary method is especially attractive. Most of these auxiliaries are derived from glycine, alanine or other α-amino acids. Three classical and commonly used auxiliaries are shown in Figure 3.6, called the Williams oxazinone (**118**),[86] the Schollkopf bis-lactim ethers (**119**),[87] and the Seebach cyclic aminal (**120**).[88]

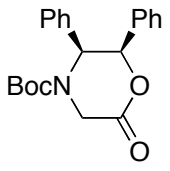

Williams auxiliary (**118**)

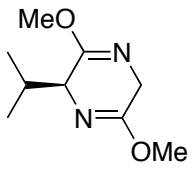

Schollkopf auxiliary (**119**)

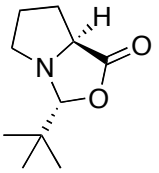

Seebach auxiliary (**120**)

Figure 3.6 Three commonly used chiral auxiliaries

In addition to these classical auxiliaries, some new auxiliaries have been reported in recent years, including the chiral tricycloiminolactones **121** and **122** developed by the Xu group (Scheme 3.5).[89] These auxiliaries are synthesized from camphor and can be considered to be glycine equivalents. The authors demonstrated that this auxiliary could be applied to the synthesis of many interesting unnatural amino acids. For instance, α-alkyl-α-amino acids and α,α-dialkyl-α-amino acids can be synthesized through mono-alkylation and bis-alkylation respectively (Scheme 3.5).[90, 91] Use of the Mannich reaction generated α,β-diamino acids,[92] while an aldol reaction gave β-hydroxy-α-amino acids as the product.[93] These auxiliaries could also participate in a Michael reaction to produce α,γ-diamino acid.[94] α-Oximino-γ-lactone was prepared by a 1,3-dipolar addition.[95] As well, these auxiliaries have been used in the synthesis of natural products, including sphingofungin F (**123**)[96] and (+)-conagenin (**124**).[97] The excellent stereoselectivity is achieved likely because the gem-dimethyl groups block the *exo*-face.

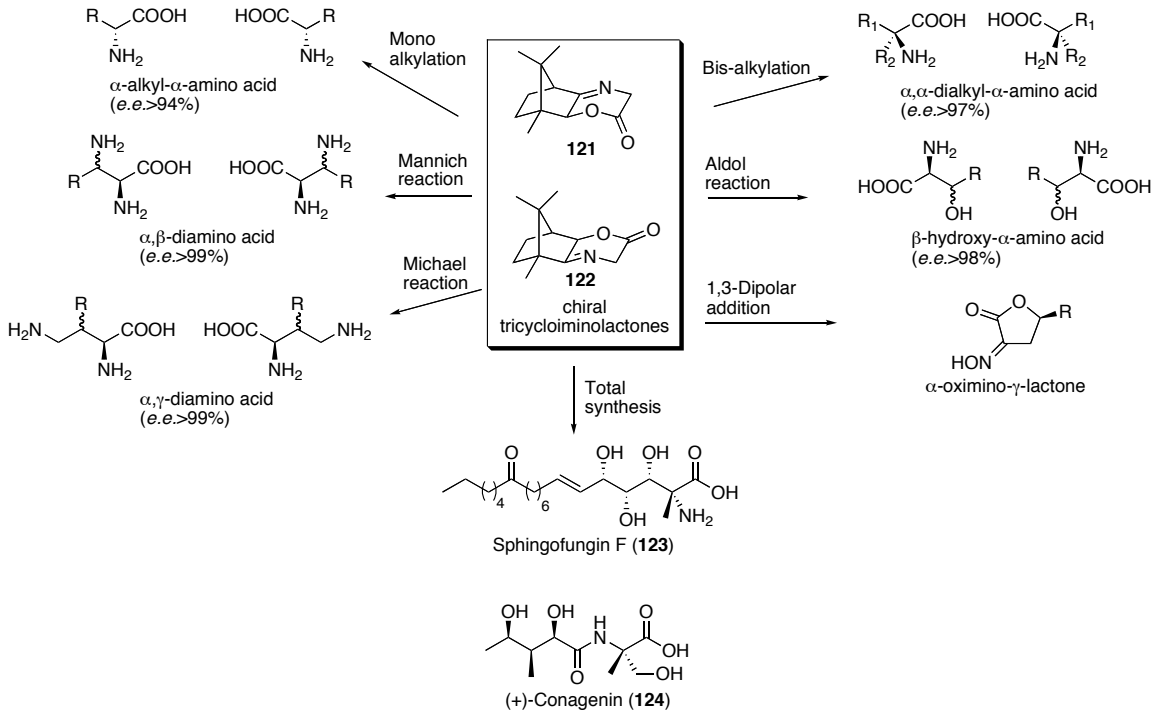

Scheme 3.5 Synthesis of unnatural amino acids using chiral tricycloiminolactones **121** and **122** [89]

We selected this type of chiral auxiliary to prepare a bis-amino acid containing a sulfur to α-carbon bridge for two principal reasons. First, excellent enantioselectivity was reported in the synthesis of α,α-dialkyl-α-amino acids (*e.e.* > 97%).[91] Second, 0.2 N HCl or even acetic acid was reported to be acidic enough conditions to remove the auxiliary.[96] These relatively mild deprotection conditions make this chiral auxiliary a good template to synthesize base-sensitive molecules, such as the bis-amino acid containing a sulfur to α-carbon bridge.

Our retrosynthetic approach towards the synthesis of bis-amino acid **125** containing a thioether bridge is shown in Scheme 3.6. Compound **125** was envisioned to be formed from the hydrolysis of compound **126**, which would be synthesized from chiral

tricycloiminolactone **129** using a stereoselective benzylation followed by a stereoselective sulfenation reaction. If compound **125** could be successfully prepared, it could then be derivatized to form the standard compound **112** for chiral GC-MS or LC-MS study.

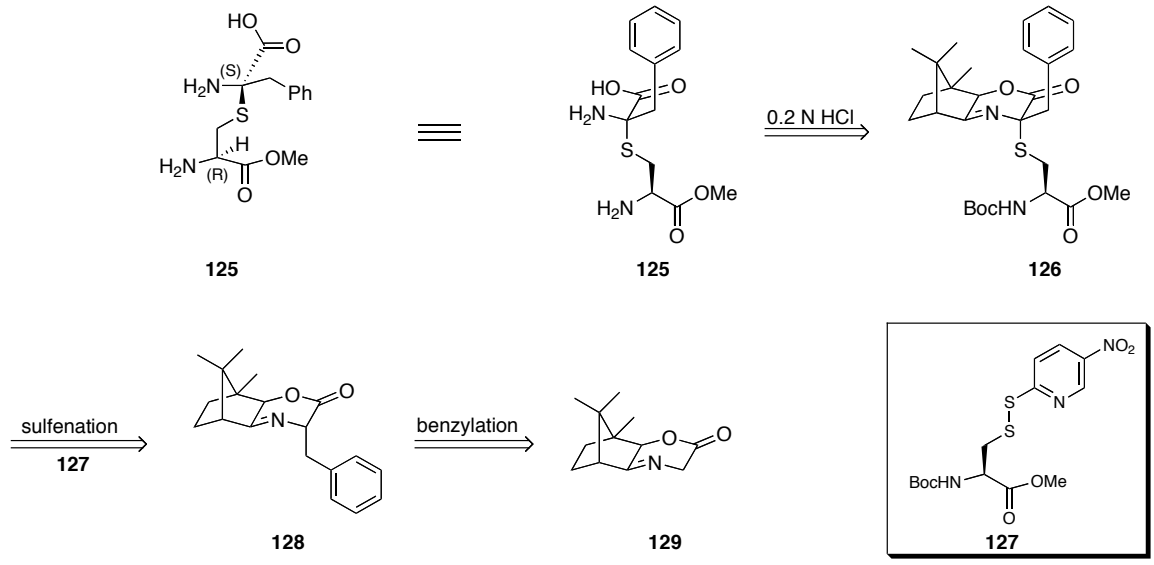

Scheme 3.6 Retrosynthetic analysis of compound **125**

Our synthesis started with the preparation of chiral tricycloiminolactones **136** and **129**. Following literature procedures,[91] (1*S*)-(-)-camphor (**130**) was oxidized using SeO_2 in refluxing Ac_2O to form camphorquinone (**131**) in excellent yield (Scheme 3.7). $NaBH_4$ reduction of **131** furnished two isomeric hydroxylketones **132** and **133**. This mixture of ketones was then directly coupled to Cbz-protected glycine (**134**) to produce inseparable esters **135** and **136** in 86% yield over two steps. According to ^1H NMR, the ratio of compounds **135** and **136** was 2:1. Finally, removal of Cbz group, followed by cyclization generated chiral tricycloiminolactones **137** and **129**. These two lactones were purified by flash chromatography with 10% and 8% isolated yields, respectively.

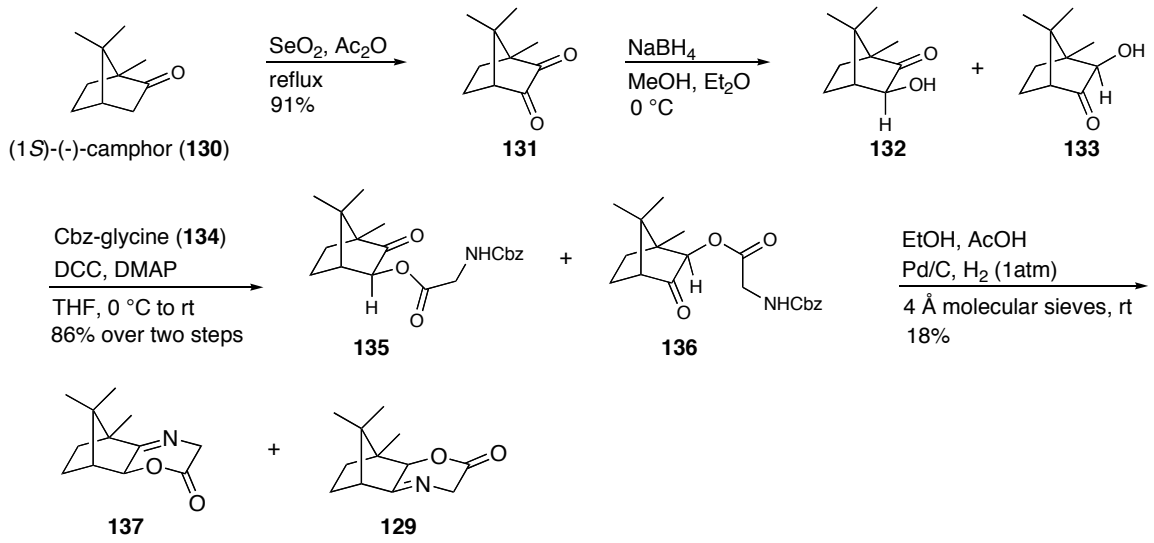

Scheme 3.7 Preparation of chiral tricycloiminolactones **137** and **129**

With chiral auxiliary **129** in hand, we were then prepared to make bis-amino acid derivative (**126**) (Scheme 3.8). Using LDA as base, **129** was deprotonated to form an enolate, which reacted with benzyl bromide to give compound **128**. This desired diastereomer was isolated in 69% yield.[91] It was envisioned that in order to form the key sulfur to α-carbon bond, an electrophilic cysteine derivative was required. Therefore, compound **127** was synthesized in a moderate yield from protected cysteine **138** and disulfide **139**. Fortunately, under similar conditions as the benzylation reaction, the desired bis-amino acid derivative **126** containing a thioether bond was isolated in 81% yield. To the best of our knowledge, this was the first successful preparation of a bis-amino acid derivative containing a thioether bridge in a stereoselective manner. Interestingly, due to the anisotropic effect of the benzene ring, the chemical shift of the methyl group in compound **126**, labeled with a star, was only 0.20 ppm in the ^{1}H NMR spectrum (Figure 3.7). In contrast, the chemical shift of the labeled methyl group in

tricycloiminolactone **129** was 0.87 ppm. These results strongly support the assigned stereochemistry at the α-carbon of compound **126**. Previously, a similar anisotropic effect was observed by the Xu group.[91]

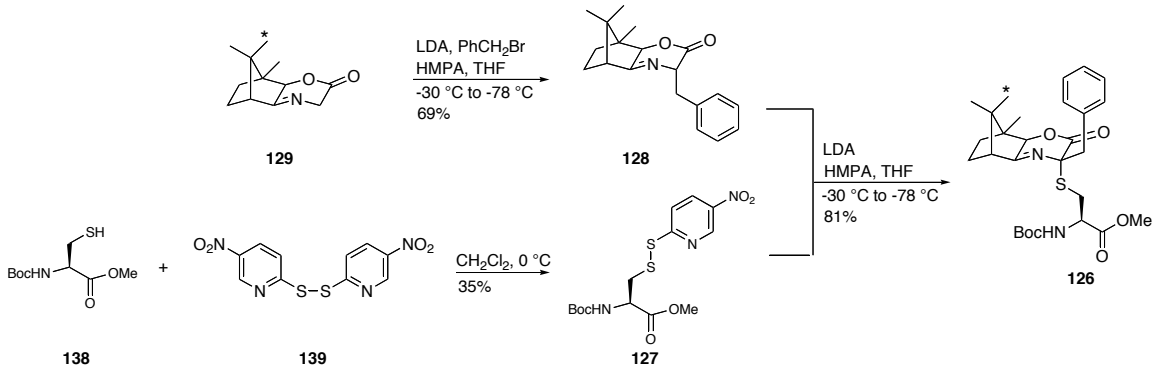

Scheme 3.8 Synthesis of bis-amino acid derivative **126**

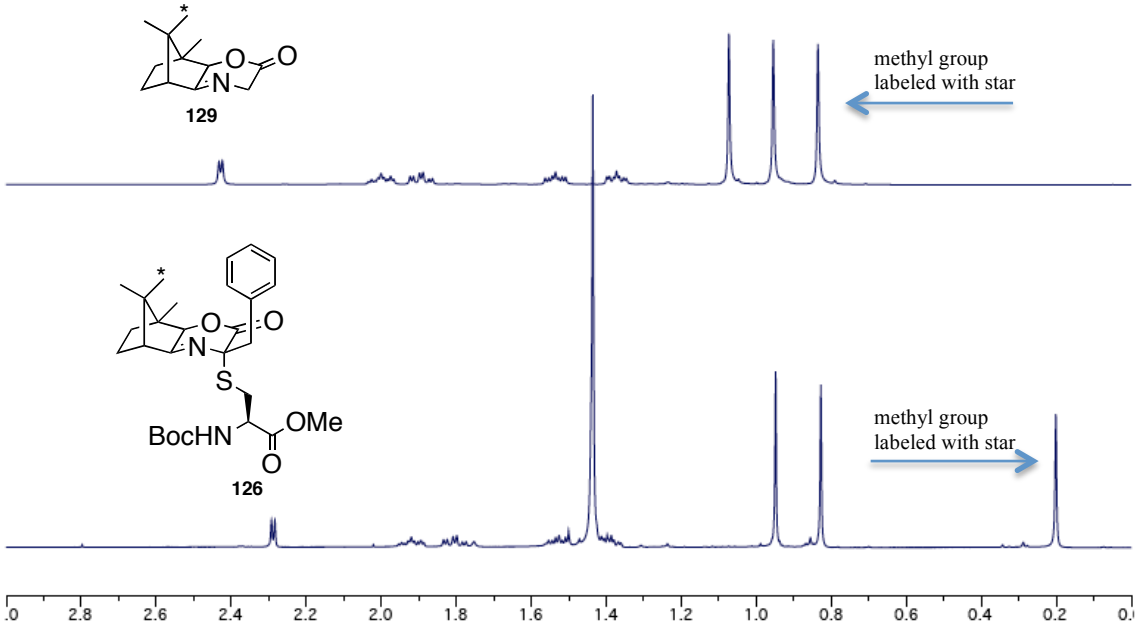

Figure 3.7 Overlayed partial ^{1}H NMR spectra of compound **129** and **126**

With the desired product **126** in hand, the next task was to remove the chiral auxiliary. Before hydrolyzing the real target **126**, a model study was performed using chiral auxiliary **137** (Scheme 3.9). Slightly modified literature conditions were used to hydrolyze tricycloiminolactone **137**.[96] Both of the two desired products **132** and glycine were isolated and confirmed by ^{1}H NMR and ESI-MS.

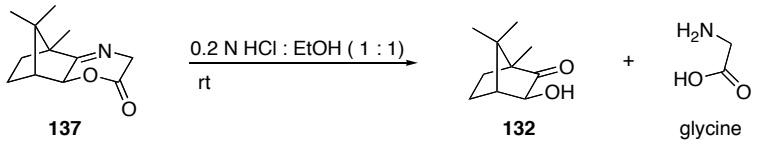

Scheme 3.9 Hydrolysis study of model chiral auxiliary **137**

After this model study, compound **126** was subjected to similar hydrolysis conditions (Scheme 3.10). Deuterated solvents were used because we wanted to use ^{1}H NMR to monitor the reaction conversion. When the starting material was completely consumed, Et_2O and H_2O were added. After this extraction step, product **133** was observed by TLC comparison to a standard. Unfortunately, the two desired products **125** and **110** were not found using ESI-MS. Instead, a peak corresponding to phenylpyruvic acid (**140**) was observed in ESI-MS. The formation of phenylpyruvic acid (**140**) was rationalized as shown in Scheme 3.11. Initial acidic cleavage of starting material **126** would furnish either species **141** or **142**. Breaking of the sulfur to α-carbon bond would generate species **145**, which could be attacked by D_2O, eventually leading to the formation of deuterated phenylpyruvic acid **149**. In the extraction step, hydrogen-deuterium exchange would produce the observed compound **140**.

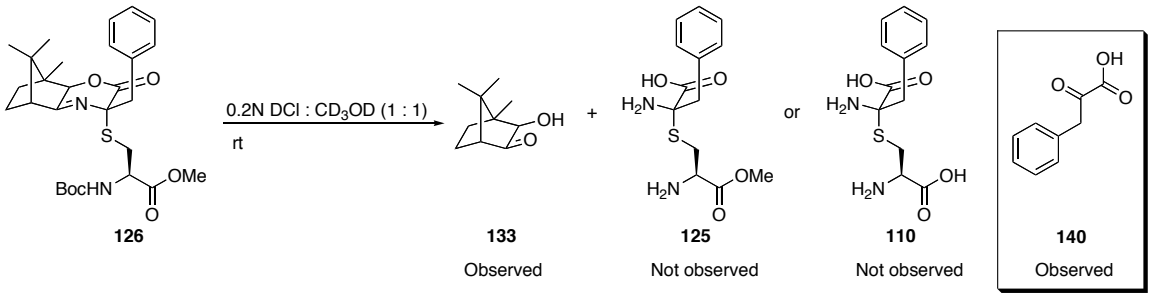

Scheme 3.10 Hydrolysis study of compound **126** under acidic conditions

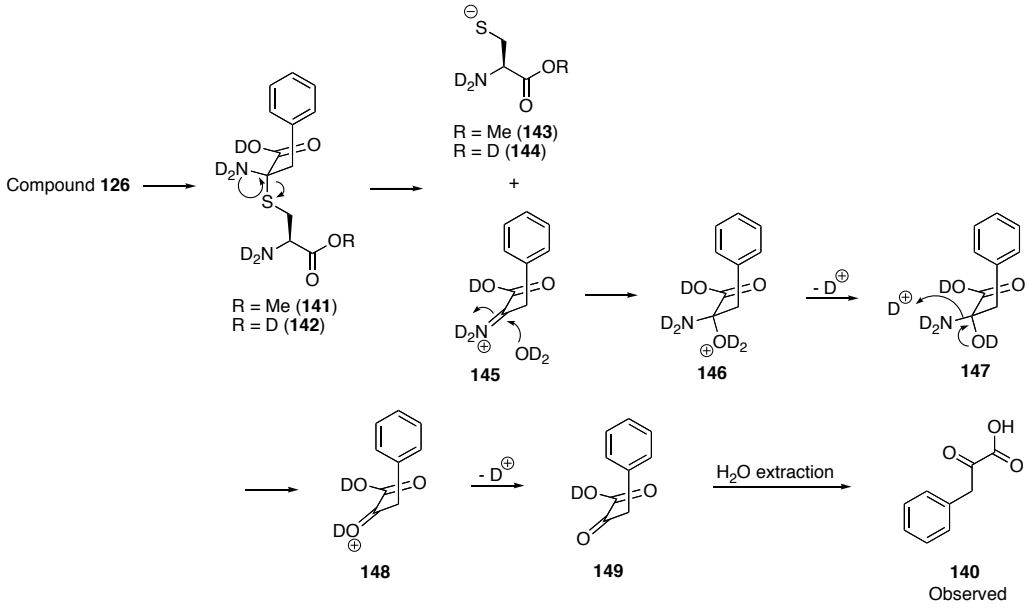

Scheme 3.11 Proposed mechanism for the formation of phenylpyruvic acid (**140**)

As the direct hydrolysis approaches failed, an indirect route to remove the camphor template was attempted (Scheme 3.12). Compound **126** was treated with hydroxylamine under mild conditions (pH adjusted to 6 to 7). Unfortunately, the desired product **150** was not observed by LC-MS. The major peak was identified as disulfide **151**.

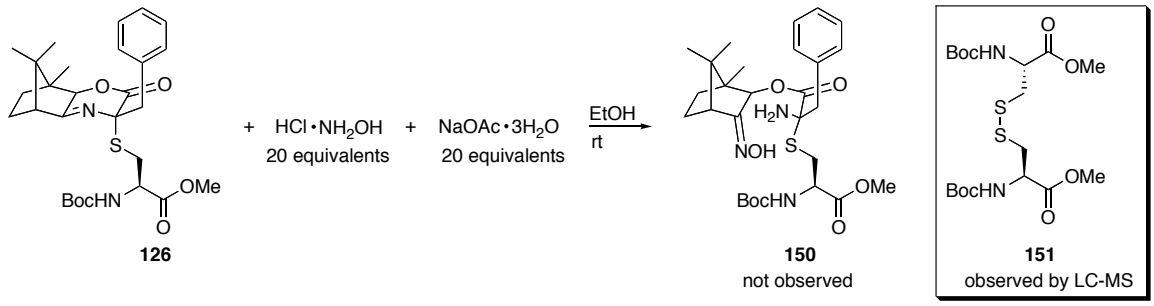

Scheme 3.12 Attempted indirect route to remove the camphor auxiliary of compound **126**

The formation of compound **151** could be rationalized in two steps (Scheme 3.13). The initially formed compound **150** was cleaved to generate cysteine derivative **138**, which was oxidized to give disulfide **151** as the major product observed in LC-MS.

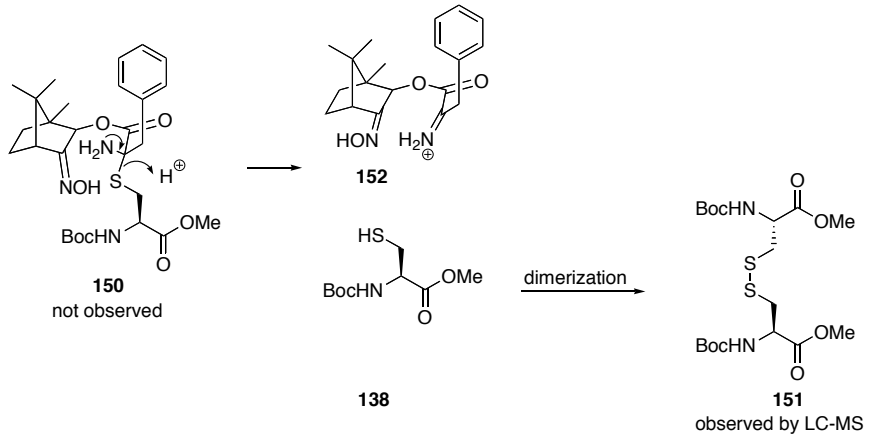

Scheme 3.13 Proposed mechanism for the formation of disulfide **151**

At this stage, it was clear that the removal of the chiral auxiliary was not trivial. Subtilosin A and thuricin-β are labile in basic conditions, but stable in moderately acidic conditions.[72, 73] In contrast, the synthetic bis-amino acid derivative (**126**) was not stable at a pH between 6 and 7. These natural peptides are highly structured and their conformation may prevent or slow the cleavage of the thioether bridges, which may

rationalize the increased stability of the thioether bridges in the natural peptides over the synthetic small molecules.

3.3.2 Structure-activity relationship study of thuricin-β

The second goal of this project was to perform an SAR study of Trn-β. Three peptide analogs with the cysteine residues replaced by glycine, serine or alanine residues were chemically synthesized and tested for antimicrobial activity.

3.3.2.1 Chemical synthesis of glycine analog (153) of thuricin-β

The glycine analog (**153**) was our first synthetic target. This peptide was synthesized from a pre-loaded Fmoc-Leu-Wang resin (**154**) using standard automated Fmoc-based SPPS methodology (Scheme 3.14). The synthesis started with the Fmoc deprotection of the pre-loaded leucine residue, followed by peptide chain elongation. The final Fmoc deprotection and resin cleavage generated the crude peptide.

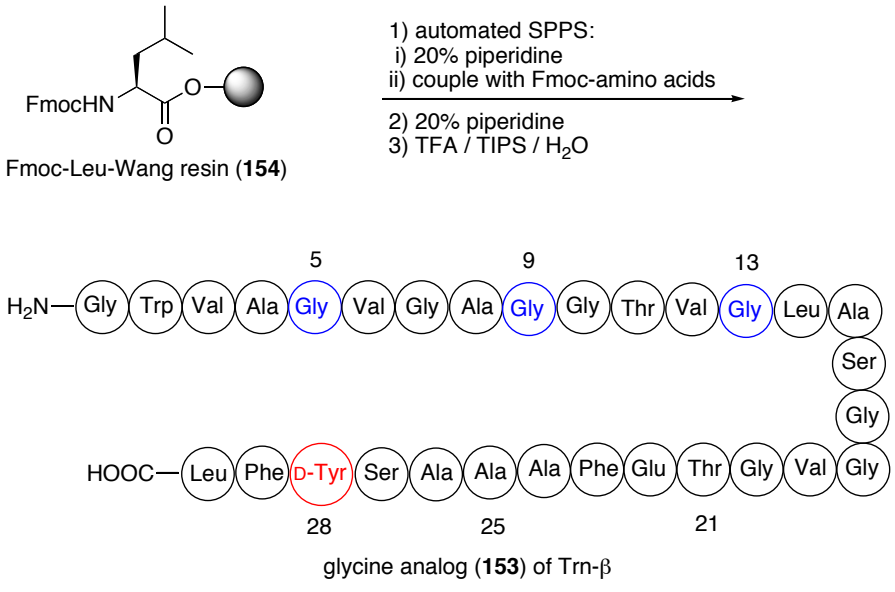

Scheme 3.14 Synthesis of glycine analog (**153**) containing D-Tyr at position 28

HPLC was used to purify this peptide, but the peptide showed poor solubility in many common HPLC solvents, such as H_2O, CH_3CN, MeOH and *i*-PrOH. We suspected that the limited solubility was likely due to the relatively hydrophobic sequence. After trying many experiments, we eventually succeeded in obtaining this peptide with good purity by using a C4-functionalized HPLC column. The correct sequence of this synthetic peptide was confirmed by LC-MS/MS (Figure 3.8), as almost all of the b-ions (charge retained at the N-terminus) and y-ions (charge retained at the C-terminus) in the sequence were observed.

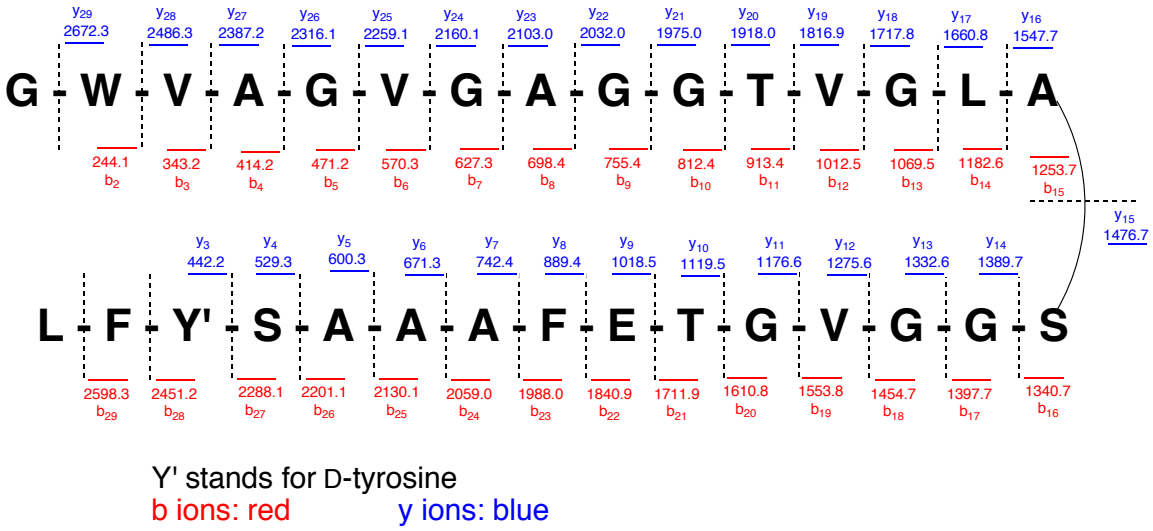

Figure 3.8 LC-MS/MS analysis of the glycine analog (**153**)

3.3.2.2 Chemical synthesis of serine analog (155) of thuricin-β

To prepare serine analog (**155**) of Trn-β, the same synthetic method was used as for the glycine analog. The MALDI-MS spectrum of the crude peptide was very complicated and several peaks were observed. Careful analysis suggested that this synthesis generated many truncated peptides in addition to the desired peptide. This result

was not unexpected, as the peptide sequence was very hydrophobic. It is well known that aggregation may occur during the Fmoc-based SPPS of long and hydrophobic peptides.[12] Peptide aggregation happens mainly through hydrogen bonding between the amide hydrogen and carbonyl oxygen of two separate growing peptide chains (Figure 3.9).[98]

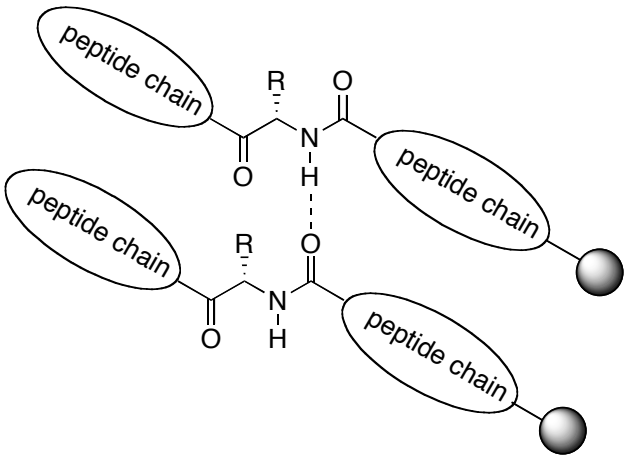

Figure 3.9 Peptide aggregation caused by hydrogen bonding between two growing peptide chains

In the literature, there are several approaches developed to address this problem. For instance, Mutter and co-workers reported that peptide aggregation could be minimized by the incorporation of pseudoproline dipeptides (**156**, **157**) (Figure 3.10).[99, 100] Alternatively, Fmoc-Ala-(Dmb)Gly-OH dipeptide (**158**) is also able to effectively decrease the peptide aggregation.[101] Following inspection of the structures of these dipeptides, it is clear that peptide aggregation is minimized due to the lack of hydrogen bonding of the amide hydrogen. Another technique used to address this problem is the use of polyethylene glycol (PEG) resin, which is found to be superior to polystyrene resin in the synthesis of hydrophobic peptides.[102]

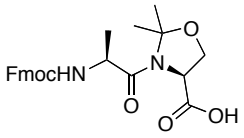

Fmoc-Ala-Ser(ψMe,Me Pro)-OH (**156**)

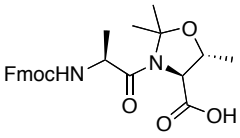

Fmoc-Ala-Thr(ψMe,Me Pro)-OH (**157**)

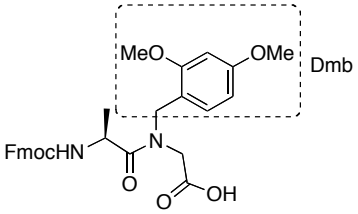

Fmoc-Ala-(Dmb)Gly-OH (**158**)

Figure 3.10 Structures of pseudoproline dipeptides (**156**, **157**) and Fmoc-Ala-(Dmb)Gly-OH dipeptide (**158**)

The improved synthesis of the serine analog (**155**) of Trn-β was achieved by using the pseudoproline Fmoc-Ala-Ser(ψMe,Me Pro)-OH (**156**) dipeptide at three positions (Scheme 3.15). All the amino acids were coupled using an automated peptide synthesizer except for the two N-terminal residues, which were coupled using manual SPPS. Following synthesis, the peptide was cleaved from the resin under acidic conditions and the pseudoproline dipeptide was converted to the normal dipeptide concomitantly. Similar to the glycine analog, this product peptide had limited solubility in H_2O, CH_3CN and MeOH. Still, relatively pure peptide was obtained after HPLC purification.

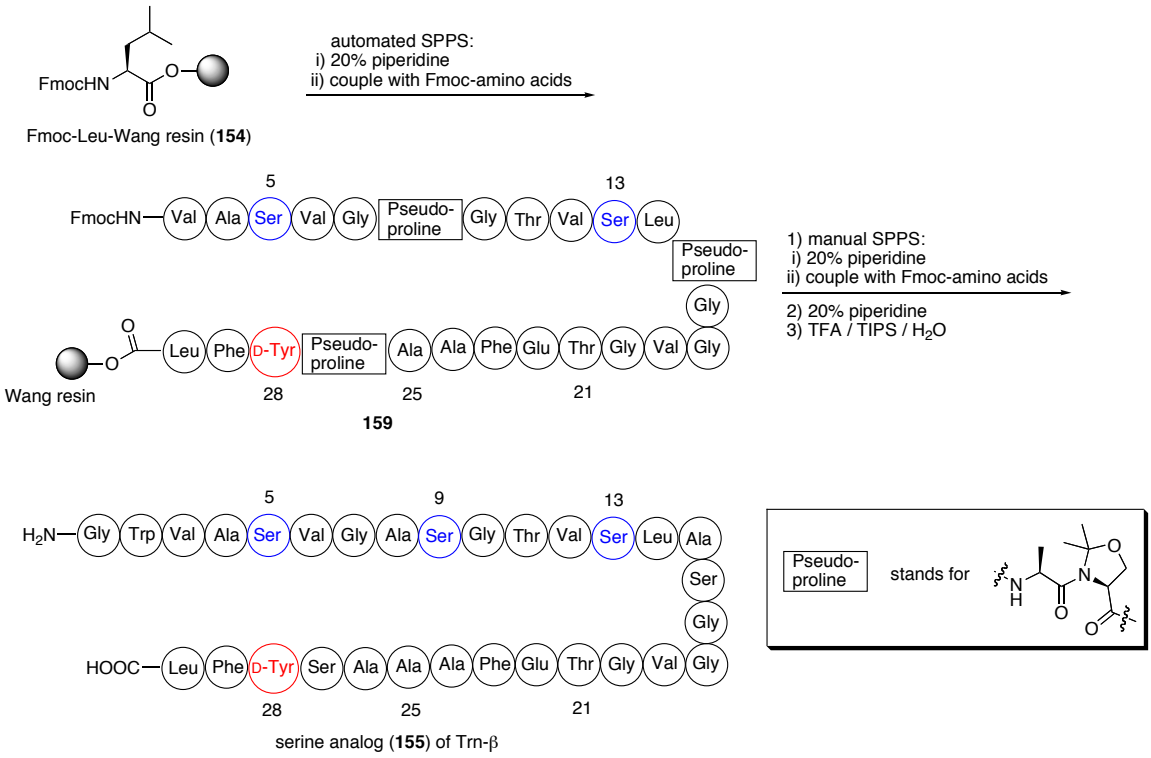

Scheme 3.15 Synthesis of serine analog (**155**) of Trn-β

3.3.2.3 Chemical synthesis of alanine analog (160) of thuricin-β

When compared to the synthesis of the serine analog, a similar synthetic route was applied in the synthesis of the alanine analog (**160**) of Trn-β except for the use of the Fmoc-Ala-(Dmb)Gly-OH dipeptide (**158**), H-Leu-HMPB-PEG resin (**161**) and a double coupling strategy (Scheme 3.16). The term double coupling means that an amino acid residue is coupled twice prior to Fmoc deprotection in order to improve the coupling efficiency.

After resin cleavage, the MALDI-MS spectrum of the above crude peptide was much cleaner than the corresponding spectrum of the crude peptide synthesized using standard SPPS methodology (Figure 3.11).

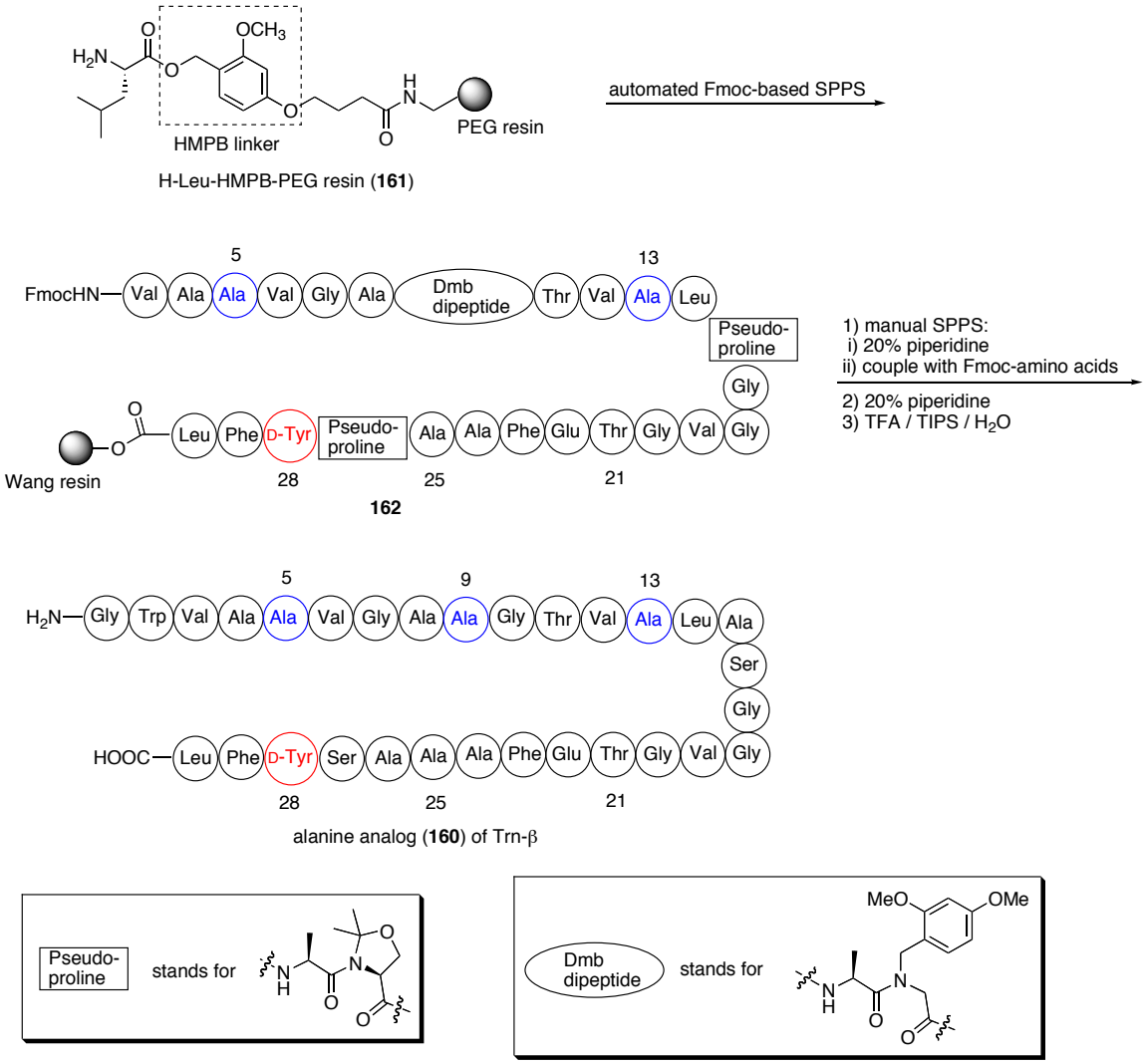

Scheme 3.16 Synthesis of alanine analog (**160**) of Trn-β

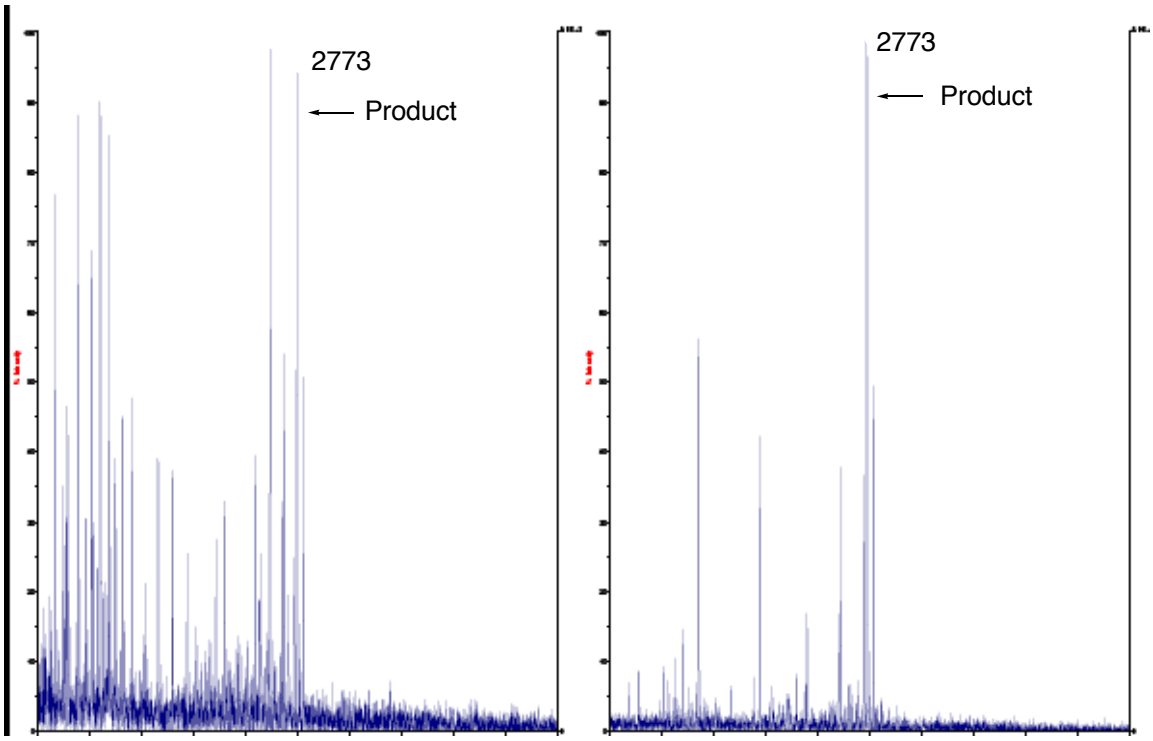

Standard SPPS method Improved SPPS method

Figure 3.11 MALDI-MS spectra of crude alanine analog (**160**) of thuricin-β synthesized using standard SPPS method (left) and improved SPPS method (right)

However, when we tried to purify this crude peptide using HPLC, the impurities seen in MALDI always co-eluted with the desired peptide. Therefore, only crude peptide was used for bioactivity testing.

3.3.3 Biological evaluation of the synthetic analogs of thuricin-β

The antimicrobial activity testing was performed using a spot-on-lawn assay using *Bacillus firmus* as an indicator strain. All the synthetic analogs were evaluated at a 200 μM concentration and the natural Trn-β in the same concentration was used as a positive

control. All of the three synthetic analogs were inactive. This result suggested that the thioether bridges are indeed essential for the bioactivity shown by the natural Trn-β. A similar result was also found for subtilosin A.[72] Taken together, thioether bridges are likely essential for the observed bioactivity, and this may be true for the whole family of peptides.

As discussed previously, the mode of action of thuricin is not yet known. These peptides may bind to a specific receptor in the membrane, or less likely, act via non-specific hydrophobic interactions. In either case, the peptide conformation is important and the lack of activity of the synthetic analogs may be attributed to different conformations compared to the natural Trn-β, which is much more restricted due to the crosslinks.

3.4 Conclusions and future directions

A novel bis-amino acid derivative (**126**) with a thioether bridge was successfully synthesized as a single diastereomer using chiral tricycloiminolactone **129**. Two methods were attempted to remove the auxiliary, using either 0.2 N HCl or hydroxylamine. However, both of these experiments lead to the cleavage of the key thioether bridge. The thioether bridge was judged to be more labile in the synthetic standard than in the natural peptides. The present results indicate that it is likely difficult to chemically prepare chiral chromatographic standards due to the instability of the thioether bridges. In order to further elucidate the stereochemistry at α-carbon of the modified residues, other approaches are required. Crystallization may be another option to achieve this goal.

Three Trn-β analogs (**153**, **155**, **160**), with the cysteine residues replaced by glycine, serine or alanine residues, were synthesized using Fmoc-based SPPS. Because of the hydrophobic nature of these peptides, the successful synthesis of the serine analog (**155**) and the alanine analog (**160**) required some special strategies, such as the use of pseudoproline dipeptide and Fmoc-Ala-(Dmb)Gly-OH dipeptide. None of the synthetic analogs showed antimicrobial activity.

As discussed previously, if the mode of action of thuricin involves non-specific hydrophobic interactions, then it may be possible to design some analogs to mimic the conformation of the natural peptides and these synthetic analogs may retain some bioactivity. One such analog (**163**) is shown in Scheme 3.17. This designed analog contains three carbon bridges instead of thioether bridges. It thus may adopt a similar geometry as the natural Trn-β, but be more metabolically stable.

Scheme 3.17 is the proposed route to the synthesis of this analog. The three required bis-amino acids (**166-168**) containing carbon bridges could be synthesized using a photolysis approach (254 nm) developed by our group.[103] Notably, the protecting groups on these building blocks need to be orthogonal. Using these building blocks, Fmoc-based SPPS would generate the resin bound peptide **169**. A combination of sequential on-resin cyclization[32] and Fmoc-based SPPS, followed by the resin cleavage would give the desired peptide analog **163** with three carbon bridges. It is hoped that biological evaluation of this cyclic analog would provide some information on the mode of action of thuricin.

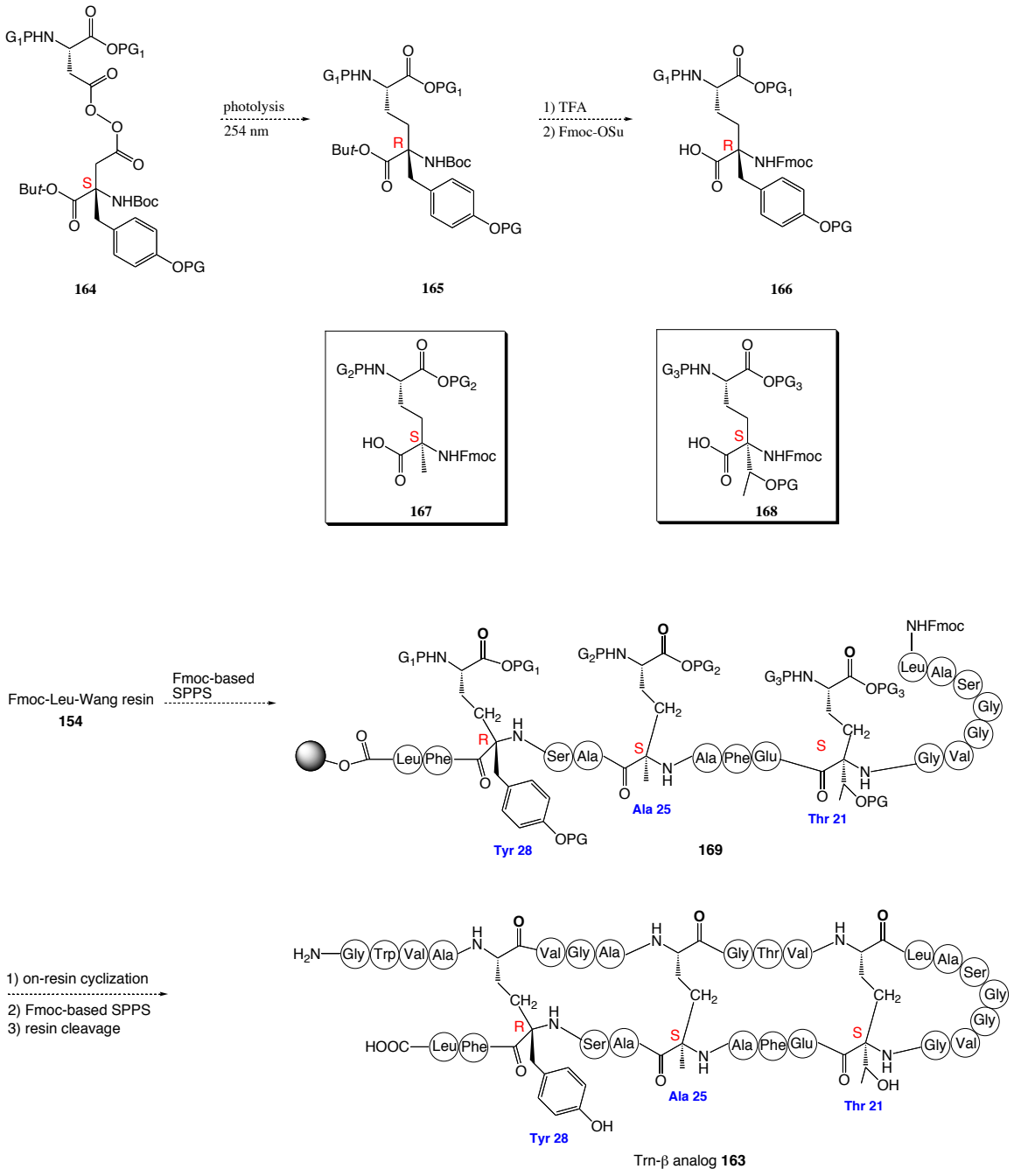

Scheme 3.17 Proposed synthetic route to thuricin-β analog **163**

Chapter 4 : Efforts Toward the Chemical Synthesis of Crocin and its Analogs

4.1 Introduction

4.1.1 Saffron and crocin

Saffron, the dried stigmas of the flower of *Crocus sativus*, is one of the most expensive spices in the world.[104] Saffron is also used as a food colorant. It is native to southwest Asia and was first cultivated in Greece.[105] The main components of saffron are shown in Figure 4.1. Crocetin (**171**) is a symmetric polyene with carboxylic acids at both ends. Crocin (**170**), the major pigment in saffron, is a crocetin-derived digentiobiosyl ester. In addition to saffron, crocin was isolated from the fruits of *Gardenia jasminoides* as well. The crocetin-derived diglucosyl ester (**172**) is also isolated from saffron, as are picrocrocin (**173**) and safranal (**174**). Picrocrocin has a bitter taste and is the chemical primarily responsible for the taste of saffron, whereas the aroma of saffron has been attributed to safranal.

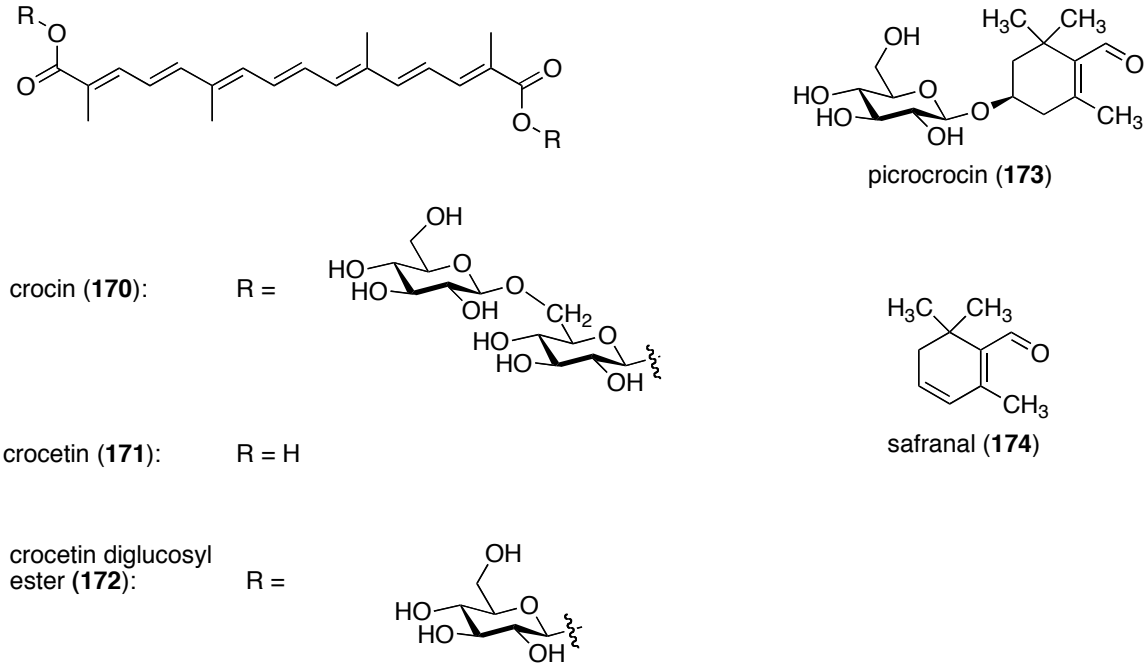

Figure 4.1 Some of the chemical components of saffron

In addition to its use as a food additive, saffron has a long history in the treatment of numerous diseases in China and India. In Chinese traditional medicine, saffron has found wide applications in the treatment of thrombus diseases, menstrual disturbances and some other diseases related to high blood viscosity.[106] Saffron has also been used to treat nervous disorders.[106] In India, saffron has been used in the treatment of cancer, heart diseases and blood diseases.[106]

Modern research has started to elucidate the component responsible for the bioactivity of saffron. Among all the components, crocin is the most interesting one as it is found to be responsible for various bioactivities. For instance, it was suggested that crocin could prevent the ethanol-induced loss of memory *in vivo*.[107] Interestingly, the authors found that the gentiobioses were important for the activity, as the crocetin diglucosyl ester was not as active as crocin. Crocin was also able to inhibit the growth of

human tumor cells *in vitro*.[108] The authors commented that due to its good water-solubility and high inhibitory growth effect, crocin was a more promising anti-cancer compound compared to other saffron components.[108] Aritake and co-workers reported that when crocin was administered to mice, non-rapid eye movement sleep was induced.[109] This result indicates that crocin has the potential to be used in the treatment of insomnia. Crocin exhibited comparable antioxidative activity to the commonly used antioxidant butylated hydroxyanisole (BHA).[110] The antioxidative activity of crocin was found to be concentration dependent. Crocin was also considered as a free radical scavenger to modulate inflammatory demyelination and neurodegeneration in multiple sclerosis,[111] and it could potentially be used in the treatment of inflammatory diseases.[111, 112] Saffron has been found to be useful in the treatment of asthma,[113, 114] although whether crocin is responsible for this activity remains to be determined.

4.1.2 Biosynthesis of crocin

Recent biosynthetic studies indicate that crocin is synthesized from zeaxanthin (**175**) (Scheme 4.1),[115, 116] one of the most common carotenoid alcohols found in nature. Zeaxanthin is biosynthesized following a mevalonate pathway, and it is produced in plants and some microorganisms. In fact, a small quantity of zeaxanthin has been isolated from saffron, which also supports these studies. In 2003, Camara and co-workers successfully expressed and purified an enzyme called zeaxanthin cleavage dioxygenase (ZCD).[115] An enzymatic reaction was performed *in vitro* using zeaxanthin as the substrate. Following the reaction, crocetin dialdehyde (**176**) was identified as the product using modern analytical techniques, such as HPLC, UV-visible spectrum and mass

spectrometry (Scheme 4.1). This enzymatic reaction was highly regio-selective, as only the 7,8 and 7',8' double bonds were cleaved. Crocetin dialdehyde is believed to be converted to crocetin (**171**) by an enzyme named aldehyde oxydoreductase, although this enzyme has not been expressed or purified to date.[115, 116]

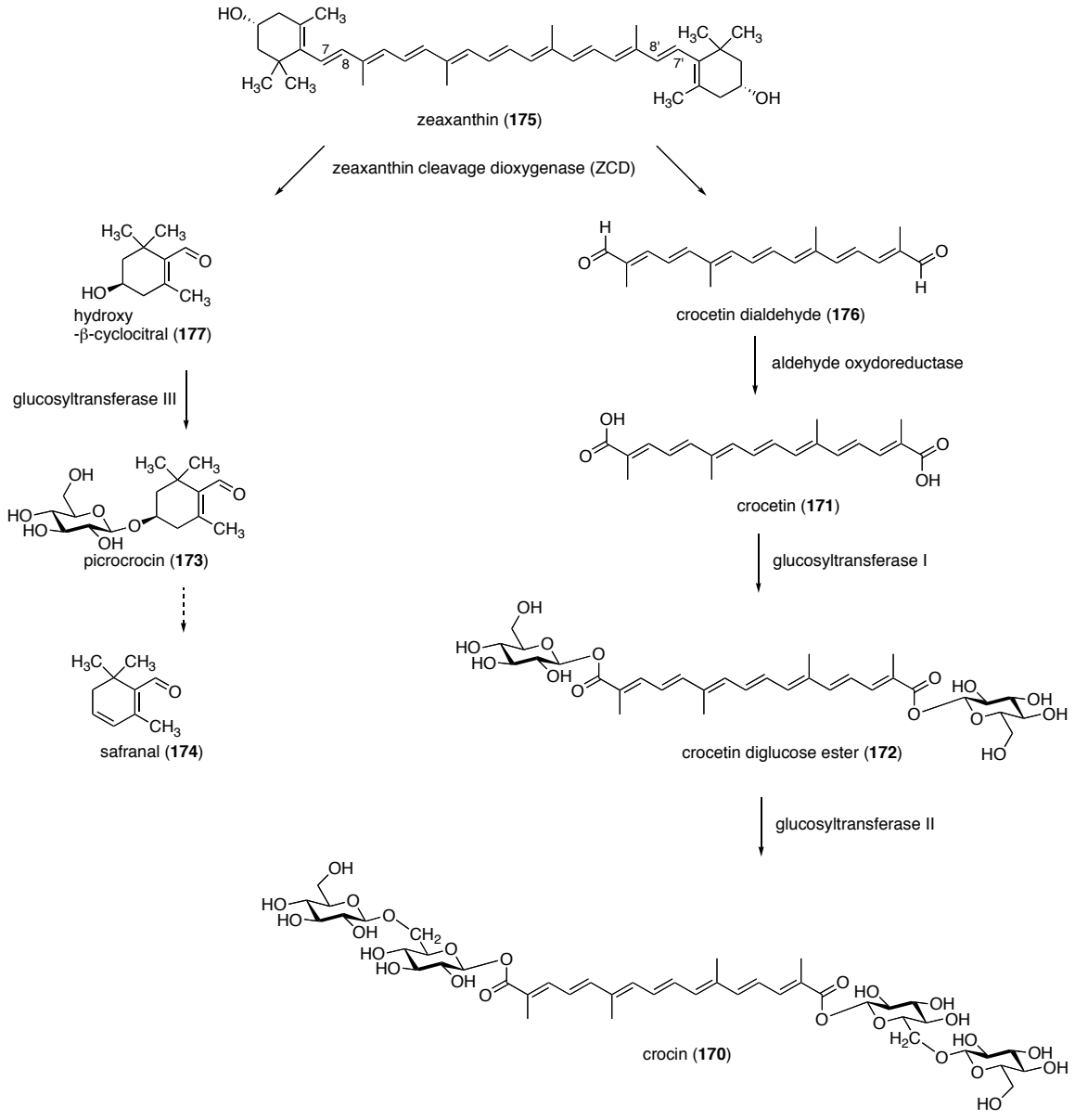

Scheme 4.1 Proposed biosynthesis of crocin (**170**)

Two UDP-glucose (UDP-Glc) glucosyltransferases are involved in the installation of the gentiobiose moiety.[117, 118] Cote and co-workers purified an enzyme from saffron cell cultures and found that this enzyme could catalyze the ester bond formation between crocetin and UDP-Glc.[117] This enzyme was highly specific for concetin and only one glucose unit was added to the carboxylic acid at each end to give crocetin diglucosyl ester as the product. No crocin was observed in this enzymatic reaction. This result indicated that more than one glucosyltransferase is involved in the biosynthesis of crocin. The second glucosyltransferase was not identified until very recently. In 2012, Mizukami and co-workers successfully expressed and purified two glucosyltransferases responsible for the final glucosylation steps in the biosynthesis of crocin in *Gardenia jasminoides*.[118] These authors found that the first glucosyltransferase UGT75L6 preferentially glucosylated the carboxylic acid of crocetin, giving crocetin diglucose ester. In contrast, a second glucosyltransferase UGT94E5 glucosylated the 6' hydroxyl groups of the glucose moiety of crocetin diglucosyl ester, yielding crocin as the product.

In addition to the evidence derived from these enzymatic reactions, the isolation of picrocrocin and safranal from saffron also supports the proposed biosynthetic pathway (Scheme 4.1).

4.1.3 Chemical synthesis of crocin related natural products

Approximately 80,000 flowers are required to harvest one kilogram of saffron.[119] Total synthesis could offer a useful alternative to obtain large quantities of crocin, however no total synthesis of crocin has been reported to date.

4.1.3.1 Chemical synthesis of carotenoids

Several synthetic strategies have been applied to the synthesis of carotenoids with symmetric polyene backbone. For instance, de Lera and co-workers reported a convergent synthesis of zeaxanthin (**175**) using a Stille reaction (Scheme 4.2).[120] Under palladium catalysis, two equivalents of iodo compound **178** were coupled to both ends of the tin compound **179** to furnish zeaxanthin in 46% yield.

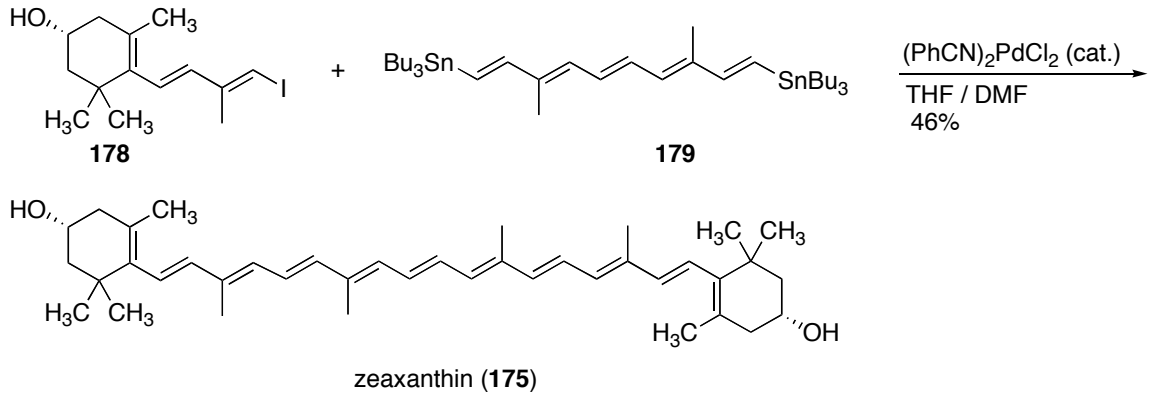

Scheme 4.2 Synthesis of zeaxanthin (**175**) using a Stille reaction[120]

Olefin metathesis is one of the most popular and efficient ways to make carbon-carbon double bonds.[121] In spite of the wide application of this reaction in the synthesis of various natural products, limited studies have been carried out to extend this methodology to the preparation of polyene natural products. Given that polyene substrates contain a large number of double bonds, site-selectivity and stereo-selectivity may become a major issue.[122] It is also possible that the polyene substrates are not stable under the reaction conditions.

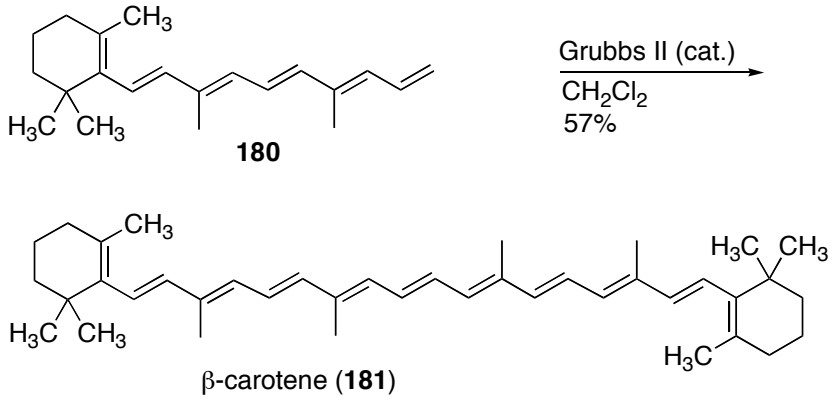

Scheme 4.3 Synthesis of β-carotene (**181**) by cross-metathesis[122]

However recent results from the de Lera group indicate that it is indeed possible to make polyene natural products effectively using olefin metathesis.[122] β-Carotene (**181**) was prepared using a Grubbs-II catalyzed cross-metathesis (CM) reaction in 57% yield (Scheme 4.3). The same protocol was also applied to the synthesis of lycopene (**182**), zeaxanthin (**175**) and isozeaxanthin (**183**) (Figure 4.2).

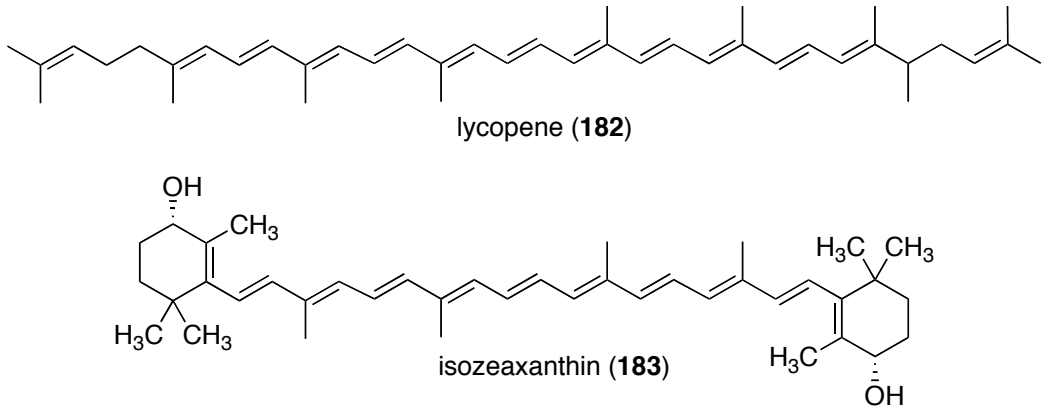

Figure 4.2 Structures of lycopene **(182)** and isozeaxanthin **(183)**

In addition to the synthesis of symmetric polyene natural products, the preparation of synthetically more challenging unsymmetric polyene compounds has also been

studied. Peridinin (**186**), a natural carotenoid, was synthesized using a modified Julia olefination reaction (Scheme 4.4).[123] Under basic conditions, the reaction of benzothiazole sulfone **184** and aldehyde **185** gave a mixture of geometric isomers **186** and **187**. The undesired *Z* isomer **187** was predominant. Fortunately, most of the *Z* isomer could be converted to the thermodynamically more stable *E* isomer by stirring in benzene for three days in the dark. Pure peridinin was isolated using preparative HPLC.

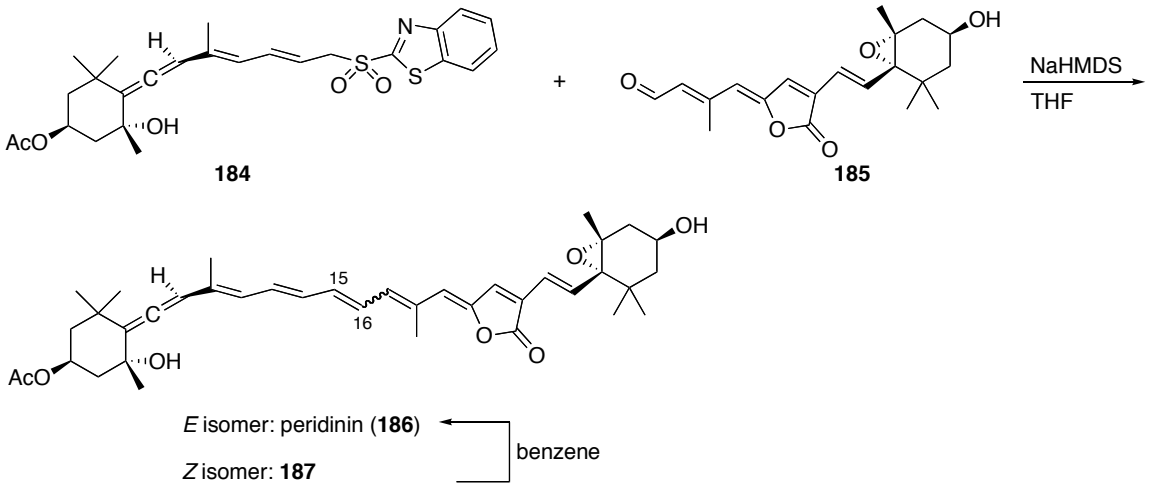

Scheme 4.4 Synthesis of peridinin (**186**) using a modified Julia olefination reaction[123]

4.1.3.2 Chemical synthesis of the polyene backbone of crocin

Crocetin dimethyl ester (**190**), a polyene backbone derivative of crocin, was synthesized using a Wittig reaction as the key step (Scheme 4.5).[124] The reaction of two equivalents of Wittig reagent **188** and dialdehyde **189** produced the desired crocetin dimethyl ester in 75% yield. Small amounts of other isomers were also isolated.

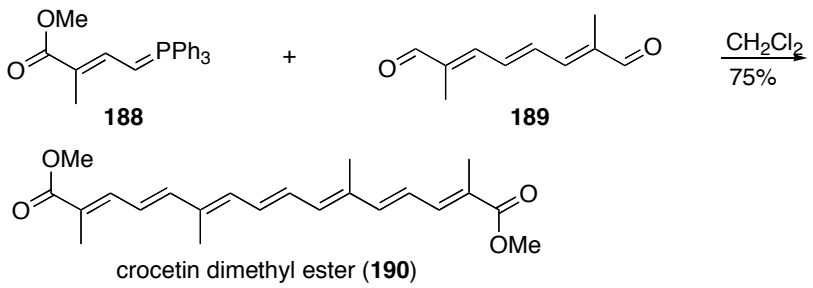

Scheme 4.5 Synthesis of crocetin dimethyl ester (**190**) using a Wittig reaction[124]

4.1.3.3 Glycosylation study of crocetin

Previously, Karrer and Kuhn were able to prepare a peracetylated derivative (**192**) of the crocetin diglucosyl ester (Scheme 4.6).[125, 126] However, the removal of acetyl groups was problematic, leading to the cleavage of the ester bond between the glucose and crocetin.

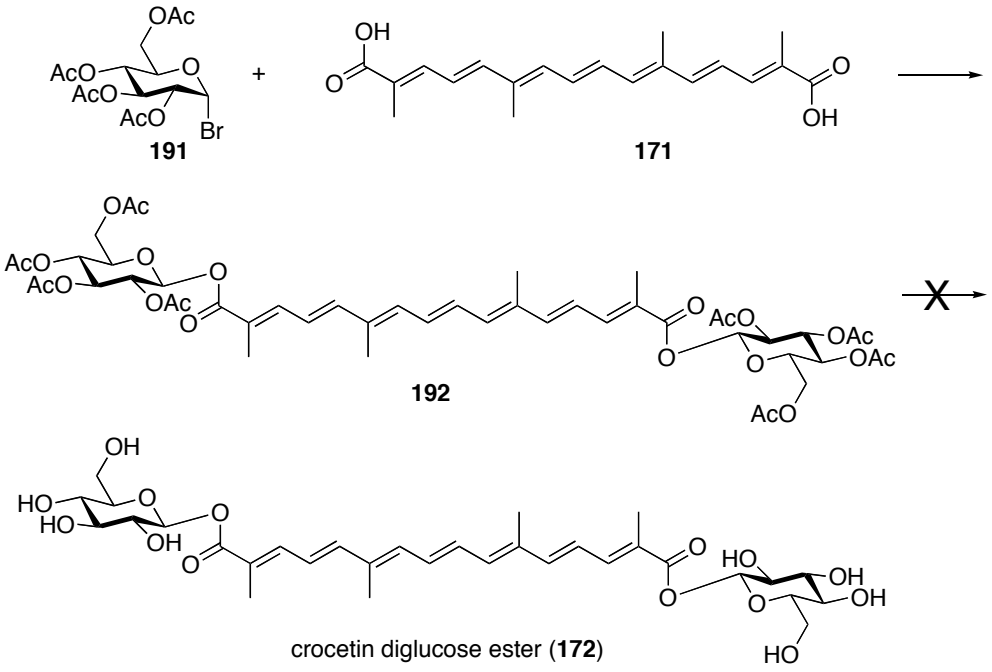

Scheme 4.6 Unsuccessful route to the synthesis of crocetin diglucosyl ester (**172**)[125, 126]

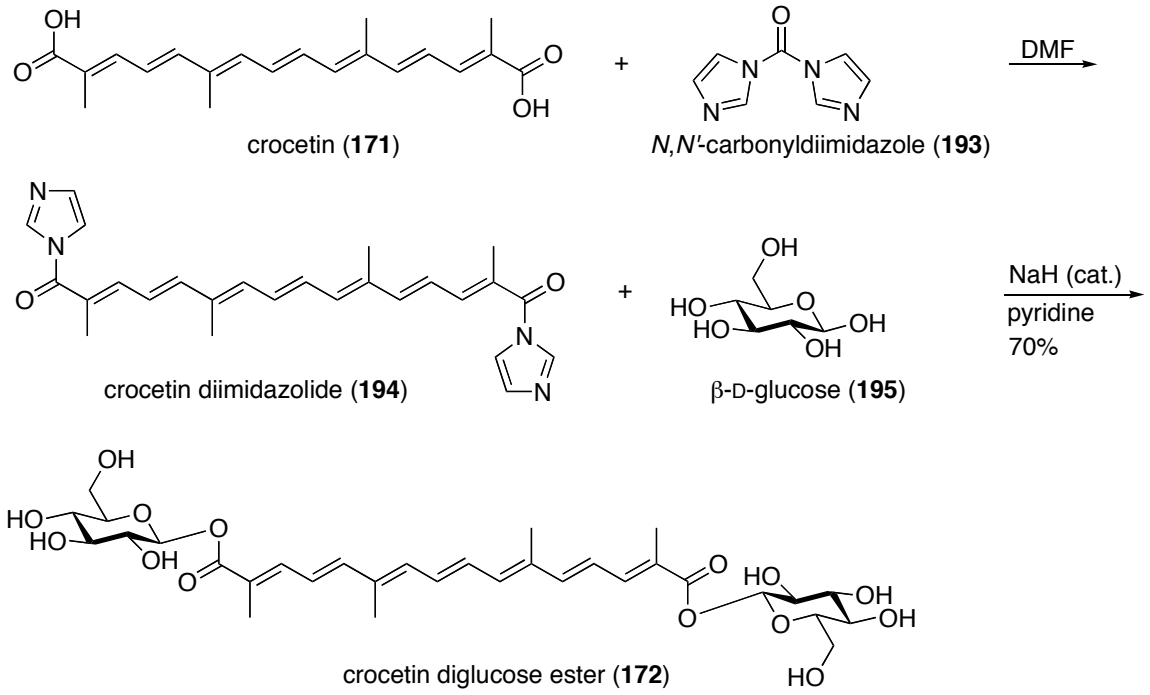

Scheme 4.7 Successful route to the synthesis of crocetin diglucosyl ester (**172**) by Pfander[125]

To solve this problem, a protecting group-free method was used by Pfander to achieve a successful synthesis of crocetin diglucosyl ester (**172**) (Scheme 4.7).[125] This synthesis involved two steps. First, the crocetin diimidazolide (**194**) was synthesized by the reaction of crocetin (**171**) with *N*,*N'*-carbonyldiimidazole (**193**). Then the desired crocetin diglucosyl ester was prepared by the reaction of the synthesized crocetin diimidazolide (**194**) with β-D-glucose (**195**) in pyridine using NaH as a catalyst. The reaction only occurred at the anomeric position, likely due to the higher acidity of the anomeric hydroxyl group compared with the other hydroxyl groups of glucose. The author also found that different reaction conditions would affect the ratio of β-anomer to

α-anomer. When DMF was used as the solvent, the undesired α-anomer was the major product.

4.2 Project objectives: chemical synthesis and biological evaluation of crocin and its analogs

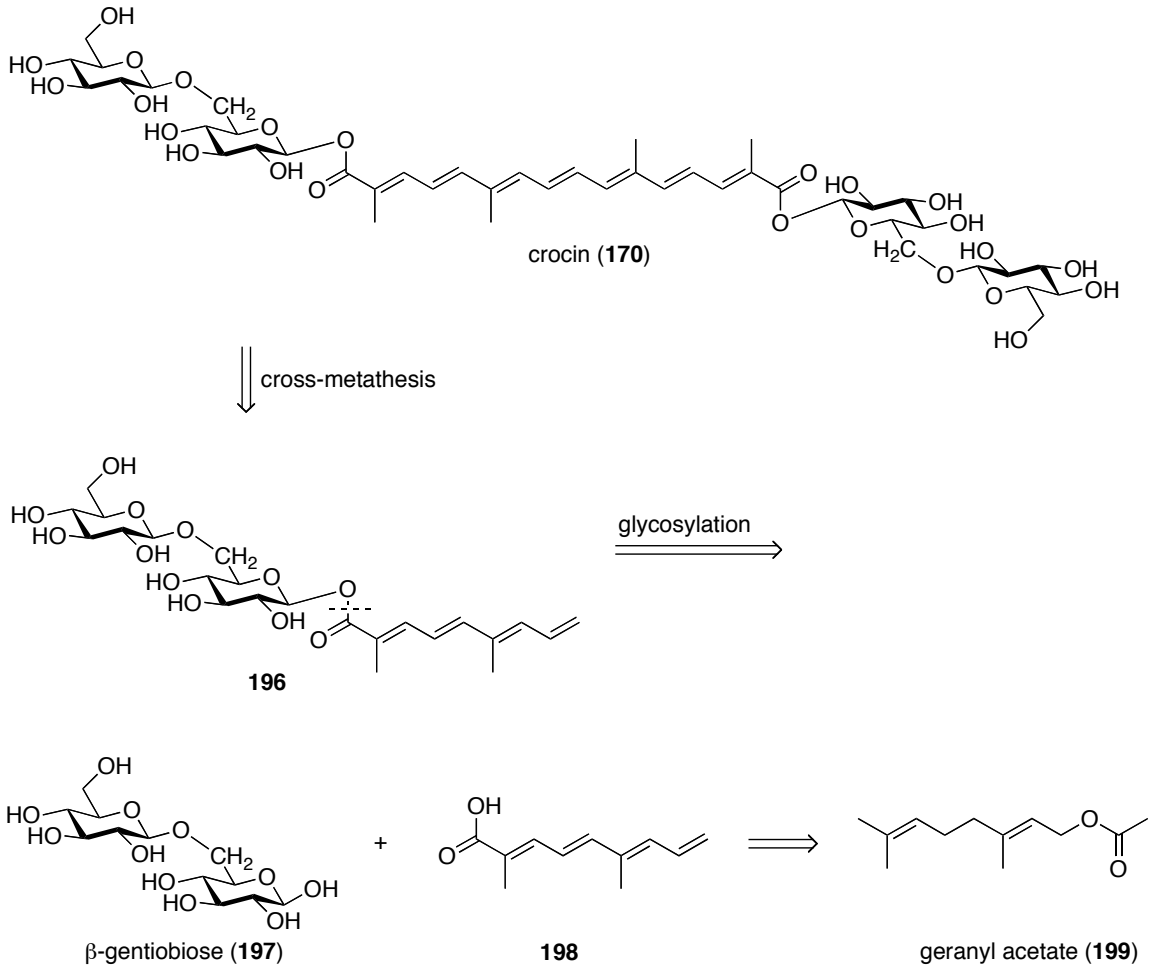

Scheme 4.8 Retrosynthetic analysis of crocin (**170**)

Through close collaboration with Dr. David Dietrich, a post-doctoral fellow in the Vederas group, the first objective was the chemical synthesis of crocin (**170**) and its analogs. The proposed retrosynthetic analysis is illustrated in Scheme 4.8. We hypothesized that crocin could be synthesized by the dimerization of compound **196** using a cross metathesis approach. To the best of our knowledge, there is no literature precedent employing a polyene-carbohydrate conjugate in an olefin metathesis. We decided to use the unprotected carbohydrate as the substrate because the deprotection might be problematic based on results observed previously by Karrer and Kuhn.[125, 126] Metathesis involving unprotected carbohydrates was achieved previously.[127, 128] Both of these two groups used aqueous conditions to solubilize the carbohydrate substrates. We envisioned that the synthesis of compound **196** could begin from acid **198** and β-gentibiose (**197**) using a protocol developed by Pfander (Scheme 4.7). The acid **198** could be readily prepared from commercially available geranyl acetate (**199**). It was expected that crocin analogs, such as crocetin diglucosyl ester (**172**), could also be prepared using the same approach. If we could successfully synthesize crocin and its analogs, the biological evaluation against inflammatory diseases, especially asthma, can be performed by the collaboration with Professor Dean Befus in the Department of Medicine, University of Alberta.

4.3 Results and discussion

4.3.1 Efforts towards chemical synthesis of crocin and its analogs

4.3.1.1 Synthesis of polyene acid 198

The synthetic route to polyene acid **198** was adapted and modified from literature procedures.[129] The commercially available geranyl acetate (**199**) was used as the starting material in our synthesis of polyene acid **198** (Scheme 4.9). SeO_2 mediated oxidation generated the desired aldehyde **200** in 30% yield.[129] The low yield was attributed to the oxidation of geranyl acetate at other allylic positions. The observation of many spots on the TLC plate after the reaction lends credence to this assumption. Attempts to further optimize the reaction were not successful. A Pinnick oxidation, followed by methylation of the resulting carboxylic acid **201** furnished methyl ester **202** in excellent yield. A second SeO_2 oxidation gave the desired racemic alcohol **203**, again in low yield. Upon conversion of this alcohol to the mesylate, exposure to DBU resulted in elimination of the mesylate yielding triene **204** as an unseparable *Z*/*E* mixture. According to the ^{1}H NMR spectrum, the ratio of *Z* to *E* isomers was 3:17. Saponification of compound **204** generated alcohol **205**, which was oxidized to the aldehyde by treatment with 2-iodoxybenzoic acid (IBX). The two isomeric aldehydes were separated by column chromatography. The desired all-*E* aldehyde **206** was obtained in 60% yield over four steps. The terminal double bond of compound **207** was installed in 94% yield using a Wittig reaction. Finally, saponification of compound **207** gave the desired polyene acid **198** in quantitative yield.

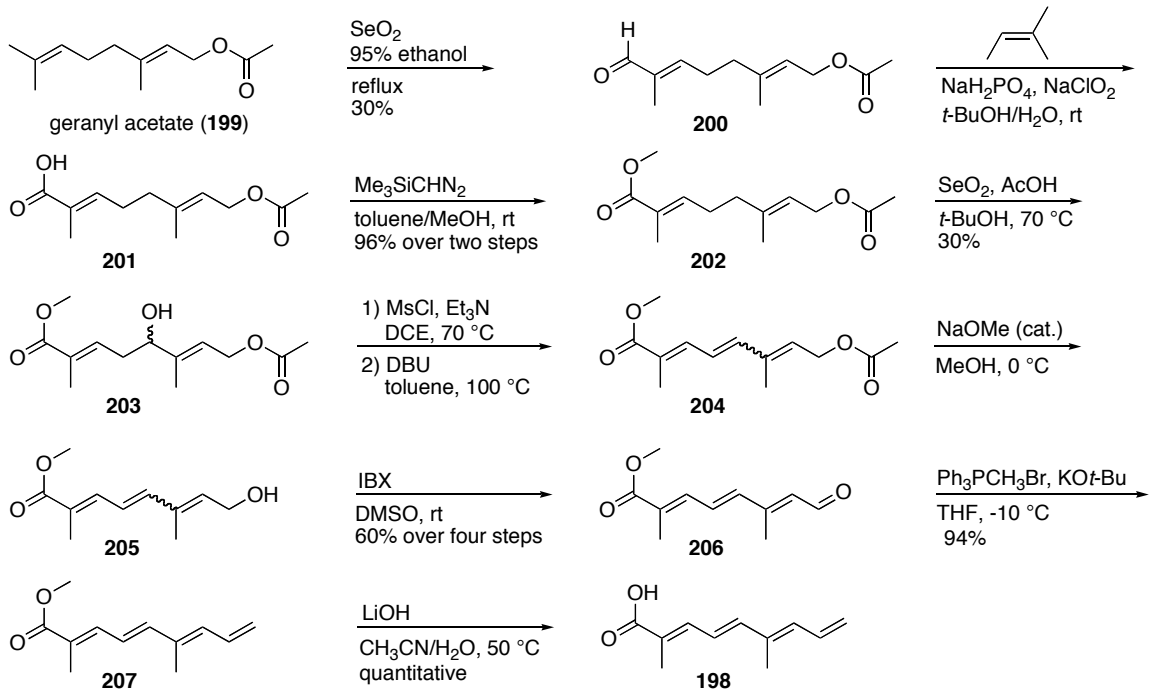

Scheme 4.9 Synthesis of polyene acid **198**

4.3.1.2 Attempts to synthesize the glucosylated polyene ester 209

With compound **198** in hand, we first tried to prepare glucosylated polyene ester **209** using the conditions reported by Pfander.[125] Compound **198** was mixed with *N,N'*-carbonyldiimidazole (**193**) in DMF (Scheme 4.10). When no starting material remained by TLC, the solvent was removed *in vacuo*. The residue was dissolved in pyridine, followed by the addition of β-D-glucose (**195**) and NaH. After workup, many signals corresponding to the anomeric proton were observed in the ^{1}H NMR spectrum. This result indicated that in our hands the glycosylation was not as selective as the literature reported.

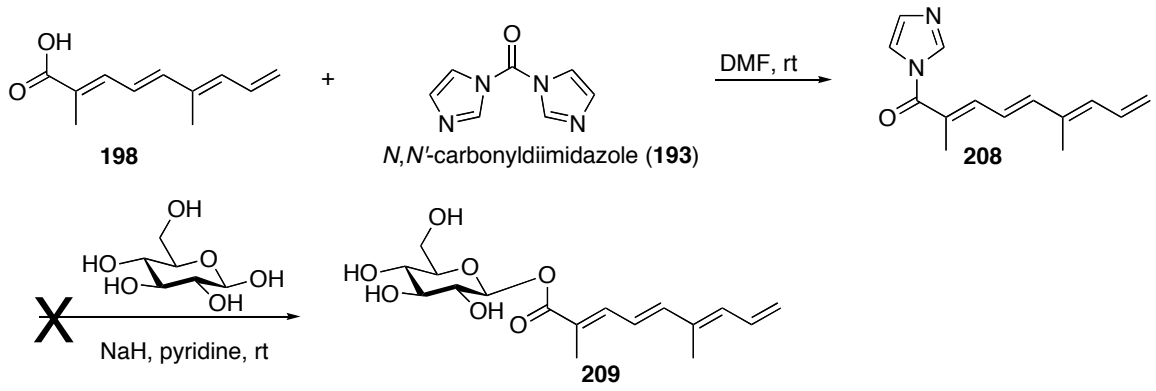

Scheme 4.10 Unsuccessful glycosylation of polyene acid **198**

After trying several different activation methods, we found that model ester **212** containing a quinoline moiety could be selectively attached to the anomeric position of β-D-glucose to give the desired glycosylated compound **213** (Scheme 4.11). In the ^{1}H NMR spectrum (Figure 4.3), only one signal corresponding to the anomeric proton was observed and the coupling constant (J = 8.0 Hz) indicating the desired β-isomer was formed.

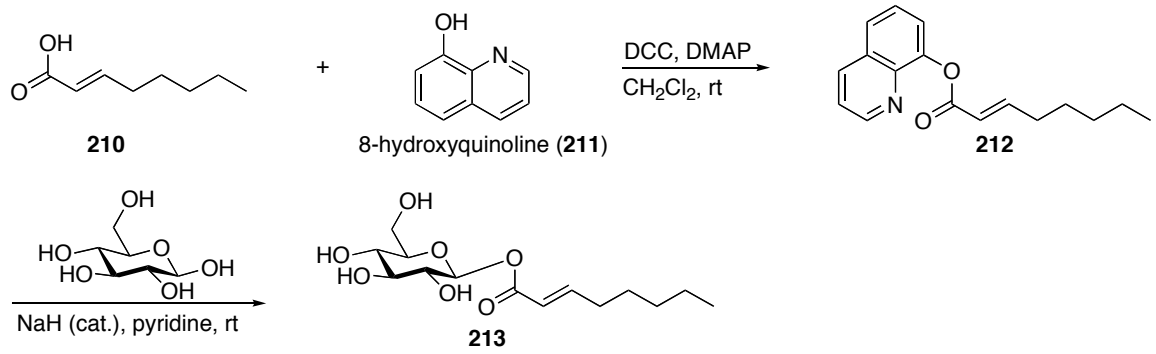

Scheme 4.11 Synthesis of the glycosylated compound **213**

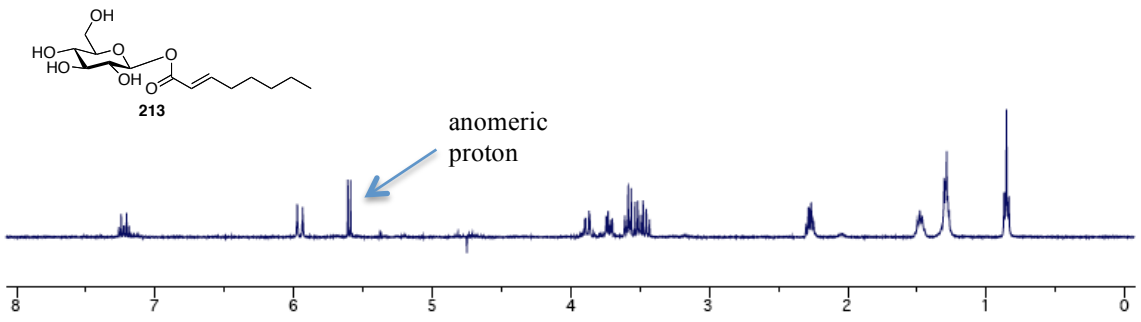

Figure 4.3 ^{1}H NMR spectrum of compound **213**

Encouraged by this result, the hydroxyquinoline esters of the polyene acid **198** and three other analogs, including retinoic acid (**219**), were synthesized in good yields (Scheme 4.12). Currently Dr. David Dietrich is working on the glycosylation of β-D-glucose with these activated esters.

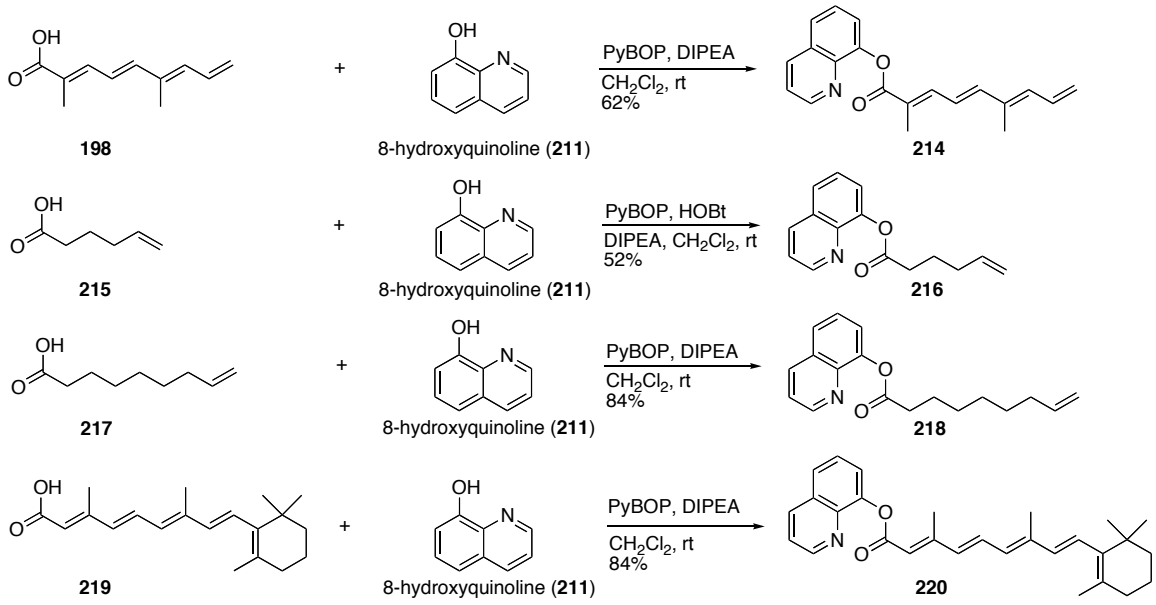

Scheme 4.12 Synthesis of the hydroxyquinoline esters of polyene acid **198** and analogs

4.4 Conclusions and future directions

Polyene acid **198** was synthesized in 10 steps from geranyl acetate with a 5% overall yield. The attempts to attach this acid to β-D-glucose using a literature method[125] were unsuccessful. In contrast, a quinoline derived activated ester **212** was reacted with β-D-glucose to give the desired product **213** as a single isomer. The hydroxyquinoline esters of the polyene acid **198** and three other analogs, including retinoic acid (**219**), were synthesized in good yields.

In the future, the activated esters will be coupled to β-D-glucose or β-gentibiose. When the glycosylated products are obtained, they will then be subjected to cross-metathesis conditions to form crocin and its analogs. Following this synthesis, the biological evaluation against inflammatory diseases, especially asthma will be conducted.

Chapter 5 : Experimental Procedures

5.1 General experimental methods

5.1.1 Reagents, solvents and purifications

All commercially available reagents were purchased from Sigma-Aldrich Canada Ltd., Fisher Scientific Ltd., Alfa Aesar Ltd., Chem-Impex International Inc., Caledon or VWR International and used without further purification unless otherwise stated. All solvents were of American Chemical Society (ACS) grade and were used without further purification unless otherwise stated. All anhydrous reactions were conducted under a positive pressure of argon using flame-dried glassware. Solvents for anhydrous reactions were distilled prior to use: dichloromethane, dichloroethane and chloroform were distilled over calcium hydride, tetrahydrofuran and diethyl ether were distilled over sodium with benzophenone as an indicator, and methanol was distilled over magnesium. HPLC grade acetonitrile, dimethylformamide, isopropyl alcohol, hexanes and methanol were used without further purification. Commercially available ACS grade solvents (>99.0% purity) were used for column chromatography without further purification. Deionized water was obtained from a Milli-Q reagent water system (Millipore Co., Milford, MA). All reactions and fractions from column chromatography were monitored by thin layer chromatography (TLC) using glass plates with a UV fluorescent indicator (normal SiO_2, Merck 60 F_{254}). One or more of the following methods were employed for visualization: UV absorption by fluorescence quenching, staining with phosphomolybdic acid in ethanol (10 g/100 mL), ninhydrin (ninhydrin : acetic acid : *n*-butanol/ 0.6 g : 6 mL : 200

mL) or permanganate ($KMnO_4$: K_2CO_3 : NaOH : H_2O/ 1.5 g : 10 g : 0.12 g : 200 mL). Flash chromatography was performed using Merck type 60, 230-400 mesh silica gel. Preparative thin layer chromatography (TLC) purification was performed using plates purchased from Analtech (1000 or 500 micros). The removal of solvents *in vacuo* was performed via evaporation under reduced pressure using a Büchi rotary evaporator.

Analytical scale high performance liquid chromatography (HPLC) was performed on one or more following systems: Beckman System Gold chromatograph equipped with a model 166 variable wavelength UV detector and a Rheodyne 7725i injector fitted with a 500 μL sample loop; Varian ProStar chromatograph equipped with model 210 pump heads, a model 325 dual wavelength UV detector, and a Rheodyne 7725i injector fitted with a 500 μL sample loop; or a Gilson chromatograph equipped with model 322 pump heads, a model 171 diode array detector, a FC 203B fraction collector, and a Rheodyne 7725i injector fitted with a 500 μL sample loop. Preparative and semi-preparative scale HPLC was performed on one or more following systems: Beckman System Gold chromatograph equipped with a model 125P solvent module, a model 166P variable wavelength UV detector, and a Rheodyne 7725i injector fitted with a 1000 μL sample loop; Gilson chromatograph equipped with model 322 pump heads, a model UV/VIS-156 detector, and a GX-271 liquid handler; Varian ProStar chromatograph equipped with model 210 pump heads, a model 325 dual wavelength UV detector, and a Rheodyne 7725i injector fitted with a 1000 μL sample loop. The columns used were Chiralcel OD column (5 μm, 4.6 x 250 mm), Vydac C_{18} (5 μm, 4.6 x 250 mm), Vydac C_8 (5 μm, 10 x 250 mm), Phenomenex C_{18} (5 μm, 21.2 x 250 mm) and Vydac C_4 (10 x 250 mm). All

HPLC solvents were filtered through a Millipore filtration system under vacuum prior to use.

5.1.2 Characterization

Optical rotations were measured on a Perkin Elmer 241 polarimeter with a microcell (10 cm, 1 mL) at ambient temperature and are reported in units of 10^{-1} deg cm^2 g^{-1}. All reported optical rotations were referenced against air and measured at the sodium D line (λ = 589.3 nm)

Infrared spectra (IR) were recorded on either a Nicolet Magna 750 FT-IR spectrometer or a Nic-Plan FT-IR microscope. The term cast refers to the evaporation of a solution on a NaCl plate.

Nuclear magnetic resonance (NMR) spectra were recorded on a Varian Inova 600, Inova 500, Inova 400, Inova 300 or Unity 500 spectrometers at 27 °C. For ^{1}H (300, 400, 500 or 600 MHz) spectra, δ values were referenced to $CDCl_3$ (7.26 ppm), CD_2Cl_2 (5.32 ppm), CD_3OD (3.30 ppm), DMSO-d_6 (2.50 ppm), or D_2O (4.79 ppm) and for ^{13}C (75, 100, 125 or 150 MHz) spectra, δ values were referenced to $CDCl_3$ (77.0 ppm), CD_2Cl_2 (53.8 ppm), CD_3OD (49.0 ppm), or DMSO-d_6 (39.5 ppm). Reported splitting patterns are abbreviated as s = singlet, d = doublet, t = triplet, q = quartet, m = multiplet.

Mass spectra (MS) were recorded on an Agilent Technologies 6220 oaTOF, a Kratos AEIMS-50, an Applied BioSystems Mariner BioSpectrometry Workstation, or a Perspective Biosystems Voyager™ Elite MALDI-TOF MS using either α-cyano-4-hydroxycinnamic acid (CHCA) or 3,5-dimethoxy-4-hydroxycinnamic acid (sinapinic acid) as a matrix. LC MS/MS was performed on a Waters (Micromass) Q-TOF Premier. For MALDI-TOF MS, a typical sample preparation is described as follows. A solution of

sample peptide (1 μL) in 0.1% TFA (aq.) is mixed in a 1:1 ratio (vol/vol) with a stock solution of sinapinic acid (10 mg/mL) in 50% acetonitrile containing 0.1% TFA (aq.). To prepare the sample plate, a sinapinic acid layer (0.7μL; 10mg/mL sinapinic acid in 3:2 acetone:methanol) is pipetted onto a stainless steel target plate. The solvent is allowed to evaporate, leaving a thin layer of sinapinic acid on the surface of the plate. The sample-matrix solution (0.6 μL) is then spotted onto the dried layer of sinapinic acid and allowed to dry.

5.1.3 General method for loading the first amino acid onto Wang resin

A 3-necked round bottom flask equipped with a stirring bar was flame dried and cooled under argon. The amino acid (10.0 equiv.) was dissolved in dry CH_2Cl_2 and cooled to 0 °C. Diisopropylcarbodiimide (DIC) (5.0 equiv.) was added and the reaction was stirred at 0 °C for 20 mins. The reaction mixture was then concentrated *in vacuo* and re-dissolved in DMF (10 mL). Wang resin (1.0 equiv.) was added to a manual SPPS vessel and washed with CH_2Cl_2 (2 x 5 mL) and DMF (5 mL). The resin was pre-swollen by bubbling with argon in DMF (5 mL) for 1 hour. The activated anhydride solution was added to the resin followed by 4-dimethylaminopyridine (DMAP) (0.1 equiv.) and bubbled with argon for 2 hours. The solvent was removed by filtration and the resin washed with DMF (3 x 5 mL). The resin was then capped by bubbling with argon in 20 % acetic anhydride in DMF (10 mL) for 15 mins and filtered. The resin was washed with DMF (3 x 5 mL) and CH_2Cl_2 (3 x 5 mL) and dried under argon.

5.1.4 General method for loading the first amino acid onto 2-chloro trityl resin

In a manual SPPS vessel 2-chlorotrityl resin (1.0 equiv.) was bubbled with argon in CH_2Cl_2 for 15 mins. The resin was then filtered and a solution of diisopropylethyl amine (DIPEA) (8.0 equiv.) and the amino acid (4.0 equiv.) in CH_2Cl_2 was added. The resulting slurry was shaking for 2.5 hours, filtered and washed CH_2Cl_2 (3 x 10 ml). The resin was then end-capped by bubbling with argon in MeOH: DIPEA: CH_2Cl_2 (10:5:85) for 15 mins. The solution was removed by filtration and the resin then washed with DMF (3 x 10 mL) and CH_2Cl_2 (3 x 10 mL) and dried under argon.

5.1.5 General method for manual solid-phase peptide synthesis

All amino acids for manual synthesis were coupled using commercially available Fmoc protected amino acid (5.0 equiv. relative to resin), benzotriazole-1-yl-oxy-tris-pyrrolidinophosphonium hexafluorophosphate (PyBOP) (4.9 equiv.) and hydroxybenzotriazole (HOBt) (5.0 equiv.) as the activating agents and *N*-methylmorpholine (4.9 equiv.) in DMF (5 mL). The above solution was pre-activated for 5 min and mixed with the pre-swelled resin. The mixture was then bubbled with argon for 2 h. The resin was capped with a solution of 20% acetic anhydride in DMF for 10 min. Removal of the Fmoc group was completed using a solution of 20% piperidine in DMF for 5 min. The completion of deprotection was monitored by disappearance of the absorbance at 301 nm (dibenzofulvene-piperidine adduct). The following side chain protecting groups were used for synthesis: Fmoc-Ser(O-*t*Bu)-OH, Fmoc-Glu(O-*t*Bu)-OH, Fmoc-Asn(Trt)-OH, Fmoc-Cys(Trt)-OH and Fmoc-Gln(Trt)-OH. Peptides were cleaved from resins using standard conditions of 95% TFA: 2.5% TIPS: 2.5% H_2O (method I) or

96% TFA: 2% TIPS: 2% H_2O (method II). Peptides were filtered through a plug of cotton or glass wool and the solvent was removed *in vacuo*. The crude peptide was then repeatedly triturated with cold ether until only a white solid was left.

5.1.6 General method for automated solid-phase peptide synthesis using ABI 433A

Automated synthesis was performed on an ABI 433A instrument (Applied Biosystems) with UV monitoring capability (Perkin Elmer) detecting at 301 nm using standard *Fastmoc*™ methodology from Applied Biosystems. This method used the coupling agents 2-(1*H*-benzotriazole-1-yl)-1,1,3,3-tetramethyl-uronium-hexafluoro-phosphate (HBTU) and hydroxybenzotriazole (HOBt) to pre-activate the corresponding Fmoc protected amino acid for 2.1 min. The pre-activated solution was then transferred to the reaction vessel and the coupling reaction occurred. After completion of coupling, the resin was capped using a solution of acetic anhydride, HOBt and diisopropylethyl amine (DIPEA). Removal of the Fmoc group was done using piperidine in *N*-methyl-2-pyrrolidone (NMP) and monitored by disappearance of the absorbance at 301 nm. The entire cycle for each residue was approximately 50 min. The following side chain protecting groups were used for synthesis: Fmoc-Ser(O-*t*Bu)-OH, Fmoc-Glu(O-*t*Bu)-OH, Fmoc-Thr(O-*t*Bu)-OH, Fmoc-D-Tyr(O-*t*Bu)-OH and Fmoc-Trp(Boc)-OH. Pseudo-proline Fmoc-Ala-Ser(ψMe,Me Pro)-OH and dipeptide Fmoc-Ala-(Dmb)Gly-OH were incorporated into certain positions to prevent peptide aggregation. Peptides were cleaved using 95% TFA: 2.5% TIPS: 2.5% H_2O (method I). Peptides were filtered through a plug of cotton or glass wool and the solvent was removed *in vacuo*. The crude peptide was then repeatedly triturated with cold ether until only a white solid remained.

5.1.7 General method for automated solid-phase peptide synthesis using CEM Liberty 1

Automated synthesis was completed on a CEM Liberty 1 Microwave Peptide Synthesizer. Commercially available Fmoc protected amino acids and synthesized amino acids were loaded onto the peptide synthesizer as 0.2 M DMF solutions. All amino acid subunits were coupled using 2-(1*H*-benzotriazole-1-yl)-1,1,3,3-tetramethyl-uronium-hexafluoro-phosphate (HBTU) and hydroxybenzotriazole (HOBt) as the activating agents and heated to 70 °C (50 °C for cysteines) for a 5 min coupling time. Removal of the Fmoc group was completed using piperidine in NMP and monitored by disappearance of the absorbance at 301 nm. The following side chain protecting groups were employed for synthesis: Fmoc-Ser(O-*t*Bu)-OH, Fmoc-Glu(O-*t*Bu)-OH, Fmoc-Asn(Trt)-OH and Fmoc-Gln(Trt)-OH. Peptides were cleaved using a standard condition of 95% TFA: 2.5% TIPS: 2.5% H_2O (method I). Peptides were filtered through a plug of cotton or glass wool and the solvent was removed *in vacuo*. The crude peptide was then repeatedly triturated with cold ether until only a white solid remained.

5.1.8 HPLC purification methods

All peptides were purified until only a single peak was seen in an HPLC chromatogram. All reported peptides were purified and assessed of purity using one of the following methods.

System A:

0-32 min: 10% isopropyl alcohol / 90% hexanes

Flow rate: 1.0 mL/min

Detected at 254 nm

System B:

0-5 min: 5% CH_3CN/ 95% H_2O (0.1% TFA)

5-30 min: 5%- 45% CH_3CN ramp

30-35 min: 45%- 95% CH_3CN ramp

35-40 min: 95% CH_3CN/ 5% H_2O (0.1% TFA)

40-45 min: 95%- 5% CH_3CN ramp

45-50 min: 5% CH_3CN/ 95% H_2O (0.1% TFA)

Column: Vydac C_{18} (5 μm, 4.6 x 250 mm)

Flow rate: 1.2 mL/min

Detected at 220 nm

System C:

0-5 min: 5% CH_3CN/ 95% H_2O (0.1% TFA)

5-30 min: 5%- 40% CH_3CN ramp

30-35 min: 40%- 95% CH_3CN ramp

35-40 min: 95% CH_3CN/ 5% H_2O (0.1% TFA)

40-41 min: 95%- 5% CH_3CN ramp

41-46 min: 5% CH_3CN/ 95% H_2O (0.1% TFA)

Column: Vydac C_{18} (5 μm, 4.6 x 250 mm)

Flow rate: 1.0 mL/min

Detected at 220 nm

System D:

0-5 min: 5% CH_3CN/ 95% H_2O (0.1% TFA)

5-30 min: 5%- 40% CH_3CN ramp

30-35 min: 40%- 95% CH_3CN ramp

35-40 min: 95% CH_3CN/ 5% H_2O (0.1% TFA)

40-41 min: 95%- 5% CH_3CN ramp

41-46 min: 5% CH_3CN/ 95% H_2O (0.1% TFA)

Column: Phenomenex C_{18} (5 μm, 21.2 x 250 mm)

Flow rate: 10 mL/min

Detected at 220 nm

System E:

0-5 min: 40% CH_3CN/ 60% H_2O (0.1% TFA)

5-35 min: 40%- 50% CH_3CN ramp

35-37 min: 50%- 90% CH_3CN ramp

37-40 min: 90% CH_3CN/ 10% H_2O (0.1% TFA)

40-42 min: 90%- 40% CH_3CN ramp

42-45 min: 40% CH_3CN/ 60% H_2O (0.1% TFA)

Column: Vydac C_4 (10 x 250 mm)

Flow rate: 5.0 mL/min

Detected at 220 nm

System F:

0-5 min: 5% CH_3CN/ 95% H_2O (0.1% TFA)

5-30 min: 5%- 95% CH_3CN ramp

30-37 min: 95% CH_3CN/ 5% H_2O (0.1% TFA)

37-40 min: 95%- 5% CH_3CN ramp

40-43 min: 5% CH_3CN/ 95% H_2O (0.1% TFA)

Column: Vydac C_8 (5 μm, 10 x 250 mm)

Flow rate: 3 mL/min

Detected at 220 nm

5.1.9 Assay for testing antimicrobial activity using a spot-on-lawn method

Antimicrobial activity was measured using a spot-on-lawn activity assay. Molten soft agar (10 mL) was inoculated with an overnight culture of *Bacillus firmus* (100 μL, 1% inoculation), and poured over a hard agar plate and allowed to solidify. Then an aliquot of the sample (10 μL) was spotted on the plate and allowed to dry. An aliquot of Trn-β (10 μL) was used as a positive control. Solvent was used as a negative control. The plate was then incubated overnight at 37 °C. Activity was measured as zones of inhibited growth.

5.1.10 Attempts of racemic crystallization of crotalphine using a robotic screen

Crystallization screening conditions were based on the commercially available kits, including JCSG I, JCSG II, Hampton index and crystal screen. Formation of crystals was attempted by vapor diffusion in sitting drops at room temperature. The drops were prepared by a robot by mixing 0.2 μL of peptide solution with 0.2 μL of reservoir solution and placed besides 1 mL of reservoir solution. The peptide solution was manually prepared and it was made of equal amount of L-crotalphine and D-crotalphine. No crystal was formed after one month.

5.2 Synthesis and characterization of compounds

(*R*)-(3-methyloxetan-3-yl)methyl 2-(((9*H*-fluoren-9-yl)methoxy)carbonylamino)-3-(*tert*-butyldisulfanyl)propanoate (29)

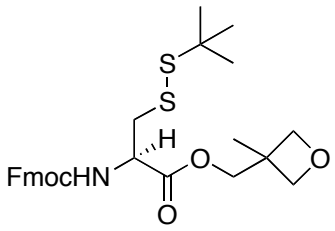

Fmoc-L-Cys(S-*t*-Bu)-OH (**26**) (21.58 g, 50.0 mmol, 1.0 equiv.) was dissolved in dry CH_2Cl_2 (200 mL) and added dropwise to a stirred solution of DCC (15.45 g, 75.0 mmol, 1.5 equiv.), DMAP (305.0 mg, 2.5 mmol, 0.05 equiv.), and 3-methyl-3-(hydroxymethyl)-oxetane (**28**) (7.41 mL, 75.0 mmol, 1.5 equiv.) cooled to 0 °C. After 90 min following completion of addition, the solution was filtered to remove dicyclohexylurea (DCU). It was then washed with 1% NH_4Cl (2 x 200 mL), 5% $NaHCO_3$ (1 x 200 mL), brine (1 x 200 mL), dried (Na_2SO_4), and evaporated to dryness, the product was purified by flash chromatography (silica gel, 2:1 hexanes : EtOAc), yielding 18.81 g (73%) of colorless sticky oil.

$[\alpha]_D$ -3.0° (*c* 1.20, $CHCl_3$); IR (Microscopy) 3312, 3065, 3018, 2962, 2875, 1725, 1529, 1451 cm^{-1}; ^1H NMR ($CDCl_3$, 400 MHz): 7.76 (d, 2H, *J* = 7.6 Hz, Fmoc-H), 7.62 (d, 2H, *J* = 7.2 Hz, Fmoc-H), 7.40 (t, 2H, *J* = 7.6 Hz, Fmoc-H), 7.32 (t, 2H, *J* = 7.6 Hz, Fmoc-H), 5.88 (d, 1H, *J* = 8.0 Hz, NH), 4.75 (m, 1H, Cys-H_α), 4.54-4.21 (m, 9H, Fmoc C<u>H</u>CH_2, Fmoc CHC<u>H</u>$_2$, 3 oxetane CH_2O), 3.26 (dd, 1H, *J* = 13.6, 4.8 Hz, Cys-$H_{\beta 1}$), 3.16 (dd, 1H, *J* = 13.6, 5.6 Hz, Cys-$H_{\beta 2}$), 1.35 (s, 3H, oxetane CH_3), 1.34 (s, 9H, -$C(CH_3)_3$); ^{13}C NMR ($CDCl_3$, 100 MHz): δ 170.6, 155.6, 143.8, 141.3, 127.7, 127.1, 125.1, 120.0,

79.4, 70.0, 67.3, 53.9, 48.4, 47.1, 42.6, 39.1, 29.8, 21.1; HRMS (ES) Calcd for $C_{27}H_{33}NO_5S_2Na[M+Na]^+$ 538.1692, found 538.1699.

(*S*)-(3-methyloxetan-3-yl)methyl 2-(((9*H*-fluoren-9-yl)methoxy)carbonylamino)-3-(*tert*-butyldisulfanyl)propanoate (30)

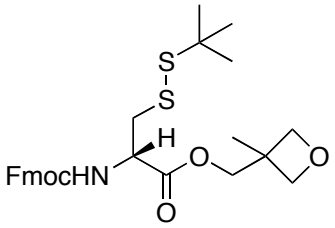

Fmoc-D-Cys(S-*t*-Bu)-OH (**27**) (9.45 g, 21.9 mmol, 1.0 equiv.) was dissolved in dry CH_2Cl_2 (100 mL) and added dropwise to a stirred solution of DCC (6.76 g, 32.8 mmol, 1.5 equiv.), DMAP (133.5 mg, 1.1 mmol, 0.05 equiv.), and 3-methyl-3-(hydroxymethyl)-oxetane (**28**) (3.24 mL, 32.8 mmol, 1.5 equiv.) cooled to 0 °C. After 70 min following completion of addition, the solution was filtered to remove DCU. It was then washed with 1% NH_4Cl (2 x 80 mL), 5% $NaHCO_3$ (1 x 80 mL), brine (1 x 80 mL), dried (Na_2SO_4), and evaporated to dryness. The product was purified by flash chromatography (silica gel, 2:1 hexanes : EtOAc), yielding 6.24 g (55%) of colorless sticky oil.

$[\alpha]_D$ 3.0° (*c* 0.91, $CHCl_3$); IR ($CHCl_3$ cast) 3320, 3066, 3018, 2962, 2875, 1725, 1529, 1451 cm^{-1}; ^1H NMR ($CDCl_3$, 500 MHz): 7.77 (d, 2H, *J* = 7.5 Hz, Fmoc-H), 7.62 (d, 2H, *J* = 7.5 Hz, Fmoc-H), 7.41 (t, 2H, *J* = 7.5 Hz, Fmoc-H), 7.32 (t, 2H, *J* = 7.5 Hz, Fmoc-H), 5.78 (d, 1H, *J* = 8.0 Hz, NH), 4.75 (m, 1H, Cys-H_α), 4.54-4.24 (m, 9H, Fmoc C<u>H</u>CH_2, Fmoc CHC<u>H</u>$_2$, 3 oxetane CH_2O), 3.26 (dd, 1H, *J* = 14.0, 5.0 Hz, Cys-$H_{\beta 1}$), 3.17

(dd, 1H, J = 14.0, 5.0 Hz, Cys-$H_{\beta 2}$), 1.36 (s, 3H, oxetane CH_3), 1.34 (s, 9H, -$C(CH_3)_3$); ^{13}C NMR ($CDCl_3$, 125 MHz): δ 170.6, 155.6, 143.8, 141.3, 127.7, 127.1, 125.2, 120.0, 79.4, 70.0, 67.3, 53.9, 48.4, 47.1, 42.6, 39.1, 29.8, 21.2; HRMS (ES) Calcd for $C_{27}H_{33}NO_5S_2Na[M+Na]^+$ 538.1692, found 538.1686.

(*R*)-(9*H*-fluoren-9-yl)methyl 2-(*tert*-butyldisulfanyl)-1-(4-methyl-2,6,7-trioxabicyclo[2.2.2]octan-1-yl)ethylcarbamate (31)

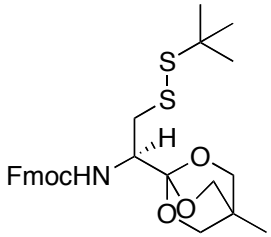

Fmoc-L-Cys(S-*t*-Bu)-oxetane ester (**29**) (11.00 g, 21.4 mmol, 1.0 equiv.) was dissolved in dry $CHCl_3$ (60 mL) and cooled to 0 °C under Ar. BF_3•Et_2O (6.70 mL, 53.4 mmol, 2.5 equiv.) was added dropwise, and the solution was stirred and warmed to room temperature. After 90 min, Et_3N (14.70 mL, 106.8 mmol, 5 equiv.) was added, and after stirring for another 10 min, the solution was evaporated to dryness. The product was purified by flash chromatography (silica gel, 3:1 hexanes : EtOAc), yielding 7.35 g (67%) of a white powder.

$[\alpha]_D$ -80.0° (*c* 1.83, CH_2Cl_2); IR (CH_2Cl_2 cast) 3349, 3065, 3019, 2960, 2880, 1729, 1517, 1451 cm^{-1}; ^1H NMR (CD_2Cl_2, 400 MHz): 7.80 (d, 2H, J = 7.6 Hz, Fmoc-H), 7.67 (d, 2H, J = 7.6 Hz, Fmoc-H), 7.42 (t, 2H, J = 7.6 Hz, Fmoc-H), 7.34 (t, 2H, J = 7.6 Hz, Fmoc-H), 5.12 (d, 1H, J = 10.4 Hz, NH), 4.46-4.24 (m, 3H, Fmoc C<u>H</u>CH_2, Fmoc CHC<u>H</u>$_2$), 4.13 (dt, 1H, J = 10.4, 3.6 Hz, Cys-H_α), 3.91 (s, 6H, 3 ortho ester OCH_2), 3.17

(dd, 1H, J = 13.6, 3.6 Hz, Cys-$H_{\beta 1}$), 2.79 (dd, 1H, J = 13.6, 3.6 Hz, Cys-$H_{\beta 2}$), 1.35 (s, 9H, -$C(CH_3)_3$), 0.79 (s, 3H, ortho ester CH_3); ^{13}C NMR (CD_2Cl_2, 100 MHz): δ 156.5, 144.6, 141.7, 128.0, 127.5, 125.7, 120.3, 108.4, 73.2, 67.2, 55.2, 48.0, 47.7, 42.8, 31.0, 30.1, 14.4; HRMS (ES) Calcd for $C_{27}H_{33}NO_5S_2Na[M+Na]^+$ 538.1692, found 538.1685. Chiral HPLC (Chiralcel OD) analyses using solvent system A indicated 99% *e.e.* t_R of the major isomer was 21.0 min and t_R of the minor isomer was 23.5 min.

(*S*)-(9*H*-fluoren-9-yl)methyl 2-(*tert*-butyldisulfanyl)-1-(4-methyl-2,6,7-trioxabicyclo[2.2.2]octan-1-yl)ethylcarbamate (32)

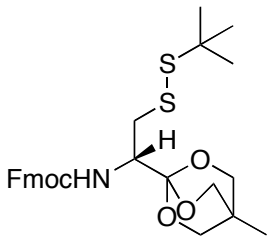

Fmoc-D-Cys(S-*t*-Bu)-oxetane ester (**30**) (6.24 g, 12.1 mmol, 1.0 equiv.) was dissolved in dry $CHCl_3$ (40 mL) and cooled to 0 °C under Ar. BF_3•Et_2O (3.81 mL, 30.3 mmol, 2.5 equiv.) was added dropwise, and the solution was stirred and warmed to room temperature. After 90 min, Et_3N (8.30 mL, 60.5 mmol, 5 equiv.) was added, and after stirring for another 15 min, the solution was evaporated to dryness. The product was purified by flash chromatography (silica gel, 3:1 hexanes : EtOAc), yielding 4.37 g (70%) of a white powder.

$[\alpha]_D$ 91.2° (*c* 1.96, CH_2Cl_2); IR (CH_2Cl_2 cast) 3347, 3065, 3019, 2960, 2880, 1728, 1517, 1451 cm^{-1}; ^1H NMR (CD_2Cl_2, 500 MHz): 7.79 (d, 2H, J = 7.5 Hz, Fmoc-H), 7.65 (d, 2H, J = 7.5 Hz, Fmoc-H), 7.41 (t, 2H, J = 7.5 Hz, Fmoc-H), 7.33 (t, 2H, J = 7.5

Hz, Fmoc-H), 5.06 (d, 1H, J = 10.5 Hz, NH), 4.44-4.24 (m, 3H, Fmoc C<u>H</u>CH_2, Fmoc CHC<u>H</u>$_2$), 4.09 (dt, 1H, J = 10.5, 3.5 Hz, Cys-H_α), 3.91 (s, 6H, 3 ortho ester OCH_2), 3.15 (dd, 1H, J = 13.5, 3.5 Hz, Cys-$H_{\beta 1}$), 2.77 (dd, 1H, J = 13.5, 3.5 Hz, Cys-$H_{\beta 2}$), 1.33 (s, 9H, -$C(CH_3)_3$), 0.80 (s, 3H, ortho ester CH_3); ^{13}C NMR (CD_2Cl_2, 125 MHz): δ 156.4, 144.6, 141.6, 128.0, 127.4, 125.6, 120.3, 108.3, 73.2, 67.2, 55.2, 48.0, 47.7, 42.8, 31.0, 30.1, 14.4; HRMS (ES) Calcd for $C_{27}H_{33}NO_5S_2Na[M+Na]^+$ 538.1692, found 538.1682. Chiral HPLC (Chiralcel OD) analyses using solvent system A indicated 99% *e.e*. t_R of the major isomer was 23.5 min and t_R of the minor isomer was 21.0 min.

(*R*)-(9*H*-fluoren-9-yl)methyl 1-(4-methyl-2,6,7-trioxabicyclo[2.2.2]octan-1-yl)-2-(pyridin-2-yldisulfanyl)ethylcarbamate (40)

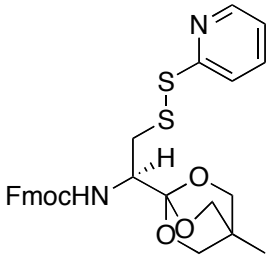

Fmoc-L-Cys(S-*t*-Bu)-cyclic-ortho-ester (**31**) (7.35 g, 14.3 mmol, 1.0 equiv.) was dissolved in THF (50 mL) and degassed for 20 min. PBu_3 (8.80 mL, 35.7 mmol, 2.5 equiv.) was added, and after stirring for 25 min, water (5 mL) was added. After stirring for another 20 h, the above solution was added dropwise to a degassed solution of 2, 2'-pyridine disulfide (**39**) (12.58 g, 57.1 mmol, 4.0 equiv.) in THF (50 mL) cooled to 0 °C under Ar. After 3.5 h following completion of addition, the solution was evaporated to dryness. The product was purified by flash chromatography (silica gel, 1:1 hexanes : EtOAc), yielding 2.34 g (31% for two steps) of a white powder.

$[\alpha]_D$ -98.9° (*c* 1.13, $CHCl_3$); IR ($CHCl_3$ cast) 3335, 3047, 2938, 2880, 1725, 1518, 1448 cm^{-1}; ^1H NMR ($CDCl_3$, 400 MHz): 8.45 (d, 1H, *J* = 4.4 Hz, Pyr-H), 7.76 (d, 2H, *J* = 7.2 Hz, Fmoc-H), 7.72-7.54 (m, 4H, 2 Fmoc-H, 2 Pyr-H), 7.39 (t, 2H, *J* = 7.2 Hz, Fmoc-H), 7.31 (t, 2H, *J* = 7.2 Hz, Fmoc-H), 7.03 (t, 1H, *J* = 6.0 Hz, Pyr-H), 5.45 (d, 1H, *J* = 10.0 Hz, NH), 4.45-4.21 (m, 4H, Cys-H_α, Fmoc C<u>H</u>CH_2, Fmoc CHC<u>H</u>$_2$), 3.88 (s, 6H, 3 ortho ester OCH_2), 3.26 (dd, 1H, *J* = 13.6, 3.6 Hz, Cys-$H_{\beta 1}$), 3.04 (dd, 1H, *J* = 13.6, 4.4 Hz, Cys-$H_{\beta 2}$), 0.77 (s, 3H, ortho ester CH_3); ^{13}C NMR ($CDCl_3$, 100 MHz): δ 160.2, 156.4, 149.6, 144.1, 141.3, 137.0, 127.6, 127.1, 125.3, 120.5, 119.9, 119.8, 108.0, 72.8, 67.0, 54.6, 47.2, 41.4, 30.6, 14.3; HRMS (ES) Calcd for $C_{28}H_{28}N_2O_5S_2Na[M+Na]^+$ 559.1332, found 559.1324.

(*S*)-(9*H*-fluoren-9-yl)methyl 1-(4-methyl-2,6,7-trioxabicyclo[2.2.2]octan-1-yl)-2-(pyridin-2-yldisulfanyl)ethylcarbamate (41)

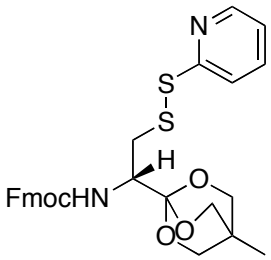

Fmoc-D-Cys(S-*t*-Bu)-cyclic-ortho-ester (**32**) (4.37 g, 8.5 mmol, 1.0 equiv.) was dissolved in THF (30 mL) and degassed for 20 min. PBu_3 (5.23 mL, 21.2 mmol, 2.5 equiv.) was added, and after stirring for 25 min, water (3 mL) was added. After stirring for another 25 h, the above solution was added dropwise to a degassed solution of 2, 2'-pyridine disulfide (**39**) (7.47 g, 33.9 mmol, 4.0 equiv.) in THF (30 mL) cooled to 0 °C under Ar. After 2.5 h following completion of addition, the solution was evaporated to

dryness. The product was purified by flash chromatography (silica gel, 1:1 hexanes : EtOAc), yielding 1.60 g (35% for two steps) of a white powder.

$[\alpha]_D$ 97.5° (*c* 0.99, $CHCl_3$); IR ($CHCl_3$ cast) 3338, 3047, 2937, 2880, 1724, 1518, 1448 cm^{-1}; ^1H NMR ($CDCl_3$, 500 MHz): 8.45 (d, 1H, *J* = 3.5 Hz, Pyr-H), 7.77 (d, 2H, *J* = 7.5 Hz, Fmoc-H), 7.73-7.54 (m, 4H, 2 Fmoc-H, 2 Pyr-H), 7.40 (t, 2H, *J* = 7.5 Hz, Fmoc-H), 7.31 (q, 2H, *J* = 7.0 Hz, Fmoc-H), 7.04 (t, 1H, *J* = 6.0 Hz, Pyr-H), 5.41 (d, 1H, *J* = 10.0 Hz, NH), 4.45-4.20 (m, 4H, Cys-H_α, Fmoc C<u>H</u>CH_2, Fmoc CHC<u>H_2</u>), 3.89 (s, 6H, 3 ortho ester OCH_2), 3.26 (dd, 1H, *J* = 14.0, 3.5 Hz, Cys-$H_{\beta 1}$), 3.05 (dd, 1H, *J* = 13.5, 4.0 Hz, Cys-$H_{\beta 2}$), 0.79 (s, 3H, ortho ester CH_3); ^{13}C NMR ($CDCl_3$, 100 MHz): δ 160.1, 156.4, 149.6, 144.0, 141.3, 137.0, 127.6, 127.0, 125.3, 120.5, 119.9, 119.8, 108.0, 72.8, 67.0, 54.6, 47.2, 41.4, 30.7, 14.3; HRMS (ES) Calcd for $C_{28}H_{28}N_2O_5S_2Na[M+Na]^+$ 559.1332, found 559.1325.

thiol resin (44)

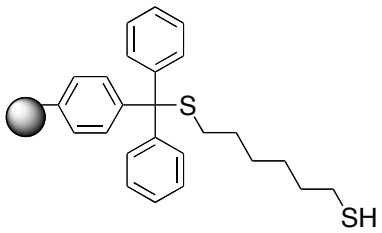

A mixed solvent system of dry CH_2Cl_2 (5 mL) and DMF (5 mL) was degassed for 15 min. Then diisopropylethyl amine (DIPEA) (0.97 mL, 5.6 mmol, 5.0 equiv.) was added under Ar, followed by 1,6-hexanedithiol (**43**) (0.85 mL, 5.6 mmol, 5.0 equiv.), and trityl chloride polystyrene resin purchased from Novabiochem (1.4 mmol/g, 0.80 g, 1.12 mmol, 1.0 equiv.). After shaking for 16 h, the resin was washed with DMF (3 x 10 mL),

CH_2Cl_2 (3 x 10 mL) and MeOH (1 x 10 mL). The resin was then dried under vacuum at 50 °C overnight.

L-cysteine cyclic ortho ester resin (45)

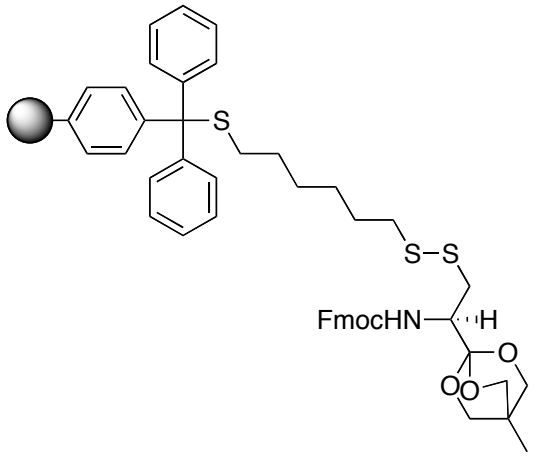

Thiol resin (**44**) (0.31 g, 0.44 mmol, 1.0 equiv) was pre-swelled in DMF (5 mL) for 30 min. To this mixture was added compound **40** (0.70 g, 1.31 mmol, 3.0 equiv.) in DMF (4 mL). After 2 h, the resin was washed with DMF (3 x 5 mL) and CH_2Cl_2 (3 x 5 mL). The loading procedure was repeated twice using fresh compound **40**.

D-cysteine cyclic ortho ester resin (46)

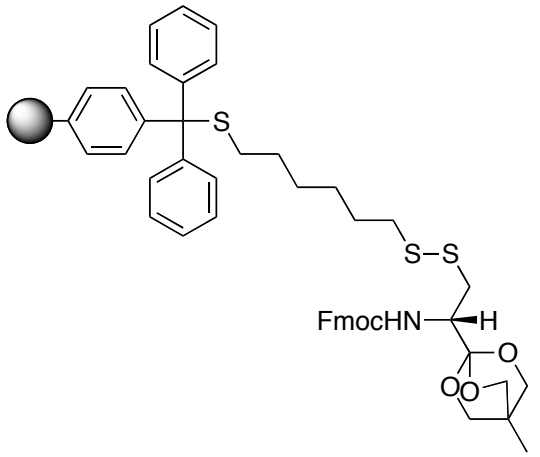

Thiol resin (**44**) (0.20 g, 0.28 mmol, 1.0 equiv) was pre-swelled in DMF (5 mL) for 30 min. To it was added compound **41** (0.44 g, 0.83 mmol, 3.0 equiv.) in DMF (3 mL). After 2 h, filtered the solution, washed the resin with DMF (3 x 5 mL) and CH_2Cl_2 (3 x 5 mL). The loading procedure was repeated twice using fresh compound **41**.

tripeptide ester (50)

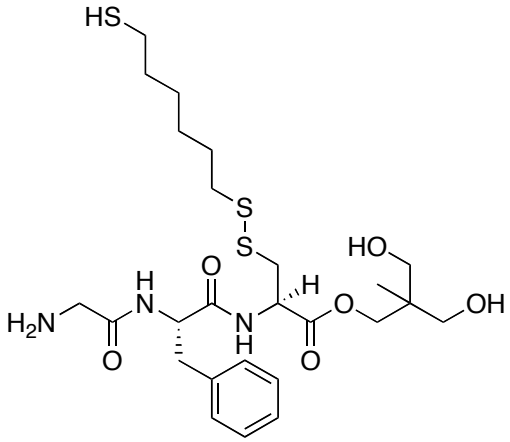

Peptide **7a** was prepared on a 0.21 mmol scale by manual synthesis (as outlined in Section 5.1.5) using resin **45**. The amino acids were coupled in the following order: Fmoc-Phe-OH and Fmoc-Gly-OH. The resin was then cleaved using 96% TFA: 2%

TIPS: 2% H_2O (method II), and purified by HPLC using solvent system B, t_R = 30.9 min. HRMS (ES) Calcd for $C_{25}H_{41}N_3O_6S_3Na[M+Na]^+$ 598.2050, found 598.2050.

tripeptide ester (51)

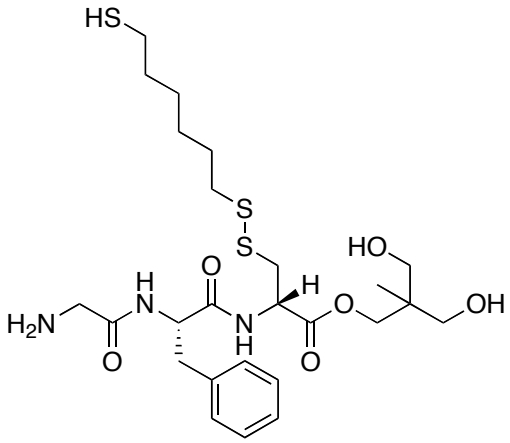

Peptide **51** was prepared on a 0.29 mmol scale by manual synthesis (as outlined in Section 5.1.5) using resin **46**. The amino acids were coupled in the following order: Fmoc-Phe-OH and Fmoc-Gly-OH. The resin was then cleaved using 96% TFA: 2% TIPS: 2% H_2O (method II), and purified by HPLC using solvent system B, t_R = 32.3 min. HRMS (ES) Calcd for $C_{25}H_{41}N_3O_6S_3Na[M+Na]^+$ 598.2050, found 598.2049.

tripeptide acid (24)

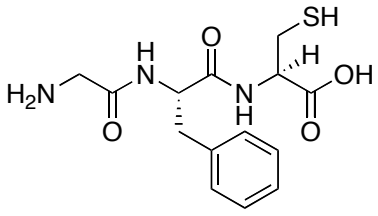

The tripeptide ester crude mixture from cleavage of resin **45** (4.8 μmol) was dissolved in a mixed solvent system of CH_3CN (0.1 mL) and H_2O (0.1 mL). To this solution, a solution of 0.437 mg / mL $LiOH•H_2O$ in H_2O (0.48 mL) was added. After 30 h, tris(2-carboxyethyl) phosphinehydrochloride (TCEP) (35.8 mg) was added. After another 4 h, using method B to purify this reaction mixture via RP-HPLC, tripeptide acid **24 (**0.4 mg**,** 1.2 μmol, 25% yield based on the initial loading of trityl chloride resin**)** was furnished, t_R = 15.5 min. HRMS (ES) Calcd for $C_{14}H_{19}N_3O_4SNa[M+Na]^+$ 348.0988, found 348.0988.

tripeptide acid (25)

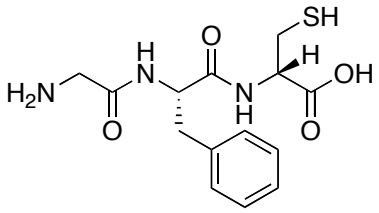

The tripeptide ester crude mixture from cleavage of resin **46** (9.8 μmol) was dissolved in a mixed solvent system of CH_3CN (0.1 mL) and H_2O (0.1 mL). To this solution, a solution of 0.437 mg / mL $LiOH•H_2O$ in H_2O (0.48 mL) was added. After 30 h, TCEP (35.8 mg) was added. After another 4 h, using method B to purify this reaction mixture via RP-HPLC, tripeptide acid **25 (**0.5 mg**,** 1.5 μmol, 15% yield based on the initial loading of trityl chloride resin**)** was furnished, t_R = 18.6 min. HRMS (ES) Calcd for $C_{14}H_{19}N_3O_4SNa[M+Na]^+$ 348.0988, found 348.0994.

tripeptide acid (24) made from H-L-Cys(Trt)-2-Cl trityl resin

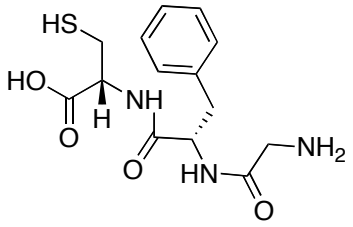

Peptide **24** was prepared on a 0.19 mmol scale by manual synthesis (as outlined in Section 5.1.5) using pre-load H-L-Cys(Trt)-2-Cl trityl resin. The amino acids were coupled in the following order: Fmoc-Phe-OH and Fmoc-Gly-OH. A portion of this resin (0.1 mmol) was then cleaved using 96% TFA: 2% TIPS: 2% H_2O (method II), and purified by HPLC using solvent system B to afford tripeptide acid **24**.

cyclic ortho ester containing resin (54)

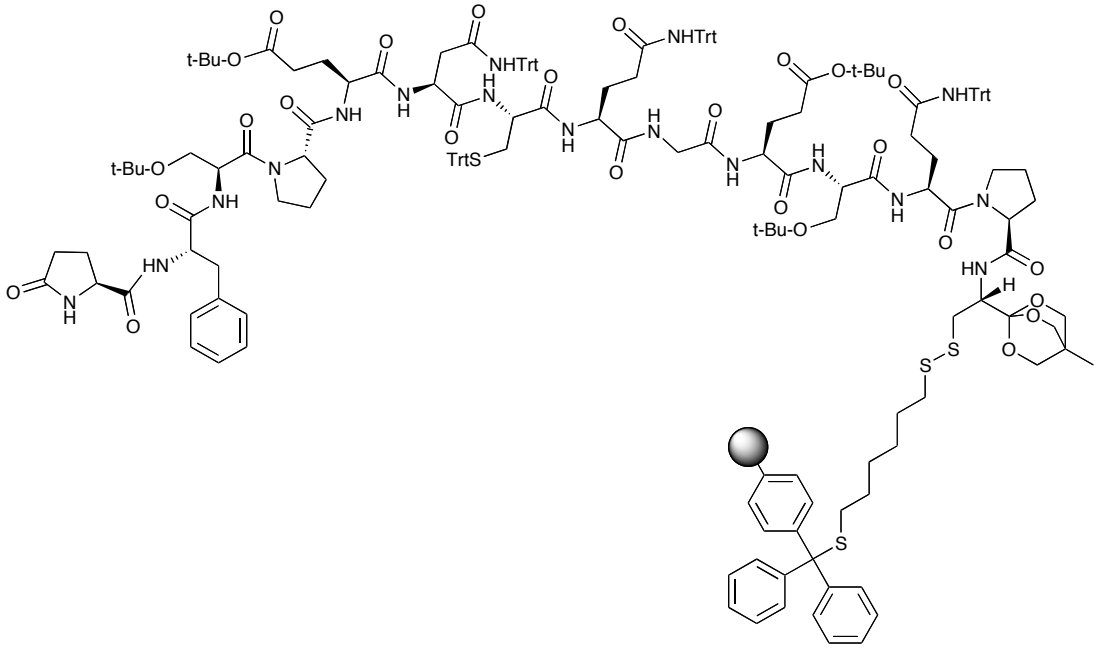

Resin **54** was prepared on a 0.59 mmol scale by manual synthesis (as outlined in Section 5.1.5) using resin **45**. The amino acids were coupled in the following order:

Fmoc-Pro-OH, Fmoc-Gln(Trt)-OH, Fmoc-Ser(O-*t*Bu)-OH, Fmoc-Glu(O-*t*Bu)-OH, Fmoc-Gly-OH, Fmoc-Gln(Trt)-OH, Fmoc-Cys(Trt)-OH, Fmoc-Asn(Trt)-OH, Fmoc-Glu(O-*t*Bu)-OH, Fmoc-Pro-OH, Fmoc-Ser(O-*t*Bu)-OH, Fmoc-Phe-OH, L-Pyroglutamic acid.

cyclic ortho ester containing resin (55)

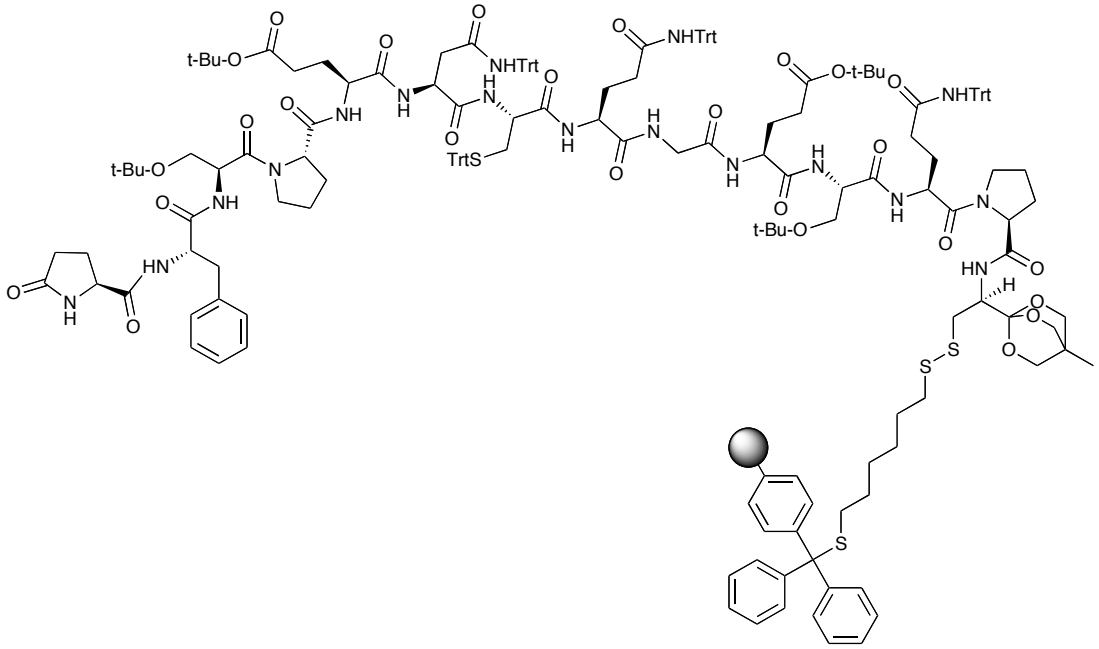

Resin **55** was prepared on a 0.27 mmol scale by manual synthesis (as outlined in Section 5.1.5) using resin **46**. The amino acids were coupled in the following order: Fmoc-Pro-OH, Fmoc-Gln(Trt)-OH, Fmoc-Ser(O-*t*Bu)-OH, Fmoc-Glu(O-*t*Bu)-OH, Fmoc-Gly-OH, Fmoc-Gln(Trt)-OH, Fmoc-Cys(Trt)-OH, Fmoc-Asn(Trt)-OH, Fmoc-Glu(O-*t*Bu)-OH, Fmoc-Pro-OH, Fmoc-Ser(O-*t*Bu)-OH, Fmoc-Phe-OH, L-Pyroglutamic acid.

crotalphine ester (56)

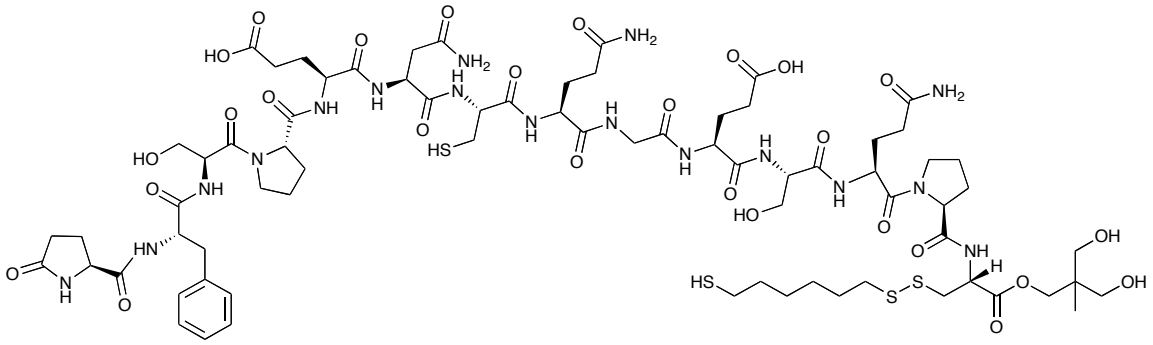

A portion of resin **54** (0.20 mmol) was cleaved using 95% TFA: 2.5% TIPS: 2.5% H_2O (method I), and purified by HPLC using solvent system C to afford crotalphine ester **56**, t_R = 30.5 min. LRMS (MALDI) Calcd for $C_{73}H_{110}N_{17}O_{27}S_4[M\text{-}H]^-$ 1784.7, found 1784.8.

crotalphine ester (57)

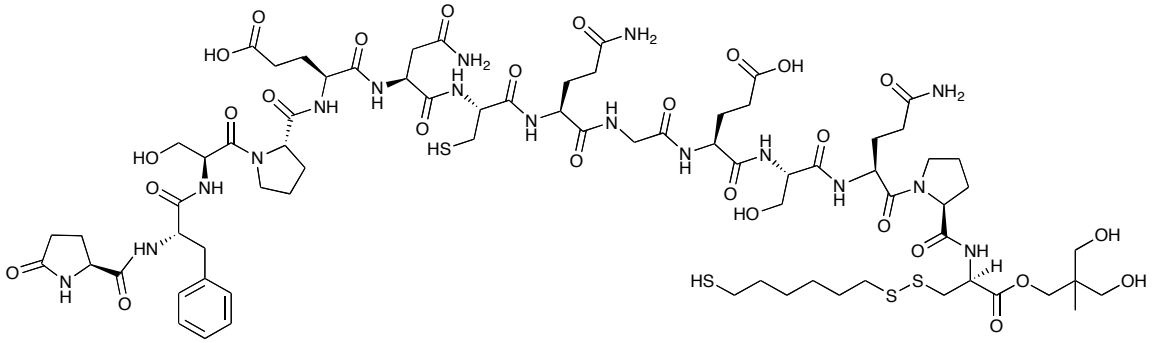

A portion of resin **55** (0.27 mmol) was cleaved using 95% TFA: 2.5% TIPS: 2.5% H_2O (method I), and purified by HPLC using solvent system C to afford crotalphine ester **57**, t_R = 31.4 min. LRMS (MALDI) Calcd for $C_{73}H_{110}N_{17}O_{27}S_4[M\text{-}H]^-$ 1784.7, found 1784.6.

crotalphine acid (free thiols) (58)

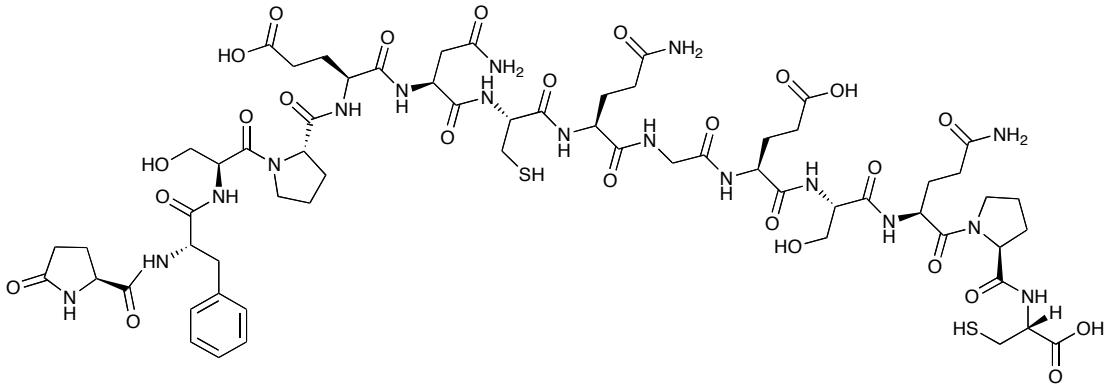

The crotalphine ester crude mixture from cleavage of resin **54** (4.0 μmol) was dissolved in mixed solvent of CH_3CN (0.1 mL) and H_2O (0.1 mL). To this solution, a solution of 0.437 mg / mL $LiOH•H_2O$ in H_2O (0.48 mL) was added. After 24 h, TCEP (35.8 mg) was added. After another 4 h, using method C to purify this reaction mixture via RP-HPLC, crotalphine acid (free thiols) **58** was furnished, t_R = 20.6 min. LRMS (MALDI) Calcd for $C_{62}H_{88}N_{17}O_{25}S_2[M-H]^-$ 1534.6, found 1534.7.

crotalphine acid (free thiols) (59)

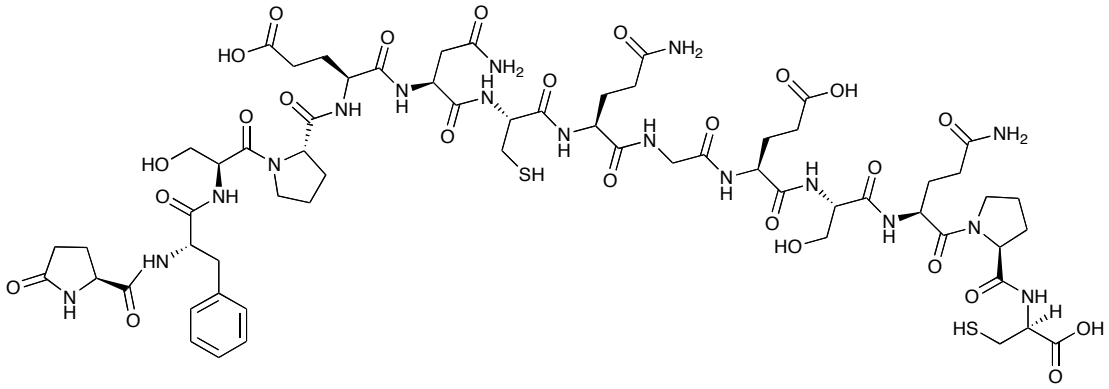

The crotalphine ester crude mixture from cleavage of resin **55** (6.7 μmol) was dissolved in mixed solvent of CH_3CN (0.1 mL) and H_2O (0.1 mL). To this solution, a

solution of 0.437 mg / mL $LiOH•H_2O$ in H_2O (0.48 mL) was added. After 24 h, TCEP (35.8 mg) was added. After another 4 h, using method C to purify this reaction mixture via RP-HPLC, crotalphine acid (free thiols) **59** was furnished, t_R = 21.2 min. LRMS (MALDI) Calcd for $C_{62}H_{88}N_{17}O_{25}S_2[M-H]^-$ 1534.6, found 1534.8.

crotalphine (2)

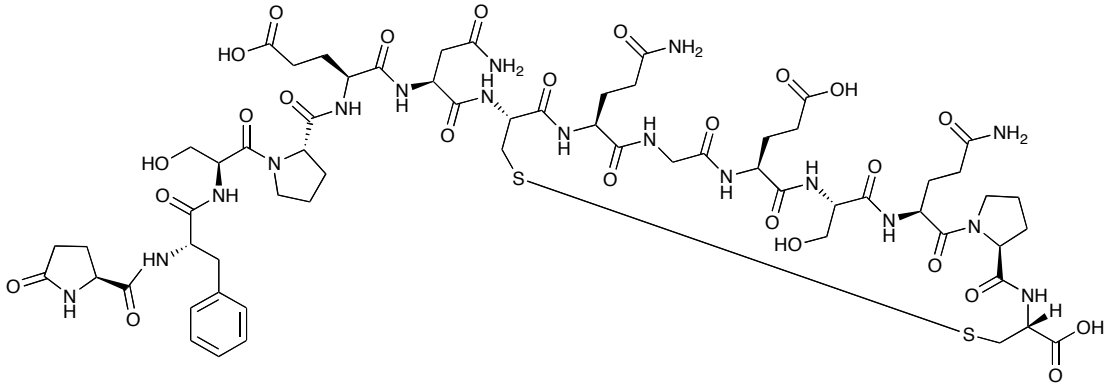

NH_4HCO_3 buffer (pH 8) (0.5 mL) was bubbled with oxygen gas for 1 h. To this solution was added pure crotalphine acid (free thiols) **58** (4.0 μmol, single diastereomer, purified from HPLC). After stirring the solution for 16h, **2 (**0.3 mg**,** 0.196 μmol, 4.9% yield based on the initial loading of trityl chloride resin**)** was purified by RP-HPLC using method C, t_R = 19.7 min. LRMS (MALDI) Calcd for $C_{62}H_{86}N_{17}O_{25}S_2[M-H]^-$ 1532.5, found 1532.9. HRMS (MALDI) Calcd for $C_{62}H_{88}N_{17}O_{25}S_2[M+H]^+$ 1534.55732, found 1534.55778.

D-Cys1 crotalphine diastereomer (53)

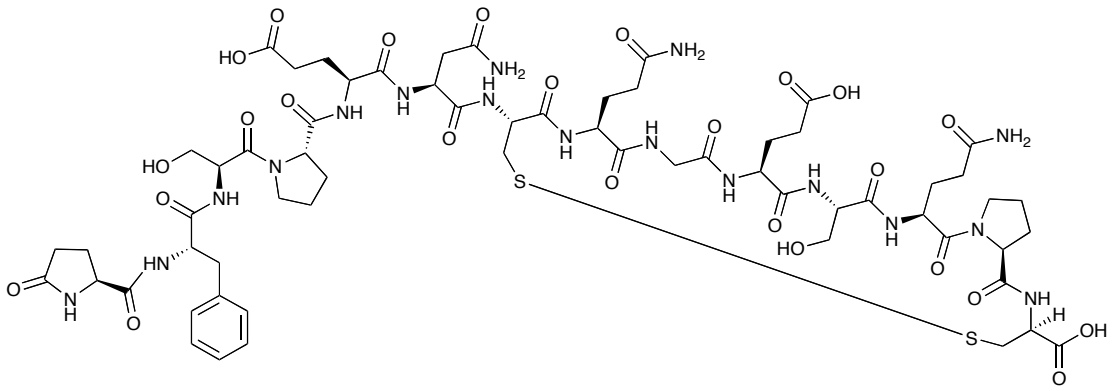

NH_4HCO_3 buffer (pH 8) (0.5 mL) was bubbled with oxygen gas for 1 h. To this solution was added pure crotalphine acid (free thiols) **59** (6.7 μmol, single diastereomer, purified from HPLC). After stirring the solution for 16h, **53 (**0.2 mg**,** 0.130 μmol, 1.9% yield based on the initial loading of trityl chloride resin**)** was purified by RP-HPLC using method C, t_R = 19.7 min. LRMS (MALDI) Calcd for $C_{62}H_{86}N_{17}O_{25}S_2[M\text{-}H]^-$ 1532.5, found 1532.6.

all-D crotalphine acid (free thiols) (63)

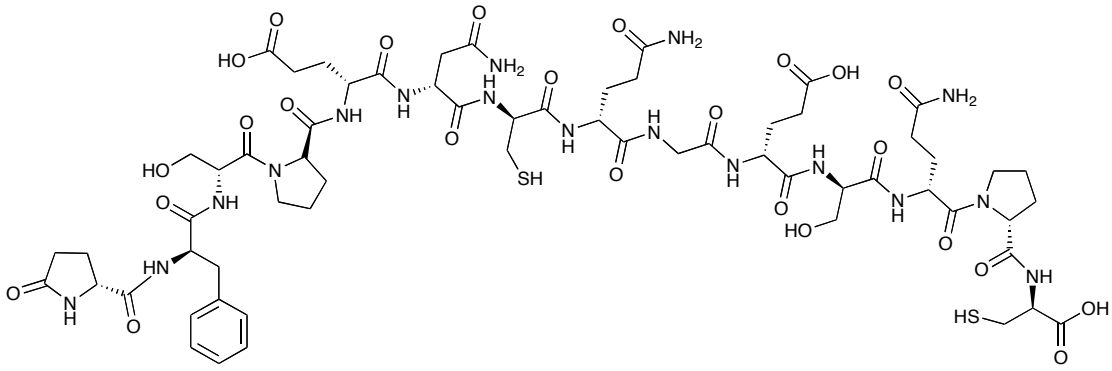

Peptide **63** was prepared on a 0.43 mmol scale by manual synthesis (as outlined in Section 5.1.5) using pre-load H-D-Cys(Trt)-2-Cl trityl resin. The amino acids were coupled in the following order: Fmoc-D-Pro-OH, Fmoc-D-Gln(Trt)-OH, Fmoc-D-Ser(O-*t*Bu)-OH, Fmoc-D-Glu(O-*t*Bu)-OH, Fmoc-Gly-OH, Fmoc-D-Gln(Trt)-OH, Fmoc-D-Cys(Trt)-OH, Fmoc-D-Asn(Trt)-OH, Fmoc-D-Glu(O-*t*Bu)-OH, Fmoc-D-Pro-OH, Fmoc-D-Ser(O-*t*Bu)-OH, Fmoc-D-Phe-OH, D-Pyroglutamic acid. The resin was then cleaved using 95% TFA: 2.5% TIPS: 2.5% H_2O (method I), and purified by HPLC using solvent system C, t_R = 20.6 min. LRMS (MALDI) Calcd for $C_{62}H_{88}N_{17}O_{25}S_2[M\text{-}H]^-$ 1534.6, found 1534.0.

all-D crotalphine (61)

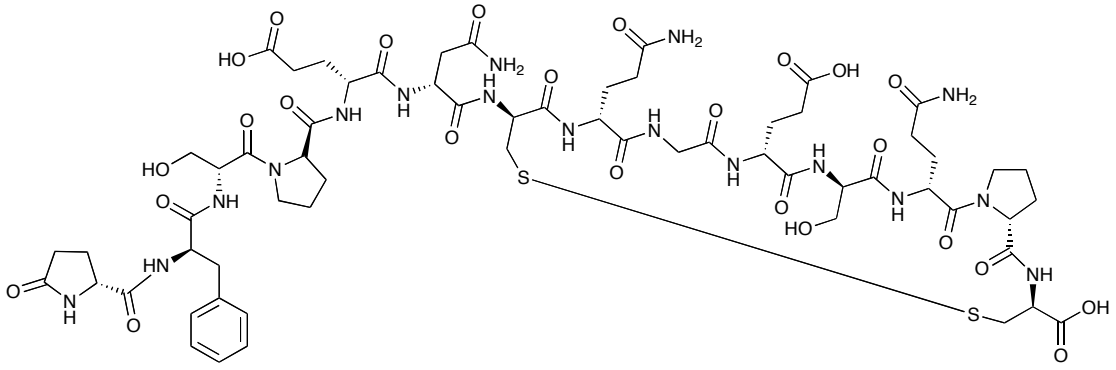

NH_4HCO_3 buffer (pH 8) was bubbled with oxygen gas for 1 h. To this solution was added crude all-D crotalphine acid (free thiols) (**63**) cleaved from the resin. After stirring the solution for 16h, all-D crotalphine (**61**) was purified by RP-HPLC using method D, t_R = 24.2 min. LRMS (MALDI) Calcd for $C_{62}H_{86}N_{17}O_{25}S_2[M\text{-}H]^-$ 1532.5, found 1532.0.

crotalphine allylser analog (88)

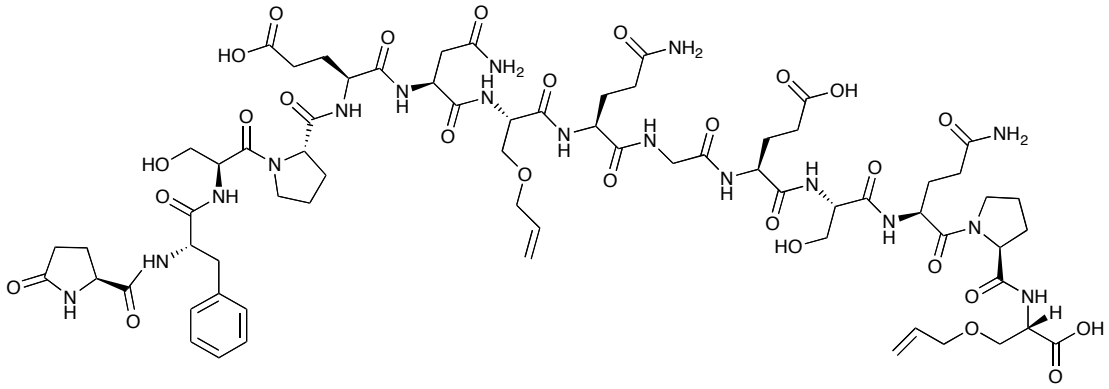

Fmoc-AllylSer-OH (**93**) was loaded onto Wang resin according to the standard procedure as described in Section 5.1.3. The peptide **88** was prepared on a 0.1 mmol scale using the above pre-loaded resin by automated synthesis according to the procedure outlined in Section 5.1.7. The amino acids were coupled in the following order: Fmoc-Pro-OH, Fmoc-Gln(Trt)-OH, Fmoc-Ser(O-*t*Bu)-OH, Fmoc-Glu(O-*t*Bu)-OH, Fmoc-Gly-OH, Fmoc-Gln(Trt)-OH, Fmoc-AllylSer-OH, Fmoc-Asn(Trt)-OH, Fmoc-Glu(O-*t*Bu)-OH, Fmoc-Pro-OH, Fmoc-Ser(O-*t*Bu)-OH, Fmoc-Phe-OH, L-Pyroglutamic acid. The resin was then cleaved using 95% TFA: 2.5% TIPS: 2.5% H_2O (method I), and purified by HPLC using solvent system D. The purity of this purified peptide was assessed using solvent system C. At solvent system C, t_R of this peptide was 21.9 min. HRMS (ES) Calcd for $C_{68}H_{98}N_{17}O_{27}[M+H]^+$ 1584.6813, found 1584.6831.

crotalphine allylcys analog (89)

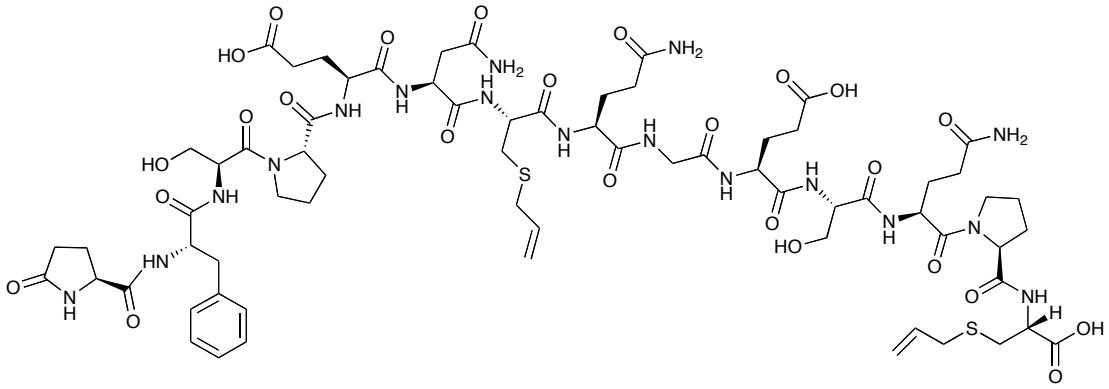

Fmoc-AllylCys-OH (**94**) was loaded onto 2-chloro trityl resin according to the standard procedure as described in Section 5.1.4. The peptide **89** was prepared on a 0.1 mmol scale using the above pre-loaded resin by automated synthesis according to the procedure outlined in Section 5.1.7. The amino acids were coupled in the following order: Fmoc-Pro-OH, Fmoc-Gln(Trt)-OH, Fmoc-Ser(O-*t*Bu)-OH, Fmoc-Glu(O-*t*Bu)-OH, Fmoc-Gly-OH, Fmoc-Gln(Trt)-OH, Fmoc-AllylCys-OH, Fmoc-Asn(Trt)-OH, Fmoc-Glu(O-*t*Bu)-OH, Fmoc-Pro-OH, Fmoc-Ser(O-*t*Bu)-OH, Fmoc-Phe-OH, L-Pyroglutamic acid. The resin was then cleaved using 95% TFA: 2.5% TIPS: 2.5% H_2O (method I), and purified by HPLC using solvent system D. The purity of this purified peptide was assessed using solvent system C. At solvent system C, t_R of this peptide was 24.1 min. HRMS (ES) Calcd for $C_{68}H_{98}N_{17}O_{25}S_2[M+H]^+$ 1616.6356, found 1616.6342.

crotalphine pentenylgly analog (90)

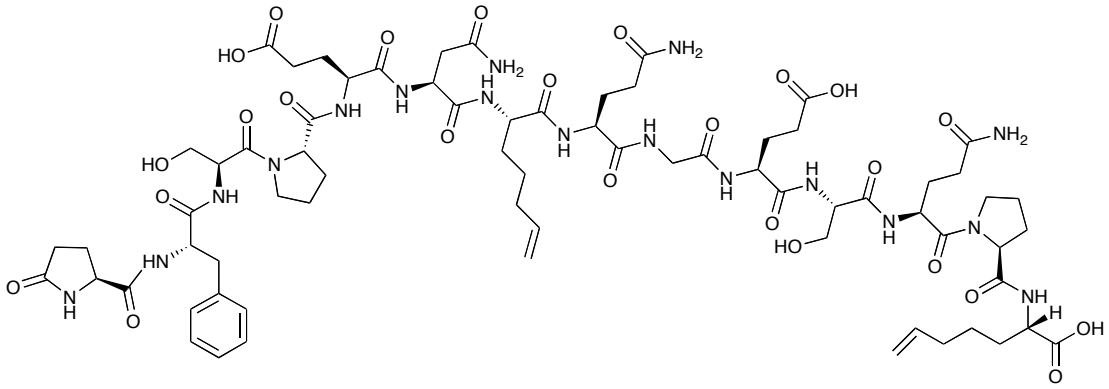

Fmoc-PentenylGly-OH (**95**) was loaded onto Wang resin according to the standard procedure as described in Section 5.1.3. The peptide **90** was prepared on a 0.1 mmol scale using the above pre-loaded resin by automated synthesis according to the procedure outlined in Section 5.1.7. The amino acids were coupled in the following order: Fmoc-Pro-OH, Fmoc-Gln(Trt)-OH, Fmoc-Ser(O-*t*Bu)-OH, Fmoc-Glu(O-*t*Bu)-OH, Fmoc-Gly-OH, Fmoc-Gln(Trt)-OH, Fmoc-PentenylGly-OH, Fmoc-Asn(Trt)-OH, Fmoc-Glu(O-*t*Bu)-OH, Fmoc-Pro-OH, Fmoc-Ser(O-*t*Bu)-OH, Fmoc-Phe-OH, L-Pyroglutamic acid. The resin was then cleaved using 95% TFA: 2.5% TIPS: 2.5% H_2O (method I), and purified by HPLC using solvent system D. The purity of this purified peptide was assessed using solvent system C. At solvent system C, t_R of this peptide was 25.3 min. HRMS (ES) Calcd for $C_{70}H_{102}N_{17}O_{25}[M+H]^+$ 1580.7227, found 1580.7229.

crotalphine allylgly analog (91)

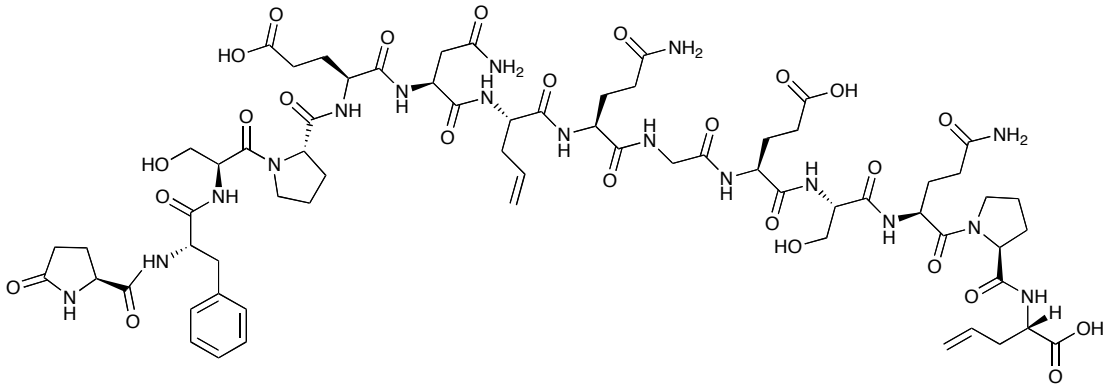

Fmoc-AllylGly-OH (**96**) was loaded onto Wang resin according to the standard procedure as described in Section 5.1.3. The peptide **91** was prepared on a 0.1 mmol scale using the above pre-loaded resin by automated synthesis according to the procedure outlined in Section 5.1.7. The amino acids were coupled in the following order: Fmoc-Pro-OH, Fmoc-Gln(Trt)-OH, Fmoc-Ser(O-*t*Bu)-OH, Fmoc-Glu(O-*t*Bu)-OH, Fmoc-Gly-OH, Fmoc-Gln(Trt)-OH, Fmoc-AllylGly-OH, Fmoc-Asn(Trt)-OH, Fmoc-Glu(O-*t*Bu)-OH, Fmoc-Pro-OH, Fmoc-Ser(O-*t*Bu)-OH, Fmoc-Phe-OH, L-Pyroglutamic acid. The resin was then cleaved using 95% TFA: 2.5% TIPS: 2.5% H_2O (method I), and purified by HPLC using solvent system D. The purity of this purified peptide was assessed using solvent system C. At solvent system C, t_R of this peptide was 20.9 min. HRMS (ES) Calcd for $C_{66}H_{94}N_{17}O_{25}[M+H]^+$ 1524.6601, found 1524.6591.

1,7,7-trimethylbicyclo[2.2.1]heptane-2,3-dione (131)[90]

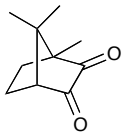

A mixture of (*S*)-(-)-camphor (**130**) (3.04 g, 20.0 mmol, 1.0 equiv.), SeO_2 (5.11 g, 46.0 mmol, 2.3 equiv.) and Ac_2O (5 mL) was refluxed for 18 h. After cooling to room temperature, CH_2Cl_2 (50 mL) was added. This solution was sequentially washed with 1 : 1 sat. NaOH : H_2O and brine, then dried over $MgSO_4$. The organic solvent was removed *in vacuo* to yield **131** as a white solid (2.96 g, 91%), which was used in the next step without further purification.

3-hydroxy-1,7,7-trimethylbicyclo[2.2.1]heptan-2-one (132)[91]

3-hydroxy-4,7,7-trimethylbicyclo[2.2.1]heptan-2-one (133)[91]

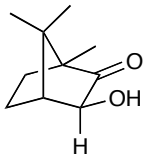

132

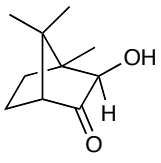

133

To an ice-cold solution of **131** (2.96 g, 17.8 mmol, 1.0 equiv.) in Et_2O (18 mL) and MeOH (18 mL) was added $NaBH_4$ (0.17 g, 4.6 mmol, 0.26 equiv.) in portions. After stirring for 30 min at 0 °C, Et_2O (20 mL) and cold H_2O (25 mL) were added. The layers were separated and the aqueous layer was back-extracted with Et_2O (2 x 20 mL). The combined organic layer was dried over $MgSO_4$. The organic solvent was removed *in vacuo* to yield **132** and **133** as a white solid which was used in the next step without further purification.

4,7,7-trimethyl-3-oxobicyclo[2.2.1]heptan-2-yl 2-(benzyloxycarbonylamino)acetate (135)[91]

1,7,7-trimethyl-3-oxobicyclo[2.2.1]heptan-2-yl 2-(benzyloxycarbonylamino)acetate (136)[91]

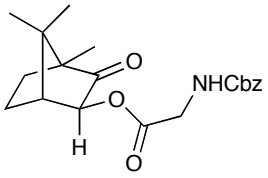

135

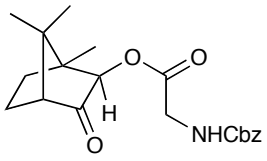

136

A solution of **132** and **133** (17.8 mmol, 1.0 equiv.), Cbz-glycine (**134**) (4.10 g, 19.6 mmol, 1.1 equiv.) and DMAP (1.09 g, 8.9 mmol, 0.5 equiv.) in THF (75 mL) was stirred at 0 °C for 20 min. Then a mixture of DCC (5.51 g, 26.7 mmol, 1.5 equiv.) in THF (50 mL) was added to the above ice-cold solution dropwise using a syringe over 20 min. This mixture was further stirred at 0 °C for 2 h, then at room temperature for 16 h. After filtering off the DCU, the organic solvent was removed *in vacuo* and the residue was purified by flash chromatography (silica gel, 6:1 hexanes : EtOAc), yielding **135** and **136** (5.51 g, 86% over two steps) as 2:1 inseparable isomers according to the ^{1}H NMR spectrum.

^{1}H NMR ($CDCl_3$, 400 MHz): 7.40-7.30 (m, 5H, Ar-H), 5.22 (bs, 1H, NH), 5.13 (s, 2H, CH_2Ar), 4.91 (s, 0.32 H, CHO), 4.84 (s, 0.63 H, CHO), 2.22 (d, 0.31H, J = 4.0 Hz, CHC(O)), 2.13 (d, 0.54H, J = 4.4 Hz, CHCHO), 2.10-1.46 (m, 4H, CH_2CH_2), 1.00-0.84 (m, 9H, CCH_3, CCH_3, CCH_3);

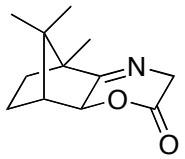

137

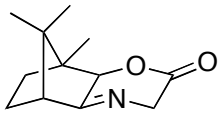

129

To a solution of **135** and **136** (2.06 g, 5.7 mmol, 1 equiv.) in anhydrous ethanol (15 mL) was added Pd/C (10% Pd on charcoal, 0.115 g), acetic acid (0.5 mL) and 4Å molecular sieves. This mixture was stirred under a hydrogen atmosphere (1 atm) at room temperature for 25 h. The crude was filtered, concentrated *in vacuo* and purified by flash chromatography (silica gel, 2:1 hexanes : EtOAc), yielding **137** (0.115 g, 10%) and **129** (0.098 g, 8%) as white solids.

(1*R*,2*S*,8*R*)-8,11,11-trimethyl-3-oxa-6-azatricyclo[6.2.1.0^{2,7}]undec-6-en-4-one (137)[91]

$[\alpha]_D$ -243.0° (*c* 1.16, $CHCl_3$); IR (CH_2Cl_2 cast) 2962, 2878, 1755, 1690, 1456 cm^{-1}; ^1H NMR ($CDCl_3$, 500 MHz): 4.57 (d, 1H, *J* = 17.9 Hz, NC<u>H</u>HC(O)), 4.51 (d, 1H, *J* = 1.8 Hz, <u>H</u>CO), 3.94 (dd, 1H, *J* = 17.9, 1.7 Hz, NCH<u>H</u>C(O)), 2.29 (d, 1H, *J* = 4.9 Hz, <u>H</u>CCO), 2.11 (m, 1H, C<u>H</u>HCHH), 1.80 (td, 1H, *J* = 12.7, 4.0 Hz, CH<u>H</u>CHH), 1.60 (ddd, 1H, *J* = 13.7, 9.0, 4.9 Hz, CHHC<u>H</u>H), 1.39 (ddd, 1H, *J* = 13.2, 9.3, 4.0 Hz, CHHCH<u>H</u>), 1.08 (s, 3H, CC<u>H</u>$_3$), 1.00 (s, 3H, CC<u>H</u>$_3$), 0.82 (s, 3H, CC<u>H</u>$_3$); ^{13}C NMR ($CDCl_3$, 125 MHz): δ 183.8, 169.0, 79.7, 52.7, 52.6, 49.1, 47.5, 29.5, 25.4, 20.0, 19.7, 9.9; HRMS (ES) Calcd for $C_{12}H_{17}NO_2Na[M+Na]^+$ 230.1151, found 230.1146.

(1*R*,2*R*,8*R*)-1,11,11-trimethyl-3-oxa-6-azatricyclo[6.2.1.0^{2,7}]-undec-6-en-4-one (129)[91]

$[\alpha]_D$ 222.7° (*c* 2.24, $CHCl_3$); IR ($CHCl_3$ cast) 2960, 2887, 1755, 1694, 1456 cm^{-1}; ^1H NMR ($CDCl_3$, 500 MHz): 4.53 (d, 1H, *J* = 18.0 Hz, NC<u>H</u>HC(O)), 4.33 (s, 1H, <u>H</u>CO),

3.92 (d, 1H, J = 17.8 Hz, NCH<u>H</u>C(O)), 2.46 (d, 1H, J = 4.4 Hz, <u>H</u>CC=N), 2.04 (m, 1H, C<u>H</u>HCHH), 1.93 (td, 1H, J = 12.6, 4.7 Hz, CH<u>H</u>CHH), 1.57 (ddd, 1H, J = 13.3, 9.1, 4.5 Hz, CHHC<u>H</u>H), 1.41 (ddd, 1H, J = 13.0, 9.3, 3.6 Hz, CHHCH<u>H</u>), 1.11 (s, 3H, CC<u>H</u>$_3$), 0.99 (s, 3H, CC<u>H</u>$_3$), 0.87 (s, 3H, CC<u>H</u>$_3$); ^{13}C NMR ($CDCl_3$, 125 MHz): δ 181.8, 168.9, 81.8, 53.3, 52.6, 49.4, 49.0, 34.1, 21.6, 20.1, 19.3, 9.9; HRMS (ES) Calcd for $C_{12}H_{18}NO_2[M+H]^+$ 208.1332, found 208.1327.

(1*R*,2*R*,5*S*,8*R*)-1,11,11-trimethyl-5-benzyl-3-oxa-6-azatricyclo[6.2.1.0^{2,7}]-undec-6-en-4-one (128)[91]

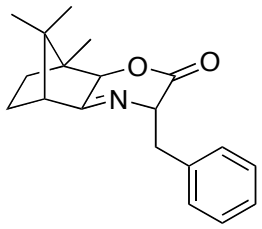

A 50 mL 3-neck flask was flame-dried and cooled to room temperature under argon. To this flask was added THF (2.1 mL) and the flask was cooled to -30 °C. Then *n*-BuLi (2.5 M in hexanes, 0.38 mL, 0.95 mmol, 1.1 equiv.) was added, and after 5 min, diisopropylamine (0.13 mL, 0.95 mmol, 1.1 equiv.) was added. After another 30 min, a solution of **129** (0.18 g, 0.86 mmol, 1.0 equiv.) in THF (13.0 mL) was added dropwise to the above freshly prepared LDA solution. This resulting solution was stirred at -30 °C for 1.5 h. After adding hexamethylphosphoramide (HMPA) (0.45 mL, 2.6 mmol, 3.0 equiv.), the mixture was cooled to -78 °C. An ice-cold solution of benzyl bromide (0.31 mL, 2.6 mmol, 3.0 equiv.) in THF (13.0 mL) was cannulated into the above mixture and the resulting solution was stirred at -78 °C for another 17 h. The reaction was quenched by

adding 2 M aqueous acetic acid (1.2 mL). The THF was removed *in vacuo*, and EtOAc (15 mL) was added to the residue. The organic solution was washed with sat. LiCl (3 x 5 mL) and dried over $MgSO_4$. The crude was filtered, concentrated *in vacuo* and purified by flash chromatography (silica gel, 2:1 hexanes : EtOAc), yielding **128** as a white solid (0.176 g, 69%).

$[\alpha]_D$ -14.8° (*c* 0.40, $CHCl_3$); IR ($CHCl_3$ cast) 2959, 2932, 1745, 1698, 1480 cm^{-1}; ^1H NMR ($CDCl_3$, 500 MHz): 7.29-7.17 (m, 5H, Ar-H), 4.81 (t, 1H, *J* = 5.1 Hz, NCHC(O)), 3.39 (dd, 1H, *J* = 13.7, 5.4 Hz, CHHAr), 3.11 (dd, 1H, *J* = 13.6, 5.0 Hz, CHHAr), 2.55 (s, 1H, HCO), 2.31 (d, 1H, *J* = 4.5 Hz, HCC=N), 1.84 (m, 1H, CHHCHH), 1.63 (td, 1H, *J* = 12.5, 5.1 Hz, CHHCHH), 1.36 (td, 1H, *J* = 8.9, 4.6 Hz, CHHCHH), 0.87 (s, 3H, CCH_3), 0.82 (s, 3H, CCH_3), 0.75 (s, 3H, CCH_3), 0.72 (m, 1H, CHHCHH); ^{13}C NMR ($CDCl_3$, 125 MHz): δ 180.3, 171.3, 136.1, 130.0, 128.7, 127.4, 80.9, 62.8, 53.8, 49.0, 48.0, 38.1, 34.5, 21.3, 19.9, 19.1, 9.4; HRMS (ES) Calcd for $C_{19}H_{23}NO_2[M+H]^+$ 298.1802, found 298.1801.

(*R*)-methyl 2-(*tert*-butoxycarbonylamino)-3-((5-nitropyridin-2-yl)disulfanyl)propanoate (127)

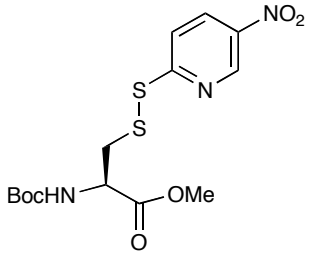

This unknown compound was prepared using an adapted literature procedure.[31]

5, 5'-dinitro-2, 2'-thiopyridine disulfide (**139**) (2.32 g, 7.5 mmol, 1.5 equiv.) was dissolved in CH_2Cl_2 (50 mL) and this solution was degassed by bubbling argon for 15 min. After cooling this solution in an ice bath, (*R*)-methyl 2-(*tert*-butoxycarbonylamino)-3-mercaptopropanoate (**138**) was added dropwise and the mixture was stirred for another 70 min. The solution was washed with sat. Na_2CO_3 (3 x 50 mL) and brine (1 x 50 mL), dried over Na_2SO_4. The crude was filtered, concentrated *in vacuo* and purified by flash chromatography (silica gel, 5:1 hexanes : EtOAc), yielding **127** as a yellow solid (0.66 g, 35%).

$[\alpha]_D$ 45.3° (*c* 0.92, $CHCl_3$); IR ($CHCl_3$ cast) 3367, 2979, 1747, 1714, 1591, 1567, 1519, 1344 cm^{-1}; ^1H NMR ($CDCl_3$, 500 MHz): 9.31 (d, 1H, *J* = 2.5 Hz, Ar-H), 8.38 (dd, 1H, *J* = 8.5, 2.5 Hz, Ar-H), 7.74 (d, 1H, *J* = 9.0 Hz, Ar-H), 6.08 (d, 1H, *J* = 4.0 Hz, NH), 4.57 (m, 1H, H_α), 3.72 (s, 3H, OCH_3), 3.37 (dd, 1H, *J* = 14.0, 5.5 Hz, $H_{\beta 1}$), 3.31 (dd, 1H, *J* = 14.0, 5.0 Hz, $H_{\beta 2}$), 1.43 (s, 9H, $OC(CH_3)_3$); ^{13}C NMR ($CDCl_3$, 125 MHz): δ 170.8, 167.4, 155.2, 145.3, 142.3, 131.6, 119.9, 80.4, 52.9, 52.8, 42.0, 28.3; HRMS (ES) Calcd for $C_{14}H_{19}N_3O_6S_2Na[M+Na]^+$ 412.0607, found 412.0607.

bis-amino acid derivative containing an sulfur to α-carbon bridge (126)

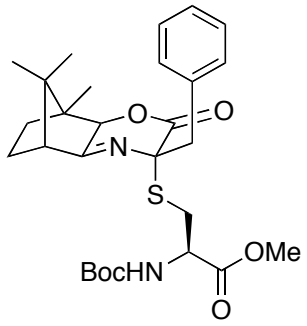

A 50 mL 3-neck flask was flame-dried and cooled to room temperature under argon. To this flask was added THF (0.97 mL) and the flask was cooled to -30 °C. Then *n*-BuLi (2.5 M in hexanes, 0.20 mL, 0.51 mmol, 1.3 equiv.) was added, and after 5 min, diisopropylamine (0.07 mL, 0.51 mmol, 1.3 equiv.) was added. After another 30 min, a solution of **128** (0.12 g, 0.40 mmol, 1.0 equiv.) in THF (6.0 mL) was added dropwise to the above freshly prepared LDA solution. This resulting solution was stirred at -30 °C for 1.5 h. After adding hexamethylphosphoramide (HMPA) (0.20 mL, 1.2 mmol, 3.0 equiv.), the mixture was cooled to -78 °C. An ice-cold solution of **127** (0.46 g, 1.2 mmol, 3.0 equiv.) in THF (6.0 mL) was cannulated into the above mixture and the resulting solution was stirred at -78 °C for another 15 h. The reaction was quenched by adding 2 M aqueous acetic acid (0.6 mL). THF was removed *in vacuo*, EtOAc (15 mL) was added to the residue. The organic solution was washed with sat. Na_2CO_3 (2 x 5 mL), sat. LiCl (1 x 5 mL) and dried over Na_2SO_4. The crude was filtered, concentrated *in vacuo* and purified by flash chromatography (silica gel, 7:1 hexanes : EtOAc), yielding **126** as a yellow solid (0.165 g, 81%).

^{1}H NMR ($CDCl_3$, 500 MHz): 7.36 (m, 2H, Ar-H), 7.15 (m, 3H, Ar-H), 5.22 (d, 1H, J = 7.6 Hz, NH), 4.63 (s, 1H, CHCO), 4.55 (m, 1H, H_α), 3.76 (s, 3H, OCH_3), 3.68 (d, 1H, J = 13.0 Hz, CHHAr), 3.31 (d, 1H, J = 13.0 Hz, CHHAr), 3.21 (dd, 1H, J = 13.0, 4.7 Hz, $H_{\beta 1}$), 3.15 (dd, 1H, J = 13.0, 6.7 Hz, $H_{\beta 2}$), 2.29 (d, 1H, J = 4.5 Hz, HCC=N), 1.92 (tt, 1H, J = 12.6, 4.1 Hz, CHHCHH), 1.80 (td, 1H, J = 12.5, 4.9 Hz, CHHCHH), 1.57 (m, 1H, CHHCHH), 1.48 (s, 9H, $OC(CH_3)_3$), 1.39 (m, 1H, CHHCHH), 0.95 (s, 3H, CCH_3), 0.83 (s, 3H, CCH_3), 0.20 (s, 3H, CCH_3); ^{13}C NMR ($CDCl_3$, 125 MHz): δ 183.7, 171.0, 162.2, 155.0, 135.4, 127.6, 126.8, 125.3, 81.1, 80.3, 65.2, 54.0, 52.9, 52.7, 49.5, 48.7,

45.2, 42.0, 34.2, 32.7, 28.2, 21.1, 19.2, 9.6; HRMS (ES) Calcd for $C_{28}H_{38}N_2O_6SNa[M+Na]^+$ 553.2343, found 553.2340.

(6*R*,11*R*)-dimethyl 2,2,15,15-tetramethyl-4,13-dioxo-3,14-dioxa-8,9-dithia-5,12-diazahexadecane-6,11-dicarboxylate (151)[130]

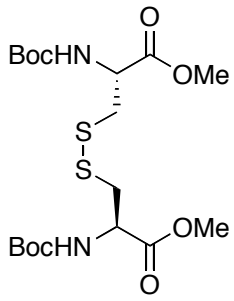

A solution of compound **126** (0.024 g, 0.045 mmol, 1.0 equiv.), HCl•NH_2OH (0.062 g, 0.90 mmol, 20.0 equiv.) and NaOAc•$3H_2O$ (0.122 g, 0.90 mmol, 20.0 equiv.) in ethanol (1.8 mL) was stirred at room temperature for 24 h. After the solid was filtered out, the filtrate was injected to LC-MS. The method is shown below:

Solvent A: H_2O

Solvent B: MeOH

0-1 min: 25%- 35% B ramp

1-2 min: 35%- 30% B ramp

2-16 min: 30%- 95% B ramp

16-21 min: 95% B/ 5% A

21-24 min: 95%- 25% B ramp

24-25 min: 25% B/ 75% A

Flow rate: 0.2 mL/min

Phenyl-Hexyl MercuryMS, 0.2x20mm

MCP: 650V; PMT:750V

Fragmentor: 85V, Skimmer 55V, Source: 3200V

Detected at 260 nm and 369 nm

Using the above method, the title compound has a t_R = 15.3 min. HRMS (ES) Calcd for $C_{18}H_{32}N_2O_8S_2Na[M+Na]^+$ 491.1492, found 491.1496.

glycine analog of thuricin-β (153)

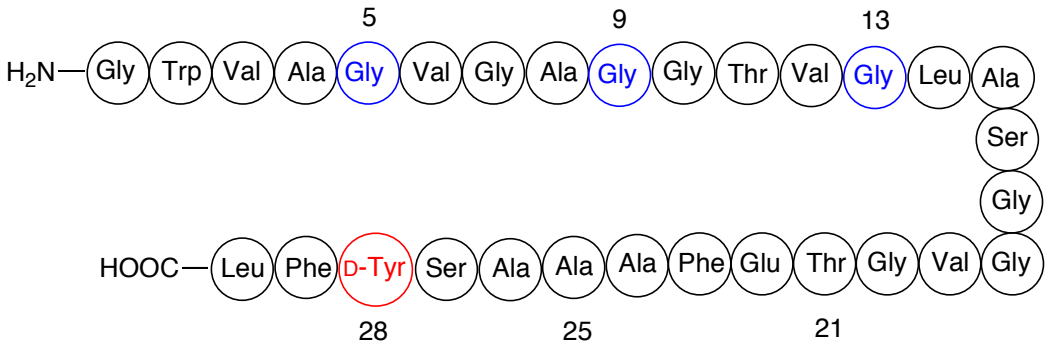

The peptide was prepared on a 0.1 mmol scale using the pre-loaded Fmoc-Leu-Wang resin (**154**) by automated synthesis according to the procedure outlined in Section 5.1.6. The amino acids were coupled in the following order: Fmoc-Phe-OH, Fmoc-D-Tyr(O-*t*Bu)-OH, Fmoc-Ser(O-*t*Bu)-OH, Fmoc-Ala-OH, Fmoc-Ala-OH, Fmoc-Ala-OH, Fmoc-Phe-OH, Fmoc-Glu(O-*t*Bu)-OH, Fmoc-Thr(O-*t*Bu)-OH, Fmoc-Gly-OH, Fmoc-Val-OH, Fmoc-Gly-OH, Fmoc-Gly-OH, Fmoc-Ser(O-*t*Bu)-OH, Fmoc-Ala-OH, Fmoc-Leu-OH, Fmoc-Gly-OH, Fmoc-Val-OH, Fmoc-Thr(O-*t*Bu)-OH, Fmoc-Gly-OH, Fmoc-Gly-OH, Fmoc-Ala-OH, Fmoc-Gly-OH, Fmoc-Val-OH, Fmoc-Gly-OH, Fmoc-Ala-OH, Fmoc-Val-OH, Fmoc-Trp(Boc)-OH and Fmoc-Gly-OH. The resin was then cleaved using 95% TFA: 2.5% TIPS: 2.5% H_2O (method I), and purified by HPLC using solvent

system E, t_R = 16.3 min. LRMS (MALDI) Calcd for $C_{125}H_{185}N_{31}O_{38}Na[M+Na]^+$ 2751.3, found 2752.6. The sequence of this peptide was confirmed by LC-MS/MS. This purified peptide was not active against *Bacillus firmus* at a concentration of 200 μmol.

serine analog of thuricin-β (155)

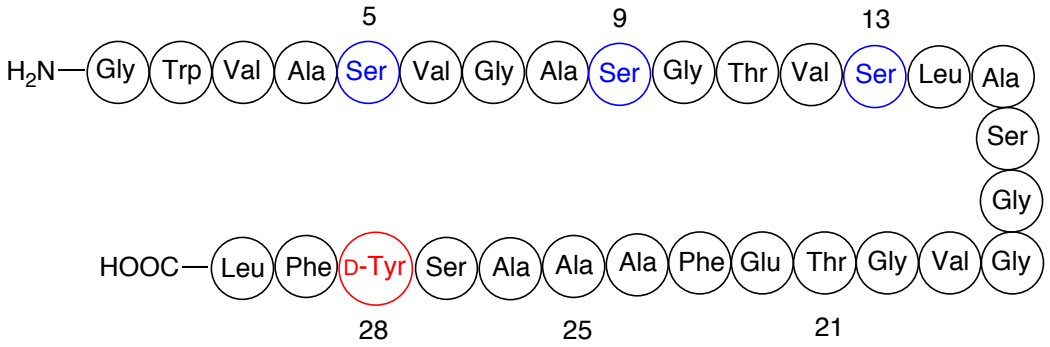

Residues 3-30 of the title peptide were prepared on a 0.1 mmol scale using the pre-loaded Fmoc-Leu-Wang resin (**154**) by automated synthesis according to the procedure outlined in Section 5.1.6. Pseudoproline dipeptide Fmoc-Ala-Ser(ψMe,Me Pro)-OH (**156**) was used at positions 8-9, 15-16 and 26-27 to minimize on-resin aggregation. The amino acids were coupled in the following order: Fmoc-Phe-OH, Fmoc-D-Tyr(O-*t*Bu)-OH, Fmoc-Ala-Ser(ψMe,Me Pro)-OH, Fmoc-Ala-OH, Fmoc-Ala-OH, Fmoc-Phe-OH, Fmoc-Glu(O-*t*Bu)-OH, Fmoc-Thr(O-*t*Bu)-OH, Fmoc-Gly-OH, Fmoc-Val-OH, Fmoc-Gly-OH, Fmoc-Gly-OH, Fmoc-Ala-Ser(ψMe,Me Pro)-OH, Fmoc-Leu-OH, Fmoc-Ser(O-*t*Bu)-OH, Fmoc-Val-OH, Fmoc-Thr(O-*t*Bu)-OH, Fmoc-Gly-OH, Fmoc-Ala-Ser(ψMe,Me Pro)-OH, Fmoc-Gly-OH, Fmoc-Val-OH, Fmoc-Ser(O-*t*Bu)-OH, Fmoc-Ala-OH and Fmoc-Val-OH. At this point, the remaining two residues Fmoc-Trp(Boc)-OH and Fmoc-Gly-OH were coupled manually according to the procedure

described in Section 5.1.5 using a double coupling method. The resin was then cleaved using 95% TFA: 2.5% TIPS: 2.5% H_2O (method I), and purified by HPLC using solvent system F, t_R = 20.5 min. LRMS (MALDI) Calcd for $C_{128}H_{192}N_{31}O_{41}[M+H]^+$ 2819.4, found 2820.4. This purified peptide was not active against *Bacillus firmus* at a concentration of 200 μmol.

alanine analog of thuricin-β (160)

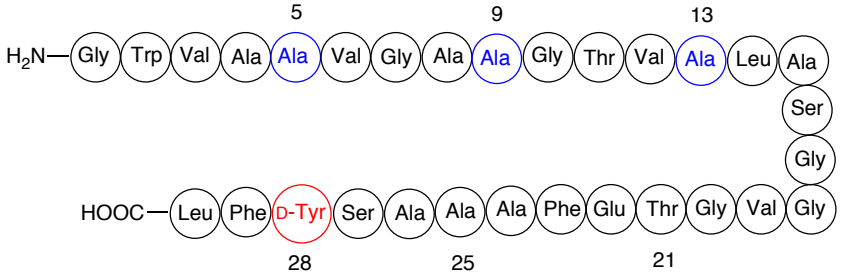

Residues 3-30 of the title peptide were prepared on a 0.1 mmol scale using the pre-loaded H-Leu-HMPB-PEG resin (**161**) by automated synthesis according to the procedure outlined in Section 5.1.6. Pseudoproline dipeptide Fmoc-Ala-Ser(ψMe,Me Pro)-OH (**156**) was used at positions 15-16 and 26-27 and a dipeptide Fmoc-Ala-(Dmb)Gly-OH (**158**) was used at positions 9-10 to minimize on-resin aggregation. Compared to Section 5.1.6, a double coupling strategy was applied. The amino acids were coupled in the following order: Fmoc-Phe-OH, Fmoc-D-Tyr(O-*t*Bu)-OH, Fmoc-Ala-Ser(ψMe,Me Pro)-OH, Fmoc-Ala-OH, Fmoc-Ala-OH, Fmoc-Phe-OH, Fmoc-Glu(O-*t*Bu)-OH, Fmoc-Thr(O-*t*Bu)-OH, Fmoc-Gly-OH, Fmoc-Val-OH, Fmoc-Gly-OH, Fmoc-Gly-OH, Fmoc-Ala-Ser(ψMe,Me Pro)-OH, Fmoc-Leu-OH, Fmoc-Ala-OH, Fmoc-Val-OH, Fmoc-Thr(O-*t*Bu)-OH, Fmoc-Ala-(Dmb)Gly-OH, Fmoc-Ala-OH, Fmoc-Gly-OH, Fmoc-Val-OH, Fmoc-Ala-OH, Fmoc-Ala-OH and Fmoc-Val-OH. At this point, the

remaining two residues Fmoc-Trp(Boc)-OH and Fmoc-Gly-OH were coupled manually according to the procedure described in Section 5.1.5 using a double coupling method. The resin was then cleaved using 95% TFA: 2.5% TIPS: 2.5% H_2O (method I) and a crude peptide was obtained. LRMS (MALDI) Calcd for $C_{128}H_{192}N_{31}O_{38}[M+H]^+$ 2771.4, found 2772.2. This crude peptide was not active against *Bacillus firmus* at a concentration of 200 μmol.

(2*E*,6*E*)-3,7-dimethyl-8-oxoocta-2,6-dienyl acetate (200)[129]

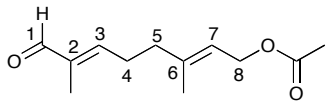

A solution of geranyl acetate (**199**) (18.00 g, 92.2 mmol, 1.0 equiv.) and SeO_2 (11.40 g, 95.9 mmol, 1.05 equiv.) in 95% ethanol (150 mL) was refluxed for 1 h. After filtering off the precipitate, the ethanol was removed *in vacuo*. Water (100 mL) was added to the residue, which was extracted with EtOAc (3 x 150 mL). The combined organic layer was dried over Na_2SO_4. The crude was filtered, concentrated *in vacuo* and purified by flash chromatography (silica gel, 4:1 hexanes : EtOAc), yielding **200** as a pale yellow oil (5.85 g, 30%).

IR ($CHCl_3$, cast film) 3022, 2919, 2850, 2717, 1735, 1686, 1644 cm^{-1}; ^1H NMR ($CDCl_3$, 500 MHz): 9.42 (s, 1H, H-1), 6.47 (t, 1H, J = 7.0 Hz, H-3), 5.41 (t, 1H, J = 7.0 Hz, H-7), 4.62 (d, 2H, J = 7.0 Hz, CH_2OAc), 2.52 (q, 2H, J = 7.5 Hz, CH_2-4), 2.26 (t, 2H, J = 7.5 Hz, CH_2-5), 2.08 (s, 3H, C(O)-CH_3), 1.78 (s, 3H, CCH_3), 1.77 (s, 3H, CCH_3); ^{13}C NMR ($CDCl_3$, 125 MHz): δ 195.1, 171.0, 153.3, 140.4, 139.7, 119.6, 61.1, 37.8, 27.0, 21.0, 16.4, 9.3; HRMS (ES) Calcd for $C_{12}H_{18}O_3Na[M+Na]^+$ 233.1148, found 233.1147.

(2*E*,6*E*)-8-acetoxy-2,6-dimethylocta-2,6-dienoic acid (201)[129]

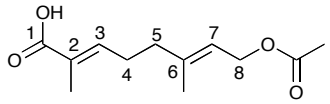

To an ice-cold solution of **200** (3.60 g, 17.0 mmol, 1.0 equiv.) and 2-methyl-2-butene (89 mL, 0.81 mol, 49.0 equiv.) in *t*-BuOH (350 mL) was added a solution of NaH_2PO_4 (30.50 g, 0.22 mol, 13.0 equiv.) and $NaClO_2$ (25.00 g, 0.22 mol, 13.0 equiv.) in H_2O (144 mL) dropwise. This resulting mixture was warmed slowly to room temperature and stirred for 13 h. The two layers were separated. The original aqueous layer was back extracted with EtOAc (3 x 110 mL). The original organic layer was concentrated *in vacuo*, followed by the addition of EtOAc (220 mL) and washed with brine (200 mL). The brine layer was further back extracted with EtOAc (2 x 110 mL). All the organic layers were combined and dried over Na_2SO_4. The crude was filtered, concentrated *in vacuo*, yielding **201** as a colorless oil which was used in the next step without further purification.

IR ($CDCl_3$, cast film) 2935, 1739, 1687, 1635, 1423, 1367 cm^{-1}; ^1H NMR ($CDCl_3$, 500 MHz): 6.88 (t, 1H, J = 7.5 Hz, H-3), 5.38 (t, 1H, J = 7.0 Hz, H-7), 4.60 (d, 2H, J = 7.0 Hz, CH_2OAc), 2.35 (q, 2H, J = 7.5 Hz, CH_2-4), 2.20 (t, 2H, J = 7.0 Hz, CH_2-5), 2.07 (s, 3H, C(O)-CH_3), 1.85 (s, 3H, CCH_3), 1.74 (s, 3H, CCH_3); ^{13}C NMR ($CDCl_3$, 125 MHz): δ 173.4, 171.1, 143.9, 140.8, 127.5, 119.3, 61.2, 37.9, 27.0, 21.0, 16.4, 12.0; HRMS (ES) Calcd for $C_{12}H_{17}O_4[M-H]^-$ 225.1132, found 225.1131.

(2*E*,6*E*)-methyl 8-acetoxy-2,6-dimethylocta-2,6-dienoate (202)[129]

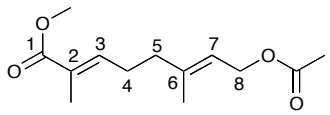

To a solution of **201** (17.0 mmol) in toluene (40 mL) and MeOH (20 mL), Me_3SiCHN_2 (2.0 M in hexanes, 9.5 mL, 19.0 mmol, 1.1 equiv.) was added dropwise over 15 min. At this point, the reaction was complete according to TLC. The crude reaction was concentrated *in vacuo* and purified by flash chromatography (silica gel, 17:3 hexanes : EtOAc), yielding **202** as a pale yellow oil (4.05 g, 96% over two steps).

IR ($CDCl_3$, cast film) 3406, 2988, 2951, 1740, 1716, 1651, 1437, 1366 cm^{-1}; ^1H NMR ($CDCl_3$, 500 MHz): 6.72 (t, 1H, *J* = 7.5 Hz, H-3), 5.37 (t, 1H, *J* = 7.0 Hz, H-7), 4.59 (d, 2H, *J* = 7.0 Hz, CH_2OAc), 3.73 (s, 3H, OCH_3), 2.31 (q, 2H, *J* = 7.5 Hz, CH_2-4), 2.16 (t, 2H, *J* = 7.5 Hz, CH_2-5), 2.05 (s, 3H, C(O)-CH_3), 1.84 (s, 3H, CCH_3), 1.72 (s, 3H, CCH_3); ^{13}C NMR ($CDCl_3$, 125 MHz): δ 171.0, 168.5, 141.4, 140.9, 127.9, 119.1, 61.2, 51.7, 38.0, 26.8, 21.0, 16.4, 12.4; HRMS (ES) Calcd for $C_{13}H_{20}O_4Na[M+Na]^+$ 263.1254, found 263.1252.

(2*E*,6*E*)-methyl 8-acetoxy-5-hydroxy-2,6-dimethylocta-2,6-dienoate (203)[129]

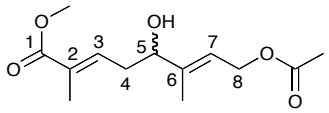

A solution of **202** (3.37 g, 14.0 mmol, 1.0 equiv.), SeO_2 (1.55 g, 14.0 mmol, 1.0 equiv.) and acetic acid (1.4 mL) in *t*-BuOH (140 mL) was heated at 70 °C for 2 h. *t*-BuOH was removed *in vacuo* and CH_2Cl_2 (150 mL) was added to the residue. This solution was washed with sat. $NaHCO_3$ (70 mL), water (70 mL) and brine (70 mL), dried over Na_2SO_4. The crude product was filtered, concentrated *in vacuo* and purified by flash chromatography (silica gel, 3:2 hexanes : EtOAc), yielding **203** as a pale yellow oil (1.07 g, 30%).

IR ($CDCl_3$, cast film) 3482, 2953, 1740, 1651, 1615 cm^{-1}; ^1H NMR ($CDCl_3$, 500 MHz): 6.74 (t, 1H, J = 7.5 Hz, H-3), 5.62 (t, 1H, J = 7.0 Hz, H-7), 4.62 (d, 2H, J = 6.5 Hz, CH_2OAc), 4.17 (t, 1H, J = 7.0 Hz, H-5), 3.73 (s, 3H, OCH_3), 2.44 (t, 2H, J = 6.5 Hz, CH_2-4), 2.05 (s, 3H, C(O)-CH_3), 1.85 (s, 3H, CCH_3), 1.72 (s, 3H, CCH_3); ^{13}C NMR ($CDCl_3$, 125 MHz): δ 170.9, 168.3, 142.2, 137.6, 130.0, 120.2, 75.6, 60.8, 51.8, 34.4, 20.9, 12.7, 12.3; HRMS (ES) Calcd for $C_{13}H_{20}O_5Na[M+Na]^+$ 279.1203, found 279.1203.

(2*E*)-methyl 8-acetoxy-2,6-dimethylocta-2,4,6-trienoate (204)[129]

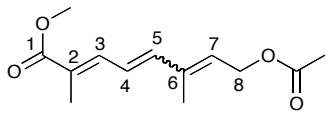

A solution of **203** (1.00 g, 3.9 mmol, 1.0 equiv.), Et_3N (1.70 mL, 12.1 mmol, 3.1 equiv.) and MsCl (0.46 mL, 5.8 mmol, 1.5 equiv.) in DCE (40 mL) was heated at 80 °C for 35 min. After CH_2Cl_2 (100 mL) was added, the solution was washed with 1 M HCl (3 x 20 mL) and brine (20 mL), and dried over Na_2SO_4. The crude product was filtered and concentrated *in vacuo*. This residue was dissolved in toluene (20 mL), followed by the addition of DBU (1.24 mL, 7.8 mmol, 2.0 equiv.). The above solution was heated at 100 °C for 30 min. The toluene was removed *in vacuo* and the residue was dissolved in CH_2Cl_2 (50 mL). This solution was washed with 1 M HCl (3 x 20 mL) and brine (20 mL) and dried over Na_2SO_4. The crude product was filtered, concentrated *in vacuo*, yielding **204** as a yellow oil which was used in the next step without further purification.

IR ($CDCl_3$, cast film) 2952, 1741, 1708, 1616, 1436, 1368 cm^{-1}; ^1H NMR ($CDCl_3$, 500 MHz): 7.29-7.21 (m, 1H, H-3), 6.90 (d, 0.3 H, J = 15.0 Hz, H-5), 6.61-6.51 (m, 1.7H, H-4, H-5), 5.74 (td, 0.7H, J = 7.0, 1.0 Hz, H-7), 5.65 (t, 0.3H, J = 7.5 Hz, H-7), 4.77-4.72 (m, 2H, CH_2OAc), 3.77 (s, 0.9H, OCH_3), 3.76 (s, 2.1H, OCH_3), 2.07 (s, 2.1H, $C(O)CH_3$), 2.06 (s, 0.9H, $C(O)CH_3$), 1.99 (d, 0.9H, J = 1.3 Hz, CH_3-C_2), 1.98 (d, 2.1H, J = 1.3 Hz, CH_3-C_2), 1.95 (s, 0.9H, CH_3-C_6), 1.89 (s, 2.1H, CH_3-C_6); ^{13}C NMR ($CDCl_3$, 125 MHz): δ 170.8, 168.8, 168.7, 142.6, 138.3, 138.0, 137.1, 134.6, 128.5, 128.0, 127.2, 126.3, 126.0, 124.0, 61.1, 60.0, 51.8, 20.9, 20.2, 12.8, 12.7; HRMS (ES) Calcd for $C_{13}H_{18}O_4Na[M+Na]^+$ 261.1097, found 261.1097.

(2*E*)-methyl 8-hydroxy-2,6-dimethylocta-2,4,6-trienoate (205)[129]

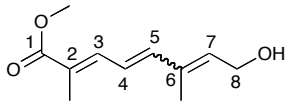

To an ice-cold solution of **204** (3.9 mmol) in MeOH (40 mL) was added freshly prepared NaOMe (1.0 M in MeOH, 0.78 mL, 0.78 mmol, 0.2 equiv.). After stirring at 0 °C for 2.5 h, the MeOH was removed *in vacuo*. The residue was dissolved in CH_2Cl_2 (50 mL). This solution was washed with 1 M HCl (3 x 10 mL) and brine (10 mL), and dried over Na_2SO_4. The crude product was filtered and concentrated *in vacuo*, yielding **205** as a yellow oil which was used in the next step without further purification.

IR (Microscope) 3454, 2952, 2926, 1709, 1613, 1437 cm^{-1}; ^1H NMR ($CDCl_3$, 500 MHz): 7.32-7.25 (m, 1H, H-3), 6.92 (d, 0.3 H, J = 15.1 Hz, H-5), 6.61-6.48 (m, 1.7H, H-4, H-5), 5.85 (t, 0.7H, J = 6.6 Hz, H-7), 5.75 (t, 0.3H, J = 6.9 Hz, H-7), 4.39-4.34 (m, 2H, CH_2OH), 3.79 (s, 0.9H, OCH_3), 3.78 (s, 2.1H, OCH_3), 2.02 (d, 0.9H, J = 1.1 Hz, CH_3-C_2), 2.01 (d, 2.1H, J = 1.0 Hz, CH_3-C_2), 1.97 (s, 0.9H, CH_3-C_6), 1.88 (s, 2.1H, CH_3-C_6); ^{13}C NMR ($CDCl_3$, 125 MHz): δ 168.9, 143.3, 138.6, 135.9, 135.2, 134.2, 126.7, 123.4, 59.5, 58.4, 51.8, 20.2, 12.8, 12.6; HRMS (ES) Calcd for $C_{11}H_{16}O_3Na[M+Na]^+$ 219.0992, found 219.0988.

(2*E*,4*E*,6*E*)-methyl 2,6-dimethyl-8-oxoocta-2,4,6-trienoate (206)[129]

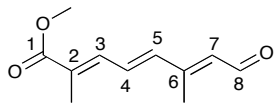

To a solution of **205** (3.9 mmol) in DMSO (18 mL) was added IBX (45% wt with stabilizer, 4.85 g, 7.8 mmol, 2.0 equiv.). After stirring at room temperature for 30 min, the solution was poured into a mixture of CH_2Cl_2 (240 mL) and sat. $NaHCO_3$ (120 mL). The layers were separated and the aqueous layer was extracted with another CH_2CL_2 (100 mL). The combined organic layer was sequentially washed with sat. $NaHCO_3$, H_2O and brine, and dried over Na_2SO_4. The crude was filtered, concentrated *in vacuo* and purified by flash chromatography (silica gel, 17:5 hexanes : EtOAc), yielding **206** as a yellow solid (0.45 g, 60% over 4 steps).

IR (Microscope) 3055, 2994, 2950, 2857, 2784, 1700, 1653, 1594, 1438 cm^{-1}; ^1H NMR ($CDCl_3$, 600 MHz): 10.15 (d, 1H, J = 7.9 Hz, H-8), 7.29-7.26 (m, 1H, H-3), 6.99 (dd, 1H, J = 15.2, 11.5 Hz, H-4), 6.63 (d, 1H, J = 15.3 Hz, H-5), 6.05 (d, 1H, J = 7.9 Hz, H-7), 3.79 (s, 3H, OCH_3), 2.34 (d, 3H, J = 1.2 Hz, CH_3-C_2), 2.05 (d, 3H, J = 1.4 Hz, CH_3-C_6); ^{13}C NMR ($CDCl_3$, 125 MHz): δ 191.1, 168.3, 152.9, 141.1, 136.8, 131.36, 131.29, 130.2, 52.1, 13.2, 13.1; HRMS (ES) Calcd for $C_{11}H_{14}O_3Na[M+Na]^+$ 217.0841, found 217.0835.

(2*E*,4*E*,6*E*)-methyl 2,6-dimethylnona-2,4,6,8-tetraenoate (207)

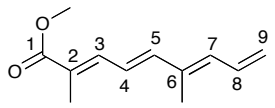

Ph_3PCH_3Br (0.14 g, 0.39 mmol, 1.0 equiv.) was suspended in THF (3 mL) at -10 °C. KO*t*-Bu (1.0 M in THF, 0.39 mL, 0.39 mmol, 1.0 equiv.) was added to the above suspension and the resulting mixture was stirred at -10 °C for an additional 30 min. Then an ice-cold solution of **206** (0.075 g, 0.39 mmol, 1.0 equiv.) in THF (3 mL) was added dropwise and stirred at -10 °C for another 1 h. After the addition of sat. NH_4Cl (5 mL), the mixture was slowly warmed to room temperature over 30 min. Then hexanes (30 mL) and brine (15 mL) were added. The layers were separated and the organic layer was dried over Na_2SO_4, filtered, concentrated *in vacuo* and purified by flash chromatography (silica gel, 9:1 hexanes : EtOAc), yielding **207** as a yellow solid (0.070 g, 94%).

IR (Microscope) 3055, 2950, 1700, 1653, 1640, 1594, 1438 cm^{-1}; ^1H NMR ($CDCl_3$, 500 MHz): 7.30 (dq, 1H, *J* = 10.7, 1.3 Hz, H-3), 6.75 (ddd, 1H, *J* = 16.7, 11.2, 10.1 Hz, H-8), 6.63-6.52 (m, 2H, H-4, H-5), 6.26 (d, 1H, *J* = 11.3 Hz, H-7), 5.38 (d, 1H, *J* = 16.7 Hz, H-9), 5.27 (d, 1H, *J* = 10.2 Hz, H-9), 3.79 (s, 3H, OCH_3), 2.02 (d, 3H, *J* = 1.3 Hz, CH_3-C_2), 1.97 (d, 3H, *J* = 0.8 Hz, CH_3-C_6); ^{13}C NMR ($CDCl_3$, 125 MHz): δ 168.9, 143.9, 138.8, 135.6, 135.1, 133.0, 126.4, 123.6, 119.6, 51.8, 12.8, 12.6; HRMS (ES) Calcd for $C_{12}H_{16}O_2Na[M+Na]^+$ 215.1048, found 215.1043.

(2*E*,4*E*,6*E*)-2,6-dimethylnona-2,4,6,8-tetraenoic acid (198)

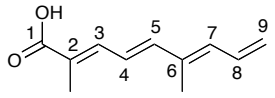

Compound **207** (0.065 g, 0.38 mmol, 1.0 equiv.) was dissolved in CH_3CN (3 mL), followed by the addition of H_2O (2 mL) and LiOH (0.09 g, 2.3 mmol, 6.0 equiv.). This mixture was heated at 50 °C for 3.5 h. H_2O (20 mL) was added and the crude product was extracted with CH_2Cl_2 (2 x 15 mL). The organic layer was extracted back with H_2O (15 mL). The combined aqueous layer was acidified to pH = 1 using 1 M HCl. This acidic solution was extracted with CH_2Cl_2 (3 x 15 mL) and the organic layer was dried over Na_2SO_4. The crude was filtered, concentrated *in vacuo*, yielding **198** as a yellow solid (0.060 g, quantitative), which was used in the next step without further purification.

IR ($CDCl_3$, cast film) 3046, 2922, 1681, 1600, 1584, 1482 cm^{-1}; ^1H NMR ($CDCl_3$, 500 MHz): 7.42 (d, 1H, J = 11.2 Hz, H-3), 6.76 (ddd, 1H, J = 16.7, 11.2, 10.2 Hz, H-8), 6.66-6.53 (m, 2H, H-4, H-5), 6.29 (d, 1H, J = 11.3 Hz, H-7), 5.40 (d, 1H, J = 16.8 Hz, H-9), 5.30 (d, 1H, J = 10.5 Hz, H-9), 2.03 (s, 3H, CH_3-C_2), 1.99 (s, 3H, CH_3-C_6); ^{13}C NMR ($CDCl_3$, 125 MHz): δ 173.8, 144.9, 140.9, 135.7, 135.5, 132.9, 125.7, 123.5, 120.0, 12.6, 12.5; HRMS (ES) Calcd for $C_{11}H_{13}O_2[M-H]^-$ 177.0921, found 177.0921.

(*E*)-quinolin-8-yl oct-2-enoate (212)

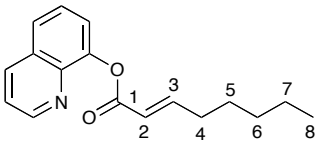

To a solution of (*E*)-2-octenoic acid (**210**) (0.28 mL, 2.0 mmol, 1.0 equiv.) and DCC (0.42 g, 2.3 mmol, 1.15 equiv.) in EtOAc (20 mL) was added 8-hydroxyquinoline (**211**) (0.29 g, 2.0 mmol, 1.0 equiv.). This resulting solution was stirred at room temperature for 1 h. The DCU was removed by filtration and the filtrate was concentrated *in vacuo* and purified by flash chromatography (silica gel, 9:1 hexanes : EtOAc), yielding **212** as a colorless oil (0.075 g, 14%).

^{1}H NMR ($CDCl_3$, 400 MHz): 8.93 (dd, 1H, J = 4.2, 1.7 Hz, Ar-H), 8.18 (dd, 1H, J = 8.4, 1.7 Hz, Ar-H), 7.73 (dd, 1H, J = 8.1, 1.4 Hz, Ar-H), 7.55 (t, 1H, J = 7.8 Hz, Ar-H), 7.48 (dd, 1H, J = 7.5, 1.5 Hz, Ar-H), 7.42 (dd, 1H, J = 8.3, 4.2 Hz, Ar-H), 7.31 (dt, 1H, J = 15.6, 6.9 Hz, H-3), 6.27 (dt, 1H, J = 15.6, 1.6 Hz, H-2), 2.34 (dq, 2H, J = 7.4, 1.5 Hz, CH_2-4), 1.61-1.33 (m, 6H, CH_2-5, CH_2-6, CH_2-7), 0.93 (t, 3H, J = 7.1 Hz, CH_3-8); HRMS (ES) Calcd for $C_{17}H_{20}NO_2[M+H]^+$ 270.1489, found 270.1484.

(*E*)-((2*S*,3*S*,4*S*,5*S*)-3,4,5-trihydroxy-6-(hydroxymethyl)tetrahydro-2*H*-pyran-2-yl) oct-2-enoate (213)

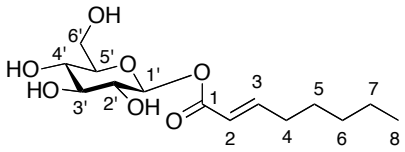

To an ice-cold solution of β-D-glucose (**195**) (0.041 g, 0.23 mmol, 1.2 equiv.) in pyridine (2 mL) was added compound **212** (0.050 g, 0.19 mmol, 1.0 equiv.) and NaH (0.1 mg, 0.004 mmol, 0.02 equiv.). This resulting suspension was stirred at room temperature overnight. The crude product was concentrated *in vacuo* and purified by flash chromatography (silica gel, 93:7 CH_2Cl_2 : MeOH), yielding **213** as a white solid.

^{1}H NMR (D_2O, 400 MHz): 7.23 (dt, 1H, *J* = 15.6, 7.0 Hz, H-3), 5.96 (dt, 1H, *J* = 15.7, 1.4 Hz, H-2), 5.60 (d, 1H, *J* = 8.0 Hz, H-1'), 3.88 (dd, 1H, *J* = 12.3, 2.2 Hz, H-6'), 3.72 (dd, 1H, *J* = 12.3, 5.4 Hz, H-6'), 3.62-3.42 (m, 4H, H-2', H-3', H-4', H-5'), 2.27 (dq, 2H, *J* = 7.1, 1.2 Hz, CH_2-4), 1.53-1.25 (m, 6H, CH_2-5, CH_2-6, CH_2-7), 0.85 (t, 3H, *J* = 7.0 Hz, CH_3-8); LRMS (ES) Calcd for $C_{14}H_{24}O_7Na[M+Na]^+$ 327.1, found 327.2.

(2*E*,4*E*,6*E*)-quinolin-8-yl 2,6-dimethylnona-2,4,6,8-tetraenoate (214)

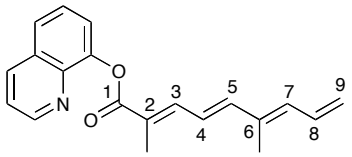

To a solution of **198** (0.030 g, 0.17 mmol, 1.0 equiv.), PyBOP (0.10 g, 0.19 mmol, 1.1 equiv.) and DIPEA (0.066 mL, 0.38 mmol, 2.2 equiv.) in CH_2Cl_2 (2.0 mL) was added 8-hydroxyquinoline (**211**) (0.028 g, 0.19 mmol, 1.1 equiv.). The resulting solution was stirred overnight. The crude was concentrated *in vacuo* and purified by flash chromatography (silica gel, 4:1 hexanes : EtOAc), yielding **214** as a yellow oil (0.032 g, 62%).

IR (CH_2Cl_2, cast film) 3048, 2924, 2856, 1719, 1621, 1586, 1501 cm^{-1}; ^1H NMR ($CDCl_3$, 500 MHz): 8.92 (dd, 1H, *J* = 4.2, 1.7 Hz, Ar-H), 8.17 (dd, 1H, *J* = 8.3, 1.7 Hz, Ar-H), 7.70 (m, 2H, Ar-H), 7.54 (t, 1H, *J* = 7.8 Hz, Ar-H), 7.48 (dd, 1H, *J* = 7.5, 1.4 Hz, H-3), 7.41 (dd, 1H, *J* = 8.3, 4.2 Hz, Ar-H), 6.75 (ddd, 1H, *J* = 16.7, 11.2, 10.2 Hz, H-8), 6.71-6.64 (m, 2H, H-4, H-5), 6.26 (d, 1H, *J* = 11.3 Hz, H-7), 5.37 (d, 1H, *J* = 16.7 Hz, H-9), 5.26 (d, 1H, *J* = 10.2 Hz, H-9), 2.21 (d, 3H, *J* = 1.3 Hz, CH_3-C_2), 1.99 (d, 3H, *J* = 0.9 Hz, CH_3-C_6); ^{13}C NMR ($CDCl_3$, 125 MHz): δ 167.2, 150.5, 148.1, 144.7, 141.6, 140.9, 135.9, 135.6, 135.5, 133.0, 129.6, 126.2, 125.6, 123.7, 121.62, 121.58, 119.8, 13.2, 12.6; HRMS (ES) Calcd for $C_{20}H_{20}NO_2[M+H]^+$ 306.1489, found 306.1483.

quinolin-8-yl hex-5-enoate (216)

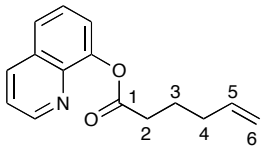

To an ice-cold solution of 5-hexenoic acid (**215**) (0.19 g, 1.7 mmol, 1.0 equiv.), PyBOP (0.88 g, 1.7 mmol, 1.0 equiv.) and HOBt (0.23 g, 1.7 mmol, 1.0 equiv.) in CH_2Cl_2 (2.5 mL) was added DIPEA (0.29 mL, 1.7 mmol, 1.0 equiv.). After stirring for 5 min, 8-hydroxyquinoline (**211**) (0.24 g, 1.7 mmol, 1.0 equiv.) was added. The resulting solution was slowly warmed to room temperature and stirred for another 17 h. The solution was washed sequentially with sat. $NaHCO_3$, H_2O and brine, dried over Na_2SO_4. The crude was filtered, concentrated *in vacuo* and purified by flash chromatography (silica gel, 4:1 hexanes : EtOAc with 1% Et_3N), yielding **216** as a colorless oil (0.21 g, 52%).

IR (CH_2Cl_2, cast film) 3074, 2935, 1760, 1640, 1596, 1500 cm^{-1}; ^1H NMR ($CDCl_3$, 300 MHz): 8.91 (dd, 1H, *J* = 4.2, 1.7 Hz, Ar-H), 8.17 (dd, 1H, *J* = 8.3, 1.7 Hz, Ar-H), 7.72 (dd, 1H, *J* = 8.2, 1.4 Hz, Ar-H), 7.54 (t, 1H, *J* = 7.8 Hz, Ar-H), 7.42 (m, 2H, Ar-H), 5.89 (ddt, 1H, *J* = 17.0, 10.2, 6.8 Hz, H-5), 5.13 (dq, 1H, *J* = 17.1, 1.8 Hz, H-6), 5.05 (ddt, 1H, *J* = 10.2, 2.1, 1.1 Hz, H-6), 2.83 (t, 2H, *J* = 7.5 Hz, CH_2-2), 2.29 (m, 2H, CH_2-4), 1.98 (m, 2H, CH_2-3); ^{13}C NMR ($CDCl_3$, 125 MHz): δ 172.4, 150.4, 147.6, 141.3, 137.8, 136.0, 129.6, 126.2, 125.8, 121.7, 121.5, 115.5, 33.5, 33.1, 24.2; HRMS (ES) Calcd for $C_{15}H_{16}NO_2[M+H]^+$ 242.1176, found 242.1170.

quinolin-8-yl non-8-enoate (218)

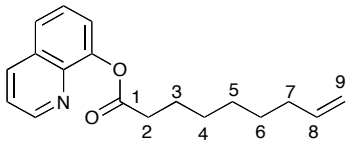

To an ice-cold solution of 8-nonenoic acid (**217**) (0.19 g, 1.2 mmol, 1.0 equiv.) and PyBOP (0.64 g, 1.2 mmol, 1.0 equiv.) in CH_2Cl_2 (2.5 mL) was added DIPEA (0.44 mL, 2.6 mmol, 2.1 equiv.). After stirring for 5 min, 8-hydroxyquinoline (0.18 g, 1.2 mmol, 1.0 equiv.) (**211**) was added. The resulting solution was slowly warmed to room temperature and stirred for another 21 h. The solution was washed sequentially with sat. $NaHCO_3$, H_2O and brine, and dried over Na_2SO_4. The crude was filtered, concentrated *in vacuo* and purified by flash chromatography (silica gel, 3:1 hexanes : EtOAc with 1% Et_3N), yielding **218** as a colorless oil (0.29 g, 84%).

IR ($CDCl_3$, cast film) 3072, 2928, 2856, 1762, 1727, 1640, 1597, 1500 cm^{-1}; ^1H NMR ($CDCl_3$, 500 MHz): 8.90 (dd, 1H, J = 4.2, 1.7 Hz, Ar-H), 8.16 (dd, 1H, J = 8.3, 1.7 Hz, Ar-H), 7.71 (dd, 1H, J = 8.2, 1.3 Hz, Ar-H), 7.54 (t, 1H, J = 7.9 Hz, Ar-H), 7.42 (m, 2H, Ar-H), 5.83 (ddt, 1H, J = 17.0, 10.3, 6.7 Hz, H-8), 5.01 (dq, 1H, J = 17.1, 1.8 Hz, H-9), 4.95 (ddt, 1H, J = 10.2, 2.2, 1.1 Hz, H-9), 2.80 (t, 2H, J = 7.5 Hz, CH_2-2), 2.08 (m, 2H, CH_2-7), 1.87 (m, 2H, CH_2-3), 1.55-1.38 (m, 6H, CH_2-4, CH_2-5, CH_2-6); ^{13}C NMR ($CDCl_3$, 125 MHz): δ 172.6, 150.4, 147.5, 141.3, 139.0, 135.9, 129.5, 126.2, 125.8, 121.7, 121.5, 114.3, 34.2, 33.7, 29.0, 28.79, 28.77, 25.0; HRMS (ES) Calcd for $C_{18}H_{22}NO_2[M+H]^+$ 284.1645, found 284.1639.

(2*E*,4*E*,6*E*,8*E*)-quinolin-8-yl 3,7-dimethyl-9-(2,6,6-trimethylcyclohex-1-enyl)nona-2,4,6,8-tetraenoate (220)

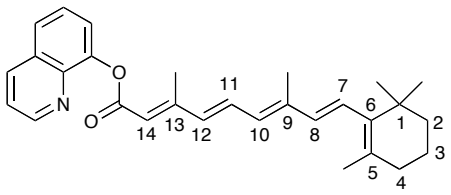

To an ice-cold solution of retinoic acid (**219**) (0.15 g, 0.5 mmol, 1.0 equiv.) and PyBOP (0.26 g, 0.5 mmol, 1.0 equiv.) in CH_2Cl_2 (1.0 mL) was added DIPEA (0.18 mL, 1.05 mmol, 2.1 equiv.). After stirring for 5 min, 8-hydroxyquinoline (**211**) (0.14 g, 0.5 mmol, 1.0 equiv.) was added. The resulting solution was slowly warmed to room temperature and stirred for another 19 h. The solution was washed sequentially with sat. $NaHCO_3$, H_2O and brine, and dried over Na_2SO_4. The crude was filtered, concentrated *in vacuo* and purified by flash chromatography (silica gel, 4:1 hexanes : EtOAc with 1% Et_3N), yielding **220** as a yellow oil (0.22 g, 84%).

IR ($CDCl_3$, cast film) 3043, 2927, 2863, 1729, 1606, 1581, 1500 cm^{-1}; ^1H NMR ($CDCl_3$, 500 MHz): 8.97 (dd, 1H, J = 4.2, 1.7 Hz, Ar-H), 8.21 (dd, 1H, J = 8.3, 1.6 Hz, Ar-H), 7.75 (dd, 1H, J = 8.2, 1.3 Hz, Ar-H), 7.58 (t, 1H, J = 7.8 Hz, Ar-H), 7.52 (dd, 1H, J = 7.5, 1.3 Hz, Ar-H), 7.45 (dd, 1H, J = 8.3, 4.2 Hz, Ar-H), 7.14 (dd, 1H, J = 15.0, 11.4 Hz, H-C_{11}), 6.47 (d, 1H, J = 15.1 Hz, H-C_{12}), 6.37-6.32 (m, 2H, H-C_7, H-C_{10}), 6.27-6.19 (m, 2H, H-C_8, H-C_{14}), 2.47 (d, 3H, J = 0.8 Hz, CH_3-C_{13}), 2.10-2.07 (m, 2H, CH_2-C_5), 2.06 (s, 3H, CH_3-C_9), 1.77 (s, 3H, CH_3-C_5), 1.69-1.63 (m, 2H, $CH_2CH_2CH_2$), 1.53-1.50 (m, 2H, CH_2-C_1), 1.08 (s, 6H, CH_3-C_1, CH_3-C_1); ^{13}C NMR ($CDCl_3$, 125 MHz): δ 165,7, 155.9, 150.6, 147.5, 141.6, 140.3, 137.7, 137.3, 136.0, 135.0, 131.9, 130.2, 129.6, 129.0,

126.2, 125.6, 121.8, 121.6, 117.2, 39.7, 34.3, 33.2, 29.0, 21.8, 19.2, 14.2, 13.0; HRMS (ES) Calcd for $C_{29}H_{34}NO_2[M+H]^+$ 428.2584, found 428.2577.

Chapter 6 : References

1. Sewald, N.; Jakubke, H., *Peptides: chemistry and biology*; Wiley: Weinheim, 2002.

2. Merrifield, R. B., Solid phase peptide synthesis .I. Synthesis of a tetrapeptide. *J. Am. Chem. Soc.* **1963,** *85*, 2149-2154.

3. Dawson, P. E.; Muir, T. W.; Clarklewis, I.; Kent, S. B. H., Synthesis of proteins by native chemical ligation. *Science* **1994,** *266*, 776-779.

4. Brazeau, P.; Vale, W.; Burgus, R.; Ling, N.; Butcher, M.; Rivier, J.; Guillemin.R., Hypothalamic polypeptide that inhibits secretion of immunoreactive pituitary growth-hormone. *Science* **1973,** *179* , 77-79.

5. Konno, K.; Picolo, G.; Gutierrez, V. P.; Brigatte, P.; Zambelli, V. O.; Camargo, A. C. M.; Cury, Y., Crotalphine, a novel potent analgesic peptide from the venom of the South American rattlesnake Crotalus durissus terrificus. *Peptides* **2008,** *29*, 1293-1304.

6. Gutierrez, V. P.; Konno, K.; Chacur, M.; Sampaio, S. C.; Picolo, G.; Brigatte, P.; Zambelli, V. O.; Cury, Y., Crotalphine induces potent antinociception in neuropathic pain by acting at peripheral opioid receptors. *Eur. J. Pharmacol.* **2008,** *594*, 84-92.

7. Williams, D. E.; Austin, P.; Diaz-Marrero, A. R.; Van Soest, R.; Matainaho, T.; Roskelley, C. D.; Roberge, M.; Andersen, R. J., Neopetrosiamides, peptides from the marine sponge Neopetrosia sp that inhibit amoeboid invasion by human tumor cells. *Org. Lett.* **2005,** *7*, 4173-4176.

8. Liu, H. Q.; Boudreau, M. A.; Zheng, J.; Whittal, R. M.; Austin, P.; Roskelley, C. D.; Roberge, M.; Andersen, R. J.; Vederas, J. C., Chemical synthesis and biological

activity of the neopetrosiamides and their analogues: revision of disulfide bond connectivity. *J. Am. Chem. Soc.* **2010,** *132*, 1486-1487.

9. Durek, T.; Torbeev, V. Y.; Kent, S. B. H., Convergent chemical synthesis and high-resolution x-ray structure of human lysozyme. *Proc. Natl. Acad. Sci. U.S.A.* **2007,** *104*, 4846-4851.

10. Pedroso, E.; Grandas, A.; Delasheras, X.; Eritja, R.; Giralt, E., Diketopiperazine formation in solid-phase peptide-synthesis using p-alkoxybenzyl ester resins and Fmoc-amino acids. *Tetrahedron Lett.* **1986,** *27*, 743-746.

11. Giralt, E.; Eritja, R.; Pedroso, E., Diketopiperazine formation in acetamido-bridged and nitrobenzamido-bridged polymeric supports. *Tetrahedron Lett.* **1981,** *22*, 3779-3782.

12. Zinieris, N.; Zikos, C.; Ferderigos, N., Improved solid-phase peptide synthesis of 'difficult peptides' by altering the microenvironment of the developing sequence. *Tetrahedron Lett.* **2006,** *47*, 6861-6864.

13. Barber, M.; Jones, J. H.; Witty, M. J., Structural factors affecting the direct exchange racemization of benzyloxycarbonyl-*S*-benzyl-L-cysteine pentachlorophenyl ester and related compounds by triethylamine in chloroform. *J. Chem. Soc. Perkin Trans. 1* **1979,** 2425-2428.

14. Hibino, H.; Nishiuchi, Y., 4-Methoxybenzyloxymethyl group, a racemization-resistant protecting group for cysteine in Fmoc solid phase peptide synthesis. *Org. Lett.* **2012,** *14*, 1926-1929.

15. Lukszo, J.; Patterson, D.; Albericio, F.; Kates, S. A., 3-(1-Piperidinyl)alanine formation during the preparation of C-terminal cysteine peptides with the Fmoc/t-Bu strategy. *Lett. Pept. Sci.* **1996,** *3*, 157-166.

16. Fujiwara, Y.; Akaji, K.; Kiso, Y., Racemization-free synthesis of C-terminal cysteine-peptide using 2-chlorotrityl resin. *Chem. Pharm. Bull.* **1994,** *42*, 724-726.

17. Barany, G.; Han, Y. X.; Hargittai, B.; Liu, R. Q.; Varkey, J. T., Side-chain anchoring strategy for solid-phase synthesis of peptide acids with C-terminal cysteine. *Biopolymers* **2003,** *71*, 652-666.

18. Blaskovich, M. A.; Lajoie, G. A., Synthesis of a chiral serine aldehyde equivalent and its conversion to chiral alpha-amino-acid derivatives. *J. Am. Chem. Soc.* **1993,** *115*, 5021-5030.

19. Rife, J.; Ortuno, R. M.; Lajoie, G. A., Stereoselective synthesis of L-2-(carboxycyclopropyl)glycines via stereocontrolled 1,3-dipolar cycloadditions of diazomethane on *Z*- and *E*-3,4-L-didehydroglutamates OBO esters. *J. Org. Chem.* **1999,** *64*, 8958-8961.

20. Blaskovich, M. A.; Evindar, G.; Rose, N. G. W.; Wilkinson, S.; Luo, Y.; Lajoie, G. A., Stereoselective synthesis of *threo* and *erythro* beta-hydroxy and beta-disubstituted-beta-hydroxy alpha-amino acids. *J. Org. Chem.* **1998,** *63*, 4560-4560.

21. Herdeis, C.; Kelm, B., A stereoselective synthesis of 3-substituted (*S*)-pyroglutamic and glutamic acids via OBO ester derivatives. *Tetrahedron* **2003,** *59*, 217-229.

22. Raghavan, B.; Johnson, R. L., Short stereoselective synthesis of alpha-substituted gamma-lactams. *J. Org. Chem.* **2006,** *71*, 2151-2154.

23. Oba, M.; Saegusa, T.; Nishiyama, N.; Nishiyama, K., Synthesis of non-proteinogenic amino acids using Michael addition to unsaturated orthopyroglutamate derivative. *Tetrahedron* **2009,** *65*, 128-133.

24. Yoo, D.; Oh, J. S.; Lee, D. W.; Kim, Y. G., Efficient synthesis of a configurationally stable L-serinal derivative. *J. Org. Chem.* **2003,** *68*, 2979-2982.

25. Hamada, M.; Shinada, T.; Ohfune, Y., Efficient total synthesis of (-)-kaitocephalin. *Org. Lett.* **2009,** *11*, 4664-4667.

26. Hansen, D. B.; Wan, X. B.; Carroll, P. J.; Joullie, M. M., Stereoselective synthesis of four stereoisomers of beta-methoxytyrosine, a component of callipeltin A. *J. Org. Chem.* **2005,** *70*, 3120-3126.

27. Hansen, D. B.; Lewis, A. S.; Gavalas, S. J.; Joullie, M. M., A stereoselective synthetic approach to (2*S*,3*R*)-N-(1 ' 1 '-dimethyl-2 ',3 '-epoxypropyl)-3-hydroxytryptophan, a component of cyclomarin A. *Tetrahedron-Asymmetry* **2006,** *17*, 15-21.

28. Zhdanko, A. G.; Nenajdenko, V. G., Nonracemizable Isocyanoacetates for Multicomponent Reactions. *J. Org. Chem.* **2009,** *74*, 884-887.

29. Zhdanko, A. G.; Gulevich, A. V.; Nenajdenko, V. G., One-step synthesis of *N*-acetylcysteine and glutathione derivatives using the Ugi reaction. *Tetrahedron* **2009,** *65*, 4692-4702.

30. Derksen, D. J., Synthesis & testing of bacteriocin analogues. *University of Alberta PhD Thesis* **2008**.

31. Huang, Z.; Derksen, D. J.; Vederas, J. C., Preparation and use of cysteine orthoesters for solid-supported synthesis of peptides. *Org. Lett.* **2010,** *12*, 2282-2285.

32. Liu, W.; Chan, A. S. H.; Liu, H. Q.; Cochrane, S. A.; Vederas, J. C., Solid supported chemical syntheses of both components of the lantibiotic lacticin 3147. *J. Am. Chem. Soc.* **2011,** *133*, 14216-14219.

33. Liu, H. Q.; Pattabiraman, V. R.; Vederas, J. C., Stereoselective syntheses of 4-oxa diaminopimelic acid and its protected derivatives via aziridine ring opening. *Org. Lett.* **2007,** *9*, 4211-4214.

34. Tegge, W.; Bautsch, W.; Frank, R., Synthesis of cyclic peptides and peptide libraries on a new disulfide linker. *J. Pept. Sci.* **2007,** *13*, 693-699.

35. Lack, O.; Zbinden, H.; Woggon, W. D., A useful disulfide linker for single-bead analysis of peptide libraries. *Helv. Chim. Acta* **2002,** *85*, 495-501.

36. Mery, J.; Brugidou, J.; Derancourt, J., Disulfide bond as peptide-resin linkage in Boc-Bzl spps, for potential biochemical applications. *Pept. Res.* **1992,** *5*, 233-240.

37. Brugidou, J.; Mery, J., 2-Hydroxypropyl-dithio-2'-isobutyric acid (Hpdi) as a multipurpose peptide-resin linker for spps. *Pept. Res.* **1994,** *7*, 40-47.

38. Merskey, H.; Bogduk, N., *Classification of chronic pain*; International Association for the Study of Pain: Seattle, 1994.

39. Woolf, C. J., Pain: Moving from symptom control toward mechanism-specific pharmacologic management. *Ann. Intern. Med.* **2004,** *140*, 441-451.

40. Edwards, C. M. B.; Cohen, M. A.; Bloom, S. R., Peptides as drugs. *Qjm-mon. J. Assoc. Phys* **1999,** *92*, 1-4.

41. Waldhoer, M.; Bartlett, S. E.; Whistler, J. L., Opioid receptors. *Annu. Rev. Biochem* **2004,** *73*, 953-990.

42. Hong, S. Y.; Oh, J. E.; Lee, K. H., Effect of D-amino acid substitution on the stability, the secondary structure, and the activity of membrane-active peptide. *Biochem. Pharmacol.* **1999,** *58*, 1775-1780.

43. Pouny, Y.; Shai, Y., Interaction of D-amino-acid ancorporated analogs of paradoxin with membranes. *Biochemistry* **1992,** *31*, 9482-9490.

44. Cribbs, D. H.; Pike, C. J.; Weinstein, S. L.; Velazquez, P.; Cotman, C. W., All-D-enantiomers of beta-amyloid exhibit similar biological properties to all-L-beta-amyloids. *J. Biol. Chem.* **1997,** *272*, 7431-7436.

45. Pritsker, M.; Jones, P.; Blumenthal, R.; Shai, Y. C., A synthetic all D-amino acid peptide corresponding to the N-terminal sequence of HIV-1 gp41 recognizes the wild-type fusion peptide in the membrane and inhibits HIV-1 envelope glycoprotein-mediated cell fusion. *Proc. Natl. Acad. Sci. U.S.A.* **1998,** *95*, 7287-7292.

46. Yan, L. Z.; Gibbs, A. C.; Stiles, M. E.; Wishart, D. S.; Vederas, J. C., Analogues of bacteriocins: antimicrobial specificity and interactions of leucocin A with its enantiomer, carnobacteriocin B2, and truncated derivatives. *J. Med. Chem.* **2000,** *43*, 4579-4581.

47. Derksen, D. J.; Stymiest, J. L.; Vederas, J. C., Antimicrobial leucocin analogues with a disulfide bridge replaced by a carbocycle or by noncovalent interactions of allyl glycine residues. *J. Am. Chem. Soc.* **2006,** *128*, 14252-14253.

48. Sit, C. S.; Lohans, C. T.; van Belkum, M. J.; Campbell, C. D.; Miskolzie, M.; Vederas, J. C., Substitution of a conserved disulfide in the type IIa bacteriocin, leucocin A, with L-leucine and L-serine residues: effects on activity and three-dimensional structure. *Chembiochem* **2012,** *13*, 35-38.

49. Miller, S. J.; Blackwell, H. E.; Grubbs, R. H., Application of ring-closing metathesis to the synthesis of rigidified amino acids and peptides. *J. Am. Chem. Soc.* **1996,** *118*, 9606-9614.

50. Williams, R. M.; Liu, J. W., Asymmetric synthesis of differentially protected 2,7-diaminosuberic acid, a ring-closure metathesis approach. *J. Org. Chem.* **1998,** *63*, 2130-2132.

51. Gao, Y.; Lane-Bell, P.; Vederas, J. C., Stereoselective synthesis of *meso*-2,6-diaminopimelic acid and its selectively protected derivatives. *J. Org. Chem.* **1998,** *63*, 2133-2143.

52. Schafmeister, C. E.; Po, J.; Verdine, G. L., An all-hydrocarbon cross-linking system for enhancing the helicity and metabolic stability of peptides. *J. Am. Chem. Soc.* **2000,** *122*, 5891-5892.

53. Berman, H. M.; Westbrook, J.; Arzberger, P.; Bourne, P.; Gilliland, G.; Fagan, P., Our vision for the new protein data bank. *Biophys. J.* **1999,** *76*, A200-A200.

54. Matthews, B. W., Racemic crystallography--easy crystals and easy structures: what's not to like? *Protein Sci.* **2009,** *18*, 1135-1138.

55. Wukovitz, S. W.; Yeates, T. O., Why protein crystals favor some space-groups over others. *Nat. Struct. Biol.* **1995,** *2*, 1062-1067.

56. Mandal, K.; Pentelute, B. L.; Tereshko, V.; Kossiakoff, A. A.; Kent, S. B. H., X-ray structure of native scorpion toxin BmBKTx1 by racemic protein crystallography using direct methods. *J. Am. Chem. Soc.* **2009,** *131*, 1362-1363.

57. Mandal, K.; Pentelute, B. L.; Tereshko, V.; Thammavongsa, V.; Schneewind, O.; Kossiakoff, A. A.; Kent, S. B. H., Racemic crystallography of synthetic protein

enantiomers used to determine the X-ray structure of plectasin by direct methods. *Protein Sci.* **2009,** *18*, 1146-1154.

58. Pentelute, B. L.; Gates, Z. P.; Tereshko, V.; Dashnau, J. L.; Vanderkooi, J. M.; Kossiakoff, A. A.; Kent, S. B. H., X-ray structure of snow flea antifreeze protein determined by racemic crystallization of synthetic protein enantiomers. *J. Am. Chem. Soc.* **2008,** *130*, 9695-9701.

59. Pentelute, B. L.; Mandal, K.; Gates, Z. P.; Sawaya, M. R.; Yeates, T. O.; Kent, S. B. H., Total chemical synthesis and X-ray structure of kaliotoxin by racemic protein crystallography. *Chem. Commun.* **2010,** *46*, 8174-8176.

60. Doi, M.; Ishibe, A.; Shinozaki, H.; Urata, H.; Inoue, M.; Ishida, T., Conserved and novel structural characteristics of enantiomorphic Leu-enkephalin - X-ray crystal analysis of Leu-enkephalin enantiomer, L-Tyr-Gly-Gly-L-Phe-L-Leu and D-Tyr-Gly-Gly-D-Phe-D-Leu. *Int. J. Pept. Protein Res.* **1994,** *43*, 325-331.

61. Toniolo, C.; Peggion, C.; Crisma, M.; Formaggio, F.; Shui, X. Q.; Eggleston, D. S., Structure determination of racemic trichogin-a-iv using centrosymmetric crystals. *Nat. Struc. Biol.* **1994,** *1*, 908-914.

62. Patterson, W. R.; Anderson, D. H.; DeGrado, W. F.; Cascio, D.; Eisenberg, D., Centrosymmetric bilayers in the 0.75 angstrom resolution structure of a designed alpha-helical peptide, D,L-Alpha-1. *Protein Sci.* **1999,** *8*, 1410-1422.

63. Jack, R. W.; Tagg, J. R.; Ray, B., Bacteriocins of gram-positive bacteria. *Microbiol. Rev.* **1995,** *59*, 171-200.

64. Kolter, R.; Moreno, F., Genetics of ribosomally synthesized peptide antibiotics. *Annu. Rev. Microbiol.* **1992,** *46*, 141-163.

65. Zheng, G. L.; Hehn, R.; Zuber, P., Mutational analysis of the sbo-alb locus of Bacillus subtilis: Identification of genes required for subtilosin production and immunity. *J. Bacteriol.* **2000,** *182*, 3266-3273.

66. Klaenhammer, T. R., Genetics of bacteriocins produced by lactic-acid bacteria. *FEMS Microbiol. Rev.* **1993,** *12*, 39-86.

67. Nes, I. F.; Hole, H., Class II antimicrobial peptides from lactic acid bacteria. *Biopolymers* **2000,** *55*, 50-61.

68. van Belkum, M. J.; Stiles, M. E., Nonlantibiotic antibacterial peptides from lactic acid bacteria. *Nat. Prod. Rep.* **2000,** *17*, 323-335.

69. Cotter, P. D.; Hill, C.; Ross, R. P., Bacteriocins: developing innate immunity for food. *Nat. Rev. Microbiol.* **2005,** *3*, 777-788.

70. Chatterjee, C.; Paul, M.; Xie, L.; van der Donk, W. A., Biosynthesis and mode of action of lantibiotics. *Chem. Rev.* **2005,** *105*, 633-684.

71. Kawulka, K.; Sprules, T.; McKay, R. T.; Mercier, P.; Diaper, C. M.; Zuber, P.; Vederas, J. C., Structure of subtilosin A, an antimicrobial peptide from Bacillus subtilis with unusual posttranslational modifications linking cysteine sulfurs to alpha-carbons of phenylalanine and threonine. *J. Am. Chem. Soc.* **2003,** *125*, 4726-4727.

72. Kawulka, K. E.; Sprules, T.; Diaper, C. M.; Whittal, R. M.; McKay, R. T.; Mercier, P.; Zuber, P.; Vederas, J. C., Structure of subtilosin A, a cyclic antimicrobial peptide from Bacillus subtilis with unusual sulfur to alpha-carbon cross-links: Formation and reduction of alpha-thio-alpha-amino acid derivatives. *Biochemistry* **2004,** *43*, 3385-3395.

73. Rea, M. C.; Sit, C. S.; Clayton, E.; O'Connor, P. M.; Whittal, R. M.; Zheng, J.; Vederas, J. C.; Ross, R. P.; Hill, C., Thuricin CD, a posttranslationally modified bacteriocin with a narrow spectrum of activity against Clostridium difficile. *Proc. Natl. Acad. Sci. U.S.A.* **2010,** *107*, 9352-9357.

74. Sit, C. S.; Mckay, R. T.; Hill, C.; Ross, R. P.; Vederas, J. C., The 3D structure of thuricin CD, a two-component bacteriocin with cysteine sulfur to alpha-carbon cross-links. *J. Am. Chem. Soc.* **2011,** *133*, 7680-7683.

75. Sit, C. S.; 3D Structures of S-linked bacteriocins. *University of Alberta PhD Thesis* **2011**.

76. Fluhe, E.; Knappe, T. A.; Gattner, M. J.; Schafer, A.; Burghaus, O.; Linne, U.; Marahiel, M. A., The radical SAM enzyme AlbA catalyzes thioether bond formation in subtilosin A. *Nat. Chem. Biol.* **2012,** *8*, 350-357.

77. Thennarasu, S.; Lee, D. K.; Poon, A.; Kawulka, K. E.; Vederas, J. C.; Ramamoorthy, A., Membrane permeabilization, orientation, and antimicrobial mechanism of subtilosin A. *Chem. Phys. Lipids* **2005,** *137*, 38-51.

78. Yamamoto, K.; Xu, J. D.; Kawulka, K. E.; Vederas, J. C.; Ramamoorthy, A., Use of a copper-chelated lipid speeds up NMR measurements from membrane proteins. *J. Am. Chem. Soc.* **2010,** *132*, 6929-6931.

79. Martin-Visscher, L. A.; van Belkum, M. J.; Vederas, J. C., Class IIc or circular bacteriocins. *In Prokaryotic Antimicrobial Peptides* **2011**, 213-236.

80. Huang, T.; Geng, H.; Miyyapuram, V. R.; Sit, C. S.; Vederas, J. C.; Nakano, M. M., Isolation of a variant of subtilosin A with hemolytic activity. *J. Bacteriol.* **2009,** *191*, 5690-5696.

81. Sit, C. S.; van Belkum, M. J.; McKay, R. T.; Worobo, R. W.; Vederas, J. C., The 3D solution structure of thurincin H, a bacteriocin with four sulfur to alpha-carbon crosslinks. *Angew. Chem. Int. Ed.* **2011,** *50*, 8718-8721.

82. Ross, A. C.; Liu, H. Q.; Pattabiraman, V. R.; Vederas, J. C., Synthesis of the lantibiotic lactocin S using peptide cyclizations on solid phase. *J. Am. Chem. Soc.* **2010,** *132*, 462-463.

83. Fu, S. C. J.; Birnbaum, S. M., The hydrolytic action of acylase-I on *N*-acylamino Acids. *J. Am. Chem. Soc.* **1953,** *75*, 918-920.

84. Banphavichit, V.; Mansawat, W.; Bhanthumnavin, W.; Vilaivan, T., A highly enantioselective Strecker reaction catalyzed by titanium-*N*-salicyl-beta-aminoalcohol complexes. *Tetrahedron* **2004,** *60*, 10559-10568.

85. Noyori, R., Chemical multiplication of chirality - science and applications. *Chem. Soc. Rev.* **1989,** *18*, 187-208.

86. Williams, R. M.; Sinclair, P. J.; Zhai, D.; Chen, D., Practical asymmetric syntheses of alpha-amino-acids through carbon carbon bond constructions on electrophilic glycine templates. *J. Am. Chem. Soc.* **1988,** *110*, 1547-1557.

87. Schollkopf, U.; Groth, U.; Deng, C., Asymmetric syntheses via heterocyclic intermediates .6. Enantioselective synthesis of (*R*)-amino acids using L-valine as chiral agent. *Angew.Chem. Int. Ed. Engl.* **1981,** *20*, 798-799.

88. Seebach, D.; Boes, M.; Naef, R.; Schweizer, W. B., Alkylation of amino-acids without loss of the optical-activity - preparation of alpha-substituted proline derivatives - a case of self-reproduction of chirality. *J. Am. Chem. Soc.* **1983,** *105*, 5390-5398.

89. Luo, Y. C.; Zhang, H. H.; Wang, Y.; Xu, P. F., Synthesis of alpha-amino acids based on chiral tricycloiminolactone derived from natural (+)-camphor. *Acc. Chem. Res.* **2010,** *43*, 1317-1330.

90. Xu, P. F.; Chen, Y. S.; Lin, S. I.; Lu, T. J., Chiral tricyclic iminolactone derived from (1*R*)-(+)-camphor as a glycine equivalent for the asymmetric synthesis of alpha-amino acids. *J. Org. Chem.* **2002,** *67*, 2309-2314.

91. Xu, P. F.; Li, S.; Lu, T. J.; Wu, C. C.; Fan, B. T.; Golfis, G., Asymmetric synthesis of alpha,alpha-disubstituted alpha-amino acids by diastereoselective alkylation of camphor-based tricyclic iminolactone. *J. Org. Chem.* **2006,** *71*, 4364-4373.

92. Zhang, H. H.; Hu, X. Q.; Wang, X.; Luo, Y. C.; Xu, P. F., A convenient route to enantiopure 3-aryl-2,3-diaminopropanoic acids by diastereoselective Mannich reaction of camphor-based tricyclic iminolactone with imines. *J. Org. Chem.* **2008,** *73*, 3634-3637.

93. Li, Q.; Yang, S. B.; Zhang, Z. H.; Li, L.; Xu, P. F., Diastereo- and enantioselective synthesis of beta-hydroxy-alpha-amino acids: application to the synthesis of a key intermediate for lactacystin. *J. Org. Chem.* **2009,** *74*, 1627-1631.

94. Huang, Y.; Li, Q.; Liu, T. L.; Xu, P. F., Diastereoselective synthesis of beta-substituted-alpha,gamma-diaminobutyric acids and pyrrolidines containing multichiral centers. *J. Org. Chem.* **2009,** *74*, 1252-1258.

95. Wang, P. F.; Gao, P.; Xu, P. F., Synthesis and 1,3-dipolar cycloadditions of two new chiral geometrically fixed alpha-alkoxycarbonylnitrones from a single chiral source. *Synlett* **2006,** 1095-1099.

96. Gan, F. F.; Yang, S. B.; Luo, Y. C.; Yang, W. B.; Xu, P. F., Total synthesis of sphingofungin F based on chiral tricyclic iminolactone. *J. Org. Chem.* **2010,** *75*, 2737-2740.

97. Wang, H. F.; Ma, G. H.; Yang, S. B.; Han, R. G.; Xu, P. F., A concise synthesis of (+)-conagenin and its isomer using chiral tricyclic iminolactones. *Tetrahedron-Asymmetry* **2008,** *19*, 1630-1635.

98. Chan, W. C.; White, P. D., *Fmoc solid phase peptide synthesis*; Oxford University Press: New York, 2004.

99. Haack, T.; Mutter, M., Serine derived oxazolidines as secondary structure disrupting, solubilizing building-blocks in peptide-synthesis. *Tetrahedron Lett.* **1992,** *33*, 1589-1592.

100. Mutter, M.; Nefzi, A.; Sato, T.; Sun, X.; Wahl, F.; Wohr, T., Pseudo-prolines (Psi-Pro) for accessing inaccessible peptides. *Pept. Res.* **1995,** *8*, 145-153.

101. Cardona, V.; Eberle, I.; Barthelemy, S.; Beythien, J.; Doerner, B.; Schneeberger, P.; Keyte, J.; White, P. D., Application of dmb-dipeptides in the Fmoc SPPS of difficult and aspartimide-prone sequences. *Int. J. Pept. Res. Ther.* **2008,** *14*, 285-292.

102. Garcia-Martin, F.; Quintanar-Audelo, M.; Garcia-Ramos, Y.; Cruz, L. J.; Gravel, C.; Furic, R.; Cote, S.; Tulla-Puche, J.; Albericio, F., ChemMatrix, a poly(ethylene glycol)-based support for the solid-phase synthesis of complex peptides. *J. Comb. Chem.* **2006,** *8*, 213-220.

103. Ross, A. C.; McKinnie, S. M. K.; Vederas, J. C., The synthesis of active and stable diaminopimelate analogues of the lantibiotic peptide lactocin S. *J. Am. Chem. Soc.* **2012,** *134*, 2008-2011.

104. Xi, L. A.; Qian, Z. Y., Pharmacological properties of crocetin and crocin (digentiobiosyl ester of crocetin) from saffron. *Nat. Prod. Commun.* **2006,** *1*, 65-75.

105. Wani, B. A.; Hamza, A. K. R.; Mohiddin, F. A., Saffron: A repository of medicinal properties. *J. Med. Plants Res.* **2011,** *5*, 2131-2135.

106. Negbi, M., *Saffron Crocus sativus L;* CRC Press: Amsterdam, 1999.

107. Sugiura, M.; Shoyama, Y.; Saito, H.; Abe, K., Crocin (crocetin di-gentiobiose ester) prevents the inhibitory effect of ethanol on long-term potentiation in the dentate gyrus in-vivo. *J. Pharmacol. Exp. Ther.* **1994,** *271*, 703-707.

108. Escribano, J.; Alonso, G. L.; CocaPrados, M.; Fernandez, J. A., Crocin, safranal and picrocrocin from saffron (Crocus sativus L) inhibit the growth of human cancer cells in vitro. *Cancer Lett.* **1996,** *100*, 23-30.

109. Masaki, M.; Aritake, K.; Tanaka, H.; Shoyama, Y.; Huang, Z. L.; Urade, Y., Crocin promotes non-rapid eye movement sleep in mice. *Mol. Nutr. Food Res.* **2012,** *56*, 304-308.

110. Pham, T. Q.; Cormier, F.; Farnworth, E.; Tong, V. H.; Van Calsteren, M. R., Antioxidant properties of crocin from Gardenia jasminoides Ellis and study of the reactions of crocin with linoleic acid and crocin with oxygen. *J. Agric. Food. Chem.* **2000,** *48*, 1455-1461.

111. Deslauriers, A. M.; Afkhami-Goli, A.; Paul, A. M.; Bhat, R. K.; Acharjee, S.; Ellestad, K. K.; Noorbakhsh, F.; Michalak, M.; Power, C., Neuroinflammation and endoplasmic reticulum stress are coregulated by crocin to prevent demyelination and neurodegeneration. *J. Immunol.* **2011,** *187*, 4788-4799.

112. Xu, G. L.; Li, G.; Ma, H. P.; Zhong, H.; Liu, F.; Ao, G. Z., Preventive effect of crocin in inflamed animals and in LPS-challenged RAW 264.7 Cells. *J. Agric. Food. Chem.* **2009,** *57*, 8325-8330.

113. Ulbricht, C.; Conquer, J.; Costa, D.; Hollands, W.; Iannuzzi, C.; Isaac, R.; Jordan, J. K.; Ledesma, N.; Ostroff, C.; Serrano, J. M.; Shaffer, M. D.; Varghese, M., An evidence-based systematic review of saffron (Crocus sativus) by the natural standard research collaboration. *J. Diet. Suppl.* **2011,** *8*, 58-114.

114. Moghaddasi, M. S., Saffron chemicals and medicine usage. *J. Med. Plants Res.* **2010,** *4*, 427-430.

115. Bouvier, F.; Suire, C.; Mutterer, J.; Camara, B., Oxidative remodeling of chromoplast carotenoids: Identification of the carotenoid dioxygenase CsCCD and CsZCD genes involved in crocus secondary metabolite biogenesis. *Plant Cell* **2003,** *15*, 47-62.

116. Pfander, H.; Schurtenberger, H., Biosynthesis of C20-carotenoids in crocus-sativus. *Phytochemistry* **1982,** *21*, 1039-1042.

117. Cote, F.; Cormier, F.; Dufresne, C.; Willemot, C., A highly specific glucosyltransferase is involved in the synthesis of crocetin glucosylesters in Crocus sativus cultured cells. *J. Plant Physiol.* **2001,** *158*, 553-560.

118. Nagatoshi, M.; Terasaka, K.; Owaki, M.; Sota, M.; Inukai, T.; Nagatsu, A.; Mizukami, H., UGT75L6 and UGT94E5 mediate sequential glucosylation of crocetin to crocin in Gardenia jasminoides. *FEBS Lett.* **2012,** *586*, 1055-1061.

119. Hill, T., *The contemporary encyclopedia of herbs and spices: seasonings for the global kitchen;* Wiley: Weinheim, 2004.

120. Vaz, B.; Alvarez, R.; de Lera, A. R., Synthesis of symmetrical carotenoids by a two-fold Stille reaction. *J. Org. Chem.* **2002,** *67*, 5040-5043.

121. Grubbs, R. H., Olefin metathesis. *Tetrahedron* **2004,** *60*, 7117-7140.

122. Fontan, N.; Dominguez, M.; Alvarez, R.; de Lera, A. R., Synthesis of C-40-symmetrical fully conjugated carotenoids by olefin metathesis. *Eur. J. Org. Chem.* **2011**, 6704-6712.

123. Furuichi, N.; Hara, H.; Osaki, T.; Mori, H.; Katsumura, S., Highly efficient stereocontrolled total synthesis of the polyfunctional carotenoid peridinin. *Angew. Chem. Int. Ed.* **2002,** *41*, 1023-1026.

124. Frederico, D.; Donate, P. M.; Constantino, M. G.; Bronze, E. S.; Sairre, M. I., A short and efficient synthesis of crocetin-dimethylester and crocetindial. *J. Org. Chem.* **2003,** *68*, 9126-9128.

125. Pfander, H., Synthesis of carotenoid glycosylesters and other carotenoids. *Pure Appl. Chem.* **1979,** *51*, 565-580.

126. Karrer, P.; Benz, F.; Stoll, M., Coloured compounds from plants XLIX. Synthesis of perhydro-crocetins. *Helv. Chim. Acta* **1933,** *16*, 297-302.

127. Kanai, M.; Mortell, K. H.; Kiessling, L. L., Varying the size of multivalent ligands: The dependence of concanavalin a binding on neoglycopolymer length. *J. Am. Chem. Soc.* **1997,** *119*, 9931-9932.

128. Lin, Y. A.; Chalker, J. M.; Floyd, N.; Bernardes, G. J. L.; Davis, B. G., Allyl sulfides are privileged substrates in aqueous cross-metathesis: Application to site-selective protein modification. *J. Am. Chem. Soc.* **2008,** *130*, 9642-9643.

129. Zhao, Y. J.; Loh, T. P., Practical synthesis of 1,5-dimethyl substituted conjugated polyenes from geranyl acetate. *Tetrahedron* **2008,** *64*, 4972-4978.

130. Zhang, J. M.; Li, S.; Zhang, D. H.; Wang, H.; Whorton, A. R.; Xian, M., Reductive Ligation Mediated One-Step Disulfide Formation of S-Nitrosothiols. *Org. Lett.* **2010,** *12*, 4208-4211.

APPENDIX : Chemical Synthesis of Standards for Elucidation of Stereochemistry of Lipid chain of Tridecaptin A

A.1 Introduction

Recently Christopher Lohans, a graduate student in the Vederas group, isolated a peptide from the strain of *Bacillus circulans* NRRL B-30644. This peptide is active against Gram-negative bacteria, including *Escherichia coli* DH5α. This peptide was characterized using MALDI-MS, LC-MS/MS, chiral GC-MS and NMR. All the data indicates it is the known peptide called tridecaptin A (Figure A.1).[A1] Notably, the stereochemistry of the lipid chain of tridecaptin A is unknown, although this peptide has been known for decades.

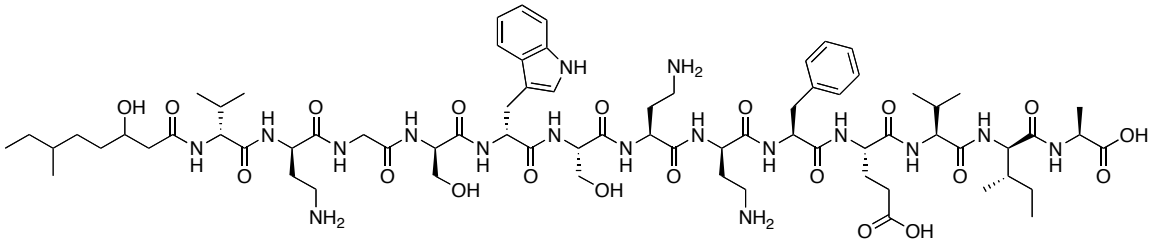

Figure A.1 Structure of tridecaptin A

A.2 Objectives

The objective of this project was to chemically synthesize all the four possible isomers (Figure A.2) as standards to elucidate the stereochemistry of the lipid chain of tridecaptin A using chiral GC-MS as a tool.

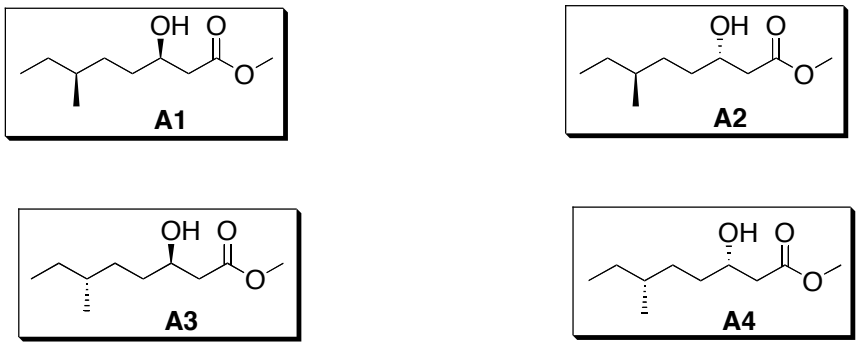

Figure A.2 Four synthetic standards (**A1**-**A4**) to elucidate the stereochemistry of tridecaptin A lipid chain

A.3 Results and Discussions

A.3.1 Retrosynthetic analysis of standards A1-A4

All of these standards were envisioned to be synthesized using an aldol reaction as the key step. Taking compound **A1** as an example, the retrosynthetic analysis is shown in Scheme 7.1. Compound **A1** could be prepared from compound A**5** which was the product of the aldol reaction of aldehyde **A6** with compound **A7**.[A2,A3] Aldehyde A**6** would be synthesized from alkene **A8** by an ozonolysis reaction. Alkene **A8** could be readily prepared from commercially available (*R*)-citronellol. On the other hand, compound **A7** could be synthesized from the Crimmins auxiliary by an acylation reaction.

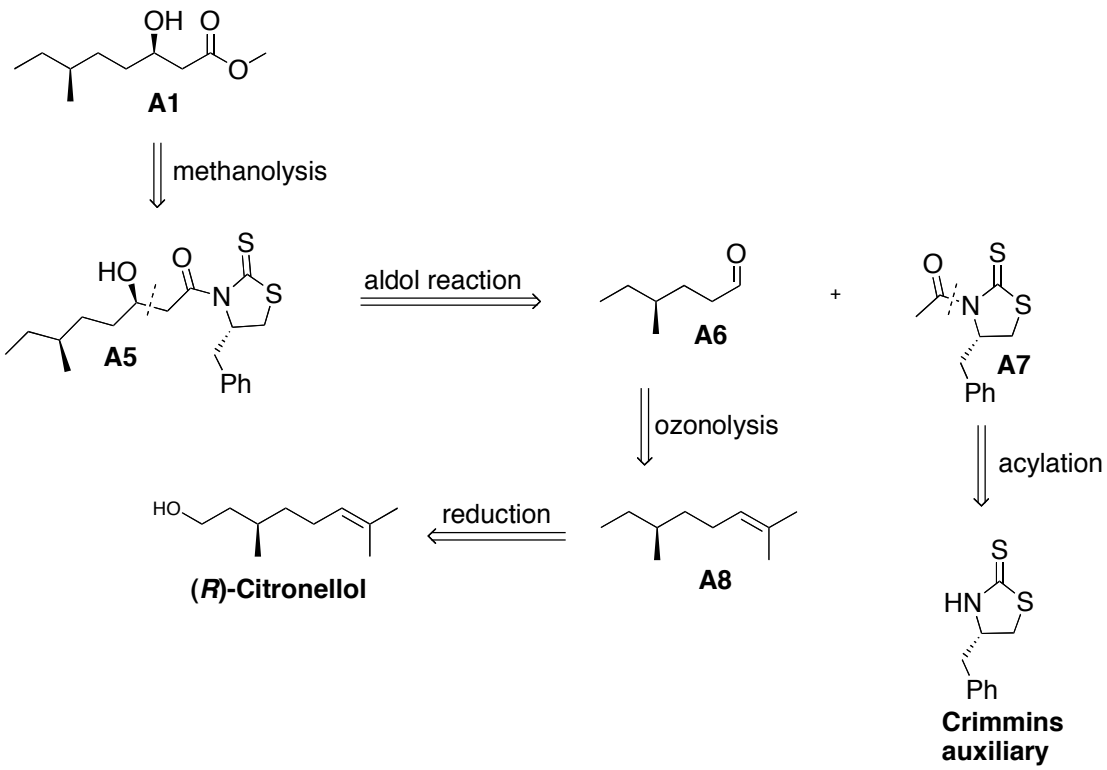

Scheme A.1 Retrosynthetic analysis of compound **A1**

A.3.2 Synthesis of standards A1-A4

The synthesis started with the preparation of compound **A7** (Scheme A.2). Acylation of the commercially available Crimmins auxiliary gave the desired product **A7** in 65% yield.

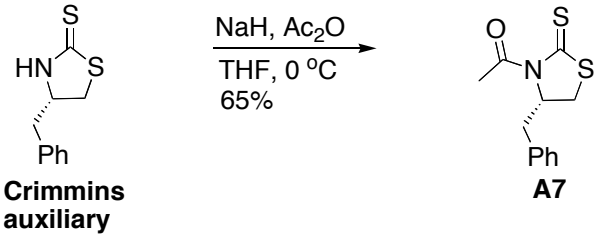

Scheme A.2 Synthesis of compound **A7**

(*R*)-citronellol was converted to the corresponding tosylate **A9**, which was reduced by $LiAlH_4$ to yield alkene **A8** (Scheme 7.3). Ozonolysis of compound **A8** generated aldehyde **A6**. The key aldol reaction of aldehyde **A6** and compound **A7** proceeded smoothly to give the desired products A**5** and **A10** in 6% and 28% yields respectively.[A2-A4] The stereochemistry of the hydroxyl group at compounds **A5** and **A10** was assigned based on the chemical shifts and coupling constants of the protons attached to carbon-7.[A5]

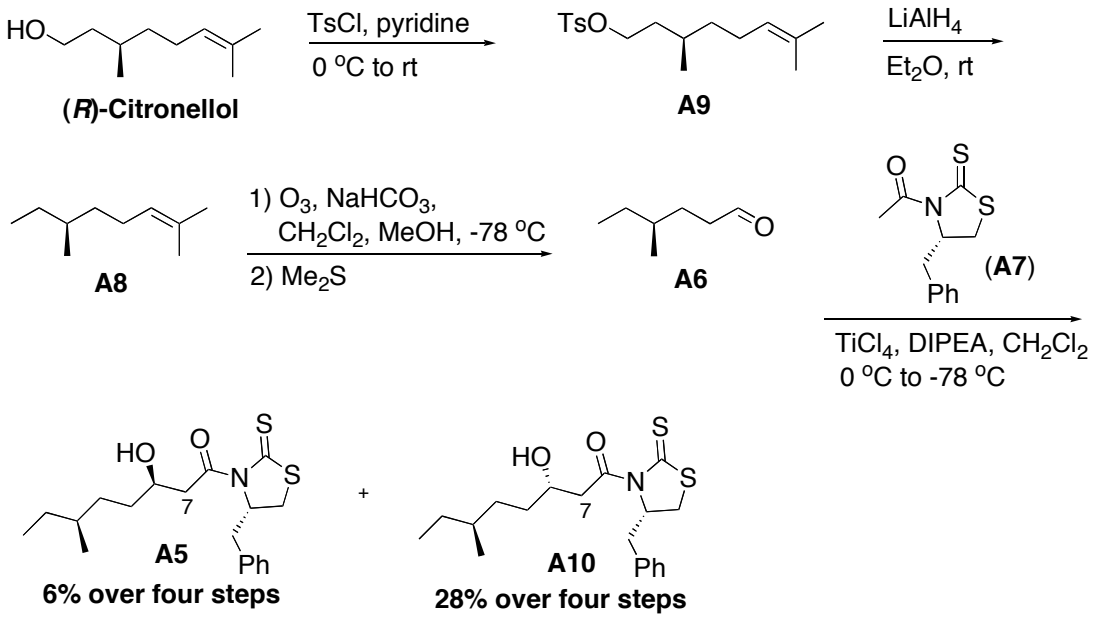

Scheme A.3 Synthesis of compounds **A5** and **A10**

Methanolysis of compounds **A5** and **A10** produced the desired standards **A1** and **A2** in moderate yields (Scheme A.4).

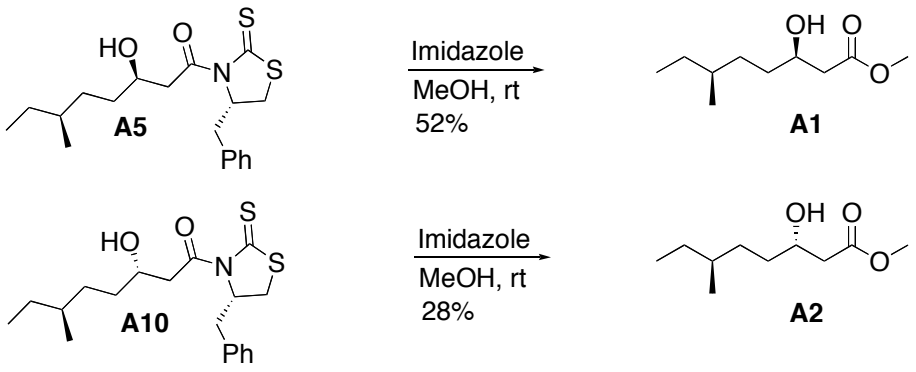

Scheme A.4 Synthesis of standards **A1** and **A2**

Standards **A3** and **A4** were also prepared in 6.8% and 23% yield respectively from (*S*)-citronellol using the same synthetic route.

A.4 Conclusions and future work

The four possible isomers of the lipid chain of tridecaptin A were synthesized using the aldol reaction as the key step. In the future, Christopher Lohans will use these synthetic standards to elucidate the stereochemistry of the lipid chain of tridecaptin A using chiral GC-MS.

A.5 Experimental

(*R*)-3,7-dimethyloct-6-enyl 4-methylbenzenesulfonate (A9)

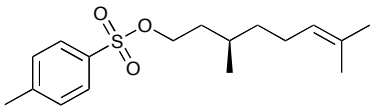

To an ice-cold solution of (*R*)-(+)-β-citronellol (3.00 g, 19.2 mmol, 1.0 equiv.) in pyridine (24 mL) was added 4-toluenesulfonyl chloride (8.00 g, 42.1 mmol, 2.2 equiv.). This mixture was slowly warmed to room temperature and stirred for another 4.5 h. H_2O (4 mL) and Et_2O (30 mL) were added and the two layers were separated. The aqueous layer was cooled in an ice bath, followed by the addition of 12 N HCl (30 mL). The original organic layer was slowly added back to the above acidic solution. The layers were separated and the aqueous layer was extracted back with Et_2O (2 x 30 mL). The combined organic layer was sequentially washed with sat. $NaHCO_3$ (50 mL), H_2O (50 mL) and brine (50 mL), and dried over Na_2SO_4. The crude was filtered, concentrated *in vacuo*, yielding **A9** as a colorless oil which was used in the next step without further purification.

(*S*)-2,6-dimethyloct-2-ene (A8)

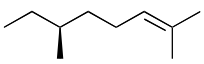

A 50 mL 3-neck flask was flame-dried and cooled to room temperature under argon. $LiAlH_4$ (0.93 g, 24.5 mmol, 1.3 equiv.) was added, followed by the addition of Et_2O (25 mL). This suspension was cooled in an ice bath and then a solution of **A9** (19.2 mmol) in Et_2O (5 mL) was added dropwise. This mixture was stirred at 0 °C for 2 h and was then poured into a 500 mL beaker. After cooling into a brine-ice bath, H_2O was

added slowly until no bubbles were evolved. 1 M NaOH (25 mL) was added and the mixture was stirred for 10 min. The mixture was filtered through a sintered glass funnel. The layers were separated and the aqueous layer was extracted back with Et_2O (50 mL). The combined organic layer was sequentially washed with 1 M NaOH, H_2O and brine, and dried over Na_2SO_4. The crude product was filtered, concentrated *in vacuo*, yielding **A8** as a colorless oil which was used in the next step without further purification.

(*S*)-4-methylhexanal (A6)

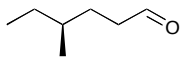

To a solution of **A8** (19.2 mmol) in CH_2Cl_2 (10 mL) and MeOH (2 mL), 0.1 g $NaHCO_3$ was added. This mixture was cooled to -78 °C and O_3 was bubbled through for 45 min. After bubbling with O_2 for 1 h, dimethyl sulfide (1 mL) was added. The solution was slowly warmed to room temperature and stirred for 1 h. H_2O (20 mL) and pentane (25 mL) were then added. The layers were separated and the aqueous layer was extracted back with pentane (2 x 25 mL). The combined organic layer was washed with H_2O and brine, and dried over Na_2SO_4. The crude product was filtered, and concentrated *in vacuo* (keeping the temperature of water bath below 25 °C), yielding **A6** as a colorless oil which was used in the next step without further purification.

(*S*)-1-(4-benzyl-2-thioxothiazolidin-3-yl)ethanone (A7)

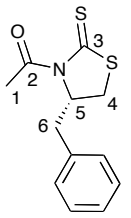

A 50 mL 3-neck flask was flame-dried and cooled to room temperature under argon. To this flask, THF (24 mL) was added and the flask was cooled to 0 °C. NaH (60% wt in mineral oil, 0.20 g, 5.0 mmol, 1.0 equiv.) was added and stirred for 20 min. Then Crimmins auxiliary (1.04 g, 5.0 mmol, 1.0 equiv.) was added and the mixture was stirred for 1 h at 0 °C. Acetic anhydride (0.57 mL, 6.0 mmol, 1.2 equiv.) was added and the mixture was stirred for another 2 h at the same temperature. The reaction was quenched by the addition of sat. NH_4Cl (10 mL). THF was removed *in vacuo* and EtOAc (30 mL) was added to the residue. The layers were separated and the organic layer was dried over Na_2SO_4. The crude product was filtered, concentrated *in vacuo* and purified by flash chromatography (silica gel, 8:1 hexanes : EtOAc), yielding **A7** as a yellow solid (0.81 g, 65%).

$[\alpha]_D$ 242.0° (*c* 0.40, $CHCl_3$); IR ($CDCl_3$, cast film) 3026, 2927, 1697, 1495, 1368 cm^{-1}; ^1H NMR ($CDCl_3$, 400 MHz): 7.38-7.28 (m, 5H, Ar-H), 5.41-5.36 (m, 1H, H-5), 3.39 (ddd, 1H, J = 11.5, 7.2, 1.1 Hz, H-4), 3.23 (dd, 1H, J = 13.2, 3.8 Hz, H-6), 3.04 (dd, 1H, J = 13.2, 10.5 Hz, H-6), 2.89 (dd, 1H, J = 11.5, 0.7 Hz, H-4), 2.80 (s, 3H, H-1); ^{13}C NMR ($CDCl_3$, 100 MHz): δ 201.2, 170.3, 136.1, 129.1, 128.5, 126.8, 67.8, 36.3, 31.4, 26.7; HRMS (ES) Calcd for $C_{12}H_{13}NOS_2Na[M+Na]^+$ 274.0331, found 274.0330.

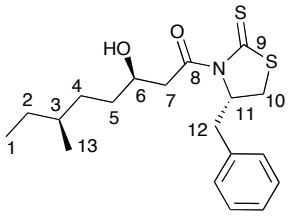

A5

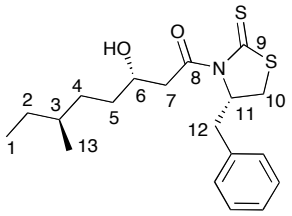

A10

A 100 mL 3-neck flask was flame-dried and cooled to room temperature under argon. To this flask was added a solution of **A7** (1.40 g, 5.6 mmol, 1.0 equiv.) in CH_2Cl_2 (28 mL) and the flask was cooled to 0 °C. Then $TiCl_4$ (1.0 M in CH2CL2, 5.60 mL, 5.6 mmol, 1.0 equiv.) was added and the mixture was stirred for 5 min at 0 °C. After cooling the above solution to -78 °C, DIPEA (0.97 mL, 5.6 mmol, 1.0 equiv.) was added and the mixture was stirred for 1 h at -78 °C. Then a solution of **A6** (0.64 g, 5.6 mmol, 1.0 equiv.) in CH_2Cl_2 (5.5 mL) was added dropwise. After stirring for another 1.5 h at the same temperature, the reaction was quenched by the addition of sat. NH_4Cl (10 mL). The layers were separated and the aqueous layer was extracted back with CH_2Cl_2 (2 x 40 mL). The combined organic layer was dried over Na_2SO_4. The crude product was filtered, concentrated *in vacuo* and purified by flash chromatography (silica gel, 6:1 then 4:1 hexanes : EtOAc), yielding **A5** (0.12 g, 6% over 4 steps) and **A10** (0.57 g, 28% over 4 steps) as yellow solids.

(3*R*,6*S*)-1-((*S*)-4-benzyl-2-thioxothiazolidin-3-yl)-3-hydroxy-6-methyloctan-1-one (A5)

$[\alpha]_D$ 126.6° (*c* 1.00, $CHCl_3$); IR ($CHCl_3$, cast film) 3458, 2958, 2929, 2872, 1693, 1455, 1342 cm^{-1}; ^1H NMR ($CDCl_3$, 500 MHz): 7.37-7.26 (m, 5H, Ar-H), 5.44-5.38 (m, 1H, H-11), 4.06-4.00 (m, 1H, H-6), 3.46 (dd, 1H, *J* = 17.5, 9.3 Hz, H-7), 3.40 (dd, 1H, *J*

= 11.2, 7.6 Hz, H-10), 3.35 (dd, 1H, *J* = 17.5, 2.6 Hz, H-7), 3.22 (dd, 1H, *J* = 13.2, 4.0 Hz, H-12), 3.04 (dd, 1H, *J* = 13.2, 10.4 Hz, H-12), 2.91 (d, 1H, *J* = 11.6 Hz, H-10), 1.65-1.10 (m, 7H, CH_2-2, CH-3, CH_2-4, CH_2-5), 0.89-0.82 (m, 6H, CH_3-1, CH_3-13); ^{13}C NMR ($CDCl_3$, 125 MHz): δ 201.4, 173.8, 136.4, 129.4, 128.9, 127.3, 68.8, 68.2, 45.6, 36.8, 34.3, 34.2, 32.2, 32.0, 29.4, 19.1, 11.4; HRMS (ES) Calcd for $C_{19}H_{27}NO_2S_2Na[M+Na]^+$ 388.1375, found 388.1368.

(3*S*,6*S*)-1-((*S*)-4-benzyl-2-thioxothiazolidin-3-yl)-3-hydroxy-6-methyloctan-1-one (A10)

$[\alpha]_D$ 175.0° (*c* 0.97, CH_2Cl_2); IR (CH_2Cl_2, cast film) 3445, 2958, 2929, 2872, 1690, 1455, 1342 cm^{-1}; ^{1}H NMR ($CDCl_3$, 500 MHz): 7.37-7.25 (m, 5H, Ar-H), 5.42-5.36 (m, 1H, H-11), 4.14-4.08 (m, 1H, H-6), 3.65 (dd, 1H, *J* = 17.7, 2.4 Hz, H-7), 3.40 (ddd, 1H, *J* = 11.5, 7.2, 0.9 Hz, H-10), 3.22 (dd, 1H, *J* = 13.2, 3.8 Hz, H-12), 3.13 (dd, 1H, *J* = 17.7, 9.4 Hz, H-7), 3.05 (dd, 1H, *J* = 13.2, 10.5 Hz, H-12), 2.90 (d, 1H, *J* = 11.6 Hz, H-10), 1.58-1.10 (m, 7H, CH_2-2, CH-3, CH_2-4, CH_2-5), 0.90-0.86 (m, 6H, CH_3-1, CH_3-13); ^{13}C NMR ($CDCl_3$, 125 MHz): δ 201.4, 173.4, 136.4, 129.5, 129.0, 127.3, 68.3, 45.9, 36.9, 34.4, 34.0, 32.4, 32.1, 29.3, 19.2, 11.4; HRMS (ES) Calcd for $C_{19}H_{27}NO_2S_2Na[M+Na]^+$ 388.1375, found 388.1370.

(3*R*,6*S*)-methyl 3-hydroxy-6-methyloctanoate (A1)

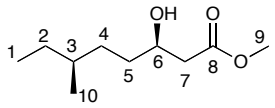

A solution of **A5** (0.06 g, 0.17 mmol, 1.0 equiv.) and imidazole (0.056 g, 0.83 mmol, 5.0 equiv.) in MeOH (2.8 mL) was stirred at room temperature for 19 h. The crude product was concentrated *in vacuo* and purified by preparative TLC (silica plate, 5:1 hexanes : EtOAc), yielding **A1** as a colorless oil (0.016 g, 52%).

$[\alpha]_D$ -11.8° (*c* 1.35, CH_2Cl_2); IR (CH_2Cl_2, cast film) 3459, 2958, 2932, 2875, 1740, 1461 cm^{-1}; ^1H NMR ($CDCl_3$, 500 MHz): 4.04-3.97 (m, 1H, H-6), 3.74 (s, 3H, CH_3-9), 2.89 (s, 1H, O-H), 2.55 (dd, 1H, *J* = 16.4, 3.1 Hz, H-7), 2.45 (dd, 1H, *J* = 16.4, 9.0 Hz, H-7), 1.61-1.14 (m, 7H, CH_2-2, CH-3, CH_2-4, CH_2-5), 0.91-0.85 (m, 6H, CH_3-1, CH_3-10); ^{13}C NMR ($CDCl_3$, 125 MHz): δ 173.5, 68.4, 51.7, 41.1, 34.3, 34.0, 32.2, 29.4, 19.1, 11.3; HRMS (ES) Calcd for $C_{10}H_{20}O_3Na[M+Na]^+$ 211.1305, found 211.1302.

(3*S*,6*S*)-methyl 3-hydroxy-6-methyloctanoate (A2)

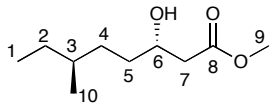

A solution of **A10** (0.071 g, 0.19 mmol, 1.0 equiv.) and imidazole (0.066 g, 0.97 mmol, 5.0 equiv.) in MeOH (3.3 mL) was stirred at room temperature for 19 h. The crude product was concentrated *in vacuo* and purified by preparative TLC (silica plate, 5:1 hexanes : EtOAc), yielding **A2** as a colorless oil (0.010 g, 28%).

$[\alpha]_D$ 24.8° (*c* 0.81, CH_2Cl_2); IR (CH_2Cl_2, cast film) 3463, 2959, 2931, 2874, 1740, 1462 cm^{-1}; ^1H NMR ($CDCl_3$, 500 MHz): 4.04-3.96 (m, 1H, H-6), 3.74 (s, 3H, CH_3-9),

2.89 (s, 1H, O-H), 2.56 (dd, 1H, *J* = 16.4, 3.0 Hz, H-7), 2.44 (dd, 1H, *J* = 16.4, 9.1 Hz, H-7), 1.55-1.10 (m, 7H, CH_2-2, CH-3, CH_2-4, CH_2-5), 0.91-0.87 (m, 6H, CH_3-1, CH_3-10); ^{13}C NMR ($CDCl_3$, 125 MHz): δ 173.5, 68.5, 51.7, 41.1, 34.4, 34.1, 32.3, 29.3, 19.2, 11.3; HRMS (ES) Calcd for $C_{10}H_{20}O_3Na[M+Na]^+$ 211.1305, found 211.1301.

(*S*)-3,7-dimethyloct-6-enyl 4-methylbenzenesulfonate (A11)

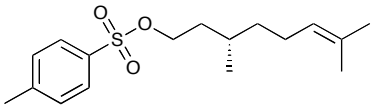

To an ice-cold solution of (*S*)-(+)-β-citronellol (3.00 g, 19.2 mmol, 1.0 equiv.) in pyridine (24 mL) was added 4-toluenesulfonyl chloride (8.00 g, 42.1 mmol, 2.2 equiv.). This mixture was slowly warmed to room temperature and stirred for another 4.5 h. H_2O (4 mL) and Et_2O (30 mL) were added and the two layers were separated. The aqueous layer was cooled in an ice bath, followed by the addition of 12 N HCl (30 mL). The original organic layer was slowly added back to the above acidic solution. The layers were separated and the aqueous layer was extracted back with Et_2O (2 x 30 mL). The combined organic layer was sequentially washed with sat. $NaHCO_3$ (50 mL), H_2O (50 mL) and brine (50 mL), and dried over Na_2SO_4. The crude was filtered, concentrated *in vacuo*, yielding **A11** as a colorless oil which was used in the next step without further purification.

(*R*)-2,6-dimethyloct-2-ene (A12)

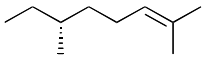

A 50 mL 3-neck flask was flame-dried and cooled to room temperature under argon. $LiAlH_4$ (0.93 g, 24.5 mmol, 1.3 equiv.) was added, followed by the addition of Et_2O (25 mL). This suspension was cooled in an ice bath and then a solution of **A11** (19.2 mmol) in Et_2O (5 mL) was added dropwise. This mixture was stirred at 0 °C for 2 h and was then poured into a 500 mL beaker. After cooling into a brine-ice bath, H_2O was added slowly until no bubbles were evolved. 1 M NaOH (25 mL) was added and the mixture was stirred for 10 min. The mixture was filtered through a sintered glass funnel. The layers were separated and the aqueous layer was extracted back with Et_2O (50 mL). The combined organic layer was sequentially washed with 1 M NaOH, H_2O and brine, and dried over Na_2SO_4. The crude product was filtered, concentrated *in vacuo*, yielding **A12** as a colorless oil which was used in the next step without further purification.

(*R*)-4-methylhexanal (A13)

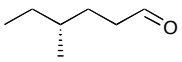

Compound **A12** (19.2 mmol) was dissolved in CH_2Cl_2 (30 mL). This solution was cooled to -78 °C and O_3 was bubbled through for 45 min. After bubbling with O_2 for 1 h, dimethyl sulfide (1 mL) was added. The solution was slowly warmed to room temperature and stirred for 1 h. H_2O (20 mL) and pentane (25 mL) were then added. The layers were separated and the aqueous layer was extracted back with pentane (2 x 25 mL). The combined organic layer was washed with H_2O and brine, and dried over Na_2SO_4. The crude product was filtered, and concentrated *in vacuo* (keeping the

temperature of water bath below 25 °C), yielding **A13** as a colorless oil which was used in the next step without further purification.

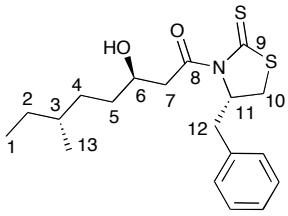

A14

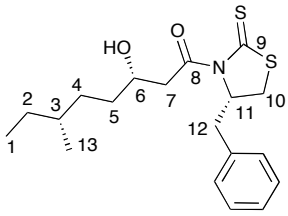

A15

A 100 mL 3-neck flask was flame-dried and cooled to room temperature under argon. To this flask was added a solution of **A7** (1.71 g, 6.8 mmol, 1.0 equiv.) in CH_2Cl_2 (34 mL) and the flask was cooled to 0 °C. Then $TiCl_4$ (1.0 M in CH2CL2, 6.80 mL, 6.8 mmol, 1.0 equiv.) was added and the mixture was stirred for 5 min at 0 °C. After cooling the above solution to -78 °C, DIPEA (1.18 mL, 6.8 mmol, 1.0 equiv.) was added and the mixture was stirred for 1 h at -78 °C. Then a solution of **A13** (0.77 g, 6.8 mmol, 1.0 equiv.) in CH_2Cl_2 (6.6 mL) was added dropwise. After stirring for another 1.5 h at the same temperature, the reaction was quenched by the addition of sat. NH_4Cl (10 mL). The layers were separated and the aqueous layer was extracted back with CH_2Cl_2 (2 x 40 mL). The combined organic layer was dried over Na_2SO_4. The crude product was filtered, concentrated *in vacuo* and purified by flash chromatography (silica gel, 6:1 then 4:1 hexanes : EtOAc), yielding **A14** (0.26 g, 11% over 4 steps) and **A15** (0.72 g, 29% over 4 steps) as yellow sticky oils.

(3*R*,6*R*)-1-((*S*)-4-benzyl-2-thioxothiazolidin-3-yl)-3-hydroxy-6-methyloctan-1-one (A14)

$[\alpha]_D$ 148.0° (*c* 0.15, $CHCl_3$); IR ($CHCl_3$, cast film) 3449, 2957, 2921, 2851, 1691, 1455, 1342 cm^{-1}; ^1H NMR ($CDCl_3$, 600 MHz): 7.36-7.24 (m, 5H, Ar-H), 5.45-5.40 (m, 1H, H-11), 4.06-4.00 (m, 1H, H-6), 3.46 (dd, 1H, *J* = 17.5, 9.4 Hz, H-7), 3.41 (ddd, 1H, *J* = 11.5, 7.2, 1.0 Hz, H-10), 3.36 (dd, 1H, *J* = 17.5, 2.6 Hz, H-7), 3.24 (dd, 1H, *J* = 13.3, 4.0 Hz, H-12), 3.11 (dd, 1H, *J* = 4.1, O-H), 3.06 (dd, 1H, *J* = 13.3, 10.4 Hz, H-12), 2.92 (d, 1H, *J* = 11.6 Hz, H-10), 1.60-1.10 (m, 7H, CH_2-2, CH-3, CH_2-4, CH_2-5), 0.89-0.86 (m, 6H, CH_3-1, CH_3-13); ^{13}C NMR ($CDCl_3$, 125 MHz): δ 201.5, 173.9, 136.4, 129.5, 129.0, 127.3, 69.0, 68.2, 45.5, 36.8, 34.4, 34.2, 32.3, 32.1, 29.3, 19.2, 11.4; HRMS (ES) Calcd for $C_{19}H_{27}NO_2S_2Na[M+Na]^+$ 388.1375, found 388.1369.

(3*S*,6*R*)-1-((*S*)-4-benzyl-2-thioxothiazolidin-3-yl)-3-hydroxy-6-methyloctan-1-one (A15)

$[\alpha]_D$ 176.1° (*c* 0.48, $CHCl_3$); IR ($CHCl_3$, cast film) 3437, 2957, 2927, 2856, 1693, 1455, 1342 cm^{-1}; ^1H NMR ($CDCl_3$, 600 MHz): 7.37-7.26 (m, 5H, Ar-H), 5.43-5.38 (m, 1H, H-11), 4.15-4.10 (m, 1H, H-6), 3.66 (dd, 1H, *J* = 17.7, 2.2 Hz, H-7), 3.41 (dd, 1H, *J* = 11.5, 7.2 Hz, H-10), 3.23 (dd, 1H, *J* = 13.3, 3.8 Hz, H-12), 3.14 (dd, 1H, *J* = 17.7, 9.4 Hz, H-7), 3.06 (dd, 1H, *J* = 13.1, 10.6 Hz, H-12), 2.91 (d, 1H, *J* = 11.5 Hz, H-10), 2.70 (s, 1H, O-H), 1.65-1.13 (m, 7H, CH_2-2, CH-3, CH_2-4, CH_2-5), 0.91-0.85 (m, 6H, CH_3-1, CH_3-13); ^{13}C NMR ($CDCl_3$, 125 MHz): δ 201.4, 173.4, 136.4, 129.5, 129.0, 127.3, 68.3, 68.2, 46.0, 36.9, 34.3, 33.9, 32.3, 32.1, 29.4, 19.1, 11.4; HRMS (ES) Calcd for $C_{19}H_{27}NO_2S_2Na[M+Na]^+$ 388.1375, found 388.1369.

(3*R*,6*R*)-methyl 3-hydroxy-6-methyloctanoate (A3)

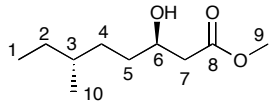

A solution of **A14** (0.099 g, 0.27 mmol, 1.0 equiv.) and imidazole (0.092 g, 1.35 mmol, 5.0 equiv.) in MeOH (4.0 mL) was stirred at room temperature for 24 h. The crude product was concentrated *in vacuo* and purified by flash chromatography (silica gel, 5:1 hexanes : EtOAc), yielding **A3** as a colorless oil (0.034 g, 68%).

$[\alpha]_D$ -22.0° (*c* 0.81, CH_2Cl_2); IR (CH_2Cl_2, cast film) 3498, 2956, 2922, 2851, 1741, 1556, 1542, 1352 cm^{-1}; ^1H NMR ($CDCl_3$, 500 MHz): 4.01-3.93 (m, 1H, H-6), 3.71 (s, 3H, CH_3-9), 2.84 (d, 1H, *J* = 3.4 Hz, O-H), 2.53 (dd, 1H, *J* = 16.4, 3.0 Hz, H-7), 2.41 (dd, 1H, *J* = 16.4, 9.1 Hz, H-7), 1.52-1.09 (m, 7H, CH_2-2, CH-3, CH_2-4, CH_2-5), 0.88-0.83 (m, 6H, CH_3-1, CH_3-10); ^{13}C NMR ($CDCl_3$, 125 MHz): δ 173.5, 68.5, 51.7, 41.0, 34.4, 34.1, 32.2, 29.3, 19.1, 11.3; HRMS (ES) Calcd for $C_{10}H_{20}O_3Na[M+Na]^+$ 211.1305, found 211.1301.

(3*S*,6*R*)-methyl 3-hydroxy-6-methyloctanoate (A4)

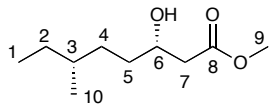

A solution of **A15** (0.129 g, 0.35 mmol, 1.0 equiv.) and imidazole (0.120 g, 1.78 mmol, 5.0 equiv.) in MeOH (6.0 mL) was stirred at room temperature for 24 h. The crude product was concentrated *in vacuo* and purified by flash chromatography (silica gel, 5:1 hexanes : EtOAc), yielding **A4** as a colorless oil (0.050 g, 76%).

$[\alpha]_D$ 11.5° (*c* 1.35, CH_2Cl_2); IR ($CHCl_3$, cast film) 3440, 2958, 2918, 2850, 1733, 1496 cm^{-1}; ^1H NMR ($CDCl_3$, 600 MHz): 4.02-3.95 (m, 1H, H-6), 3.72 (s, 3H, CH_3-9), 2.84 (d, 1H, *J* = 3.6 Hz, O-H), 2.53 (dd, 1H, *J* = 16.4, 3.0 Hz, H-7), 2.43 (dd, 1H, *J* = 16.4, 9.1 Hz, H-7), 1.59-1.11 (m, 7H, CH_2-2, CH-3, CH_2-4, CH_2-5), 0.89-0.84 (m, 6H, CH_3-1, CH_3-10); ^{13}C NMR ($CDCl_3$, 125 MHz): δ 173.5, 68.4, 51.7, 41.1, 34.3, 34.0, 32.2, 29.4, 19.1, 11.3; HRMS (ES) Calcd for $C_{10}H_{20}O_3Na[M+Na]^+$ 211.1305, found 211.1301.

A.6 References

A1. Kato, T.; Hinoo, H.; Shoji, J., Studies on antibiotics from genus Bacillus. 24. Structure of Tridecaptin-A. *J. Antibiot.* **1978,** *31*, 652-661.

A2. Crimmins, M. T.; King, B. W.; Tabet, E. A., Asymmetric aldol additions with titanium enolates of acyloxazolidinethiones: Dependence of selectivity on amine base and Lewis acid stoichiometry. *J. Am. Chem. Soc.* **1997,** *119*, 7883-7884.

A3. Crimmins, M. T.; Chaudhary, K., Titanium enolates of thiazolidinethione chiral auxiliaries: Versatile tools for asymmetric aldol additions. *Org. Lett.* **2000,** *2*, 775-777.

A4. Zhou, H.; Gao, Z.; Qiao, K.; Wang, J.; Vederas, J. C.; Tang, Y., A fungal ketoreductase domain that display substrate-dependent stereospecificity. *Nat. Chem. Biol.* **2012,** *8*, 331-333.

A5. Hodge, M. B.; Olivo, H. F., Stereoselective aldol additions of titanium enolates of *N*-acetyl-4-isopropyl-thiazolidinethione. *Tetrahedron* **2004,** *60*, 9397-9403.